Predictive models for intra-articular drug delivery (Alternative format thesis).

Nikolettos, John

Award date:
2018

Awarding institution:
University of Bath

Predictive Models for Intra-Articular Drug Delivery

Ioannis (John) Nikolettos

A thesis submitted for the degree of Doctor of Philosophy (PhD)

University of Bath
Department of Pharmacy & Pharmacology
March 2018

Table of Contents

List of Figures

List of Tables

Acknowledgements

Completing this PhD required a combination of my personal efforts and help offered by many special people around me through all these years. This journey has had many difficult and beautiful moments (mainly difficult) that I shared and discussed in detail with all of them. I greatly appreciate their outstanding support that led to ways of moving forward, in situations during which that extra push was needed!

I would like to express my sincere gratitude to my lead supervisor **Dr. Nikoletta Fotaki**, for her continuous and encouraging support through all these moments of hard work (which would also include a great amount of panic and anxiety), during my time in the lab. Her guidance was always of the highest importance, helping me overcome experimental obstacles and theoretical barriers. The completion of this thesis would not have been possible without her presence. I would also like to thank my second supervisor Dr. **Maria Marlow** for her valuable suggestions throughout this process and her contributions towards the making of this thesis. I would also like to express my gratitude towards Dr. **Jesper Østergaard** and Professor **Randall Mrsny** for accepting to evaluate this work.

My deepest thanks also go to those who assisted with my experiments and were kind enough to provide me with the use of instruments available in their lab: **Fernando Acosta** from the Analytical Systems lab for his help and advice, Professor **Karen Edler** for her help with the surface tension measurements, Professor **Jean van den Elsen** and Dr. **Albert Bolhuis** for their support with the sonication process of developing microparticles, Dr. **Paul De Bank**, Dr. **Ian Eggleston** and Dr. **Matthew Lloyd** for their support with the freeze-drying stage of developing microparticles and also Dr. **Olga Savvidou** and Dr. **Pelagia Katsimbri** from the Attikon University Hospital, Athens, Greece, for collecting and providing disease state synovial fluid for my experiments.

Most importantly, I would like to thank my family and especially my parents, **Nicos and Georgia**, for believing in me all these years by motivating me daily and financing my education until the end. I would not have reached this stage in life without their love and support during the expected and unexpected parts of this long journey. I can't thank you enough and I hope my accomplishments in life will prove worthy of everything you have offered me. I would also like to thank my partner, **Carrie**, for smiling every day and being inspiring and positive while providing endless support during the final stages of my PhD.

I would also like to thank my **friends and colleagues** inside and outside of the lab for being there during this time and for motivating and supporting me when tough times would approach. Thank you **μυστικοί 7, ομάδα πύραυλος** and everyone at **5W 3.22.** Special thanks should also be given to all the members of the "Dr. Fotaki team" (especially **Fotios, Ricardo, Joanna** and **Nota**) for the support we offered each other through this process!

Declaration

The experiments described in sections 2.3.6.3 up to 2.3.6.6. of Chapter 2 were conducted and the data was collected by the 4th year MPharm project students, Victor Lee Nien Kit, Timothy Chan and Ching Hoi (University of Bath, UK, 2015), under my support in their experimental work and the supervision of Dr. Nikoletta Fotaki.

Abstract

Intra-articular (IA) administration is used for the symptomatic treatment of disorders such as Osteoarthritis (OA) and Rheumatoid Arthritis (RA) providing a local effect while avoiding systemic side effects. For appropriate IA formulations to be developed and for quality control purposes, appropriate dissolution models have significant importance. Developing these models poses a great challenge, while at the moment, there is no regulatory approved standard methods for testing drug dissolution from parenteral formulations. The principal aim of this thesis is the development of appropriate *in-vitro* compendial and biorelevant dissolution models of drug absorption after IA administration. A vast number of dissolution methods were investigated, based on their potential and suitability as compendial methods (USP apparatus I, II, III and IV, dialysis methods and bi-phasic models) and their applicability in simulating *in-vivo* conditions for the biorelevant dissolution aspect (Side-Bi-Side diffusion cells and bi-phasic models). Various parameters of the setups were successfully evaluated towards their effect in drug dissolution. The discrimination ability of the USP apparatus IV was demonstrated showing the significant potential of this method in order to be considered for compendial testing. For the biorelevant dissolution testing, biorelevant synovial fluids (BSFs) of healthy and disease states were developed according to performed *in-vivo* studies of physicochemical properties and solubility values of Triamcinolone Acetonide (TA). These media were also used in biorelevant dissolution testing, showing the ability of the tested systems to discriminate between these media. Finally, surface dissolution imaging has permitted direct visualisation of the solvation and dissolution of TA with a detailed insight in the characterisation of the dissolution process by evaluating the effect of surfactants and increased viscosity of the medium. Overall, this thesis provides essential information on the potential of dissolution models for being the primary method upon which the drug dissolution of IA formulations may be established.

List of Abbreviations

ASF	Artificial Synovial Fluid
BBB	Blood Brain Barrier
BBMEC	Bovine Brain Microvessel Endothelial Cells
BSA	Bovine Serum Albumin
BSF	Biorelevant Synovial Fluid
CA	Cellulose Acetate
CMC	Carboxymethylcellulose
CTAB	Cetrimonium Bromide
DPS	Dips Per Minute
ECM	Extracellular Matrix
EDTA	Ethylenediaminetetraacetic Acid
GF	Glass Microfiber
GI	Gastrointestinal
HA	Hyaluronic Acid
HBSS	Hank's Balanced Salt Solution
HMW	High Molecular Weight
HPLC	High Pressure Liquid Chromatography
HS	Healthy State
IA	Intra-articular
IDR	Intrinsic Dissolution Rate
IGF	Insulin-Like Growth Factor
IL	Interleukin
IVIVC	*In-vitro-In-vivo* Correlation
LMW	Low Molecular Weight
MMP	Matrix Metalloproteinase
MPa	Microparticles a
MPb	Microparticles b
MWCO	Molecular weight cut off
OA	Osteoarthritis
PBS	Phosphate Buffer Saline
PC	Phosphatidylcholine
PLA	Poly- (l-lactid)

PLGA	Poly(lactic-co-glycolic acid)
PTFE	Polytetrafluoroethylene
RA	Rheumatoid Arthritis
RC	Regenerated Cellulose
RPM	Rotations Per Minute
SD	Standard Deviation
SDI	Surface Dissolution Imaging
SEM	Scanning Electron Microscopy
SLS	Sodium Lauryl Sulfate
SMD	Sample Mass Dissolved
TA	Triamcinolone Acetonide
TGF	Transforming Growth Factor
USP	United States Pharmacopoieia
UV	Ultraviolet
W	Watt

Chapter 1: Introduction

Overview

Intra-articular (IA) is a type of medical administration which delivers the drug directly to the joint (local administration) while reducing the systemic side effects. With this type of delivery, most of the drug administered, is directly released in the targeted area allowing even drugs with poor oral bioavailability to achieve their pharmacological purpose against diseases affecting the joint. The most important among these are Osteoarthritis (OA) and Rheumatoid Arthritis (RA). Both these diseases have in common the gradual damage of the articular cartilage and the bones involved in the joint [1]. The IA pharmacological treatment available [corticosteroids and hyaluronic acid (HA)] does not cure or prevent arthritic disorders but reduces moderate to severe pain and slows down the progression of the disease [2]. A significant drawback of formulations given through the IA route, is that they exit the joint rapidly and distribute through the body. This takes place due to the continuous transynovial flow of the synovial fluid in and out of the joint, resulting in the need for multiple injections, to maintain the desired drug concentration. This is a major issue, with promising strategies available to overcome it, such as formulations that stay in the joint longer and are released in a longer length of time [3]. In order to develop and characterise these potential drug formulations, specific *in-vitro* tests need to be performed to establish drug dissolution. Currently, there is no official standard method for testing drug dissolution from IA formulations. Instead, widely used *in-vitro* dissolution methods include: 1) sample and separate, 2) dialysis and 3) continuous flow through (USP apparatus IV). A main issue with these setups is that they are designed for testing dissolution of different drug delivery systems and they do not fully cover the dissolution of the drug given through the IA route [1]. The goal of this project is the development of appropriate and validated *in-vitro* compendial and biorelevant dissolution models of the drug after IA administration. For biorelevant dissolution testing, biorelevant synovial fluids of healthy and disease state will be developed for the prediction of *in-vivo* performance by characterising *in-vivo* disease state synovial fluids (OA and RA). Surface dissolution imaging will also be used for characterisation of the dissolution process of IA drugs. The methods developed will be used for defining critical formulation variables and setting dissolution testing specifications, with the biorelevant aspect being used to predict *in-vivo* performance. These tests may be used for other parenteral formulations as well.

1.1. Anatomy of the synovial joint and synovial fluid composition

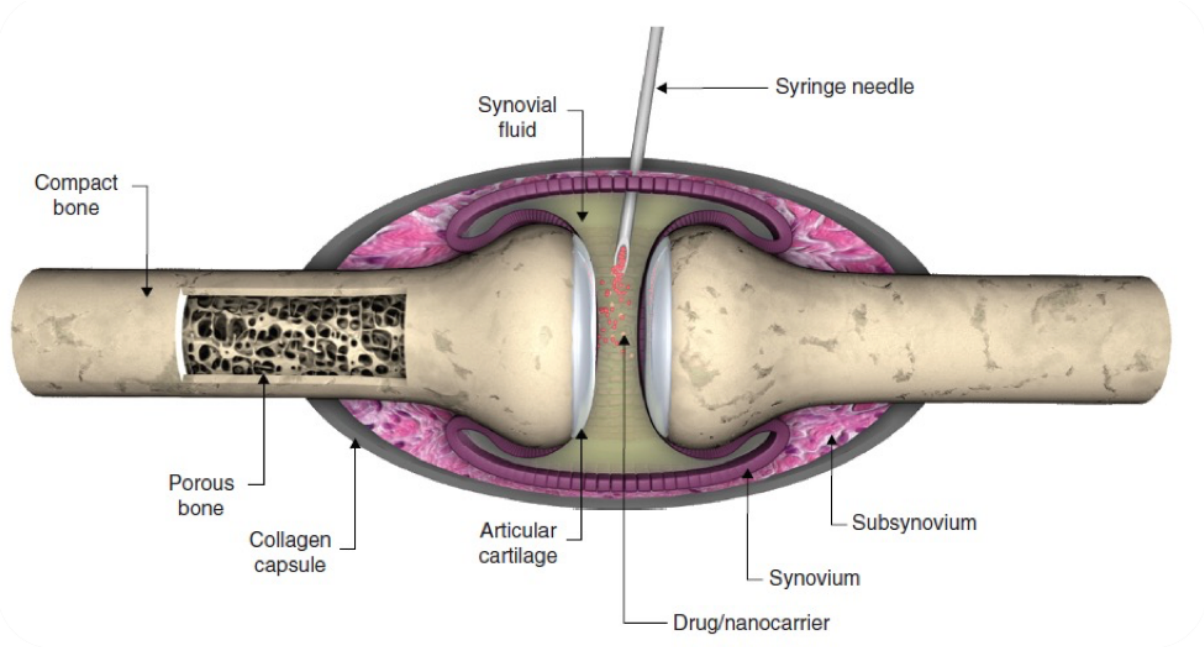

Fig. 1.1. The synovial joint and IA drug delivery. Reproduced with kind permission from [2].

A synovial joint, which is one of the most common joints in the body, has specific anatomic properties which make IA delivery feasible. It consists of parts connecting the bones involved in the cavity, in which movement takes place and stability is needed (Fig. 1.1). At the end parts of the two bones, there is a layer, the articular (hyaline) cartilage, and between the bones inside the synovial cavity, there is the synovial fluid that lubricates the joint and reduces friction during applied pressure. The synovial fluid also supplies the oxygen and nutrients to the articular cartilages for the growth, restoration and viability of the bone [1, 2]. This synovial cavity is then "encapsulated" in a membrane, the synovium. The last part involved in the synovial joint is the outer fibrous collagen capsule which is in direct contact with the subsynovium and the blood circulation.

1.1.1. Articular cartilage

The articular (hyaline) cartilage covers the end part of the bone involved in the joint and has a thickness of 1-5 mm [4]. This tissue provides a near no-friction surface when the bones come into contact, with reversible deformation properties, meaning that after stress is applied to the membrane, it can return to its original state. Apart from reversible compression, the articular cartilage can reduce contact pressure and compression (due to water absorbance) between the bones and apply any change in stress evenly to the bone surface. These properties exist due to

an extensive extracellular matrix (ECM), which has layers of glycosaminoglycans and collagen fibres (that also provide the articular cartilage with tensile strength). For the growth, restoration and viability of the bone, nutrients and oxygen, are able to diffuse through the articular cartilage, from the synovial fluid and reach the chondrocytes [1, 4]. The articular cartilage is separated from the bone by a calcified cartilage layer.

1.1.2. Synovial fluid

The synovial fluid is the liquid in which the IA injection is administered. It is located in the synovial cavity and surrounded by the synovium, which also forms a thin film over the inner cavity. The synovial fluid is a non-Newtonian thixotropic fluid meaning that it is viscous and with increased stress conditions, its viscosity decreases and it may flow easier. The composition of the synovial fluid of the healthy, OA and RA joint (volume in knee joint: 0.5-2 mL, >3.5 mL and up to 100 mL respectively) can be seen in Table 1.1.

Table 1.1. Healthy and disease state (OA and RA) synovial fluid composition

Components (mg/mL)	Healthy state	OA	RA
Total protein	10-30 [4] 10.4-15.8 [5] 12-30 [6] 13.1-21.3 [7] 18 [8]	15-45 [4] 17-56.8 [9]	31.6-66.2 [10] 19.8-49.5 [5]
Albumin	8-13 [4] 7-18 [11] 11 [12] 4-10 [13] 12-20 [14]	8-13 (Similar to Healthy state) [4]	20.25 [15-17]
γ-globulin	0.5-2.9 [8]	0.5-2.9 (Similar to Health state) [4]	24.75[15, 17]
a2-Macroglobuline	0.31 [4]	-	-

Hyaluronic acid	3.5 [4] 1–4 [18] 2-4 [19] 2.5-3.65 [20] 1.45-2.94 [5] 2-4 [21] 0.35-4.22 [22] 1-4 [23] 2.83 [8]	<2.2 [4] 0.1-1.3 [18]* 1-2 [10] 1.07-2.60 [20] 0.32-3.61 [10] 1.24-2.22 [22]	0.39-2.19 [20] 0.7-3.74 [10] 0.37-1.88 [5] 0.19-1.26 [24] 0.35-2.41 [22] 0.8-1.7 [25]
Lubricin	0.05 [4] 0.05-0.35 [18]	-	-
Glucose	0.66 [4]	0.66 (Similar to Health state) [4]	-
Urea	0.04 [4]	0.04 (Similar to Health state) [4]	-
Lactate	0.09-0.162 [4]	-	-
Ca^{+}	0.48-0.96 [4]	0.48-0.96 (Similar to Health state) [4]	-
Cl^{-}	3.81 [4]	3.81 (Similar to Health state) [4]	-
Na^{+}	3.33 [4]	3.33 (Similar to Health state) [4]	-
K^{+}	0.16 [4]	0.16 (Similar to Health state) [4]	-
Zn^{2+}	1.26 [4] 1.14 ± 0.56 [26]	1.56 ± 1.31 [26]	1.7 ± 0.75 [26]
Fe^{2+}	2.28 [4] 2.18 ± 0.64 [26]	2.28 (Similar to Health state) [4] 3.259 ± 1.781 [26]	1.91 ± 1 [26]
Cu^{2+}	2.47 [4] 2.81 ± 0.71 [26]	2.47 (Similar to Health state) [4]	5.66 ± 3.48 [26]

		4.85 ± 2.85 [26]	
Phospholipids	0.1-0.2 [18] 0.13-0.15 [27] 0.14 [8] 0.1 [28]	0.2-0.3 [28] 0.26-0.98 [27]	0.4-1.4 [27]
Total Cholesterol	0.07-0.08 [27]	0.04-1.69 [27]	0.76-1.30 [27]
Total Triglycerides	0 [27]	0.12-0.59 [27]	0.17-1 [27]

* Classified for arthritic disease (i.e. OA)

The synovial fluid composition is very similar to that of blood plasma with concentrations of small, low molecular weight molecules and electrolytes being similar in both fluids, leading to the consideration of the synovial fluid as plasma ultra-dialysate. Larger molecules though, such as proteins and polymers (albumin, fibrinogen and globulins) are present in lower concentrations in synovial fluid or may not be present at all, compared to plasma, due to filtration by the synovial capillary walls. The synovial fluid also contains components not present in the plasma, such as HA and lubricin which play a major role in the viscoelastic and lubricating ability of this fluid [4, 29]. In addition, the HA is useful for bringing together the opposing surfaces of the joints by creating tensile strength with little or no shear stress. This allows the surfaces to slide easier across each other with limited friction [4].

1.1.2.1. Transynovial flow

The pathway followed by the blood and eventually the synovial fluid in the synovial joint is through a continuous flow. The synovial fluid is drained from the synovial cavity into the sub-synovial lymphatics and capillaries (subsynovium) while it is produced by the vascularised synovial membrane, by filtering the blood into the cavity, with the addition of HA and lubricin produced by type B synoviocytes (Fig. 1.1) [2]. The two pathways which regulate the flow of the synovial fluid through the synovial membrane are:

- Synovial cavity → subsynovium through the full thickness of the synovial lining and
- Superficial plasma → synovial cavity through ultrafiltration by the capillary wall and overlying synovial interstitium [29, 30]

This turnover flow is the trans-synovial flow and depends on local intra-extravascular pressures [4]. By this, most of the proteins and the water in the synovial fluid are changed approximately every 2 hours and the HA every 38 hours [1].

1.1.3. Synovium

The synovium, the membrane surrounding the synovial fluid, is comprised of two layers. The deep layer consists of adipose, fibrous or areolar tissue and an ECM with main contents being collagen (e.g. types I, III, V, VI), proteoglycans (eg. decorin, biglycan), HA and fibronectin [1, 4]. The second and superficial part of the synovium contains type A and type B synoviocyte cells [1]. Type A synoviocytes act as macrophages which consist ~30% of the intima and subintima cells [31] and type B synoviocytes, which appear more frequently and act similarly to fibroblasts [1]. These similarities between the synoviocytes and the mentioned cells, mean that type A synoviocytes express specific markers with a haematopoietic origin and type B synoviocytes secrete specific collagens, vimentin and Cluster Differentiation (CD) 90 [32]. Both type of synoviocytes are important in creating the joint's immune system and in helping with the clearance of waste products. The synovium has several major roles, including:

- Playing the role of a diffusion membrane for solutes between the synovial fluid solution and the fenestrated microvessels and lymphatic vessels
- Providing a large proportion of filtration to the plasma (mostly with the ECM and type B synoviocytes) for passing the capillary walls and into the joint cavity
- Removing (through type A synoviocytes) the foreign fragments from the synovial fluid, with type A synoviocytes also producing chemokines
- Synthesis of HA and lubricin (through type B synoviocytes)
- Generation of the synovial fluid [4]

Finally, outside of the ECM (consisting the synovium) there is a fenestrated capillary network with lymphatic vessels and loose areolar connective tissue, the subsynovium [1, 33].

1.2. Pathophysiology of the joint in Osteoarthritis and Rheumatic Arthritis

IA drug delivery is useful for treating symptoms such as pain and inflammation in the joint while it is effective against a range of diseases such as arthritic disorders (OA and RA). OA has a prevalence of about 7% [1] and after the age of 65 years it appears in 60% of men and 70% of women [4] while in the US it is the cause of more than 500,000 total joint replacements

every year [1]. RA has a prevalence of 1% in the population and affects, in average, 1.5 men and 3.6 women per 10,000 people each year [34].

The arthritic joint, involved in conditions such as OA or RA, has several differences to a healthy state joint (Fig. 1.2. A) associated with the articular cartilage, the components of the synovial fluid and the synovium [35]. The volume of the synovial fluid increases while the synovial tissue becomes enlarged due to a different balance between intravascular pressure and synovial interstitial pressure. An increased amount of proteins appears in the synovial fluid, reaching the amount present in the blood plasma (Table 1.1.) [2].

OA is mainly described as a disease where degeneration and loss of articular cartilage takes place while the synovium cells become enlarged (Fig. 1.2. B). Bone remodelling and new bone formation takes place in the degenerated articular cartilage due to the local presence of osteophytes in the cartilage and the bone [4]. In patients with OA, one of the first differences observed in the joint are fissures on the surface of the articular cartilage, which may then spread and penetrate into the cartilage and then enter the bone [4]. While degeneration expands in the articular cartilage, numerous results take place such as loss of collagen and proteoglycans (the main components of the articular cartilage), production of specific cytokines (eg. IL-1), growth factors (eg. IGF-1, TGFb) and proteases, leading to impairment of the collagen network. This means that the thickness of the articular cartilage is slowly lost, with the growth factors playing, most likely, a major role in the synthetic processes of OA [4]. The loss of collagen and proteoglycans and the production of cytokines, growth factors and proteases are mainly caused by the matrix metalloproteinases (MMP's), which lead to the cleavage of macromolecules belonging to the articular cartilage such as type II collagen and the proteoglycan aggrecan [35]. The products of macromolecule degradation (involving the cytokines mentioned) also cause the degradation of the articular cartilage creating a positive feedback loop.

RA is a chronic inflammatory disease which is mainly caused from interactions between cells starting with interactions between the antigen presenting cells and the CD4 + T cells (Fig. 1.2. C) [2]. The synovial joint becomes damaged and many cell types appear within it, such as T cells, B cells, dendritic cells, macrophages, fibroblasts, mast cells and neutrophils. The physiology of the joint is changed due to the appearance of the mentioned cells, with an increase in the volume of the synovial fluid, the temperature and the inner pressure. The activity arising from the inflammation present is considered to be a chain event, as the T cells activated are responsible for producing interferon c and specific cytokines (TNF and interleukins) [2] that activate synovial macrophages, fibroblasts, chondrocytes and osteoclasts, causing the inflammation of synovial tissues [35]. The macrophages and fibroblasts then, produce TNF-a

and IL-1, IL-6, IL-15, IL-18. The TNF-a and Interleukin cytokines, together with specific growth factors, are responsible for the activation of B cells and neutrophils. The neutrophils, that also play a role in the articular cartilage degradation, accumulate in the synovial fluid. The articular cartilage is then impaired by the MMP's similarly to the events taking place in OA [2]. The B cells and the dendritic cells together with the T cells and tissue macrophages, form aggregates. The synovial lining (synovium) becomes enlarged from 1-20 cells in depth due to a large amount of type A and B synoviocytes present, leading to an increase in molecule transportation from the subsynovium to the synovium and synovial fluid [1, 32] The synovium also becomes pannus tissue at the cartilage-bone interface (an abnormal layer of fibrovascular tissue) containing mainly macrophages and osteoclasts. While the panus tissue continues its growth it can enter the bone and may also include growth of blood vessels (angiogenesis) [32, 35]

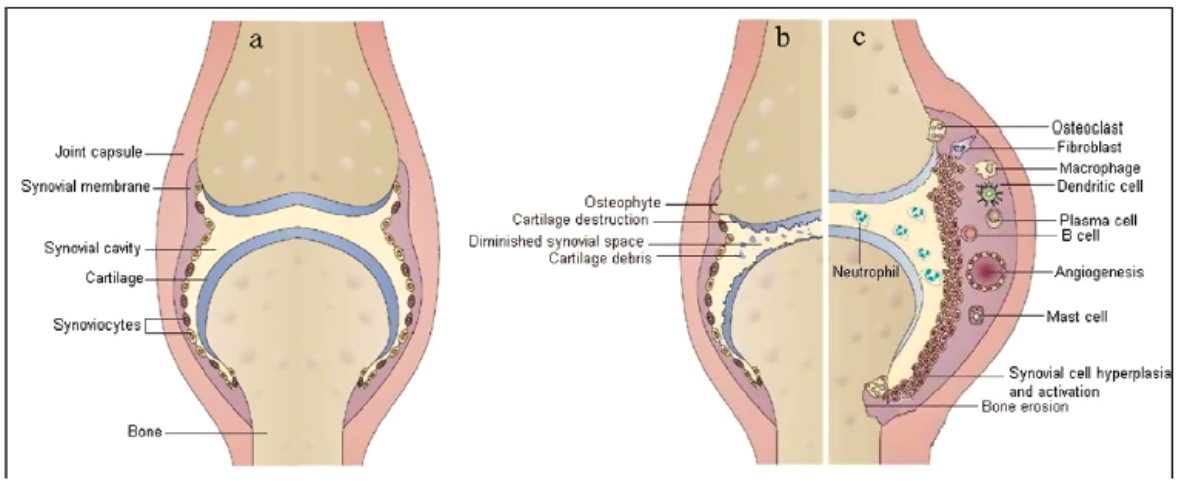

Fig. 1.2. Representation of a) healthy state joint, b) Osteoarthritis joint, c) Rheumatic arthritis joint. Reproduced with kind permission from [35]

1.3. Physicochemical properties of synovial fluid in the healthy, OA and RA synovial joint

1.3.1. pH of synovial fluid

The pH value of the synovial fluid may have a significant effect on the dissolution of the drug administered through the joint as it affects the solubility of weak acidic and basic drugs. In literature, the pH of human synovial fluid (normal and disease state) is measured directly from

the samples collected with pH electrodes. More specifically, measurements were performed with a pH meter [36, 37] or radiometer [38], with a specific pH electrode made from antimony also been used in combination with a radiometer pH meter [39], while in another study a McInnis glass electrode applied [7].

1.3.1.1. Healthy state

Considering that synovial fluid is a dialysate of blood with the addition of HA and lubricin, the pH is near the physiological value (~7.4) [38] agreeing to previous animal studies and post mortem samples [7]. Results from one study that shows a mean value of 7.7 for healthy adult subjects (Table 1.2.). The same paper explains that an important factor affecting the pH, is the age of the subjects. At a young age of 7-19 the mean value of the pH was at 8.1 while from 20 years and onwards the pH stabilises at around 7.7 (Fig. 1.3.) [36].

1.3.1.2. Osteoarthritis

The OA synovial fluid pH, seems to be lower than the healthy state synovial fluid pH in between the ages of 30-78 with a mean of 7.5 [36]. No test was performed on early age patients while only 3 patients were aged 30-49 years out of the 41 OA patients that were tested. In another study the mean synovial fluid pH of 16 OA patients tested was relatively higher than that noted as the value was 7.9 (Table 1.2.) [36, 37]. A higher pH may be estimated due the hydrogen ion concentration measurement technique, as oxygenation may take place when samples are withdrawn from the synovial cavity, increasing the hydrogen ion concentration [39].

1.3.1.3. Rheumatoid arthritis

Tests on patients with RA have shown that the pH of their synovial fluid is lower than healthy and OA values. A mean value of 7.22 was measured which can be attributed to a topical lactic-acid acidosis taking place due to the inflammation of the joint. The synovial membrane in this condition has acid producing villi formed in its surface that may entrap synovial fluid in its folds; if synovial fluid is withdrawn from that area the pH will be lower than the actual value [38]. It was also noticed that the position of the needle when withdrawing fluid was important for maintaining similar readings, which was not an issue for healthy state joints. Other measurements showed a lower mean value of 6.61 explained by the acidity present in inflamed joints [39] while in another study, the mean pH value was measured at 7.5 which was higher than studies conducted before [37] due to the possible oxygenation of the withdrawn samples (Table 1.2.) [39].

Table 1.2. pH values of synovial fluid in healthy and disease state

Mean value	Range	Subjects	Age	State	Reference
7.39	7.29-7.45	6	-	Healthy	[7]
7.7	6.5-8.9	91	7-78	Healthy	[36]
7.43	7.31-7.64	5	-	Healthy	[38]
7.3	7.1-7.4	10	23-73	Healthy	[39]
7.55	7.49-7.6	41	30-78	OA	[36]
7.9	7.4-8.1	16	-	OA	[37]
7.22	7.08-7.28	6	-	RA	[38]
6.61	6-7.3	10	48-74	RA	[39]
7.5	7.4-.76	6	-	RA	[37]

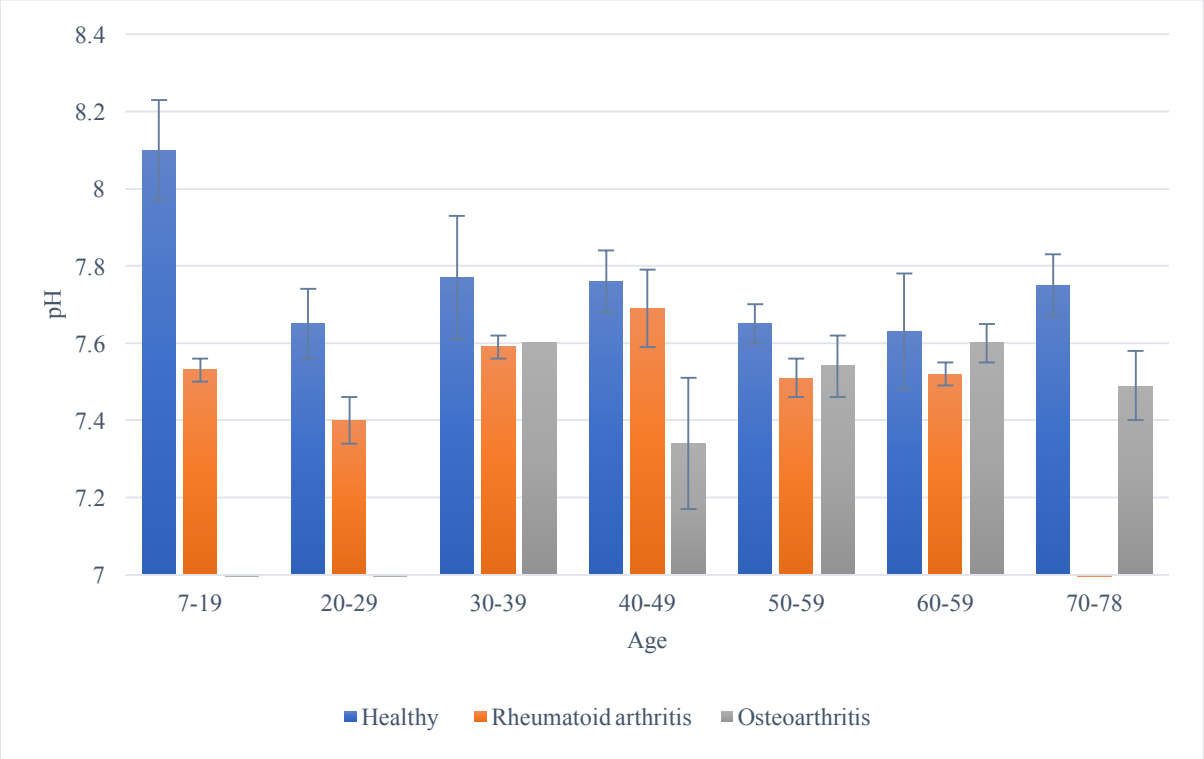

Fig. 1.3. Mean ± SD % of healthy and disease state synovial fluid pH as a function of age [36]

1.3.2. Osmolality of synovial fluid

Osmolality is a percentage (%) of the total number of particles dissolved per kilogram of solvent which can affect the osmotic pressure that shows how possible it is for the solvent molecules to pass through a semipermeable membrane, such as the one involved in a synovial joint [40]. Osmolality is usually measured by a freezing point depression osmometer or a vapour pressure depression osmometer [40-42]. The freezing point depression is considered more accurate, as the vapour pressure method is more useful for viscous and non-volatile solutions [41, 42].

1.3.2.1. Healthy state

One of the first studies conducted for measuring osmolality from healthy patients showed that the range changed over time, with the first measurement giving a mean value of 404 ± 57 mmol/kg and after twenty minutes the same samples gave a mean value of 369 ± 50 mmol/kg [41]. This difference in osmolality over time may be explained by the conformational changes of HA due to entropy, influence the amount of bound water, which can be released in exchange for salt particles. In addition, stress conditions in the joint can affect the conformational state of HA. Another study showed slightly lower values in a range of 295-340 mmol/kg, which was justified by the technique used to measure osmolality, as a freezing point was used instead of vapour pressure (Table 1.3.) [42].

1.3.2.2. Osteoarthritis

The osmolality measured in synovial fluid from OA patients is significantly lower than that of healthy subjects. The first explanation as to why this occurs, focused on the change of HA in the diseased state synovial fluid. Due to the conformational changes and the difference in molecular weight of the HA there is an increase of bound water instead of salt and so the osmolality decreases [40, 41]. Secondly, the chondrocytes present in the articular cartilage seem to be affected by osmolarity difference and regulate gene expression of chondrogenic transcription factors together with ECM constituents [42].

1.3.2.3. Rheumatoid arthritis

The osmolality of the synovial fluid of patients with RA is also lower than that of healthy subjects. From the studies conducted it is shown that the values are slightly lower than those of the OA patients due to the change of the constituent concentrations through the disease, such as total protein which is lower in OA and also due to lytic enzymes and cell debris in RA [40].

Table 1.3. Osmolality of healthy and disease state synovial fluid

Mean value (mmol/kg)	Range (mmol/kg)	Subjects	Age	State	Reference
404 +/- 57 **369 +/- 50**	N/A	15	22-35	healthy	[41]
-	295–340	N/A	>30	healthy	[42]
297 +/- 16.9	270-334	15	38-74	OA	[40]
-	249-277	3	>30	OA	[42]
280 +/- 7.7	265-290	15	55-86	RA	[40]
-	273-283	3	>30	RA	[42]

1.3.3. Surface tension of synovial fluid

The surface tension shows the resistance of a liquid surface to an external force and affects the wetting of drug particles and consequently the surface area for drug dissolution [43]. Components such as phospholipids [44] and HA [43] are mainly responsible for changing the surface tension of the synovial fluid. There is limited data for the surface tension of the synovial fluid, with one study showing the values measured in healthy subjects and one more for patients with RA, with no measurements found for OA. The surface was measured by a Wilhelmy plate method [43] or a tensiometer [45].

1.3.3.1. Healthy state

When the amount of phospholipids present in synovial fluid are in healthy state levels, the surface tension is approx. 50 mN/m (Table 1.4.).

1.3.3.2. Rheumatoid arthritis

In RA, the composition of the synovial fluid is altered and the synovium is degenerated which can affect the presence of bound surface active phospholipids. The surface tension is affected by these changes [46] which means that the dissolution rate of poor soluble drugs could also be different in the disease state (Table 1.4.).

Table 1.4. Surface tension of healthy and disease state synovial fluid

Mean value(mN/m)	Range (mN/m)	Subjects	Age	State	Reference
50.6	48-52	5	-	Healthy	[45]
47.99 +/- 4.59	31.15–52.61	19	-	RA	[43]

1.3.4. Viscosity of synovial fluid

As healthy synovial fluid has non-Newtonian shear thinning properties with viscosity decreasing as the shear rate becomes higher [9, 45, 47, 48], it is common in the literature to present figures with viscosity values against shear rates, as a specific viscosity or values over time, are difficult to interpret [49]. The viscosity of synovial fluid has been measured with a rotational cone in cone viscometer [47, 50, 51], a low shear rotational viscometer [52, 53], a Weissenberg rheogoniometer [48] and also a capillary tube method [49].

1.3.4.1. Healthy state

The viscosity of synovial fluid at a shear rate of 0.1 s^{-1} is approx. 100 Pa s (Table 1.5.). With the shear rate decreasing, due to non-Newtonian behaviour, viscosity reaches a value of approx. 0.1 Pa s with 0.001 s^{-1} [48-53]. The presence of the HA protein complex with its high molecular weight (10^7 Da) is responsible for maintaining the viscosity of synovial fluid [9, 52].

1.3.4.2. Osteoarthritis

OA synovial fluid has shear-thinning behaviour in accordance with synovial fluid from a healthy subject, but with lower viscosity at the same shear rates [47, 48, 53] (Table 1.5.). This is attributed to the decreased HA concentration due to dilution (higher volume of synovial fluid) and its lower molecular weight (10^6 Da) due to depolymerisation in OA [9]. Depolymerisation is caused by specific components present in blood, such as ascorbic acid, produced by the increased amount of leukocytes in the diseased synovial joint [54]. With lower viscosity, the synovial fluid is no longer able to provide lubrication and protection of the bone [9].

1.3.4.3. Rheumatoid arthritis

The synovial fluid in RA contains a smaller amount of HA compared to the OA fluid, with the molecular weight of HA in RA synovial fluid being higher (compared to OA), but still lower

than in healthy state synovial fluid (Table 5) [9]. This can explain its Newtonian properties (shear thinning behaviour) in comparison with the non-Newtonian properties of healthy and OA synovial fluids [50], resulting to the viscosity not being highly affected by the changing shear rate [48, 53]. The components of synovial fluid change similarly to OA due to the disease state affecting the concentration and molecular weight of HA [9].

Table 1.5. Viscosity vs. shear rate of healthy and disease state synovial fluid

Shear rate (1/s)	Mean (Pa s)	Viscosity Range (Pa s)	Subjects	Age	State	Reference
0-5	-	0-0.5	6	<40	healthy	[49]
0.1-1000	-	0.1-100	3	43-48	healthy	[48]
0.001-1000	-	1-40	200	-	healthy	[53]
0.001-1000	-	6-175	7	~60	healthy	[51]
0.001-1000	-	0-10	4	-	healthy	[52]
0.01-100	-	0.01-10	4	40-48	healthy	[50]
0.1-1000	-	0.01-0.5	4	-	OA	[48]
0.001-1000	-	0.1-1	200	-	OA	[53]
0.01-1000	-	0.01-10	22	-	OA	[47]
0.1-1000	-	0.01-0.05	4	-	RA	[48]
0.001-1000	-	0.004-0.007	200	-	RA	[53]

1.4. Intra-Articular injection pathways

When drug molecules are administered into the synovial fluid via IA injection, they follow specific pathways through the joint as shown in Fig. 1.4.

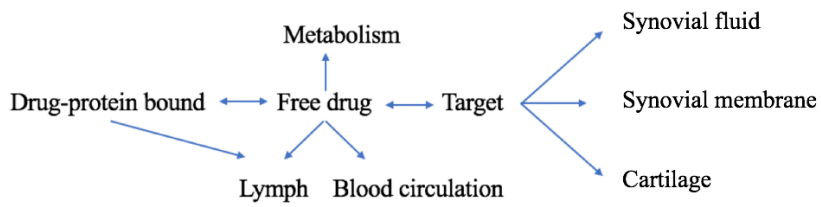

Fig. 1.4. Drug transport and distribution through synovial joint. Reproduced with kind permission from [1]

The drug molecules can, simultaneously, bind to components of the synovial fluid, spread to the synovium and articular cartilage or be uptaken by the chondrocytes and synoviocytes present in the articular cartilage and synovium respectively [1].

In summary, the pathways followed by the drug after IA delivery according to the size of the drug molecules are [3, 55]:

Less than 60 nm: The first pathway (Fig. 1.5. B) is through convective transport between the liquid articular cartilage matrix and the nanoparticulates containing the drug. This takes place during the dynamic compression of the cartilage (due to applied pressure through movement) where the nanoparticulates are integrated between the collagen fibres of the extracellular matrix or they can also be integrated within the chondrocytes of the articular cartilage [56]. Studies have shown that nanoparticles with a mean volume diameter of 31 and 38 nm were able to enter the articular cartilage ECM, whereas larger nanoparticles with a mean volume diameter of 96 nm could not. This was attributed to the 60 nm pore size of the dense collagen network [57].

Between 1-10 μm: The second pathway (Fig. 1.5. A) is through phagocytosis by type A synoviocytes (macrophages) located in the synovium. In this pathway, the drug entrapped in the formulation can either be released within the targeted type A synoviocytes or transferred through the cell junction into the subsynovium. In this case, particles of size < 250 nm can escape freely from the joint cavity, whereas those with a diameter between 1-10 μm are effectively phagocytosed by the synovial macrophages [55, 58-60].

Between 35-105 μm: The third pathway (Fig. 1.5. C) involves the synovial fluid at which the formulation (microparticulates) either adhere to the articular cartilage and synovium or becomes entrapped inside the synovial folds. The drug is then dissolved into the synovial fluid and transfers via passive diffusion to the tissues, lymphatic system and capillaries of the joint, being cleared into the systemic circulation due to the transynovial flow [61-63]. The appropriate size of microspheres without causing harmful effects has been tested in rats and was 35-105 μm [64].

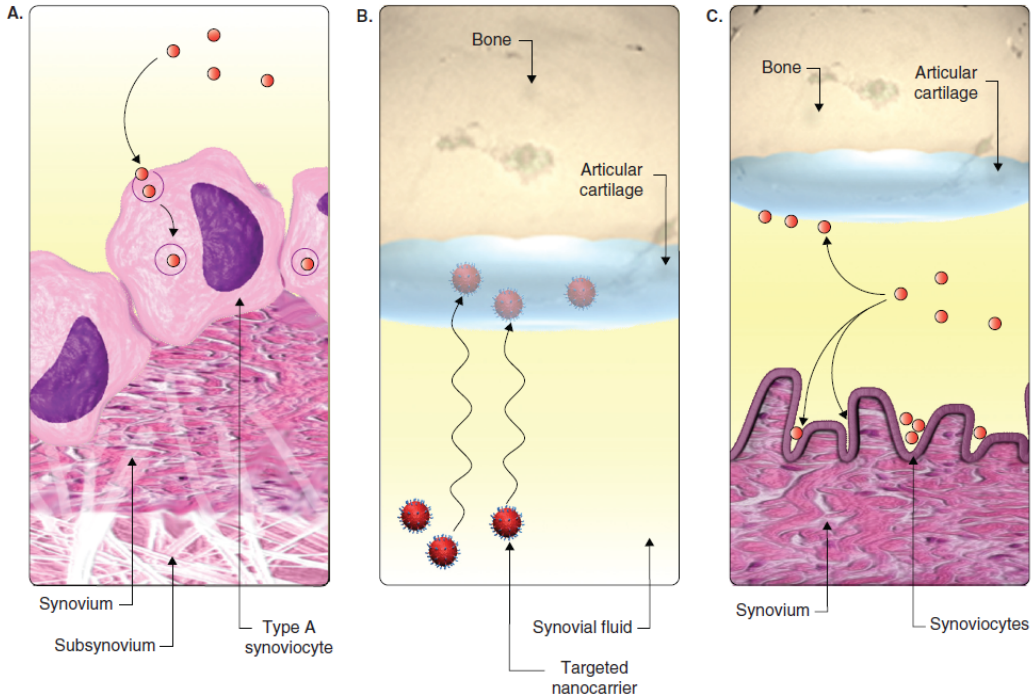

Fig. 1.5. Pathways followed by drug molecules after IA injection: A. Phagocytosis by Type A synoviocytes. B. Convective transport of drug nanoparticulates into the cartilage matrix. C. Microparticulates in synovial fluid adhering to the articular cartilage and synovium Reproduced with kind permission from [2].

1.5. Advantages and disadvantages of Intra-Articular drug administration

The IA drug delivery has a vast number of advantages and disadvantages which define its effectiveness and safety. This type of delivery is localised, performed directly into the site of action (joint) and so systemic exposure is minimised which means that side effects of the drug distributed are also reduced [3, 4]. Due to the direct delivery, the amount of drug needed to achieve high concentrations in the joint is quite low which means lower toxicity and fewer side effects. Furthermore, due to the high concentration of the drug localised in the joint, there is a high efficacy, so drugs developed for IA delivery may have a low bioavailability [4].

Despite these advantages, there are still drawbacks associated with IA delivery. The most common ones are pain caused by administration and the discomfort caused by needle placement, reducing patient compliance. The cost and time needed to perform IA injections also provide a negative aspect [4, 65] as they might be quite challenging and a specialist may be needed to perform the injection correctly [66]. Another issue is the possible risk of infection and induction of septic arthritis [67], as during administration bacteria may contaminate the

joint space leading to the number of IA injections per year reduced to the minimum possible (every 3-4 months) [68, 69]. One of the most significant challenges met in IA delivery is the residence time of the drug, which can be quite short and the efflux is rapid, due to the quick uptake of the drugs through blood circulation [4, 70]. The clearance is rapid as the direct equilibrium between the synovial fluid and the blood circulation is regenerated very fast, even though, it is falsely considered that the synovial fluid is "entrapped" by the synovium. This is due to a discontinuous layer of synoviocytes on the synovial surface, with no presence of a basement membrane and with intercellular gaps of 0.1-5.5 μm, allowing a more direct continuity between the synovial cavity and the intercellular spaces of the synovium. The synovial joint is in direct equilibrium with the rest of the circulation, so absorption and re-distribution is about the same between IA delivery and other non-intravenous parenteral routes [69, 71].

1.6. Current available IA drugs/formulations and future research

A vast amount of studies have been done to develop IA formulations with a continuous controlled release and sufficient drug retention in the joint cavity for a prolonged period of time. The "ideal" formulation should have [2]:

- Particle size according to the tissue targeted in the joint
- Particles with good drug loading capacity
- Biocompatible drug carrier which when degraded will not be toxic
- Sterility

The available drugs for IA administration are specific corticosteroids, HA and topical anaesthetic drugs given in combination with corticosteroids [72] (Table 1.6.). Corticosteroids provide anti-inflammatory, immunosuppressive action that can increase mobility and reduce joint deformity [73], while HA is an effective lubricant providing anti-inflammatory activity and also relieves pain [74]. The local anaesthetic provides an additional temporary analgesic effect and is administered in combination with the corticosteroid. The formulation containing the anaesthetic is Depo-Medrol® with lidocaine (Pfizer), containing methylprednisolone acetate (40 mg/mL) and lidocaine hydrochloride (10 mg/mL).

For the IA drug delivery to be more efficient, several delivery systems such as micro/nanoparticles, liposomes and hydrogels are in pharmaceutical development to offer a

prolonged release of the drug over a period of time (weeks/months), which may also reduce the number of injections. The formulations available in the market for IA, are solutions, suspensions, hydrogels, and a liposome formulation (Lipotalon®) licensed only in Germany. The active ingredient of Lipotalon® (Merckle Recordati) is dexamethasone 21-palmitate, encapsulated in lecithin coated vesicles with a particle size of ~200 nm [75]. In some occasions, the formulations are available in dry powder form re-suspended with sterile water, mostly due to stability issues [4]. Comparing the residence time in the joint of poorly soluble glucocorticoids administered in suspension or solution, suspensions tend to stay longer in the joint, as molecules already dissolved are easily cleared from the synovial cavity in comparison to suspended particles which dissolve in the joint before exiting via lymphatic clearance [76, 77]. Other studies show that when a steroid is used via IA delivery in its crystalline form compared to a non-salt form, the drug retention is increased, as the drug is complexed with the salt and so isolated from the synovial fluid which leads to a slower clearance from the synovial cavity. This might not reduce the side effects of corticosteroid injections but it may provide increased anti-inflammatory potential [78-81].

1.6.1. Liposomes

Promising formulations under development, for increased drug retention in the joint include liposomes, with drug activity potentially extending and due to encapsulation, the formulation may become more biocompatible [35]. The potential use of liposomes for increasing drug retention time was first studied in the late 70's, showing promising results with an increase in cortisol palmitate efficacy compared to free cortisol [82]. A liposomal formulation of triamcinolone also showed that encapsulated triamcinolone had better efficacy than free triamcinolone due to the extended residence time of the drug delivery system after the IA injection in rabbits, while similar results were shown with clodronate compared to the free drug [83, 84]. Other studies involving radio-labelled methotrexate showed that the liposomes used, accumulate in the synovial membrane, where they slowly dissolve releasing the drug [85, 86]. Another study showed that liposomes can reduce inflammatory reactions that can be experienced with crystalline suspension formulations of glucocorticoids, highlighting the biocompatibility of this formulation [87]. Drawbacks of liposomes include the osmolarity and surface charge inside the formulation interfering with stability, reducing the effectiveness of the drug and its delivery [84].

1.6.2. Nano and Microparticles

Nano- and micro-particles have been developed mostly targeting the articular cartilage (Fig. 1.5. B). The efficacy of microparticles is shown with studies such as the reported prolonged half-life of triamcinolone and prednisolone when encapsulated with albumin microspheres (23 μm) and also in studies with albumin microspheres loaded with diclofenac sodium, which provided an extended release of drug in the joint [88]. The most suitable size of microparticles used for IA delivery is proven to be 1-10 μm as they become captured by the synovial macrophages (similar action as phagocytosis) increasing their residence time in the joint [55]. Encapsulating iodide into albumin microspheres of a size lower than 6 μm, leads to a slower drug clearance in rabbit joints due to the uptake by synovial macrophages [89-92]. Smaller particles have been shown to be phagocytosed more easily. Comparing PLGA nanospheres (265 nm) and microparticles (26 μm) encapsulating betamethasone sodium phosphate, showed that the nanoparticles have a more potent action (increased drug concentration in damaged cells, drug stayed longer in the joint and side effects were reduced) [59]. With even smaller nanoparticles, a study in which collagen II binding peptides were used for coating, showed that nanoparticles lower than 60 nm would enter the cartilage matrix through convective transport and use it as a reservoir, but larger nanoparticles due to the dense collagen II network would not be able to access the matrix. (Fig. 1.5. B). [56, 90]. Extended retention in the joint has also been shown with encapsulation material such as gelatin microspheres which contained flubiprofen, showing that the drug may stay for more than 24-h in the joint compared to injected flubiprofen with a retention time of 8-h [93]; chitosan microspheres containing celecoxib, where the drug release and the entrapment efficiency was shown to be dependent on the concentration of chitosan and other factors such as SPAN-85 and glutarldehyde which were part of the microspheres [94]; calcium alginate encapsulating TGF-β growth factor, that was released in a slow and steady rate (~0.3% per hour) in the target area improving the repair rate of the articular cartilage [95]; poly (l-lactic acid) microspheres encapsulating methotrexate compared to methotrexate solution (both through IA injection), showing a higher concentration in the synovial tissues and a higher retention time [96] and PLGA [poly(lactic-co-glycolic acid)], which were compared with Bovine Serum Albumin (BSA) loaded microspheres (both with Naproxen Sodium) showing that PLGA was more promising for a longer retention time in the joint [97, 98]. One of the problems with nanoparticles and microparticles is the burst release effect, during which the drug release is not in a slowly controlled manner. This leads to a higher concentration present in the joint after the burst release, creating problems such as

increased side effects for drugs administered frequently. In addition, developing macromolecules, peptides, proteins and generally soluble materials for drug encapsulation (e.g. by using a mixture of gelatine and chondroitine sulphate) is far more complex compared to the manufacturing of PLGA coated particles that require usage of organic solvents and increase in temperature [99] leading to albumin or PLGA being the most commonly used, also due to their biocompatibility and biodegradability.

1.6.3. Hydrogels

Hydrogels are insoluble colloidal dispersions that can swell in water mainly due to their macromolecular chains. Swelling seems to minimize non-wanted particles entering the joint through the injection and it can also provide a higher biocompatibility to the formulation [97]. Hydrogels mainly contain hydrophilic chains of homopolymers or copolymers which are connected via cross-linking [100]. Because of their semi-solid structure, hydrophilic environment and ability to increase retention time of the encapsulated drug, they show significant potential in IA drug delivery [101-103]. The hydrogel formulation may be available for corticosteroids and also for encapsulating HA [4]. An important type of hydrogel studied, is the stimuli-responsive polymers [poly(ethylene oxide) based photo-polymerising hydrogel and sodium alginate gels] which are made after phase transition under external factors (e.g. temperature and light) and were used to deliver growth factors TGF-b1 and IGF-I [103-106]. The examination of synthetic acrylic hydrogel microspheres for IA delivery was also performed to show whether it would provide improved residence time in the joint and reduced side effects with results being positive as the hydrogels were present in the synovial membrane and fluid degrading in a slow manner, increasing the retention time with less side effects [97]. Hydrogels also have certain drawbacks influencing their effectiveness, such as the potential cytotoxicity of the chemically cross-linked hydrogel which may cause problems in the *in-vivo* applications [107, 108].

Table 1.6. Marketed IA drugs and formulations

Compound		**Chemical structure**	**Brand Name**	**Type of formulation**	**Excipients**	**Company**
Triamcinolone	Acetonide	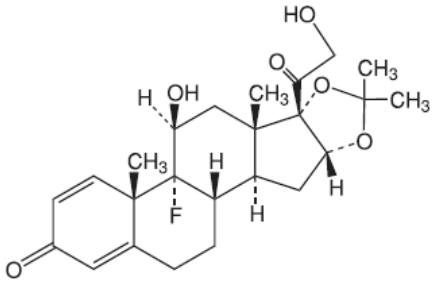	Kenalog-10® Kenalog-40®	Suspension 10 mg/mL 40 mg/mL	Sodium chloride Benzyl alcohol Carboxymethylcellulose sodium Polysorbate 80 Sodium hydroxide/ hydrochloric acid	Bristol-Myers Squibb
			Trivaris®	Suspension 80 mg/mL	Sodium hyaluronate Sodium chloride Dibasic sodium phosphate, heptahydrate Mobobasic sodium phosphate, monohydrate	Allergan Inc.

	Diacetate	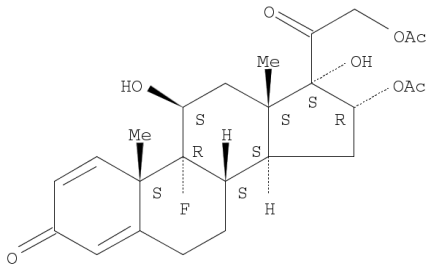	Aristocort Forte®	<u>suspension</u> 40 mg/mL	Polysorbate 80 Polyethylene Glycol Sodium Chloride Benzyl Alcohol	Sandoz Inc
	Hexacetonide	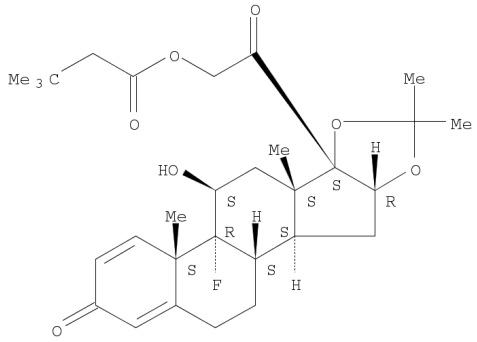	Aristospan®	<u>suspension</u> 20 mg/mL	Polysorbate 80 Sorbitol Solution USP Hydrochloric Acid/ Sodium Hydroxide Benzyl Alcohol	Sandoz Inc.
Betamethasone acetate and Betamethasone sodium phosphate		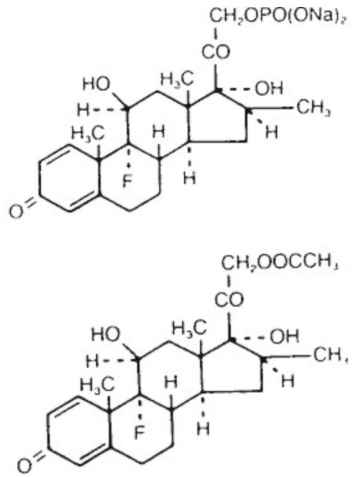	Celestone Soluspan®	<u>suspension</u> 6 mg/mL (3 mg/mL-3 mg/mL)	Dibasic sodium phosphate Monobasic sodium phosphate Edetate disodium Benzalkonium chloride	Schering-Plough

Methylprednisolone acetate	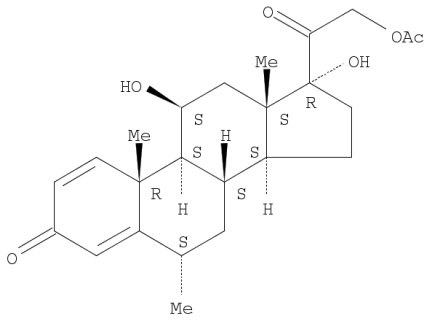	Depo-Medrol®	<u>suspension</u> 20/40/80 mg/mL	Methylprednisolone acetate Polyethylene glycol 3350 Polysorbate 80 Monobasic sodium phosphate Dibasic sodium phosphate USP Sodium Chloride Sodium hydroxide/ hydrochloric acid	Pfizer
Prednisolone acetate	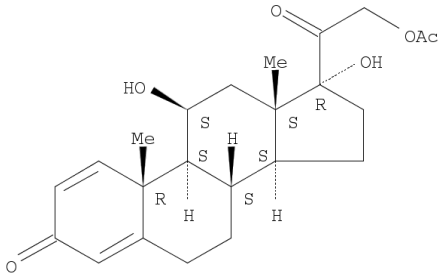	Deltastab®	<u>suspension</u> 25 mg/mL	Sodium chloride Benzyl alcohol Sodium carboxymethylcellulose (Blanose 7M8SF) Polysorbate 80	Sovereign Medical

				Sodium hydroxide/hydrochloric acid	
Dexamethasone sodium phosphate	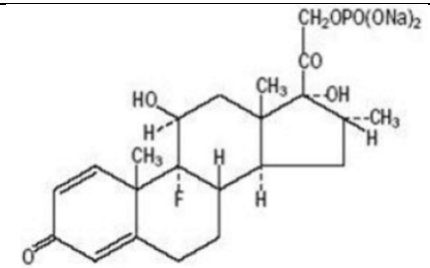	Hexadrol®	<u>Solution</u> 4/10 mg/mL	sodium sulphite Benzyl alcohol Sodium citrate	MSD
Hydrocortisone acetate	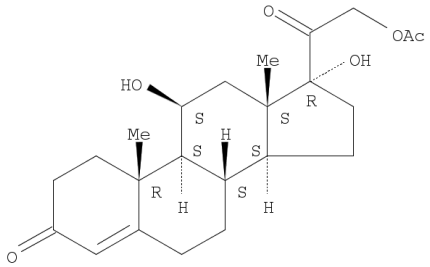	Hydrocortistab®	<u>Suspension</u> 25 mg/mL	Benzyl alcohol Sodium chloride Sodium carboxymethylcellulose (Blanose 7M8SF) Polysorbate 80 Sodium hydroxide/hydrochloric acid	Sovereign Medical

Compound	**Chemical structure**	**Brand Name**	**Type of formulation** Solution	**Excipients**	**Company**
Hyaluronic acid (Sodium hyaluronate)	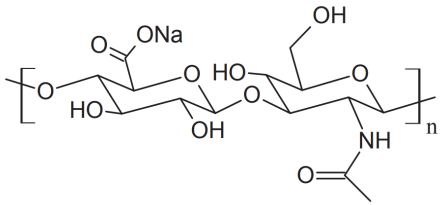	Hyalgan® Suparz® Euflexxa® Ostenil®	10 mg/mL	Sodium chloride Monobasic sodium phosphate Dibasic sodium phosphate Sodium chloride	Fidia Pharm Bioventus Ferring Pharmaceuticals TRB Chemedica
		Orthovisc®	15 mg/mL		DePuy Mitek (Johnson & Johnson)

		RenehaVis®	LMW Sodium hyaluronate 15.4mg/0.7mL HMW Sodium hyaluronate 7.0mg/0.7mL	<u>Chamber 1</u>: Sodium hyaluronate Low Molecular Weight (LMW) 0.7mL sterile <u>Chamber 2</u>: Sodium hyaluronate High Molecular Weight (HMW) 0.7ml sterile	MDT Int'l s.a.
		Suplasyn®	10 mg/mL		Bioniche Pharma
		Synocrom®			Croma-Pharma GmbH
Hylan G-F 20 (Derivative of Sodium hyalyronate)		Synvisc-One®	8 mg/mL	Sodium chloride Monobasic sodium phosphate	Genzyme

				Dibasic sodium phosphate	

1.7. *In-vitro* dissolution testing for intra-articular formulations

1.7.1. Compendial dissolution

In the pharmaceutical industry, *in-vitro* drug dissolution testing is an important tool for evaluating and demonstrating product performance and product control. More specifically:

- Quality control for assuring consistent batch to batch release and conformance to product specifications as a discriminating tool
- Indirect measurement of drug availability, release, stability and effectiveness in formulation and drug development
- Biopharmaceutical characterisation of product (chemical elucidation, physical characterisation, pre-formulation data)
- Substantiation of label claim of product (showing product efficacy)
- Assess critical manufacturing and formulation variables that might influence bioavailability
- Compedial testing
- Biorelevant testing with *in-vitro in-vivo* correlation (IVIVC) (reducing the regulatory burden of bioequivalence testing)
  [1, 31, 109-111]

As parenteral formulations include solutions, suspensions, emulsions, sterile powders for solutions and suspensions, developing a single compendial dissolution method to determine quality control and product performance for such various types of parenteral drug products becomes challenging [112]. Compendial dissolution tests will offer the possibility to optimise the therapeutic effectiveness of the product during development, with limited ability to assess biopharmaceutical properties and predict results of *in-vivo* bioavailability and behaviour [111]. Until today, there is a lack of regulatory standards available for testing *in-vitro* drug dissolution from parenteral formulations, including IA formulations[1, 31, 112, 113]. The methods currently studied and used for this type of products are divided into three categories which are briefly described below (in detail, Chapter 2 Introduction):

- Sample and separate method
- Continuous flow through method
- Dialysis membrane technique
  [31, 110, 114].

1.7.1.1. Sample and separate method

The sample and separate method (Fig. 1.6.) involves the drug being placed in a flask (or vial) containing the dissolution medium, usually positioned in a water bath. Drug release from the formulation is measured in specific time intervals. After sampling, centrifugation and filtration of the supernatant takes place to remove any undissolved drug [115].

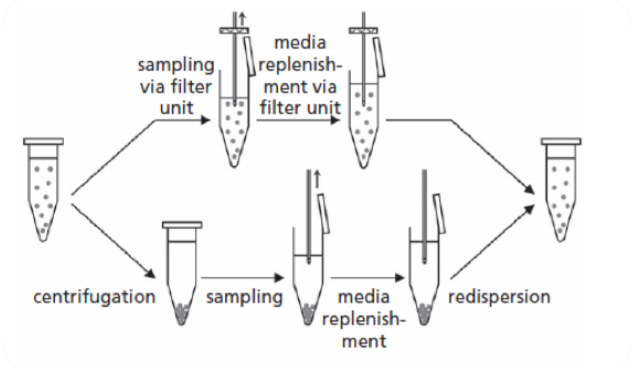

Fig. 1.6. Sample and separate methodology. Reproduced with kind permission from [116]

1.7.1.2. Continuous flow through (USP apparatus IV) method

The continuous flow through method with the USP apparatus IV, consists of the medium flown through a pump and into the flow through cell (Fig. 1.7.), causing elution, while containing mainly glass beads and the drug formulation. A filter is placed in the top ("filter head") of the cell, above the existing sieve, in order to avoid removal of undissolved drug from the cell, with the dissolved drug eluate filtered through and collected for analysis [117, 118].

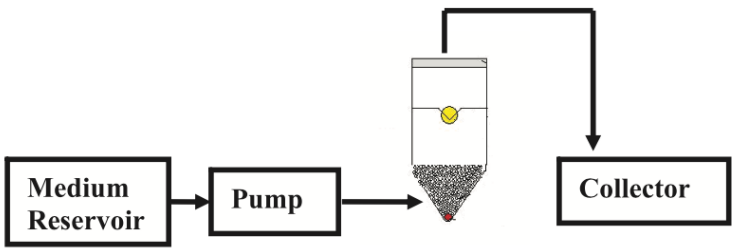

Fig. 1.7. Open system setup with USP apparatus IV. Reproduced with kind permission from [118]

The amount of glass beads and type of filter with adequate loading capacity should be carefully chosen as obstructions in the flow through cell may cause back-pressure against the desired flow [31, 119].

1.7.1.3. Dialysis membrane technique

A basic setup of the dialysis bag technique consists of the drug formulation being placed into the bag which is then placed in a vessel containing buffer (Fig. 1.8.). The drug dissolves inside the bag and diffuses from the dialysis bag into the receptor phase [115]. Agitation in the vessels eliminates the unstirred water layer, leading to a homogeneous sample with a faster diffusion rate through the membrane and into the receptor phase. The commonly used types of membrane include regenerated cellulose [113, 115], microporous cellulose [120] or cellulose acetate [121]. For sink conditions to be present, the volume of the media should be at least three times higher than the volume in which the drug would saturate according to the USP guidelines [116]. A more advanced model of dialysis used for IA dissolution testing, is shown through a three-compartment oil/water model in Fig. 1.9. [122, 123]. The oil drug solution ($[X]_o$) is placed in the aqueous donor compartment ($[X]_{Dw}$) and the dialysis membrane separates it from the aqueous acceptor compartment ($[X]_A$). The drug, after dissolving, diffuses through the dialysis membrane due to the concentration gradient between the two compartments as drug molecules transfer from areas of higher to lower concentration [124]. This continues until an equilibrium of drug molecules will be present between both phases.

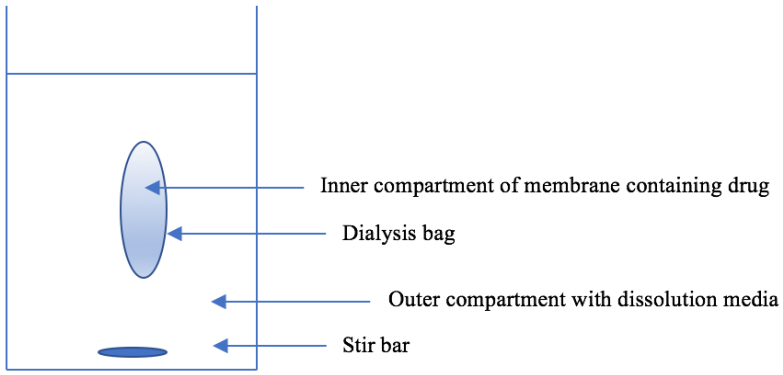

Fig. 1.8. A simple dialysis model

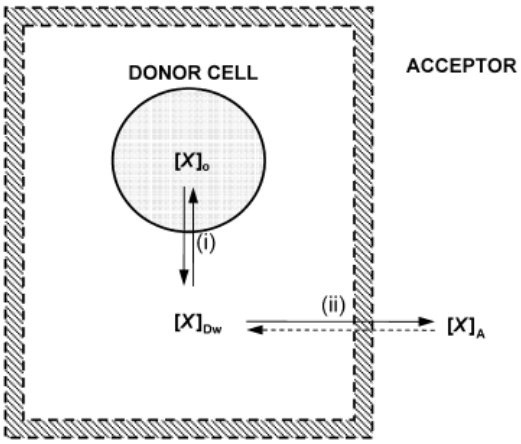

Fig. 1.9. Three compartment model (due to oil-water separation). $[X]_o$ is the oil drug solution, $[X]_{Dw}$ is the aqueous donor compartment and $[X]_A$ is the aqueous acceptor compartment. Reproduced with kind permission from [122]

1.7.2. Biorelevant dissolution

In summary (Chapter 4 Introduction, in detail), it is vital to design biorelevant dissolution tests for parenteral drugs, performed under simulated *in-vivo* conditions, mimicking in detail how the drug dissolves in the body. Biorelevant dissolution tests may reduce the amount of bioequivalence studies performed in various stages of the drug/formulation approval process, improve product quality and reduce relevant regulatory procedures [125]. The choice of apparatus is also important in order to resemble with more precision *in-vivo* conditions, with specifically designed setups or modifications of already established apparatus. Importance is also given to establishing suitable instrument parameters and appropriate biorelevant media (Chapter 3 Introduction, in detail).

At the moment, validated biorelevant dissolution methods for parenteral formulations, including IA, do not exist. For IA formulations, biorelevant dissolution would be performed under simulated *in-vivo* conditions for predicting the dissolution of drugs administered into the joint and subsequently the synovial fluid, for providing a more accurate prediction of *in-vivo* behaviour. Artificial synovial fluids have been previously developed, mostly for tribological and rheological testing purposes [12, 45, 126, 127] and so may not contain all appropriate components that would affect the dissolution of the drug inside the synovial cavity with a result of not effectively predicting *in-vivo* performance.

1.8. Thesis aims and objectives

This project aims at developing compendial and biorelevant *in-vitro* dissolution studies for IA formulations. The main target is to evaluate the applicability of setups such as USP apparatus and UV imaging on the dissolution of IA drug formulations. A vital part is to evaluate the parameters of the tested systems such as hydrodynamics and formulation variables that would affect drug dissolution of IA formulations, to design a refined compendial method, used for characterising the drug product and ensuring reproducible product quality. Our approach was to test methods currently studied such as USP apparatus I, II, III, IV, the dialysis membrane and the bi-phasic system, with the discriminatory ability of the most suitable system being evaluated (Chapter 2). An important aspect we aimed for was to develop biorelevant synovial fluid in different states, to simulate the conditions found in the joint, according to *in-vivo* measurements of physicochemical properties and solubility measurements of Triamcinolone Acetonide (TA). By developing biorelevant synovial fluid media in three states (healthy state, OA and RA) reflecting changes in composition during the disease states and by choosing components according to the significance of their effect in the dissolution of the drug in the media, would lead to prediction of *in-vivo* performance (Chapter 3) through appropriate biorelevant tests (Chapter 4). The amounts of components added, were chosen according to the average amounts found in literature, while measurements of physicochemical properties of *in-vivo* disease state synovial fluid (OA and RA) would guide the development of the biorelevant synovial fluid (BSF). Developing biorelevant dissolution tests for IA formulations involved the evaluation of the side-Bi-side diffusion cell in different setups mimicking the conditions of the joint and also a bi-phasic dissolution setup in which the organic phase is used as the reservoir of the dissolved drug transferred from the aqueous phase, simulating the diffusion of the dissolved drug from the synovial joint into the blood circulation. Variables of these setups are evaluated towards their effect in drug dissolution, while the developed biorelevant synovial fluids are applied to simulate *in-vivo* behavior and improve the biorelevance of the tested system (Chapter 4). Finally, to fully investigate the drug dissolution process and to have a better understanding of the events taking place near the surface of the IA drug under test, the use of UV imaging as a dissolution test for IA formulation is described, with parameters of the sample preparation process optimised. The application of the UV imaging system for artificial synovial fluids in healthy and disease state is also described, evaluating the effect of the viscosity of the synovial fluid (Chapter 5).

1.9. References

1. Larsen, C., Ostergaard, J., Larsen, S.W., Jensen, H., Jacobsen, S., Lindergaard, C., Andersen, P.H., *Intra-articular depot formulation principles: role in the management of postoperative pain and arthritic disorders.* J Pharm Sci, 2008. **97**(11): p. 4622-54.
2. Burt, H.M., Tsallas, A., Gilchrist, S., Liang L.S., *Intra-articular drug delivery systems: Overcoming the shortcomings of joint disease therapy.* Expert Opin Drug Deliv, 2009. **6**(1): p. 17-26.
3. Edwards, S.H., *Intra-articular drug delivery: the challenge to extend drug residence time within the joint.* Vet J, 2011. **190**(1): p. 15-21.
4. Gerwin, N., C. Hops, and A. Lucke, *Intraarticular drug delivery in osteoarthritis.* Adv Drug Deliv Rev, 2006. **58**(2): p. 226-42.
5. Balazs, E.A., Watson, D., Duff IF., Roseman, S., *Hyaluronic acid in synovial fluid. I. Molecular parameters of hyaluronic acid in normal and arthritis human fluids.* Arthritis Rheum, 1967. **10**(4): p. 357-76.
6. Koopman, W.J., and Moreland, L.W., *Arthritis and allied conditions : a textbook of rheumatology*. 2005.
7. Ropes, M.W., E.C. Rossmeisl, and W. Bauer, *The origin and nature of human synovial fluid.* J Clin Invest, 1940. **19**(6): p. 795-9.
8. Bole, G.G., *Synovial fluid lipids in normal individuals and patients with rheumatoid arthritis.* Arthritis Rheum, 1962. **5**: p. 589-601.
9. Fam, H., J.T. Bryant, and M. Kontopoulou, *Rheological properties of synovial fluids.* Biorheology, 2007. **44**(2): p. 59-74.
10. Gomez, J.E. and G.B. Thurston, *Comparisons of the oscillatory shear viscoelasticity and composition of pathological synovial fluids.* Biorheology, 1993. **30**(5-6): p. 409-27.
11. Kitano, T., Ateshian, G.A., Mow, V.C., Kadoya, Y., Yamano, Y., *Constituents and pH changes in protein rich hyaluronan solution affect the biotribological properties of artificial articular joints.* J Biomech, 2001. **34**(8): p. 1031-7.
12. Oates, K.M.N., Krause, W.E., Jones, R.L., Colby, R.H., *Rheopexy of synovial fluid and protein aggregation.* J R Soc Interface, 2006. **3**(6): p. 167-74.
13. Majd, S.E., Kuijer, R., Kowitsch, A., Groth, T., Schmidt, T.A., Sharma, P.K., *Both Hyaluronan and Collagen Type II Keep Proteoglycan 4 (Lubricin) at the Cartilage Surface in a Condition That Provides Low Friction during Boundary Lubrication.* Langmuir, 2014. **30**(48): p. 14566-72.
14. Scott, D., Coleman, P.J., Mason, R.M., Levick J.R., *Interaction of intraarticular hyaluronan and albumin in the attenuation of fluid drainage from joints.* Arthritis Rheum, 2000. **43**(5): p. 1175-82.
15. Wang, A., A. Essner, and G. Schmidig, *The effects of lubricant composition on in-vitro wear testing of polymeric acetabular components.* J Biomed Mater Res B Appl Biomater, 2004. **68**(1): p. 45-52.
16. Wilkinson, M. and B.S. Jones, *Serum and Synovial Fluid Proteins in Arthritis.* Ann Rheum Dis, 1962. **21**(1): p. 51-8.
17. Winchester, R.J., V. Agnello, and H.G. Kunkel, *Gamma globulin complexes in synovial fluids of patients with rheumatoid arthritis. Partial characterisation and relationship to lowered complement levels.* Clin Exp Immunol, 1970. **6**(5): p. 689-706.
18. Schmidt, T.A., Gastelum, N.S., Nguyen, Q.T., Schumacher, B.L., Sah, R.L., *Boundary lubrication of articular cartilage: role of synovial fluid constituents.* Arthritis Rheum, 2007. **56**(3): p. 882-91.

19. Gigante, A. and L. Callegari, *The role of intra-articular hyaluronan (Sinovial) in the treatment of osteoarthritis.* Rheumatol Int, 2011. **31**(4): p. 427-44.
20. Decker, B., McGuckin, W.F., McKenzie, B.F., Slocumb, C.H., *Concentration of hyaluronic acid in synovial fluid.* Clin Chem, 1959. **5**: p. 465-9.
21. Levick, J.R., Price, F.M., and Mason, R.M., *Synovial matrix-synovial fluid system of joints*, in *Extracellular Matrix, Tissue Function*, W.D. Comper, Editor. 1996, Harwood Academic Publishers: Amsterdam. p. 348–354.
22. Bollet, A.J., *The intrinsic viscosity of synovial fluid hyaluronic acid.* The Journal of Laboratory and Clinical Medicine. **48**(5): p. 721-728.
23. Blewis, M.E., Nugent-Derfus, G.E., Schmidt, T.A., Schumacher, B.L., Sah, R.L., *A model of synovial fluid lubricant composition in normal and injured joints.* Eur Cell Mater, 2007. **13**: p. 26-39.
24. Dahl, L.B., Dahl, I.M., Engstrom-Laurent, A., Granath, K., *Concentration and molecular weight of sodium hyaluronate in synovial fluid from patients with rheumatoid arthritis and other arthropathies.* Ann Rheum Dis, 1985. **44**(12): p. 817-22.
25. Swann, D.A., Radin, E.L., Nazimiec, M., Weisser, P.A., Curran, N., Lewinnek, G., *Role of hyaluronic acid in joint lubrication.* Annals of the Rheumatic Diseases, 1974. **33**(4): p. 318-326.
26. Yazar, M., Sarban, S., Kocyigit, A., Isikan, U.E., *Synovial fluid and plasma selenium, copper, zinc, and iron concentrations in patients with rheumatoid arthritis and osteoarthritis.* Biological Trace Element Research, 2005. **106**(2): p. 123-132.
27. Prete, P.E., A. Gurakar-Osborne, and M.L. Kashyap, *Synovial fluid lipoproteins: review of current concepts and new directions.* Semin Arthritis Rheum, 1993. **23**(2): p. 79-89.
28. Kosinska, M.K., Liebisch, G., Lochnit, G., Wilhelm, J., Klein, H., Kaesser, U., Lasczkowski, G., Rickert, M., Schmitz, G., Steinmeyer, J., *A lipidomic study of phospholipid classes and species in human synovial fluid.* Arthritis Rheum, 2013. **65**(9): p. 2323-33.
29. Knox, P., J.R. Levick, and J.N. McDonald, *Synovial fluid--its mass, macromolecular content and pressure in major limb joints of the rabbit.* Q J Exp Physiol, 1988. **73**(1): p. 33-45.
30. Levick, J.R. and J.N. McDonald, *Synovial capillary distribution in relation to altered pressure and permeability in knees of anaesthetized rabbits.* J Physiol, 1989. **419**: p. 477-92.
31. Brown, C.K., Friedel, H.D., Barker, A.R., Buhse, L.F., Keitel, S., Cecil, T.L., Kraemer, J., Morris, J.M., Reppas, C., Stickelmeyer, M.P., Yomota, C., Shah, V.P., *FIP/AAPS joint workshop report: dissolution/in-vitro release testing of novel/special dosage forms.* AAPS PharmSciTech, 2011. **12**(2): p. 782-94.
32. Bartok, B. and G.S. Firestein, *Fibroblast-like synoviocytes: key effector cells in rheumatoid arthritis.* Immunol Rev, 2010. **233**(1): p. 233-55.
33. Evans, C.H., V.B. Kraus, and L.A. Setton, *Progress in intra-articular therapy.* Nat. Rev. Rheumatol., 2013. **-**(-): p. -.
34. NICE, *Rheumatoid arthritis in adults: Management, Clinical Guideline [CG79]*, N. Guidance, Editor. 2009.
35. Butoescu, N., O. Jordan, and E. Doelker, *Intra-articular drug delivery systems for the treatment of rheumatic diseases: a review of the factors influencing their performance.* Eur J Pharm Biopharm, 2009. **73**(2): p. 205-18.
36. Jebens, E.H. and M.E. Monk-Jones, *On the viscosity and pH of synovial fluid and the pH of blood.* J Bone Joint Surg Br, 1959. **41-B**(2): p. 388-400.

37. Kitano, T., Ohasi, H., Kadoya, Y., Kobayashi, A., Yutani, Y., Yamano, Y., *Measurements of zeta potentials of particulate biomaterials in protein-rich hyaluronan solution with changes in pH and protein constituents.* J Biomed Mater Res, 1998. **42**(3): p. 453-7.
38. Cummings, N.A. and G.L. Nordby, *Measurement of synovial fluid pH in normal and arthritic knees.* Arthritis Rheum, 1966. **9**(1): p. 47-56.
39. Goldie, I. and A. Nachemson, *Synovial pH in rheumatoid knee-joints. I. The effect of synovectomy.* Acta Orthop Scand, 1969. **40**(5): p. 634-41.
40. Shanfield, S., Campbell, P., Baumgarten, M., Bloebaum, R., Sarmiento, A., *Synovial fluid osmolality in osteoarthritis and rheumatoid arthritis.* Clin Orthop Relat Res, 1988(235): p. 289-95.
41. Baumgarten, M., Bloebaum, R.D., Ross, S.D., Campbell, P., Sarmiento, A., *Normal human synovial fluid: osmolality and exercise-induced changes.* J Bone Joint Surg Am, 1985. **67**(9): p. 1336-9.
42. Bertram, K.L. and R.J. Krawetz, *Osmolarity regulates chondrogenic differentiation potential of synovial fluid derived mesenchymal progenitor cells.* Biochem Biophys Res Commun, 2012. **422**(3): p. 455-61.
43. Jeleniewicz, R., Majdan, M., Zwolak, R., Dryglewska, M., *Synovial fluid surface tension in inflammatory joint diseases.* Reumatologia, 2005. **43**(6): p. 331–334.
44. Hills, B.A. and B.D. Butler, *Surfactants identified in synovial fluid and their ability to act as boundary lubricants.* Ann Rheum Dis, 1984. **43**(4): p. 641-8.
45. Bingol, A.O., Lohmann, D., Puschel, K., Kulicke, W.M., *Characterisation and comparison of shear and extensional flow of sodium hyaluronate and human synovial fluid.* Biorheology, 2010. **47**(3-4): p. 205-24.
46. Fuchs, A., *Evaluation of the Influence of Different Bile Salts and Phospholipids on the Surface Tension of Conventional Biorelevant Media.* AAPS - Annual Meeting and Exposition, San Antonio, USA., 2013.
47. Bhuanantanondh, P., D. Grecov, and E. Kwok, *Rheological Study of Viscosupplements and Synovial Fluid in Patients with Osteoarthritis.* Journal of Medical and Biological Engineering, 2012. **21**(1): p. 12-16.
48. Cooke, A.F., D. Dowson, and V. Wright, *The Rheology of Synovial Fluid and Some Potential Synthetic Lubricants for Degenerate Synovial Joints.* Engineering in Medicine, 1978. **7**(2): p. 66-72.
49. Barnett, C.H., *Measurement and interpretation of synovial fluid viscosities.* Ann Rheum Dis, 1958. **17**(2): p. 229-33.
50. Bloch, B. and L. Dintenfass, *RHEOLOGICAL STUDY OF HUMAN SYNOVIAL FLUID.* Aust N Z J Surg, 1963. **33**: p. 108-13.
51. Rainer, F. and V. Ribitsch, *[Viscoelastic properties of normal human synovia and their relation to biomechanics].* Z Rheumatol, 1985. **44**(3): p. 114-9.
52. Schurz, J., *Rheology of Synovial Fluids and Substitute Polymers.* Journal of Macromolecular Science, Part A: Pure and Applied Chemistry, 1996. **33**(9): p. 1249-126.
53. Schurz, J. and V. Ribitsch, *Rheology of synovial fluid.* Biorheology, 1987. **24**(4): p. 385-99.
54. Tercic, D. and B. Bozic, *The basis of the synovial fluid analysis.* Clin Chem Lab Med, 2001. **39**(12): p. 1221-6.
55. Butoescu, N., Jordan, O., Burdet, P., Stadelmann, P., Petri-Fink, A., Hofmann, H., Doelker, E., *Dexamethasone-containing biodegradable superparamagnetic microparticles for intra-articular administration: physicochemical and magnetic*

properties, in-vitro and in-vivo drug release. Eur J Pharm Biopharm, 2009. **72**(3): p. 529-38.
56. Rothenfluh, D.A., Bermudez, H., O'Neil, C.P., Hubbell, J.A., *Biofunctional polymer nanoparticles for intra-articular targeting and retention in cartilage.* Nat Mater, 2008. **7**(3): p. 248-54.
57. Kang, M.L. and Im, G.I., *Drug delivery systems for intra-articular treatment of osteoarthritis.* Expert Opin Drug Deliv, 2014. **11**(2): p. 269-82.
58. Edwards, S.H., Cake, M.A., Spoelstra, G., Read, R.A., *Biodistribution and clearance of intra-articular liposomes in a large animal model using a radiographic marker.* J Liposome Res, 2007. **17**(3-4): p. 249-61.
59. Horisawa, E., Hirota, T., Kawazoe, S., Yamada, J., Yamamoto, H., Takeuchi, H., Kawashima, Y., *Prolonged anti-inflammatory action of DL-lactide/glycolide copolymer nanospheres containing betamethasone sodium phosphate for an intra-articular delivery system in antigen-induced arthritic rabbit.* Pharm Res, 2002. **19**(4): p. 403-10.
60. Thakkar, H., Kumar Sharma, R., and Murthy, R.S., *Enhanced retention of celecoxib-loaded solid lipid nanoparticles after intra-articular administration.* Drugs R D, 2007. **8**(5): p. 275-85.
61. Chowdhury, A.K. and Islam, S., *In-vitro-in-vivo correlation as a surrogate for bioequivalence testing: the current state of play.* Asian Journal of Pharmaceutical Sciences, 2011. 6(3-4): 176-190.
62. Liang, L.S., Jackson, J., Min, W., Risovic, V., Wasan, K.M., Burt, H.M., *Methotrexate loaded poly(L-lactic acid) microspheres for intra-articular delivery of methotrexate to the joint.* J Pharm Sci, 2004. **93**(4): p. 943-56.
63. Liang, L.S., W. Wong, and H.M. Burt, *Pharmacokinetic study of methotrexate following intra-articular injection of methotrexate loaded poly(L-lactic acid) microspheres in rabbits.* J Pharm Sci, 2005. **94**(6): p. 1204-15.
64. Liggins, R.T., Cruz, T., Min, W., Liang, L., Hunter, W.L., Burt, H.M., *Intra-articular treatment of arthritis with microsphere formulations of paclitaxel: biocompatibility and efficacy determinations in rabbits.* Inflamm Res, 2004. **53**(8): p. 363-72.
65. Waddell, D.D., *The tolerability of viscosupplementation: low incidence and clinical management of local adverse events.* Curr Med Res Opin, 2003. **19**(7): p. 575-80.
66. Lopes, R.V., Furtado, R.D., Parmigiani, L., Rosenfeld, A., Fernandes, A.R., Natour, J., *Accuracy of intra-articular injections in peripheral joints performed blindly in patients with rheumatoid arthritis.* Rheumatology (Oxford), 2008. **47**(12): p. 1792-4.
67. Tsumura, H., S. Ikeda, and T. Torisu, *Debridement and continuous irrigation for the treatment of pyogenic arthritis caused by the use of intra-articular injection in the osteoarthritic knee: indications and outcomes.* Journal of Orthopaedic Surgery, 2005(13): p. 52–57.
68. Hunneyball, I., *Intra-articular administration of drugs.* Pharmacy International, 1986: p. 118–122.
69. Owen, S.G., H.W. Francis, and M.S. Roberts, *Disappearance kinetics of solutes from synovial fluid after intra-articular injection.* Br J Clin Pharmacol, 1994. **38**(4): p. 349-55.
70. Ayral, X., *Injections in the treatment of osteoarthritis.* Best Pract Res Clin Rheumatol, 2001. **15**(4): p. 609-26.
71. Schurman, D.J. and G. Kajiyama, *Antibiotic absorption from infected and normal joints using a rabbit knee joint model.* J Orthop Res, 1985. **3**(2): p. 185-8.
72. Lavelle, W., E.D. Lavelle, and L. Lavelle, *Intra-articular injections.* Anesthesiol Clin, 2007. **25**(4): p. 853-62, viii.

73. Pekarek, B., Osher, L., Buck, S., Bowen, M., *Intra-articular corticosteroid injections: a critical literature review with up-to-date findings.* Foot (Edinb), 2011. **21**(2): p. 66-70.
74. Mountziaris, P.M., P.R. Kramer, and A.G. Mikos, *Emerging intra-articular drug delivery systems for the temporomandibular joint.* Methods, 2009. **47**(2): p. 134-40.
75. Bias, P., R. Labrenz, and P. Rose, *Sustained-Release Dexamethasone Palmitate.* Clinical Drug Investigation, 2001. **21**(6): p. 429-436.
76. Derendorf, H., Mollmann, H., Gruner, A., Haack, D., Gyselby, G., *Pharmacokinetics and pharmacodynamics of glucocorticoid suspensions after intra-articular administration.* Clin Pharmacol Ther, 1986. **39**(3): p. 313-7.
77. Derendorf, H., Mollmann, H., Voortman, G., can den Ouweland, F.A., van de Putte, L.B., Gevers, G., Dequeker, J., van Vliet-Daskalopoulou, E., *Pharmacokinetics of rimexolone after intra-articular administration.* J Clin Pharmacol, 1990. **30**(5): p. 476-9.
78. Bellamy, N., Campbell, J., Robinson, V., Gee, T., Bourne, R., Wells, G., *Intraarticular corticosteroid for treatment of osteoarthritis of the knee.* Cochrane Database Syst Rev, 2006(2): p. CD005328.
79. Caldwell, J.R., *Intra-articular corticosteroids. Guide to selection and indications for use.* Drugs, 1996. **52**(4): p. 507-14.
80. MacMahon, P.J., S.J. Eustace, and E.C. Kavanagh, *Injectable corticosteroid and local anesthetic preparations: a review for radiologists.* Radiology, 2009. **252**(3): p. 647-61.
81. Rull, M., Clayburne, G., Sieck, M., Shumacher., H.R., *Intra-articular corticosteroid preparations: different characteristics and their effect during inflammation induced by monosodium urate crystals in the rat subcutaneous air pouch.* Rheumatology (Oxford), 2003. **42**(9): p. 1093-100.
82. Dingle, J.T., Gordon, J.L., Hazleman, B.L., Knight, C.G., Page Thomas, D.P., Phillips, N.C., Shaw, I.H., Fildes, F.J.T., Oliver, J.E., Jones, G., Turner, E.H., Lowe, J.S., *Novel treatment for joint inflammation.* Nature, 1978. **271**(5643): p. 372-373.
83. Lopez-Garcia, F., Vazquez-Auton, J.M., Gil, F., Latoore, R., Moreno, F., Villalain, J., Gomez-Fernandez, J.C., *Intra-articular therapy of experimental arthritis with a derivative of triamcinolone acetonide incorporated in liposomes.* J Pharm Pharmacol, 1993. **45**(6): p. 576-8.
84. Monkkonen, J. and Urtti, A., *Studies on liposome formulations for intra-articular delivery of clodronate.* Journal of Controlled Release, 1995(35): p. 145-154.
85. Foong, W.C. and K.L. Green, *Retention and distribution of liposome-entrapped [3H]methotrexate injected into normal or arthritic rabbit joints.* J Pharm Pharmacol, 1988. **40**(7): p. 464-8.
86. Nesic, D., Whiteside, R., Brittberg, M., Wendt, D., Martin, I., Mainil-Varlet, P., *Cartilage tissue engineering for degenerative joint disease.* Adv Drug Deliv Rev, 2006. **58**(2): p. 300-22.
87. Zhang, W., Moskowitz, R.W., Nuki, G., Abramson, S., Altman, R.D., Arden, N., Bierma-Zeinstra, S., Brandt, K.D., Croft, P., Doherty, M., Dougados, M., Hochberg, M, Hunter, D.J., Kwoh, K., Lohmander, L.S., Tugwell, P., *OARSI recommendations for the management of hip and knee osteoarthritis, Part II: OARSI evidence-based, expert consensus guidelines.* Osteoarthritis Cartilage, 2008. **16**(2): p. 137-62.
88. Tuncay, M., Calis, S., Kas, H.S>, Ercan, M.T., Peskoy, I., Hincal, A.A., *In-vitro and in-vivo evaluation of diclofenac sodium loaded albumin microspheres.* J Microencapsul, 2000. **17**(2): p. 145-55.

89. Burgess, D.J. and S.S. Davis, *Potential use of albumin microspheres as a drug delivery system: II. In-vivo deposition and release of steroids.* International Journal of Pharmaceutics, 1988. **46**(1–2): p. 69-76.
90. Holland, T.A. and A.G. Mikos, *Advances in drug delivery for articular cartilage.* J Control Release, 2003. **86**(1): p. 1-14.
91. Horisawa, E., Kubota, K., Tuboi, I., Sato, K., Yamamoto, H., Takeuchi, H., Kawashima, Y., *Size-dependency of DL-lactide/glycolide copolymer particulates for intra-articular delivery system on phagocytosis in rat synovium.* Pharm Res, 2002. **19**(2): p. 132-9.
92. Ratcliffe, J.H., Hunneyball, I.M., Wilson, C.G., Smith, A., Davis, S.S., *Albumin microspheres for intra-articular drug delivery: investigation of their retention in normal and arthritic knee joints of rabbits.* J Pharm Pharmacol, 1987. **39**(4): p. 290-5.
93. Lu, Y., Zhang, G., Sun, D., Zhong, Y., *Preparation and evaluation of biodegradable flubiprofen gelatin micro-spheres for intra-articular administration.* J Microencapsul, 2007. **24**(6): p. 515-24.
94. Thakkar, H.,Sharma, R.K., Mishra, A.K., Chuttani, K., Murthy, R.S., *Celecoxib Incorporated Chitosan Microspheres: In-vitro and In-vivo Evaluation.* Journal of Drug Targeting, 2004. **12**(9-10): p. 549-557.
95. Mierisch, C.M., Cohen, S.B., Jordan, L.C., Robertson, P.G., Balian, G., Diduch, D.R., *Transforming growth factor-beta in calcium alginate beads for the treatment of articular cartilage defects in the rabbit.* Arthroscopy, 2002. **18**(8): p. 892-900.
96. Liang, L.S., W. Wong, and H.M. Burt, *Pharmacokinetic study of methotrexate following intra-articular injection of methotrexate loaded poly(L-lactic acid) microspheres in rabbits.* Journal of Pharmaceutical Sciences, 2005. **94**(6): p. 1204-1215.
97. Bédouet, L., Pascale, F., Moine, L., Wassef., M., Ghegediban, S.H., Nguyen, V.N., Bonneau, M., Labarre, D., Laurent, A., *Intra-articular fate of degradable poly(ethyleneglycol)-hydrogel microspheres as carriers for sustained drug delivery.* International Journal of Pharmaceutics, 2013. **456**(2): p. 536-544.
98. Bozdag, S., Calis, S., Kas, H.S., Ercan, M.T., Peskoy, I., Hical, A.A., *In-vitro evaluation and intra-articular administration of biodegradable microspheres containing naproxen sodium.* Journal of Microencapsulation, 2001. **18**(4): p. 443-456.
99. Brown, K.E., Leong, K., Huang, C.H., Dalal, R., Green, G.D., Haimes, H.B., Jimenez, P.A., Bathn, J., *Gelatin/chondroitin 6-sulfate microspheres for the delivery of therapeutic proteins to the joint.* Arthritis Rheum, 1998. **41**(12): p. 2185-95.
100. Lowman, A. and N. Peppas, *Hydrogels*, in *Encyclopedia of Controlled Drug Delivery*, E. Mathiowitz, Editor. 1999, Wiley: New York. p. 397–418.
101. Barbucci, R., Lamponi, S., Borzacchiello, A., Ambrosio, L., Fini, M., Torricelli, P., Giardino, R., *Hyaluronic acid hydrogel in the treatment of osteoarthritis.* Biomaterials, 2002. **23**(23): p. 4503-13.
102. Drury, J.L. and D.J. Mooney, *Hydrogels for tissue engineering: scaffold design variables and applications.* Biomaterials, 2003. **24**(24): p. 4337-51.
103. Lin, C.C. and A.T. Metters, *Hydrogels in controlled release formulations: network design and mathematical modeling.* Adv Drug Deliv Rev, 2006. **58**(12-13): p. 1379-408.
104. Betre, H., Liu, W., Zalutsky, M.R., Chilkoti, A., Kraus, V.B., Setton, L.A., *A thermally responsive biopolymer for intra-articular drug delivery.* J Control Release, 2006. **115**(2): p. 175-82.

105. Elisseeff, J., McIntosh, W., Fu, K., Blunk, B.T., Langer, R., *Controlled-release of IGF-I and TGF-beta1 in a photopolymerizing hydrogel for cartilage tissue engineering.* J Orthop Res, 2001. **19**(6): p. 1098-104.
106. Gombotz, W.R. and S.F. Wee, *Protein release from alginate matrices.* Advanced Drug Delivery Reviews, 2012. **64, Supplement**(0): p. 194-205.
107. Peppas, N.A.,Bures, P., Leobandung, W., Ichikawa, H., *Hydrogels in pharmaceutical formulations.* Eur J Pharm Biopharm, 2000. **50**(1): p. 27-46.
108. Temenoff, J.S., Shin, H., Conway, D.E., Engel, P.S., Mikos, A.G., *In-vitro cytotoxicity of redox radical initiators for cross-linking of oligo(poly(ethylene glycol) fumarate) macromers.* Biomacromolecules, 2003. **4**(6): p. 1605-13.
109. Bhardwaj, U. and D.J. Burgess, *A novel USP apparatus 4 based release testing method for dispersed systems.* Int J Pharm, 2010. **388**(1-2): p. 287-94.
110. D'Souza, S.S. and P.P. DeLuca, *Methods to assess in-vitro drug release from injectable polymeric particulate systems.* Pharm Res, 2006. **23**(3): p. 460-74.
111. Wang, Q.X., N. Fotaki, and Y. Mao, *Biorelevant Dissolution: Methodology and Application in Drug Development.* Dissolution Technologies, 2009. **16**(3): p. 6-12.
112. Shah, V.P., J. DeMuth, and D.G. Hunt, *Performance Test for Parenteral Dosage Forms.* Dissolution Technologies, 2015. **22**(4): p. 16-21.
113. Sterner, B., Harms, M., Weigandt, M., Windbergs, M., Lehr, C.M., *Crystal suspensions of poorly soluble peptides for intra-articular application: A novel approach for biorelevant assessment of their in-vitro release.* Int J Pharm, 2013.
114. Larsen, S.W., Frost, A.B., Ostergaard, J., Marcher, H., Larsen, C., *On the mechanism of drug release from oil suspensions in-vitro using local anesthetics as model drug compounds.* Eur J Pharm Sci, 2008. **34**(1): p. 37-44.
115. D'Souza, S.S. and P.P. DeLuca, *Development of a dialysis in-vitro release method for biodegradable microspheres.* AAPS PharmSciTech, 2005. **6**(2): p. E323-8.
116. Seidlitz, A. and W. Weitschies, *In-vitro dissolution methods for controlled release parenterals and their applicability to drug-eluting stent testing.* J Pharm Pharmacol, 2012. **64**(7): p. 969-85.
117. Bhattachar, S.N., Wesley, J.A., Fioritto, A., Martin, P.J., Babu, S.R., *Dissolution testing of a poorly soluble compound using the flow-through cell dissolution apparatus.* Int J Pharm, 2002. **236**(1-2): p. 135-43.
118. Fotaki, N., *Flow-Through Cell Apparatus (USP Apparatus 4): Operation and Features.* Dissolution Technologies, 2011.
119. Zolnik, B.S., J.L. Raton, and D.J. Burgess *Application of USP Apparatus 4 and In Situ Fiber Optic Analysis to Microsphere Release Testing.* Dissolution Technologies, 2005.
120. Pedersen, B.T., Ostergaard, J., Larsen, S.W., Larsen, C., *Characterisation of the rotating dialysis cell as an in-vitro model potentially useful for simulation of the pharmacokinetic fate of intra-articularly administered drugs.* Eur J Pharm Sci, 2005. **25**(1): p. 73-9.
121. Dong, J., Jiang, D., Wang, Z., Wu, G., Miao, L., Huang, L., *Intra-articular delivery of liposomal celecoxib–hyaluronate combination for the treatment of osteoarthritis in rabbit model.* International Journal of Pharmaceutics, 2013. **441**(1–2): p. 285-290.
122. Larsen, S.W., Ostergaard, J., Friberg-Johansen, H., Jessen, M.N., Larsen, C., *In-vitro assessment of drug release rates from oil depot formulations intended for intra-articular administration.* Eur J Pharm Sci, 2006. **29**(5): p. 348-54.
123. Washington, C., *Evaluation of non-sink dialysis methods for the measurement of drug release from colloids: effects of drug partition.* International Journal of Pharmaceutics, 1989. **56**(1): p. 71-74.

124. Frost, A.B., Larsen, F., Ostergaard, J., Larsen, S.W., Lindergaard, C., Hansen, H.R., Larsen, C., *On the search for in-vitro in-vivo correlations in the field of intra-articular drug delivery: administration of sodium diatrizoate to the horse.* Eur J Pharm Sci, 2010. **41**(1): p. 10-5.
125. Fotaki, N. and M. Vertzoni, *Biorelevant dissolution methods and their applications in in-vitroin-vivo correlations for oralformulations.* The Open Drug Delivery Journal, 2010. **4**(1): p. 2-13.
126. Smith, A.M., Fleming, L., Wudebwe, U., Bowen, J., Grover, L.M., *Development of a synovial fluid analogue with bio-relevant rheology for wear testing of orthopaedic implants.* J Mech Behav Biomed Mater, 2014. **32**: p. 177-84.
127. Zhang, Z., S. Barman, and G.F. Christopher, *The role of protein content on the steady and oscillatory shear rheology of model synovial fluids.* Soft Matter, 2014. **10**(32): p. 5965-73.

Chapter 2: Development of compendial dissolution tests for intra-articular formulations

Abstract

Purpose: To develop appropriate compendial dissolution tests for IA formulations and investigate the effect of various dissolution method parameters on drug dissolution.

Methods: Different setups of dissolution tests and apparatus accepted by the Pharmacopoeia were evaluated such as the USP apparatus I, II, III and IV, a dialysis membrane setup, a monophasic and bi-phasic setup. For each method, several factors were tested involving the hydrodynamics of the system, the formulation type and various dissolution media, to establish their impact on drug dissolution. Drug quantification was done with the HPLC and drug dissolution over time was measured.

Results: Testing the USP apparatus I and III with the use of float-A-lyzers (ready to use dialysis membranes), generally did not lead to drug permeation through the membrane. The dissolution method designed with the USP apparatus IV in open system discriminated between particle sizes of TA, with all factors tested showing significant effect on drug dissolution. The results with the bi-phasic setup dissolution method with the USP apparatus IV in closed system, showed that most of the examined factors would affect mostly the partitioning of the drug rather than the dissolution rate. Changing the aqueous and organic phase ratio in the system or the size of the oil/water interface area between the two phases, resulted in a dissolution rate faster than the partitioning rate. Regarding the dialysis studies performed in glass bottles, having a high difference of osmolality between the aqueous and organic phase (due to the presence of methanol in the receptor phase), a larger dialysis membrane surface area or an increase in the temperature of the dissolution medium, would lead to the drug dissolving and permeating through the membrane in a significant rate. Results were consistent with the hypothesis that the osmolality gradient drives dissolution from IA formulations and permeation through the dialysis membrane faster than permeation due to the concentration gradient.

Conclusions: A better understanding of the factors involved in the performed dissolution tests provides higher feasibility to develop a compendial dissolution method for IA formulations. The promising results from the continuous flow through cell method (USP apparatus IV) may address the lack of an *in-vitro* compendial dissolution test for IA formulations.

2.1. Introduction

IA administration is a type of parenteral injection taking place in the synovial joint [1-3]. Long acting corticosteroid and HA formulations [4, 5] are used today in diseases such as OA and RA as they provide anti-inflammatory effects in the joint cavity. IA injections are administered in patients with moderate to severe pain and inflammation, who do not respond appropriately to oral analgesic and anti-inflammatory agents [3, 6]. The IA injection leads to a localised delivery of the drug, reducing side effects as systemic exposure is minimised [4, 7]. With a lower dose administered, appropriate concentrations of the drug can be present in the joint. Based on this fact, there are better efficacy drugs with low bioavailability that can have a potentially more significant effect [4]. By considering the structure of the synovial joint, when an IA formulation is injected in the synovial cavity, it can be retained due to the synovial membrane lining that separates the internal part of the cavity from the external blood and lymph vessels [8, 9]. The drug can then follow different pathways, primarily according to its particle size, following IA injection: i) Phagocytosis and transfer of the drug molecules to the synovial membrane or subsynovium [10, 11], ii) convection of drug molecules with the articular cartilage or ECM [12] and iii) dissolution of drug molecules in the synovial fluid and transfer to the articular cartilage and synovium, or entrapment inside synovial folds [13, 14].

To demonstrate the rate with which the tested drug will dissolve in the joint, it is of vital importance to have a suitable *in-vitro* dissolution model that can also provide an appropriate characterisation and evaluation of the IA formulation under test [15]. Currently, there is no regulatory approved, standard compendial method for assessing drug dissolution from parenteral formulations, including IA formulations [16]. To develop an appropriate dissolution method, it is essential to study and define the effect of various factors of different dissolution methods on drug dissolution. Dissolution can be affected by drug substance factors, dosage form factors and may vary according to the methods used for its assessment [17]. The dissolution method development consists of the selection of appropriate media and suitable hydrodynamics and also the understanding of their effect on the drug dissolution. By having a better understanding of these factors, it becomes more feasible to develop a compendial dissolution method for IA formulations.

Dissolution testing is an important tool in the pharmaceutical industry as it has primary significance in drug/formulation development and quality control [18]. An official compendial dissolution method would be used to set specification criteria for ensuring product quality

(batch-to-batch consistency), while providing a biopharmaceutical characterisation of the product and so defining critical formulation variables of dissolution [16, 19]. Since there are significant differences in the formulation design between dosage forms, leading to different physicochemical and dissolution characteristics, a single dissolution method cannot be a good fit for all. A suitable dissolution technique and an apparatus with appropriate hydrodynamic conditions should be used to accommodate the dosage form in test.

For formulation development and quality control testing of parenteral (including IA) administered drugs, the *in-vitro* dissolution methods that are widely used according to literature are: i) sample and separate methods [20, 21], ii) continuous flow methods [22] and iii) dialysis techniques [23].

The sample and separate method has been a widely used technique for testing drug dissolution from parenteral systems [24]. This method involves the drug formulation being placed into a vessel which contains the media and samples taken over time to assess drug dissolution. Centrifugation or filtration of the sample is an important step, to remove any undissolved drug before measuring dissolution [25]. Parameters that can affect the amount of drug dissolved include the container size, the type of agitation and the methods of sampling [24].

The dialysis membrane method seems to be an interesting option for the dissolution testing of parenteral formulations (including IA). A small volume drug-donor phase is present in a membrane, separated from the larger volume receptor phase containing the buffer [26]. In the dialysis method, there are three steps that may be rate limiting to the dissolution/permeation of the drug: i) the dissolution of the drug in the donor phase, ii) the migration of the drug to the membrane and iii) the permeation of the drug through the membrane and into the receptor phase [27]. As the dissolution of the drug and its permeation through the membrane can take a long time [16] accelerated dissolution techniques may be appropriate for providing a rapid evaluation of the dissolution method in test [26]. It is suggested that the receptor phase volume should be at least 6- to 10-fold higher than the volume present in the dialysis membrane in order to have a driving force present for drug diffusion [24] or the saturation solubility of the drug tested should be at least three times above the drug concentration in the system [28] for appropriate sink conditions to be present in the receptor phase.

The continuous flow cell method has been mostly suggested for dissolution testing of parenteral formulations, with the drug placed on glass beads in an appropriate cell according to the formulation type [25, 29]. Two setups can be used, an open system with the medium flowing through the cell and then being collected, or in a closed system where the medium is

circulated through the cell and back to the medium reservoir [30]. A combination of a bi-phasic method with the use of the flow through cell method (USP apparatus IV) could also provide meaningful results, by taking into account that low solubility drugs would lead to non-sink conditions in the closed-monophasic system setup (one aqueous phase) [24]. The use of a bi-phasic dissolution model (aqueous and organic phase in equilibrium) can be used to facilitate the achievement of sink conditions with a smaller volume of medium in use compared to an open system. The setup involves an aqueous medium and an immiscible organic solvent, with the drug being dissolved in the aqueous phase and then partitioning into the organic layer. The organic phase in this setup acts as a reservoir in which the dissolved drug can diffuse, allowing more drug to dissolve in the aqueous medium [28]. The dissolution of the drug in the aqueous layer and then the partition to the organic phase takes place by exploiting the lipophilicity (logP) of the drug. In a bi-phasic system, it is important for the aqueous layer not to be saturated and also for the total dose of drug studied to be less than 20% of its solubility, in the volume of organic phase in the bi-phasic system [28, 31], for sink conditions to be maintained.

In the present study, the aim of our research was to design a developed and refined compendial method, used for characterising the drug product and ensuring reproducible product quality. Various parameters of the dialysis membrane method were assessed, such as the effect of surfactant, increase in osmolality in each phase, membrane length and dissolution medium temperature, addition of medium in donor phase and addition of organic solvent in the receptor phase in order to find appropriate method conditions and also to determine their effect in drug dissolution. Furthermore, different parameters of the USP apparatus IV affecting the hydrodynamics of the system were also evaluated according to their effect on drug dissolution, such as the effect of flow rate, cell size and different surfactant type added to the dissolution medium. The effect of the formulation type tested and the cell setup involving the placement of the drug in the USP apparatus IV cell were also investigated as they may have a vital part in drug dissolution [25]. The bi-phasic setup was combined with the continuous flow cell method for assessing parameters that would affect drug dissolution and partitioning to the organic phase such as the addition of surfactant in the aqueous phase, flow rate, cell size, volume of the phases, organic solvent and oil/water interface area. The synthetic corticosteroid TA has been chosen as a model drug due to its physical properties. A weak base with a pKa of 11.75 and a low solubility of 17.5 μg/mL in water [32] and 5.2 mg/mL in octanol [11], it has similar values to the remaining corticosteroids administered through the IA route. TA has been used to evaluate different dissolution setups, intended for IA formulations. The tested suspensions

are Kenalog 40® (TA, 40 mg/mL) and Adcortyl® (TA, 10 mg/mL), while a microparticle formulation in two sizes containing TA was also developed for testing dissolution method discrimination between particle sizes.

2.2. Materials and methods

2.2.1. Materials

TA (98+%, fine chemical) was purchased from Alfa Aesar (UK), Kenalog 40® (40 mg/mL) and Adcortyl® (10 mg/mL), both IA suspensions of TA, were purchased from Bristol-Myers Squibb (UK). For all experiments, ultra-pure (Milli-Q purification device) water was used. The composition of PBS included sodium chloride (≥ 99.9%), potassium dihydrogen orthophosphate (≥ 99.5%), di-sodium hydrogen orthophosphate, anhydrous dried (≥ 99.5%) and potassium chloride (≥ 99.5%) purchased from Sigma-Aldrich (UK). Tween 80 (polysorbate) was bought from VWR (UK) and sodium dodecyl sulphate (SDS/SLS) (≥ 99.0%) and CTAB (≥ 99.0%) were purchased from Sigma-Aldrich (UK). For the experiments with alterations in osmolality, sucrose and di-potassium hydrogen orthophosphate (≥ 99.5%) were purchased from Sigma-Aldrich (UK). The organic solvents used, methanol (MeOH), ethanol (EtOH) and ethyl acetate (all HPLC grade), were also purchased from Sigma-Aldrich (UK) while 1-octanol (99%, pure) was purchased from Fisher Scientific (UK). Cellulose acetate dialysis membranes (MWCO: 14 kDa) were purchased from Sigma-Aldrich (UK) while the pre-assembled dialysis tubes, Spectra/Por Float-A-lyzer, (MWCO: 25 kDa, volume size 1 mL) cellulose ester dialysis membranes were kindly donated from Agilent (US). Whatman glass fibre filters (GF/F 0.7 µm pore size, GF/D: 2.7 µm pore size) and hydrophilic polysulfone membrane disc filter (HT Tuffryn, 0.2 µm, Sigma-Aldrich, UK) were used in the USP apparatus IV experiments. For the development of nanoparticles poly-(l-lactide) (PLA) with inherent viscosity of ~1 dL/g, 0.1 % (w/v) in chloroform (25 ^{o}C), dichloromethane and poly (vinyl alcohol) (MW: 30,000-70,000) were purchased from Sigma-Aldrich (UK).

2.2.2. Solubility studies

The solubility of TA in PBS, PBS with methanol (50% v/v) and PBS with surfactants [PBS with Tween 80 (1% v/v), PBS with SLS (1% w/v) and PBS with CTAB (1% w/v)] was determined at 37 ^{o}C. The shake-flask method was used with an excess amount of TA added to the medium in test (n=3). The suspensions were then shaken in a water bath at 37 ± 0.5 ^{o}C (Grant SBB Aqua Plus, UK) for 24-h. Samples were then withdrawn, filtered with 0.45 µm RC filters and diluted with the corresponding medium where appropriate before analysis, with the amount of TA then quantified in the HPLC.

2.2.3. Measurement of osmolality

Osmolality values were measured in triplicate by freezing-point depression of the media using an Advanced Micro-Osmometer Model 3300 (Advanced Instruments Inc.)

2.2.4. Development of Triamcinolone Acetonide loaded microparticles

2.2.4.1. Preparation of microparticles

Microparticles were developed according to a modification of a published o/w emulsion-solvent evaporation method [33, 34] with the modification related to the sonication power and sonication duration. PLA polymer (200 mg) was dissolved in 5 mL dichloromethane and was then added to a 1 mL suspension of TA (100 mg) in dichloromethane. The drug polymer solution was then transferred to 30 mL of pre-chilled aqueous polyvinyl alcohol (2% w/v), acting as the emulsifier, in an ice bath under sonication to prepare an o/w emulsion. The sonication took place with the use of a probe sonicator (Branson, Digital Sonifier, US) with a power of 10 W for 1 min (Microparticles b, MPb) and at 20 W for 2 min (Microparticles a, MPa). The primary o/w emulsion obtained after the sonication was then transferred to 100 mL of chilled aqueous polyvinyl alcohol solution (2% w/v) in an ice bath under probe sonication. The sonication was done at 30 W for 3 min for both size microparticles to stabilise the emulsion. Afterwards, the emulsion obtained was stirred for 3-h in room temperature on a magnetic stirrer (to evaporate the organic solvent and harden the microparticles). The microparticles formed were then centrifuged for 20 min at 28,000 x *g* at 4 ^{o}C using a centrifuge (Beckman Coulter, J2-MC High Speed Centrifuge, UK) to obtain a pellet of microparticles. The microparticle pellet was then washed twice with 30 mL distilled, de-ionized water for further removal of any free drug present or other additives. The final pellet was then re-dispersed in 10 mL distilled, de-ionized water and frozen by storing at -80 ^{o}C for 30 min. Finally, after freezing, the microparticles were lyophilized in a freeze dryer (Labfreez FD-10 Series, UK) at -40 ^{o}C and at a pressure of 0.1 mBar for 24-h.

2.2.4.2. Characterisation of microparticles

2.2.4.2.1. Particle size

Lyophilized particles (1 mg) were re-suspended in 5 mL of distilled, de-ionized water for measuring particle size and size distribution with the use of a Mastersizer X standard bench and a Small Volume Sample Dispersion Unit (MAM 5000, Malvern Inc., US). The particle

size and size distribution for Adcortyl® and TA powder in PBS (10 mg/mL) was measured with the same equipment.

2.2.4.2.2. Surface morphology of particles

The surface morphology was examined with a scanning electron microscope (Jeol, SEM 6480LV, UK). The particles were mounted on a piece of carbon sticky aluminium stubs and stored in a desiccator overnight to remove the residual moisture. Following this, they were sputter coated with a thin layer of gold (SC7620 sputter coater, Quorum Technologies Ltd., UK) to reduce charging and improve image quality. Images of TA microparticles were then collected.

2.2.4.2.3. Drug content of particles

5 mg of lyophilized TA loaded microparticles were dissolved in 25 mL dichloromethane and the solution was stirred for 1-h at room temperature. From this solution, 1 mL was mixed with 50 mL of methanol, in order to measure TA content with the HPLC. TA amounts were calculated according to a calibration curve (range 2-10 μm/mL) in methanol. Calibration curves were prepared with the use of a stock solution of TA in methanol (100 μg/mL). The working calibration standards were prepared by diluting the stock solution accordingly with the selected medium [35]. All measurements were performed in triplicates. Drug loading (%) and the encapsulation efficacy (%) were calculated based on:

$$Drug\ loading\ (\%) = \frac{mass\ of\ drug\ in\ microparticles}{mass\ of\ microparticles} \times 100 \qquad \text{(Eq. 1)}$$

$$Encapsulation\ efficiency\ (\%) = \frac{experimental\ drug\ loading}{theoretical\ drug\ loading} \times 100 \qquad \text{(Eq. 2)}$$

2.2.5. *In-vitro* dissolution studies

2.2.5.1. In-vitro dissolution studies with USP apparatus I

Dissolution experiments were performed with a USP apparatus I (Agilent 708-DS Dissolution Apparatus, UK) with the use of a dialysis membrane instead of the cylindrical baskets. The modification was designed in co-operation with Agilent and consisted of a special adjustment of the metal probe, with a specially designed plastic part placed instead of the basket, which on its end part, would fit the upper plastic cap of the Float-A-lyzer (ready-to-use lab dialysis membrane, volume: 1 mL) and would hold it in position. The Float-A-lyzers were pre-wetted

and treated for use according to the manufacturer (Spectrum, US). The dose used was 1 mL of TA suspension 40 mg/mL (Kenalog 40®). The Float-A-lyzer height in the USP apparatus I was adjusted according to the <711> Dissolution General Chapter of the US Pharmacopoeia which suggests that the bottom of the basket and the inside bottom part of the vessel should be in a constant distance of 25 ± 2 mm during the test. The volume of the dissolution medium [PBS or PBS with Tween 80 (0.5% v/v)], was 900 mL at 37 ± 0.5 ^{o}C and the rotational speed was set at 150 rotations per minute (rpm). At appropriate time intervals (every 30 min for 8-h) 5 mL samples were withdrawn from the vessel with a glass syringe attached to a cannula, set at a specific height in the apparatus (half distance from the bottom of the vessel to the surface of the medium). 5 mL of fresh buffer was then replaced in the vessel and samples were then analysed with HPLC. The experiment was done in triplicate and results after the analysis of TA are presented as Mean (% dissolved over time) ± S.D.

2.2.5.2. In-vitro dissolution studies with USP apparatus II

A dissolution experiment was performed with the USP apparatus II (Agilent 708-DS Dissolution Apparatus, UK). The paddle height in the USP apparatus II was adjusted according to the <711> Dissolution General Chapter of the US Pharmacopoeia. The volume of the dissolution medium, PBS, was 900 mL, at 37 ± 0.5 ^{o}C and the rotational speed was set at 100 rpm. A dose of 1 mL of TA suspension 40 mg/mL (Kenalog 40®) was placed into the vessel and at specific time intervals (every 10 min for 1-h and then every 30 min for 2-h) 5 mL samples were withdrawn from the vessel with a glass syringe attached to a cannula which was set at a specific height in the apparatus (half distance from the bottom of the vessel to the buffer surface). 5 mL of fresh buffer was then replaced in the vessel and all samples were diluted with PBS before analysis with the HPLC. The experiment was done in triplicate and results after the analysis of TA are presented as Mean (% dissolved over time) ± S.D.

2.2.5.3. In-vitro dissolution studies with USP apparatus III

Dissolution experiments were performed with a USP apparatus III (Agilent Bio-Dis Reciprocating cylinder apparatus, UK). The glass reciprocating cylinders commonly used were replaced with Float-A-lyzers. The modification was designed in co-operation with Agilent and consisted of a special adjustment to the inert fittings of the evaporation cap, which on its end part, would fit the upper plastic cap of the Float-A-lyzer (Ready-to-use lab dialysis membranes, volume: 1 mL) and would hold it in position. The Float-A-lyzers were pre-wetted and treated

for use, according to the manufacturer (Spectrum, US). The dose used was 1 mL of TA suspension 40 mg/mL (Kenalog 40®) and the volume of PBS or PBS with Tween 80 (1% v/v) was 200 mL in each of the vessels, at 37 ± 0.5 °C and dip rates were set at 30 and 60 dips per minute (DPS). Samples were collected at appropriate time intervals (every 30 min for 5-h, 7-h and 72-h). The samples were analysed with HPLC. The experiment was done in triplicate and results after the analysis of TA are presented as Mean (% dissolved over time) ± S.D.

2.2.5.4. In-vitro dissolution studies with USP apparatus IV

Dissolution experiments were performed with the USP apparatus IV (Flow-through cell system) (Erweka DFZ 720, UK) connected with a piston pump (Erweka, HKP720). The small and large cells for tablets and capsules used in the experiments have three parts, the lower cone, the middle cylindrical portion and the filter head on top. A glass bead of 6 mm is positioned in the tip of each cell for tablets and capsules and on top, glass beads are added, to fill the cell up to the score of the tablet holder. The medium flows in tubes and enters the cell from the lower cone towards the filter head top. The cone and filter head are separated by a #40 mesh screen and added filter(s). The USP apparatus IV was used in two modes: open and closed. In the open system, fresh medium would flow continuously through the cell and would then be collected, while in the closed system, a specific volume of medium is recycled through the system [30]. The drug suspension was loaded onto the glass beads with a disposable dropping pipette. Samples for all experiments were collected with glass volumetric cylinders in specific time points, then were diluted with the corresponding medium, where appropriate, before analysing with the HPLC to determine the amount of TA dissolved. The % dissolved was calculated according to a calibration curve (2-10 μm) in the corresponding medium [35]. The experiments were performed at 37 ± 0.5 °C in triplicate and results are presented as Mean (% dissolved over time) ± S.D.

2.2.5.4.1. Open Mode Setup

2.2.5.4.1.1. Flow rate

The flow rate (4, 8, 16 mL/min) was evaluated with the large cell and the small cell for tablets and capsules filled up to the score of the tablet holder with 1 mm glass beads. The filter top of the cell contained two glass fibre filters (GF/F: 0.7 μm pore size and GF/D 2.7 μm pore size). The dose used was 1 mL of TA suspension 40 mg/mL (Kenalog 40®) and the medium used was PBS. Samples were collected with glass volumetric cylinders every 15 min.

2.2.5.4.1.2. Cell size

The cell size of the cell for tablets and capsules [internal diameter: 12 mm (small cell), 22.6 mm (large cell)] was evaluated with the cell filled up to the score of the tablet holder with 1 mm glass beads. The filter top of the cell contained two glass fibre filters (GF/F: 0.7 µm pore size and GF/D 2.7 µm pore size). The dose used was 1 mL of TA suspension 40 mg/mL (Kenalog 40®) and the medium used was PBS with a flow of 4 and 8 mL/mL. Samples were collected with glass volumetric cylinders every 15 min.

2.2.5.4.1.3. Glass bead size

The glass bead size (1 and 2 mm) was evaluated with the large cell and the small cell for tablets and capsules filled up to the score of the tablet holder with the glass beads. The filter top of the cell contained two glass fibre filters (GF/F: 0.7 µm pore size and GF/D: 2.7 µm pore size). The dose used was 1 mL of TA suspension 40 mg/mL (Kenalog 40®) and the medium used was PBS with a flow of 4 mL/min. Samples were collected with glass volumetric cylinders every 15 min.

2.2.5.4.1.4. Sample position

The positioning of the sample was evaluated with three different cell setups (Fig. 2.1.). Fig. 2.1. A is the setup described in 2.2.5.4.1.1. with the large cell for tablets and capsules in use. Fig. 2.1. B is the setup described in 2.2.5.4.1.1. with the large cell for tablets and capsules in use, with the difference of the filter head top part of the cell being replaced by the semisolid cell (an accessory part, set in the filter head instead of the sieve), with GF/F and GF/D filters placed above the sieve of the semisolid cell. The drug suspension in this occasion was placed inside the compartment of the semisolid cell, below the sieve. Fig. 2.1. C is the setup described in 2.2.5.4.1.1. with the large cell for tablets and capsules in use with the difference of a GF/F filter placed on the 1 mm glass beads and the suspension placed on top of that filter. The dose used was 1 mL of TA suspension 40 mg/mL (Kenalog 40®) and the medium used was PBS with Tween 80 (1% v/v) with a flow of 4 mL/mL. Samples were collected with glass volumetric cylinders every 15 min.

2.2.5.4.1.5. Filter type

The filter type (GF/F + GF/D, HT Tuffryn) on the filter head top of the cell for tablets and suspensions was evaluated with the large cell for tablets and capsules filled up to the score of the tablet holder with 1 mm glass beads. The dose used was 1 mL of TA suspension 10 mg/mL (Adcortyl®) and the medium used was PBS with a flow of 4 mL/min. Samples were collected with glass volumetric cylinders every 30 min up to 1-h and the every 1-h up to 6-h.

2.2.5.4.1.6. Surfactant type added to the dissolution medium

The effect of the dissolution medium containing surfactant was evaluated, involving different types and concentrations of surfactants in PBS [Tween 80 (0.5, 1% v/v), SLS (1% w/v) or CTAB (1% w/v)] with the large cell for tablets and capsules filled up to the score of the tablet holder with 1 mm glass beads. The filter top of the cell contained two glass fibre filters (GF/F: 0.7 µm pore size and GF/D 2.7 µm pore size). The dose used was 1 mL of TA suspension 40 mg/mL (Kenalog 40®) and the medium had a flow of 4 mL/min. Samples were collected with glass volumetric cylinders every 15 min for 6-h.

2.2.5.4.1.7. Drug concentration in the suspension

The drug concentration in the suspension [TA suspension 40 mg/mL (Kenalog 40®) and TA suspension 10 mg/mL (Adcortyl®)] was evaluated with the large cell for tablets and capsules filled up to the score of the tablet holder, with 1 mm glass beads. The filter top of the cell contained two glass fibre filters (GF/F: 0.7 µm pore size and GF/D 2.7 µm pore size). The dose used was 1 mL and the dissolution medium was PBS with Tween 80 (1% v/v) with a flow of 4 mL/mL. Samples were collected with glass volumetric cylinders every 15 min for 6-h.

2.2.5.4.1.8. Particle size

The particle size of the suspension [developed microparticle powder of small vs. large size re-suspended in PBS, TA suspension 10 mg/mL (Adcortyl®) vs. TA powder in PBS 10 mg/mL] was evaluated in different conditions. Developed microparticle powder or small and large size were tested with the small cell for tablets and capsules filled up to the score of the tablet holder, with 1 mm glass beads. The filter top of the cell contained a HT Tuffryn filter. The amount of PLA-TA microparticle powder corresponding to 0.1 mg TA was suspended in 1 mL of PBS and the suspension was loaded on top of 1 mm glass beads in the small cell. The dissolution medium used was PBS with a flow of 4 mL/mL. TA suspension 10 mg/mL (Adcortyl®) vs. TA powder in PBS (10 mg/mL) were tested with the large cell for tablets and capsules filled up to

the score of the tablet holder, with 1 mm glass beads. The filter top of the cell contained two Whatman glass fibre filters (GF/F: 0.7 µm pore size and GF/D 2.7 µm pore size). The dose used was 1 mL of TA suspension 10 mg/mL (Adcortyl®) and 1 mL of PBS containing 10 mg of TA powder. The dissolution medium used was PBS with a flow of 4 mL/min. Samples were collected with glass volumetric cylinders every 15 min for 6-h.

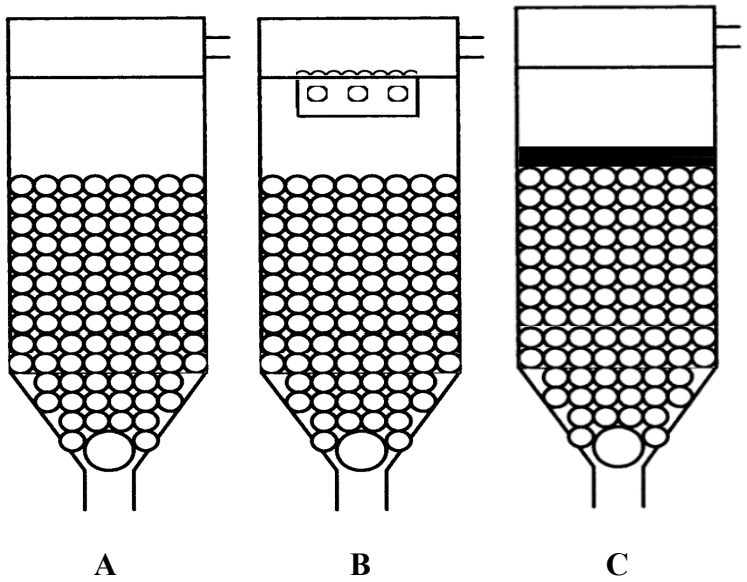

Fig. 2.1. Schematic diagrams showing the setup of the cell: A. Large cell with glass beads. B. Large cell with glass beads with semisolid cell in placed in filter top. C. Large cell with glass beads and GF/F filter placed on top of glass beads. Modified from [29]

2.2.5.4.2. Closed Mode Setup

2.2.5.4.2.1. Monophasic dissolution setup

The monophasic dissolution system experiments were performed with the use of a USP apparatus IV (Erweka, DFZ 720, UK) connected to a piston pump (Erweka, HKP720) in a closed system setup. The medium flows in tubes and into the cell from the lower cone towards the filter head top. In the closed system bi-phasic setup, the aqueous medium is pumped through tubing, circulating for each cell. An agitation of 300 rpm with a magnet in the bi-phasic system of the glass bottle was present. The volume used for the monophasic closed system was 60 mL of PBS with Tween 80 (1% v/v) and the dose used was 1 mL of TA suspension 40 mg/mL (Kenalog 40®) and the medium had a flow of 8 mL/min. The experiments were performed at 37 ± 0.5 ^{o}C in triplicate and 1 mL samples were collected from both phases every 30 minutes for 1-h and then each hour until 6-h (with replacement of the corresponding medium).

2.2.5.4.2.2. Biphasic dissolution setup

The two-phase dissolution system experiments were performed with the use of a USP apparatus IV (Erweka, DFZ 720, UK) in a closed system setup, with the dissolution medium placed in a glass bottle (Volume area of bottle for the small volumes used: 16.6 cm^2 and for the larger volumes used: 58.1 cm^2). The medium flows in tubes and into the cell from the lower cone towards the filter head top. In the closed system bi-phasic setup, the aqueous medium (saturated with the organic solvent) is pumped through tubing, circulating for each cell. An agitation of 300 rpm with a magnet in the bi-phasic system of the glass bottle was present. The experiments were performed at 37 ± 0.5 ^oC in triplicate and 1 mL samples were collected from both phases every 30 minutes for 1-h and then each hour until 6-h (with replacement of the corresponding medium). Samples from the aqueous phase would be used to measure the amount of TA dissolved and samples from the organic phase would be used to measure the amount that partitions from the aqueous phase. Samples for all experiments were collected with glass syringes attached to a cannula which was set at a specific height in the glass bottle (half distance from the bottom of the vessel to the aqueous medium surface, for aqueous phase samples and half distance from the top of the aqueous medium surface to the top of the organic medium surface, for organic phase samples) every 30 min for 1-h and then every hour for 6-h, then were diluted with the corresponding medium, where appropriate, before analysing with the HPLC. The % dissolved and partitioned was calculated according to calibration curves (2-10 μm) in the corresponding medium [35]. The experiments were performed at 37 ± 0.5 ^oC in triplicate and results are presented as Mean (% dissolved over time) ± S.D.

2.2.5.4.2.2.1. Surfactant in aqueous phase

The effect of the dissolution medium containing surfactant was evaluated, involving different types of surfactants in PBS [Tween 80 (1% v/v) and SLS (1% w/v)] with the small cell for tablets and capsules filled up to the score of the tablet holder with 1 mm glass beads. The organic solvent used was 1-octanol. The filter top of the cell contained two glass fibre filters (GF/F: 0.7 μm pore size and GF/D 2.7 μm pore size). The volumes used in the glass bottle were for the aqueous phase 40 mL and the organic phase 10 mL or for the aqueous phase 300 mL and for the organic phase 200 mL. The dose used was 1 mL of TA suspension 10 mg/mL (Adcortyl®) and the medium had a flow of 8 mL/min.

2.2.5.4.2.2.2. Flow rate

The flow rate (2 and 8 mL/min) was evaluated with the small cell for tablets and capsules filled up to the score of the tablet holder with 1 mm glass beads. The aqueous medium used was PBS with Tween 80 (1% v/v) and the organic medium used was 1-octanol. The filter top of the cell contained two glass fibre filters (GF/F: 0.7 µm pore size and GF/D 2.7 µm pore size). The volumes used in the glass bottle were for the aqueous phase 40 mL and the organic phase 10 mL. The dose used was 1 mL of TA suspension 10 mg/mL (Adcortyl®).

2.2.5.4.2.2.3. Cell size

The cell size of the tablets and capsules (small and large) filled up to the score of the tablet holder with 1 mm glass beads was evaluated. The aqueous medium used was PBS with Tween 80 (1% v/v) and the organic medium used was 1-octanol. The filter top of the cell contained two glass fibre filters (GF/F: 0.7 µm pore size and GF/D 2.7 µm pore size). The volumes used in the glass bottle were for the aqueous phase 40 mL and the organic phase 10 mL. The dose used was 1 mL of TA suspension 10 mg/mL (Adcortyl®) and the medium had a flow of 8 mL/min.

2.2.5.4.2.2.4. Organic phase/aqueous phase interface area

The effect of the organic phase/aqueous phase interface area (58.1 cm^2 and 145.2 cm^2) on the dissolution of TA from the formulation was evaluated with the small cell for tablets and capsules filled up to the score of the tablet holder with 1 mm glass beads. The aqueous medium used was PBS with Tween 80 (1% v/v) and the organic medium used was 1-octanol. The filter top of the cell contained two glass fibre filters (GF/F: 0.7 µm pore size and GF/D 2.7 µm pore size). The volumes used in the glass bottle were for the aqueous phase 300 mL and the organic phase 200 mL. The dose used was 1 mL of TA suspension 10 mg/mL (Adcortyl®) and the medium had a flow of 8 mL/min.

2.2.5.5. In-vitro dissolution with dialysis membrane method in glass bottles

A cellulose acetate dialysis membrane with a MWCO of 14 kDa (Sigma-Aldrich, UK) was chosen for the permeation of TA (according to the drug's molecular weight of 434.5 g/mol). The dialysis membrane was then securely sealed with membrane clips. The system was agitated on a magnetic stirrer (300 rpm) and held at 37 ^oC. At selected time intervals (30 min, 1-h, 2-h and then every 2-h up to 12-h and then at 24-h), 1 mL samples were collected from the receptor compartment and replaced with fresh corresponding medium. Samples were then diluted with

the corresponding medium where appropriate, before analysing with the HPLC to determine the amount of TA dissolved. The % dissolved was calculated according to a calibration curve (2-10 µm) in the corresponding medium [35]. The experiments were performed in triplicate and results are presented as Mean (% dissolved over time) ± S.D. Sink conditions were maintained throughout the experiments as the saturation solubility of TA was at least three times above the drug concentration in the system [28].

2.2.5.5.1. Effect of surfactant

The effect of the surfactant added to the receptor phase [PBS, PBS with SLS (1% w/v)] was evaluated with a volume of 100 mL in the glass bottle with a dose of 1 mL or 0.1 mL of TA suspension 10 mg/mL (Adcortyl®). The dose was placed in a 1.5-cm length dialysis membrane. The effect of surfactant was also tested with a similar setup containing with a dose of 1 mL of TA suspension 10 mg/mL (Adcortyl®) and containing a different surfactant (PBS, PBS with Tween 80 (1 and 10% v/v)].

2.2.5.5.2. Effect of increased osmolality in the donor phase

The effect of increased osmolality resulting by the addition of sodium chloride (from 382 to 500 mOsm) in the donor phase was evaluated with a volume of 100 mL PBS with Tween 80 (1% v/v) in the glass bottle with a dose of 1 mL or 0.1 mL of TA suspension 10 mg/mL (Adcortyl®). The dose was placed in a 1.5-cm length dialysis membrane.
The effect of increased osmolality resulting by the addition of a higher amount of sodium chloride (from 382 to 2000 mOsm) in the donor phase was also tested with a similar setup containing a volume of 1000 mL of PBS with Tween 80 (1% v/v) and the dose of the drug being placed in a 20-cm length dialysis.

2.2.5.5.3. Effect of increased osmolality in the receptor phase

The effect of increased osmolality resulting by the addition of di-potassium hydrogen orthophosphate (from 382 to 1000 mOsm) or sucrose (from 382 to 500, 1000 and 1500 mOsm) in the receptor phase of PBS with Tween 80 (1% v/v) was evaluated with a volume of 1000 mL in the glass bottle with a dose of 1 mL of TA suspension 10 mg/mL (Adcortyl®). The dose was placed in a 1.5-cm length dialysis membrane.

2.2.5.5.4. Effect of dialysis membrane length

The effect of the dialysis membrane length (1.5, 10 and 20 cm) was evaluated with the receptor phase containing 1000 mL of PBS with Tween 80 (1% v/v) in the glass bottle with a dose of 1 mL of TA suspension 10 mg/mL (Adcortyl®).

The effect of the dialysis membrane length between 10- and 20-cm was also evaluated with the receptor phase containing 1000 mL of PBS with Tween 80 (1% v/v) in the glass bottle and the donor phase containing 1 mL of TA suspension 10 mg/mL (Adcortyl®) with an additional volume of medium added [total volume in donor phase: 1 mL Adcortyl® + 9 mL of PBS with Tween 80 (1% v/v)].

2.2.5.5.5. Effect of temperature

The effect of temperature (37 ^{o}C and 60 ^{o}C) was evaluated with the receptor phase containing 1000 mL of PBS with Tween 80 (1% v/v) in the glass bottle with a dose of 1 mL of TA suspension 10 mg/mL (Adcortyl®). The dose was placed in dialysis membranes with lengths of 1.5-, 10- and 20-cm.

2.2.5.5.6. Effect of additional volume of the donor phase (additional medium added)

The effect of the additional medium in the donor phase (addition of 9 mL of PBS with Tween 80 (1% v/v)] containing a dose of 1 mL of TA suspension 10 mg/mL (Adcortyl®) was evaluated with a volume of 1000 mL PBS with Tween 80 (1% v/v) in the glass bottle. The dose was placed in 10- and 20-cm length dialysis membranes.

2.2.5.5.7. Organic solvent in receptor phase

2.2.5.5.7.1. Drug concentration in the suspension

The effect of the drug concentration in the suspension [TA suspension 10 mg/mL (Adcortyl®) and 40 mg/mL (Kenalog 40®)] was evaluated with a volume of 100 mL of PBS with MeOH (50% v/v) in the glass bottle. The dose of 1 mL was placed in a 1.5-cm length dialysis membrane.

2.2.5.5.7.2. Formulation type (solution, suspension and suspension developed with the addition of different volumes of methanol)

The effect of the formulation type, with a suspension [0.5 mL of TA suspension 10 mg/mL (Adcortyl®) compared to 1 mL of TA solution 5 mg/mL (TA powder in MeOH) and TA

suspensions (TA 10 mg/mL) with different volumes of methanol [TA powder in 1 mL PBS with MeoH (90% v/v) and TA powder in 1 mL PBS with MeOH (50% v/v)] was evaluated with a volume of 100 mL of PBS with MeOH (50% v/v) in the glass bottle. The dose was placed in a 1.5-cm length dialysis membrane.

2.2.5.5.7.3. Organic solvent type

The effect of the organic solvent type in the receptor phase [PBS with MeOH (50% v/v), PBS with Ethanol (1% v/v) and (10% v/v)] was evaluated with a volume of 100 mL in the glass bottle. The dose of 1 mL of TA suspension 10 mg/mL (Adcortyl®) was placed in a 1.5-cm length dialysis membrane.

2.2.6. Triamcinolone Acetonide HPLC Analysis

The samples obtained from the *in-vitro* dissolution experiments and standard solutions were analysed using an Agilent 1100 series HPLC system (Agilent, UK) consisting of a G1329A autosampler, a G1330A ALS thermostat, a G1316A thermostatted column compartment, a G1315A DAD, a G1322A degasser and a G1311A quaternary pump. A modification of a published method was used [64]. Reversed phase chromatography was performed using an Agilent Eclipse XDB-C18 column (2.6 x 250 mm, 5µm pore size) (Agilent, UK). The flow rate was set at 1 mL/min, temperature at 25 ^{o}C, the UV detection signal was set at 240 nm, run time for 8 min and injection volume 20 µL. The mobile phase was run at an isocratic mode with 65:35 (methanol/water). Samples were diluted with the corresponding medium where appropriate, before analysing with the HPLC to determine the amount of TA dissolved. The % dissolved was calculated according to a calibration curve (2-10 µm) in the corresponding medium [35]. Calibration curves were prepared with the use of a stock solution of TA (100 µg/mL) in methanol. The working calibration standards were composed after diluting the stock solution accordingly with the selected medium.

2.2.7. Dissolution profile comparisons

The use of f_2 similarity factor was chosen for comparing dissolution profiles. [36]. The percentages of dissolution for all time points were considered until the drug reached 85% dissolution of the plateau value; in this occasion one time point after the 85% dissolution was taken into account [37]. The similarity factor f_2 from 50-100 showed similarity of the compared dissolution profiles.

The equation used was:

$$f_2 = 50 \times \log\left\{\left[1 + \left({}^{1}/_{n}\right)\sum_{t=1}^{n}\left(R_t - T_t{}^{2}\right)\right]^{-0.5} \times 100\right\} \quad \text{(Eq. 3)}$$

where:

n is the number of time points

Rt is the dissolution value of the reference at time t

Tt is the dissolution value of the test at time t.

The calculations were done with the DDsolver Add-In (DDsolver, Add-In, Microsoft Excel) software program [38] using the dissolution profiles from the amount of drug dissolved over time.

2.3. Results and Discussion

2.3.1. Solubility studies

The equilibrium solubility of TA after 24-h is shown in Fig. 2.2. The addition of surfactants to the medium shows a significant increase in the solubility of TA as confirmed from the experimental data [solubility value of TA in PBS: 28.5 ± 0.7 µg/mL (n=3); solubility value of TA in PBS with Tween 80 (1% v/v): 91.6 ± 9.65 µg/mL (n=3); solubility value of TA in PBS with SLS (1% w/v): 478 ± 8.3 µg/mL (n=3); solubility value of TA in PBS with CTAB (1% w/v): 1041.2 ± 6.9 µg/mL (n=3)]. Similar results have been observed in the literature for TA [39]. The molecular weight of Tween 80 is larger compared to the anionic surfactants used [40] and so with similar surfactant molar concentrations, more drug molecules will be encapsulated in the SLS micelles, leading to lower diffusivity of the drug-micelle complex and so less drug will be dissolved from the formulation. Furthermore, ionic surfactants such as SLS and CTAB have higher surface activities with a stronger solubilising effect than non-ionic surfactants such as Tween 80 leading to higher drug solubilisation [39]. In addition, considering the critical micelle concentration values of the surfactants used in PBS (Tween 0.05 mM, CTAB: 1 mM and SLS: 1.1 M) [41], Tween 80 (and non-ionic surfactants) has a much lower CMC value and higher aggregation numbers than its ionic counterparts with similar hydrocarbon chains leading to less drug encapsulated and so a smaller solubilization capacity. The addition of organic solvent to the medium also leads to a significant increase in the solubility of TA, confirmed from the experimental data [solubility value of TA in PBS with MeOH (50% v/v): 536.7 ± 63.5 µg/mL (n=3)]. Adding methanol to the aqueous PBS medium leads to a reduction of water-to-water interactions due to the presence of hydrogen bond donating or accepting regions and also hydrocarbon regions. This leads to the system being more beneficial for non-polar solutes [42] and so increasing the solubility of TA in the medium.

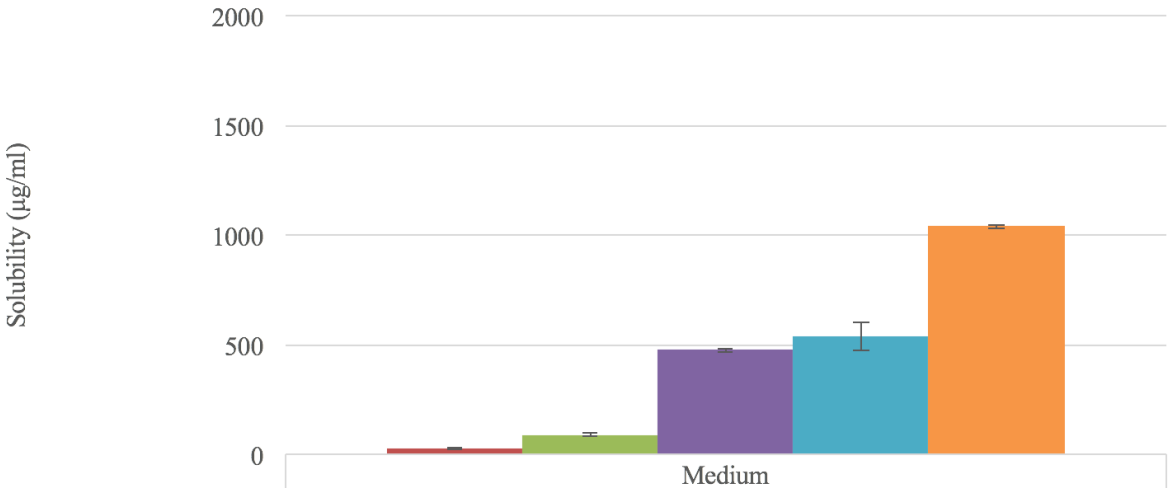

	Medium
PBS	28.5
PBS + Tween 80 (1%)	91.6
PBS + SLS (1%)	478
PBS + MeOH (50%)	536.7
PBS + CTAB (1%)	1041.2

Fig. 2.2. Solubility of TA samples in several media (n=3)

2.3.2. *In-vitro* dissolution studies with USP apparatus I

There was no significant drug dissolution noted in PBS or in PBS with Tween 80 (0.5% v/v) (data not shown). As Adcortyl® is an aqueous suspension, after a short amount of time it seems to sediment and form particle aggregates in the float-A-lyzer setup [43]. Particle aggregation took place due to the lack of agitation within the membrane which caused problems to the diffusion of the drug [26].

2.3.3. *In-vitro* dissolution studies with USP apparatus II

Dissolution studies with the USP apparatus II showed that due to non-sink conditions (40 mg of TA in 900 mL PBS) the % of drug dissolution reached a plateau from the first sampling point at 10 minutes, as the suspension would dissolve rapidly when in contact with PBS (results not shown). The percentage of the drug dissolved is approx. 40% due to the solubility of TA in PBS (28.5 µg/mL) (Fig. 2.2.).

2.3.4. *In-vitro* dissolution studies with USP apparatus III

Dissolution of TA in PBS was negligible in the modified USP apparatus III at 30 and 60 dpm as the drug did not permeate through the dialysis membrane (data not shown). Adding 0.5% v/v of Tween 80 into PBS, at 30 dpm, similarly did not lead to significant dissolution from the

dialysis membrane (data not shown). The reasoning for the drug not exiting the dialysis membrane in all conditions tested [30 and 60 dpm in PBS, 30 dpm in PBS with Tween 80 (0.5% v/v), 60 dpm in PBS with Tween 80 (1% v/v) for 72-h] was due to the lack of agitation within the membrane [26].

2.3.5. *In-vitro* dissolution with USP apparatus IV

2.3.5.1. Open system setup

2.3.5.1.1. Effect of flow rate

Results with the large cell showed that an increase in the flow rate from 4 to 8 mL/min, to 16 mL/min had an effect on the dissolution of TA from Kenalog 40® in PBS ($f_{2_{4-8}} = 56.34$ and $f_{2_{4-16}} = 52.18$ respectively and $f_{2_{8-16}} = 79.09$) (Fig. 2.3) [44]. With the use of the small cell, increasing the flow rate from 4 to 8 mL/min increased the TA dissolution significantly ($f_{2_{4-8}} = 30.07$) (Fig. 2.3). The increase in drug dissolution relates to the increased hydration of the material in test, as a higher volume of medium is flown through the cell [45, 46].

2.3.5.1.2. Effect of cell size

The effect of the cell size on the TA dissolution from Kenalog 40® was more significant at 8 mL/min reaching a difference of approx. 30% in the dissolution between the small and large cell in 6-h ($f_{2_{12-22.6}} = 32.03$). At 4 mL/min the difference in dissolved drug between the small and large cell was ≅ 10% ($f_{2_{12-22.6}} = 63.6$) in 6-h (Fig. 2.3). Using a smaller diameter cell size and increasing the flow rate, leads to the medium being flown through the cell with a higher pressure [47, 48]. Consequently, the medium will flow through the cell with a higher linear velocity related to the volumetric rate, through the cross-sectional area of the two size cells. As the linear velocity is inversely related through the ratio of the squared radii, at a specific volumetric flow, the linear velocity of the small cell will be greater than that of the large cell, resulting to a higher amount of drug dissolving with the use of the smaller cell [49, 50].

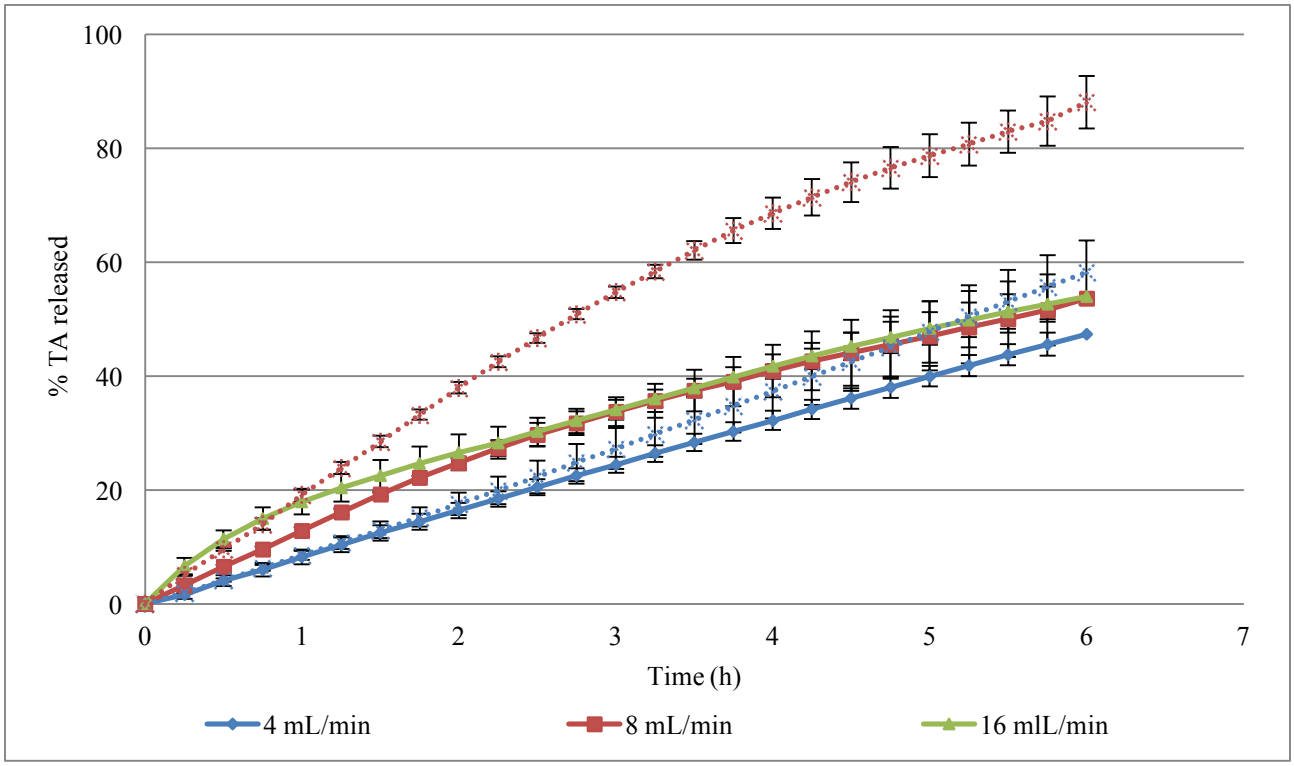

Fig. 2.3. Mean ± SD of TA dissolved from Kenalog 40® in PBS with different flow rates in the USP apparatus IV in open mode [Glass bead size: 1 mm, Cell size: large (solid lines), 12 mm (dashed lines)]

2.3.5.1.3. Effect of cell setup

2.3.5.1.3.1. Effect of glass bead size

In both cells, changing the glass bead size, from 1 to 2 mm, did not affect the dissolution of TA significantly. At 4 mL/min, the TA dissolution profiles from the dissolution of TA with the use of 1 mm and 2mm glass beads were similar in the large cell ($f_{2_{1-2}} = 94.16$) and in the small cell ($f_{2_{1-2}} = 63.63$) (Fig. 2.4). The use of glass beads results in a flow closer to a "laminar" type (fluid particles moving in parallel to the direction of flow), with the fluid entering the cell with a relatively faster speed in comparison to a "jet" type (fluid particles moving rapidly in all direction within the direction of the flow) with no glass beads present in the cell [44, 48]. A "jet" flow type of hydrodynamics leads to a more turbulent agitation of the sample. With glass beads in the cell, the fluid particles move close to parallel with each other and to the direction of the flow [30]. In both cells, increasing the size of the glass beads results in more space available in the cell due to bigger gaps present in the packed column, allowing the medium to have a slightly different velocity and therefore slower flow.

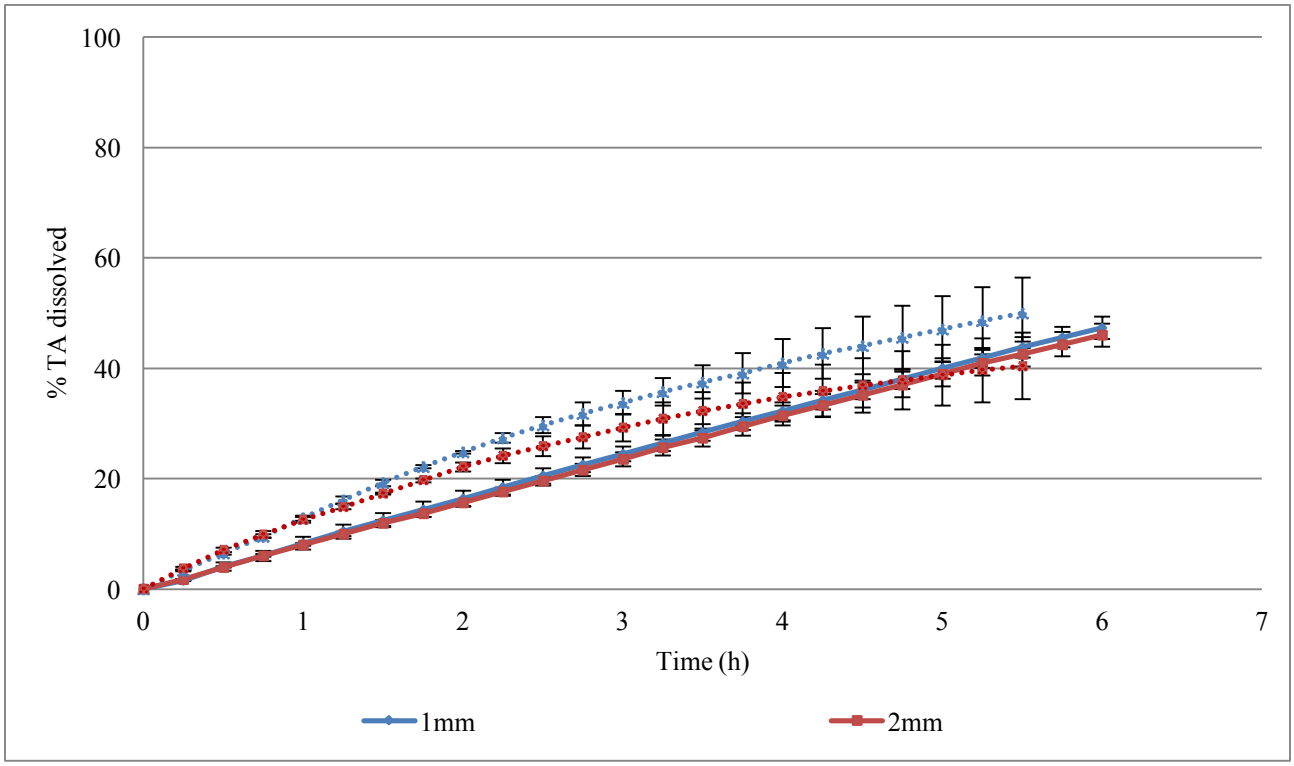

Fig. 2.4. Mean ± SD of TA dissolved from Kenalog 40® in PBS with different glass bead sizes in the USP apparatus IV in open system [Flow rate: 4 mL/min, Cell size: large (solid line), 12 mm (dashed line)]

2.3.5.1.3.2. Effect of sample position

TA dissolution from the formulation was significantly different with the sample placed on the glass beads directly compared to the sample placed on the GF/F filter on top of the glass beads, ($f_{2_{filter-22.6\,mm}} = 46$) (Fig. 2.5). The dissolution of TA from Kenalog 40® in the tested setups revealed a high variation, indicating low reproducibility. When the sample was placed in the semisolid cell, in 6-h there was a significant difference observed in TA dissolved from the formulation compared to the setup involving the placement of the suspension on the glass beads ($f_{2_{semisolid-22.6\,mm}} = 18.46$). The time it takes for the medium to reach the suspension and for the dissolution to take place when the drug is placed on the glass beads is shorter, might have an effect, leading to a faster dissolution (Fig. 2.5).

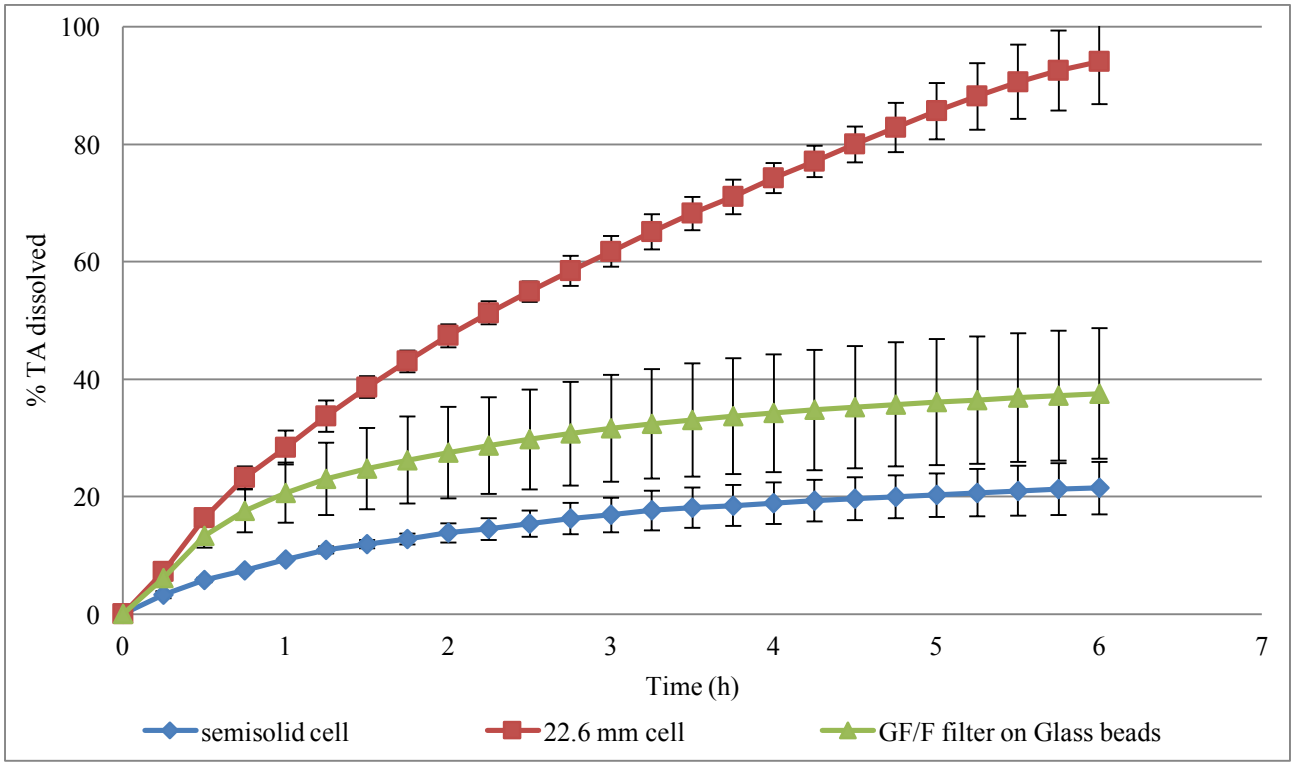

Fig. 2.5. Mean ± SD of TA dissolved from Kenalog 40® in PBS with Tween 80 (1% v/v) with different sample positions and different concentrations used in the USP apparatus IV in open system (Flow rate: 4 mL/min, Glass bead: 1 mm, Cell size: large)

2.3.5.1.3.3. Effect of filter type

Comparing the dissolution of TA from Adcortyl® with the glass microfiber filters [(GF/D + GF/F) with pore sizes of 2.7 µm and 0.7 µm respectively], and the Hydrophilic Polysulfone membrane disc filters [0.2 µm], showed that a filter with a smaller pore size and drug loading capacity will allow less amount of dissolved drug to diffuse through the filter used in the setup ($f_{2_{GFF+GFD-HT\ Tuffryn}}$ = 19.28). In a USP apparatus IV setup, the use of a durable filter in the filter head is vital, in order to avoid collecting undissolved drug material [46]. As the drug material starts to disintegrate into finer particles due to the contact with the medium [51], it will be able to pass through filters with larger pores faster (Fig. 2.6).

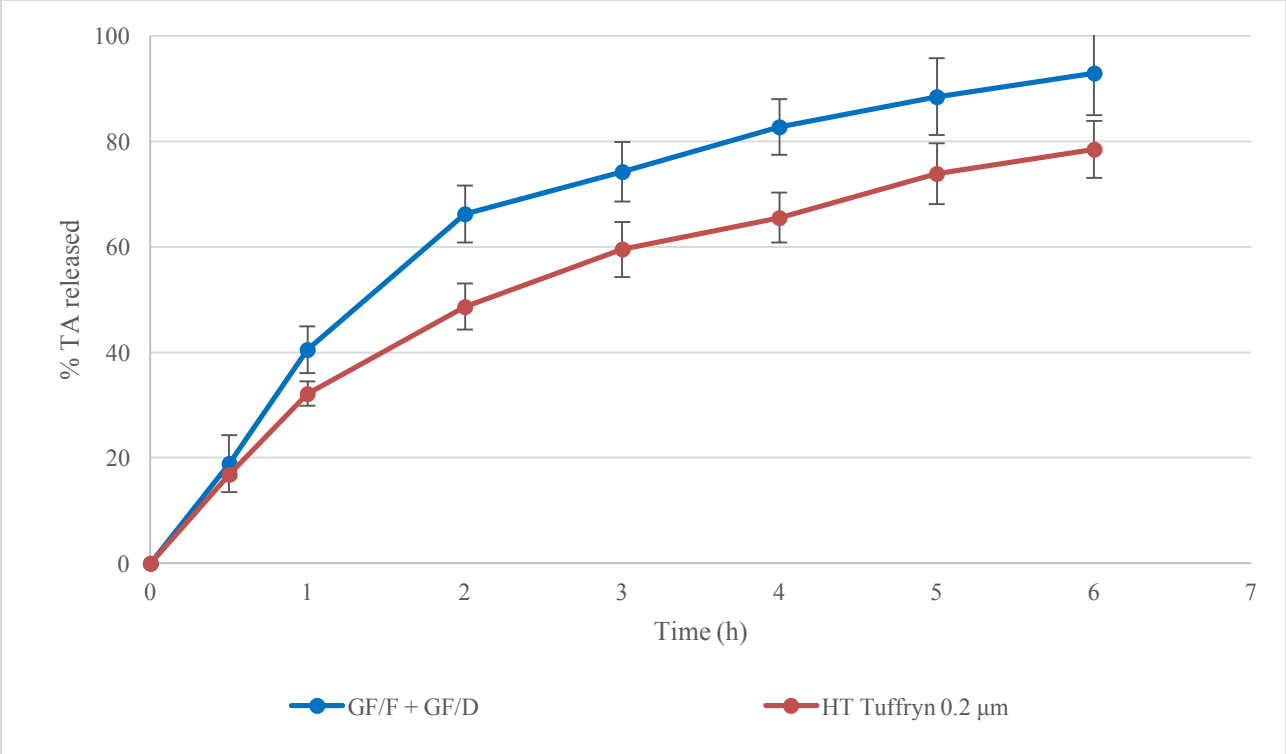

Fig. 2.6. Mean ± SD of TA dissolved from Adcortyl® in PBS with different filters in the filter head in different drug amounts in the USP apparatus IV in open system. (Flow rate: 4 mL/min, Glass bead: 1 mm, Cell size: large)

2.3.5.1.4. Effect of dissolution medium: surfactant type and concentration

The addition of cationic surfactant (CTAB) aids the system to reach complete dissolution of TA from the suspension after 1-h, while with the anionic surfactant (SLS), complete dissolution is reached at approx. 4-h. With the non-ionic surfactant (Tween 80), approx. 95% of total TA dissolution from the formulation is reached after 6-h. The TA dissolution profiles with all surfactants seems to follow a pattern of first order release. The media containing ionic surfactants (1% w/v) showed a higher % of TA dissolution from Kenalog 40® than the non-ionic Tween 80 (1% v/v) ($f_{2_{Tween\ 80-SLS}}$ =20.95 and $f_{2_{Tween\ 80-CTAB}}$ = 3.66). Similarity was noted between TA dissolution profiles in media with CTAB and SLS ($f_{2_{SLS-CTAB}}$ = 29.14). A faster initial dissolution from the suspension is shown with the use of CTAB (1% w/v) and SLS (1% w/v) compared to Tween 80 (1% v/v) (Fig. 2.7). Similar results have been observed in the literature [39]. The molecular weight of Tween 80 is larger compared to the molecular weight of the anionic surfactants used [40] and so with similar surfactant molar concentrations, more drug molecules will be encapsulated in the SLS micelles, leading to lower diffusivity of the drug-micelle complex and so less drug is dissolved from the formulation. Furthermore,

ionic surfactants such as SLS and CTAB have higher surface activities with a stronger solubilising effect than non-ionic surfactants such as Tween 80, leading to higher drug solubilisation [39].

The effect of the concentration of surfactant in the medium [PBS with Tween 80 (0.5% v/v and 1% v/v)] on the dissolution of the drug from the formulation has a significant effect [52] on the dissolution of TA from the formulation ($f_{2_{0-0.5}} = 28.7$ and $f_{2_{0.5-1}} = 48.61$ respectively). Adding surfactant to the medium, reduces the surface tension due to adsorption at the liquid-air interface and improves the wetting properties of the drug. The addition of surfactant also increases the amount of drug encapsulated in the created micelles, and subsequently increases the dissolution rate of the drug (Fig. 2.7) [53].

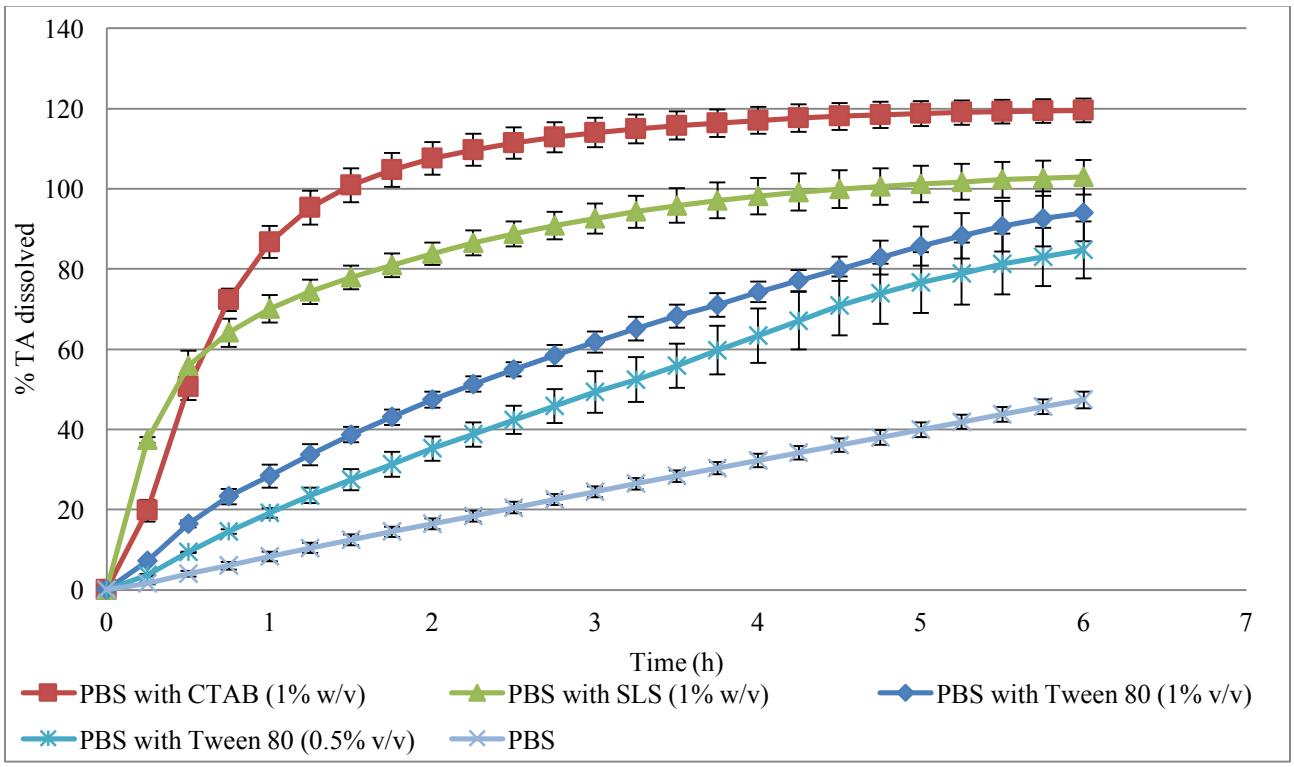

Fig. 2.7. Mean ± SD of TA dissolved from Kenalog 40® with different types of surfactant and in different amounts in the USP apparatus IV in open system (Flow rate: 4 mL/min, Glass bead: 1 mm, Cell size: large).

2.3.5.1.5. Effect of formulation factors

2.3.5.1.5.1. Effect of drug concentration in the suspension

Changing the concentration of the formulation placed on the glass beads had a significant effect on the TA dissolution rate, with the smaller concentration reaching higher % of dissolution

faster. Results show that the % of drug dissolved with the use of 1 mL Adcortyl® (TA 10 mg/mL) seems to reach completion faster than 1mL Kenalog 40® (TA 40 mg/mL) (Fig. 2.8). In terms of absolute amounts of TA dissolved at 6-h, 37.6 mg were dissolved from the Kenalog 40 and 9.9 mg from Adcortyl.

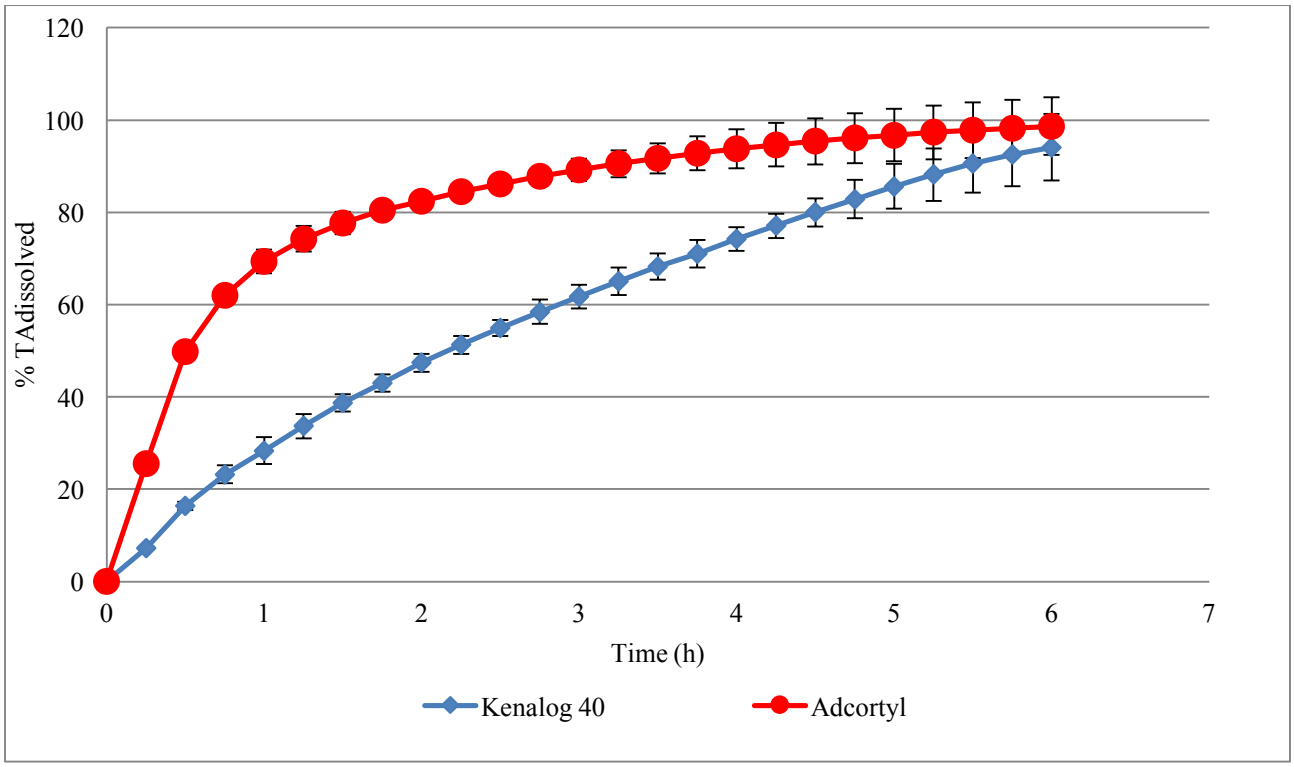

Fig. 2.8. Mean ± SD of TA dissolved in PBS with Tween 80 (1% v/v) from suspensions with different concentrations of TA, in the USP apparatus IV in open system (Flow rate: 4 mL/min, Glass bead: 1 mm, Cell size: large mm, Membrane: GF/F + GF/D)

2.3.5.1.5.2. Effect of formulation type: suspension vs. microparticles

2.3.5.1.5.2.1. Preparation and characterisation of microparticles

The loading of TA was 13.6 and 28.53% for the small and large microparticles developed, respectively, while the particle size was respectively 3.46 and 85.92 µm, with the particle size distribution analysis presented in Table 2.1. Scanning electron microscopy (SEM) revealed that the particles were spherical in shape and mostly appeared in aggregates in both MPa (Fig. 2.9) and MPb (Fig. 2.10) microparticles developed.

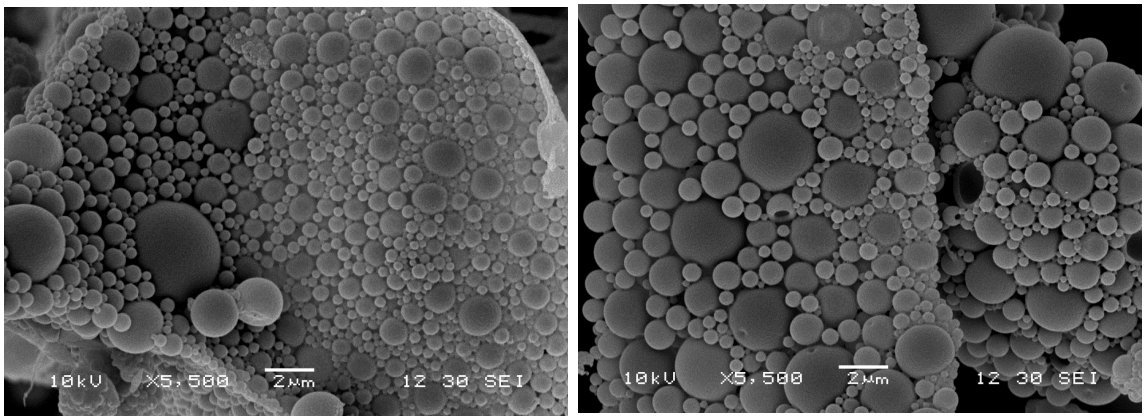

Fig. 2.9. SEM micrographs of the size and surface morphology of MPa

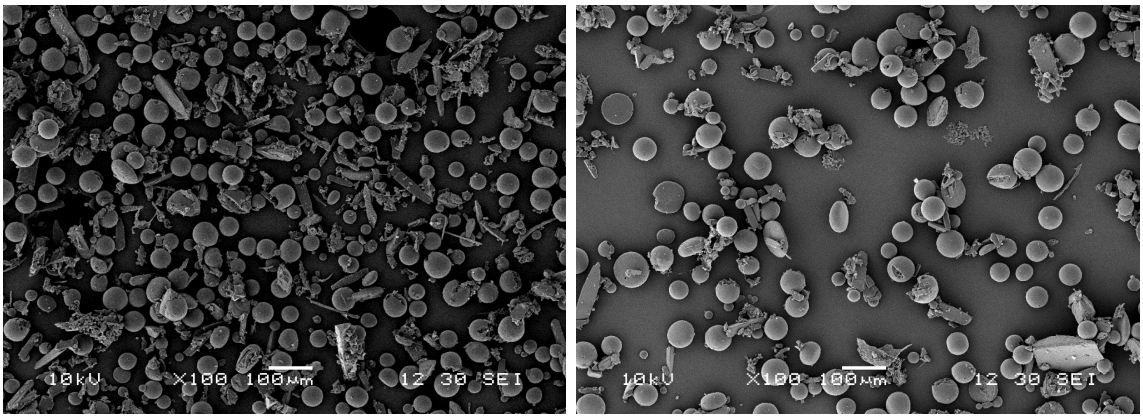

Fig. 2.10. SEM micrographs of the size and surface morphology of MPb

Table 2.1. Physicochemical Characterisation of TA loaded PLA microparticles

Batch	D (v, 0.1) (µm)	D (v, 0.5) (µm)	D (v, 0.9) (µm)	Triamcinolone Acetonide loading (% w/w)	Triamcinolone Acetonide encapsulation efficiency (% w/w)
MPa	3.09	3.46	3.94	13.6 +/- 5.36	41.3 +/- 16.25
MPb	38.42	85.92	141.38	28.53 +/- 1.68	86.45 +/- 5.09
Adcortyl®	4.26	8.45	13.65	-	-
TA powder	82.11	171.43	263.55	-	-

2.3.5.1.5.2.2. In-vitro drug release

The difference in TA release between the suspensions of different particle size (MPa and MPb) was highly significant showing that the dissolution from the large microparticles (MPb) was faster than the small ones (MPa) over a period of 6-h ($f_{2_{small-large}}$= 5.02) (Fig. 2.11). Even though, according the Noyes-Whitney equation [49], increasing the particle size should lead to

decreased dissolution as lower drug diffusion rates result from a smaller particle surface area, here we notice the opposite

The rationale behind the obtained results can be attributed to the properties of the MP suspension in PBS. The formulation containing the MPb powder [D (v, 0.5: 85.92)] has a much higher encapsulation efficacy compared to the formulation containing the MPa powder [D (v, 0.5: 3.46)], meaning that the amount of the poly-lactic acid (PLA) in the MPb powder, for encapsulating the same drug amount (0.1 mg/mL), is lower, affecting wettability (Table 2.1). Poor wettability leads to poor dissolution of the particles and hence drug dissolution from the suspension does not follow the Noyes-Whitney equation [49]. It was also noticeable that the MPa did not dissolve in a similar way with the MPb powder. The small microparticles form a uniformed homogenous milky white suspension in PBS, in comparison with the large microparticles that wouldn't seem to mix properly in the PBS, with the suspension drug particles being visible.

The discriminating ability of the method used with the open system USP apparatus IV, can also be shown when comparing the Adcortyl® suspension (10 mg/mL) with a suspension of TA powder in PBS (10 mg/mL) ($f_{2_{Adcortyl-TA\ powder}}$ = 19.9) (Fig. 2.12). Measuring the particle sizes showed that the TA particles in Adcortyl® are approx. 20x smaller than in the TA powder (Table 2.1). The TA dissolution from the suspensions in this case follow the Noyes-Whitney equation, as increased particle size leads to decreased dissolution, showing that the TA from the Adcortyl® suspension has a faster dissolution rate than the TA powder suspension.

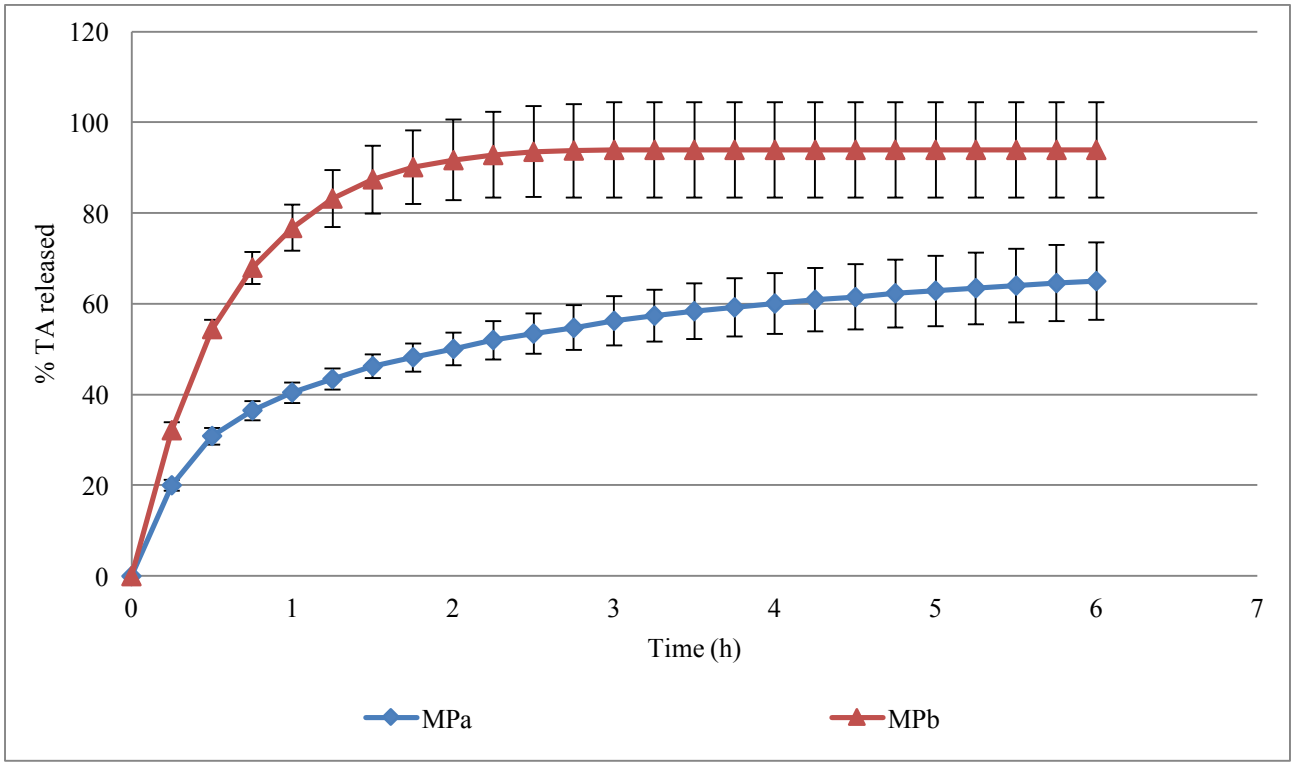

Fig. 2.11. Mean ± SD of TA released from PLA-TA microparticle suspensions in PBS with different particle sizes (Flow rate: 4 mL/min, Glass bead: 1 mm, Cell size: small, filter: Polysulfone 0.2 µm)

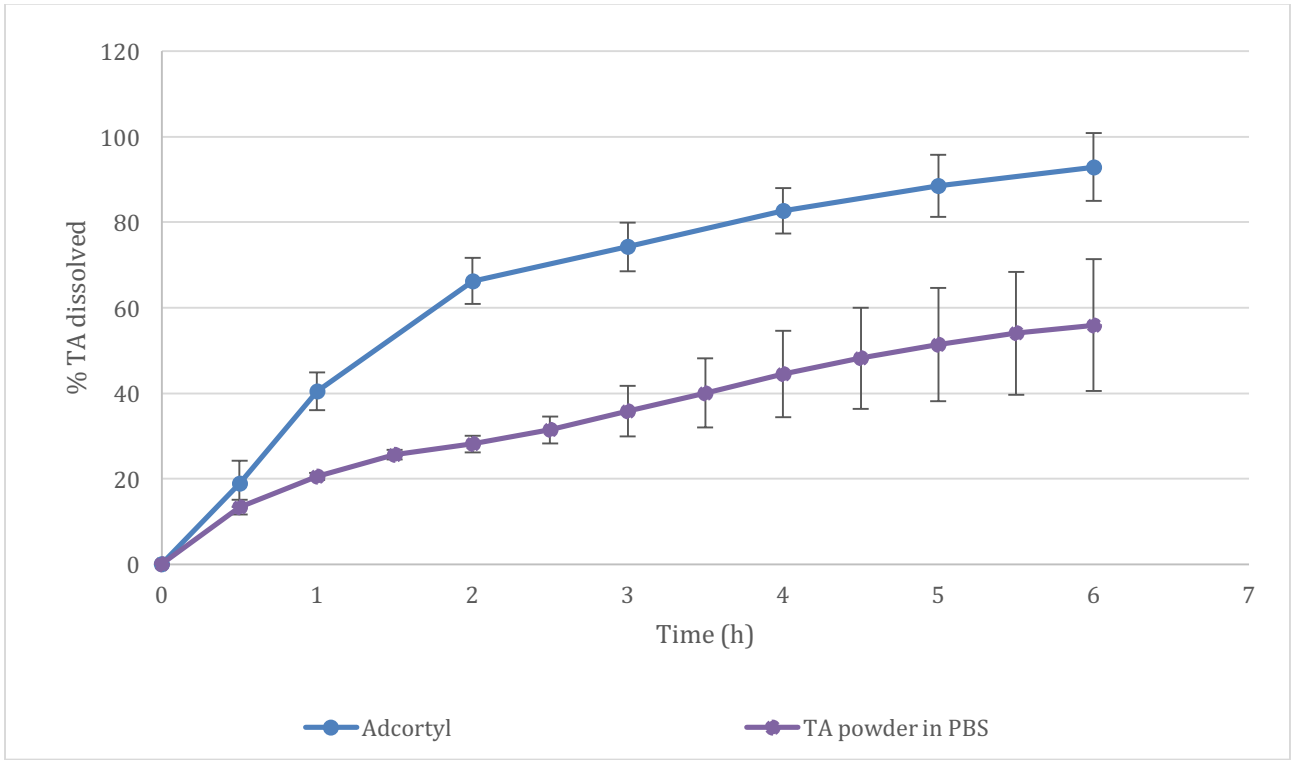

Fig. 2.12. Mean ± SD of TA dissolved from different suspensions in PBS (Flow rate: 4 mL/min, Glass bead: 1 mm, Cell size: large, membrane: GF/F + GF/D, drug amount: 10 mg/mL)

2.3.5.2. Closed mode setup

2.3.5.2.1. Monophasic dissolution setup

Results in the monophasic setup with the closed system of the USP apparatus IV with 60 mL of PBS with Tween 80 (1% v/v) and a dose of 1 mL of TA suspension 40 mg/mL (Kenalog 40®), showed that with no sink conditions present, the % of drug dissolution reached a plateau from the first sampling point and onwards. In order to have had sink conditions for 1 mL of Kenalog 40®, a volume of ~ 9 L of PBS with Tween 80 (1% v/v) is needed, according to the solubility of TA in this medium (91.6 μg/mL) which should be at least 3 times surpassed with the volume of the medium in the receptor phase (Fig. 2.2).

2.3.5.2.2. Bi-phasic dissolution setup

2.3.5.2.2.1. In low volumes (aqueous phase: 40 mL, organic phase: 10 mL)

2.3.5.2.2.1.1. Effect of surfactant in aqueous phase

Using low volumes for the organic (10 mL) and the aqueous phase (40 mL) and ensuring sink conditions as the total dose of drug (10 mg TA) is less than 20% of its solubility in the volume of organic phase (5.2 mg/mL) [28, 31, 54] the partitioning of the drug to the organic phase is significantly higher when the surfactant in the aqueous phase is SLS (1% w/v) compared to Tween 80 (1% v/v) with a difference in dissolution of 20% in 6-h ($f_{2_{SLS-Tween\ 80}}$ = 33.38) (Fig. 2.13). In the aqueous layer with Tween 80 (1% v/v), the % of TA dissolved reaches a plateau, showing that the drug in the aqueous phase is saturated in the setup, while with the use of SLS (1% w/v) in PBS, the % of TA dissolved does not reach a plateau, rather reaches a peak at 30 min and decreases (Fig. 2.13). The partition kinetics of the drug from the aqueous to the organic phase is described by Eq. 4 [55]:

$$\frac{dC_w}{dt} = C_w^2 a + C_w \mathrm{b} + \mathrm{f} \qquad \text{(Eq. 4)}$$

where:

$$a = \frac{A}{V_o}\left(\frac{k_{OW}}{C_{SW}} - \frac{k_{WO}}{C_{SO}}\right)$$

$$b = A\left(\frac{k_{WO}}{C_{SO}V_W}\left(\frac{M_0}{V_o} - C_{SO}\right) - \frac{k_{OW}}{C_{SW}V_o}\left(\frac{M_0}{V_W} - C_{SW}\right)\right)$$

$f = Ak_{OW}\frac{M_0}{V_W V_o}$

and

C_w is the drug concentration in the water phase
t is the time
A is the oil-water interface area
V_o is the oil phase volume
k_{OW} is the oil-water rate partition constant
$C_{SW}$is the drug solubility in the water phase
k_{WO} is the water-oil rate partition constant
C_{SO} is the drug solubility in the oil phase
V_W is the water phase volume
M_0 is the total drug amount present in the two-phases system

A higher amount of drug is dissolved in the aqueous phase when containing PBS with SLS (1% w/v) compared to PBS with Tween 80 (1% v/v) as the solubility of TA is higher in the first compared to the latter (478.01 μg/mL and 91.6 μg/mL respectively) (Fig. 2.2), and subsequently, with a higher drug concentration in the water phase (C_w), partitioning of TA to the organic phase is higher [55]. As the C_w increases (drug dissolution increasing from 56.1 to 70.6%), the rate of partitioning becomes faster than the rate of dissolution, reducing the % of drug dissolved over time in the aqueous phase rather than the plateau previously noticed in PBS with Tween 80 (1% v/v). As the lipophilicity of the drug is exploited in a biphasic system, using different surfactants (anionic, SLS and non-ionic, Tween 80) could influence partitioning; the rate of the partition constant between the aqueous and organic phase (k_{OW} and k_{WO}) changes and so does the partition coefficient, as the solubility of TA in PBS with SLS (1% v/v) is different than in PBS with Tween (1% v/v) (Fig. 2.14) [55, 56]. In addition, due to the ability of the surfactant to increase the hydrophilicity of the suspension [as the non-polar (hydrophobic) region of the created micelles have minimised contact with the aqueous medium], drug partitioning to the organic phase will be reduced [28]. Mixed micelles created by 1-octanol and ionic surfactants can affect drug partitioning, as their relative concentrations may lead to 1-octanol decreasing the critical micelle concentration of the ionic surfactant, leading to increased ionisation of the micelles and changes into the micellar size and structure [55].

2.3.5.2.2.1.2. Effect of flow rate

TA dissolution results with different flow rates showed that sink conditions in the aqueous phase were not maintained in both setups as the % of TA dissolved reaches a plateau from the first sampling point at approximately 20% [according to the solubility of TA in PBS with Tween 80 (1% v/v) being 91.6 μg/mL, Fig. 2.2.] (Fig. 2.13). Dissolution takes place faster than the partitioning of the drug leading to the non-sink conditions in the aqueous phase [31]. Different flow rates (2 and 8 mL/min) showed that by increasing the flow, partitioning to the organic phase increases; with ~55% TA dissolved compared to 40% TA dissolved respectively in the aqueous phase [PBS with Tween 80 (1% v/v)] from the Adcortyl® formulation ($f_{2_{2-8}}$ = 47.29). (Fig. 2.13). Considering the increased partition of TA with the increasing flow rate in the method, the drug can be dissolved faster in the aqueous phase, which consequently can have an effect on partitioning, as there will be an increase in the total drug present in the system (M_0) [56].

2.3.5.2.2.1.3. Effect of cell size

With both the cells tested (large compared to small), the % of TA dissolved from Adcortyl® in the aqueous phase reached a plateau. In the organic solvent, the % of TA dissolved from Adcortyl® with the use of the large cell was 33% in 6-h compared to 18.7% with the use of the small cell ($f_{2_{12-22.6}}$ = 52.46) (Fig. 2.13). By using a large cell in the USP apparatus IV, the interface of the suspension in contact with the aqueous media is increased meaning that there is a higher amount of drug dissolved over time and so a higher concentration of drug present (C_w) [30]. The partitioning kinetics suggest that by increasing the drug dissolved in the aqueous phase (C_w), the total amount present in the system (M_0) increases [56]. This leads to the partitioning of the drug also increasing, resulting in a higher % of TA partitioned to the organic phase [56].

2.3.5.2.2.2. In high volumes (aqueous phase: 300 mL, organic phase: 200 mL)

2.3.5.2.2.2.1. Effect of the presence of surfactant

Results showed that with no surfactant present in the aqueous phase, the % of drug dissolved in PBS reaches a lower plateau at compared to PBS with Tween 80 (1% v/v), which can be explained from the solubility of TA in these media (Fig. 2.14). It is also shown that the % of TA dissolved in the aqueous layer without surfactant (PBS), although reaches a plateau from

1- to 3-h, it seems to reduce and at 6-h it is approximately 10% lesser. This indicates that although the drug present in the aqueous phase was saturated for a 2-h period, drug partitioning then becomes faster than drug dissolution. This does not seem to take place with the presence of a surfactant in the aqueous phase [PBS with Tween 80 (1% v/v) and PBS with SLS (1% v/v)] which increases the hydrophilicity of the suspension [28] that leads to less drug being partitioned into the organic phase. In the organic phase, results confirmed that the amount of drug being partitioned is higher when no surfactant is present with Tween 80 ($f_{2_{no\ surfactant-Tween\ 80}}$ = 62.07) and with SLS ($f_{2_{no\ surfactant-SLS}}$ = 69.16) (Fig. 2.14).

2.3.5.2.2.2.2. Effect of volume and surface area in the aqueous and organic phase

By increasing the volume (High volume, aqueous phase: 300 mL, organic phase: 200 mL) and surface area (High volume in 145.2 cm^2 and low volume in of 58.1 cm^2) in both phases the amount of drug dissolved in the aqueous phase is increased compared to lower volumes (Low volume, aqueous phase: 40 mL, organic phase: 10 mL), with a plateau reached at a higher % of TA dissolved (Fig. 2.13, 2.14). Partitioning takes place in a slower rate than dissolution, which is the reason the plateau is reached. In the organic phase, the partitioning in the lower volume is higher than the partitioning in the high volume ($f_{2_{low-high}}$ = 40) (Fig. 2.13). This can be explained as the TA concentration in the aqueous phase (C_w) is higher in the small volume (0.06 mg/mL) compared to the concentration of TA present in the high volume, (0.02 mg/mL.) (Fig. 2.14) and so with a higher C_w there is higher partitioning to the organic phase [55, 56].

2.3.5.2.2.2.3. Oil-water interface area (A)

The dissolution of TA in the aqueous phase from Adcortyl® in the setup with an oil-water interface area of 145.2 cm^2 compared to the setup with an oil-water interface area of 58.1 cm^2 seems to take place in a slower rate compared to the partitioning of the drug into the organic phase. In the beginning of the experiment TA dissolves faster than it partitions to the organic phase which can explain the peak of the % of TA dissolved in the aqueous phase in 1-h. The increased oil-water interface area (A) (Eq. 4) leads to a faster partitioning rate than dissolution as indicated by the reducing percentage of the drug dissolved in the aqueous phase after 1-h (Fig. 2.14). The % of TA partitioning into the organic phase, happens faster with the use a higher surface area (57%) compared to 13% with the use of a lower surface area ($f_{2_{58.1-145.2}}$ = 28.19) (Fig. 2.14).

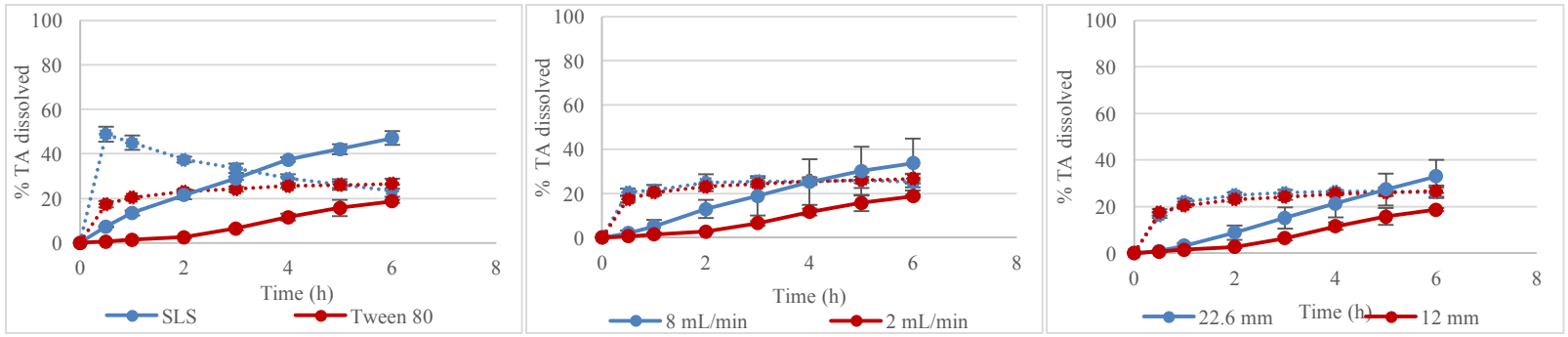

Fig. 2.13. Mean ± SD of % TA dissolved from Adcortyl® in aqueous phase 40 mL (dotted line) and in organic phase (solid line) 10 mL (cell size: small, flow rate 8 mL/min), with the USP apparatus IV in closed system.

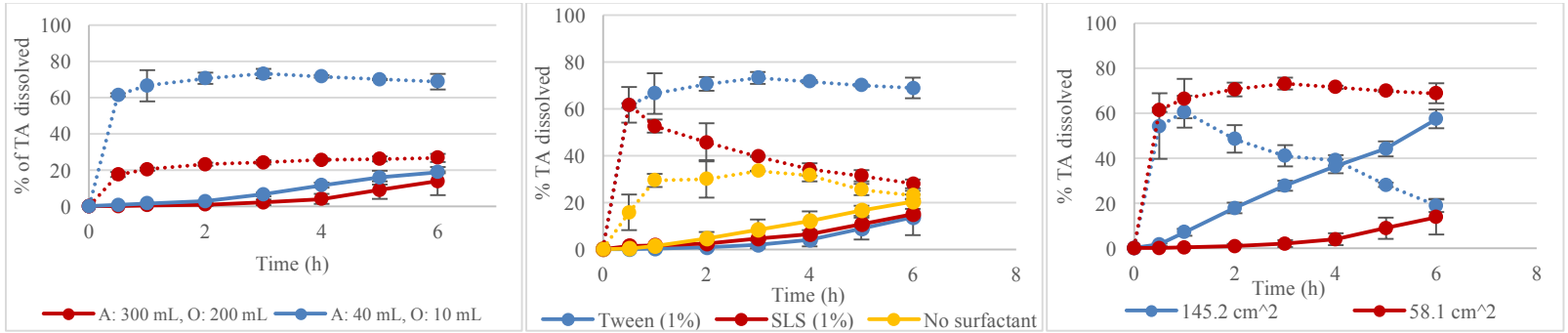

Fig. 2.14. Mean ± SD of % TA dissolved from Adcortyl® in aqueous phase 300 mL (dotted line) and in organic phase (solid line) 200 mL (cell size: small, flow rate 8 mL/min), using with the USP apparatus IV in closed system.

2.3.6. *In-vitro* dissolution studies with the dialysis membrane method in glass bottles

2.3.6.1. Effect of type and amount of surfactant

With 1 mL of Adcortyl® placed in a 1.5 cm length dialysis membrane (donor phase) in 100 mL of PBS with SLS (1% w/v) (receptor phase), there was no significant permeation measured up to 12-h (data not shown). This could be explained from the length of the dialysis membrane, as a small surface-area-to-volume ratio leads to a slower dialysis. Also, as drug dissolution is rapid when the drug is in medium, there are no sink conditions within the membrane, making the diffusion through the membrane, the rate limiting step [26, 46]. As Adcortyl® is an aqueous suspension, after a short amount of time, the drug seems to sediment and form particle aggregates in the dialysis membrane [43]. This happened due to the lack of agitation within the membrane causing problems to the diffusion of the drug [26]. No significant drug dissolution from the formulation was also noted by reducing the amount of drug in the donor phase (from 1 mL [(10 mg TA) to 0.1 mL (1 mg TA)] showing that the amount of drug present in the system is not the primary cause of the method not providing significant results (data not shown), as lack of agitation would still be the key issue. Increasing the volume of medium in the receptor phase and using a different surfactant, [1000 mL of PBS with Tween 80 (1% v/v)] also did not provide significant results (data not shown). By increasing the amount of Tween 80 in the medium, from 1% to 10%, results were not as expected; increasing the amount of surfactant, theoretically, increases the solubility of TA in the medium and so more drug should be dissolved [39, 40]. Results showed that in PBS with Tween 80 (1% v/v), the dissolution is 5% in 12-h compared to TA dissolution in PBS with Tween 80 (10% v/v), where at the same time point it is 0.5%. A higher amount of Tween 80 seems to lead to an increase of the medium viscosity, by forming a barrier on the membrane, decreasing the rate of drug diffusion [22, 27, 57, 58].

2.3.6.2. Effect of increased osmolality in the donor phase

The addition of 400 mg of NaCl to 1 mL of Adcortyl® in the donor phase increases the osmotic pressure in the membrane (from 382 to 500 mOsm) and water diffusion from the lower concentration to the higher concentration through the semi permeable membrane would be expected [59]. According to the phase in which the osmolality will be higher and following the net movement of water, the membrane will swell or shrink. Based on osmosis, where increase of the osmotic pressure occurs inside the membrane, dissolved drug will be diffused to the receptor phase [59-61]. Despite this theoretical reasoning, the dissolved drug measured in the

receptor phase was not significant (data not shown). In order to test if results were influence by the significance of the increase in osmolality, a study was performed with a higher increase in osmolality (from 382 to 2000 mOsm) in the Adcortyl® suspension and a higher receptor volume [PBS with Tween 80 (1% v/v), from 100 to 1000 mL) and an increase in the dialysis membrane length, resulting in an increased surface area (from 1.5 to 20 cm). Results showed that the % of TA dissolved in 8-h was similar (9.3 to 9.7%) showing that the increase in osmolality in the donor phase, does not have a significant effect in TA dissolution from the formulation.

2.3.6.3. Effect of increased osmolality in the receptor phase

Theoretically, increasing the osmolality in the receptor phase would cause the net movement of water from inside the membrane towards the outer part and thus the osmosis of the solvent in the dialysis sac towards the receptor phase. Visually the membrane would shrink due to the movement of the solvent towards the outside compared to increased osmolality inside the membrane, which would cause it to "balloon" and potentially burst or collapse if too much water migrated across it (due to osmotic pressure drawing water in the tubing) [59, 61]. These experiments showed that in a receptor phase of PBS with Tween 80 (1% v/v) with the addition of 6% Potassium Phosphate Dibasic (K_2HPO_4), leading to an osmolality of 1000 mOsm, did not results in significant TA dissolution, while the addition of sucrose in PBS with Tween 80 (1% v/v) (calculated according to the calibration curve presented in Fig. 2.16) led to slightly higher, yet non-significant TA dissolution from the formulation (Fig. 2.15). Addition of different amounts of sucrose [6.4% (500 mOsm) compared to 17% (1000 mOsm)] led to similar non-significant dissolution results with 1% difference at 12-h between the TA dissolved from the formulation (Fig. 2.15). The addition of 28% sucrose (1500 mOsm) gave lower dissolution results than with the lower concentrations of sucrose added to the receptor phase, at 12-h. It was visible that a high addition of sucrose leads to high medium viscosity, which affects the diffusion process similarly to the addition of a high amount of Tween 80.

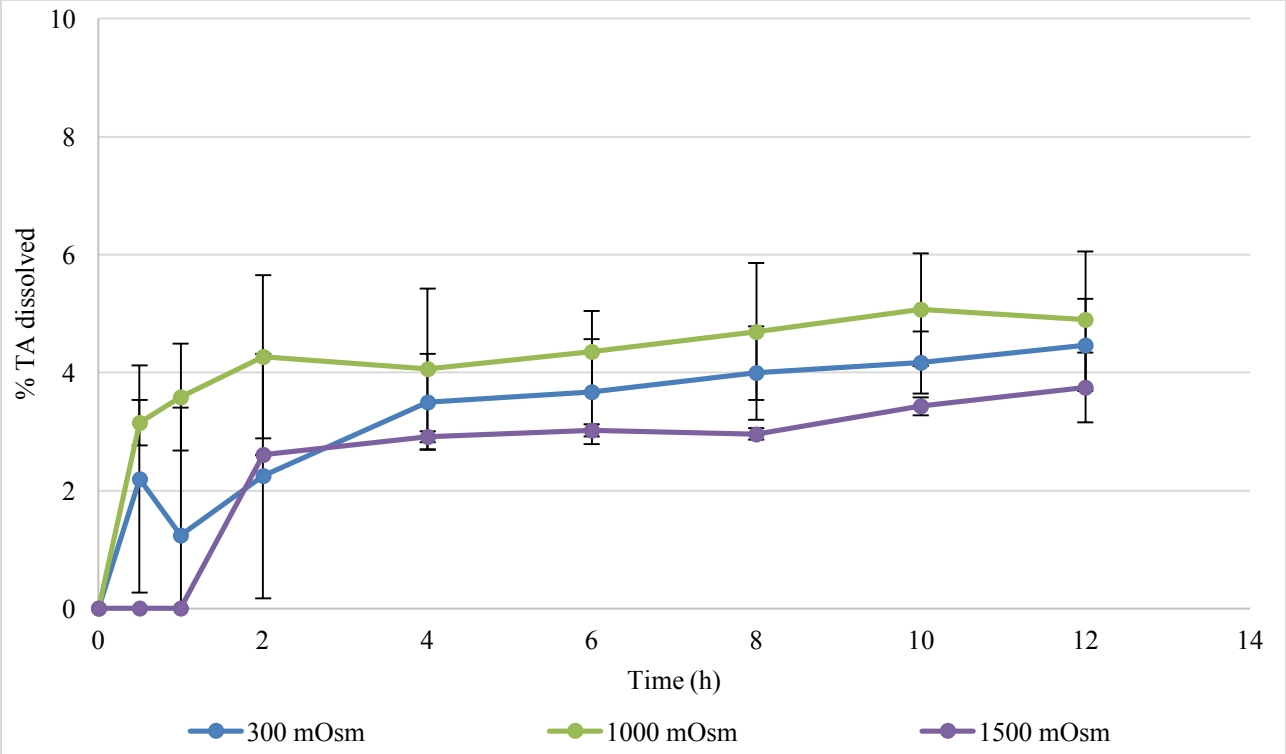

Fig. 2.15. Mean ± SD of TA dissolved from Adcortyl® (1 mL) in 1000 mL PBS with Tween 80 (1% v/v) with different osmolality due to the addition of sucrose

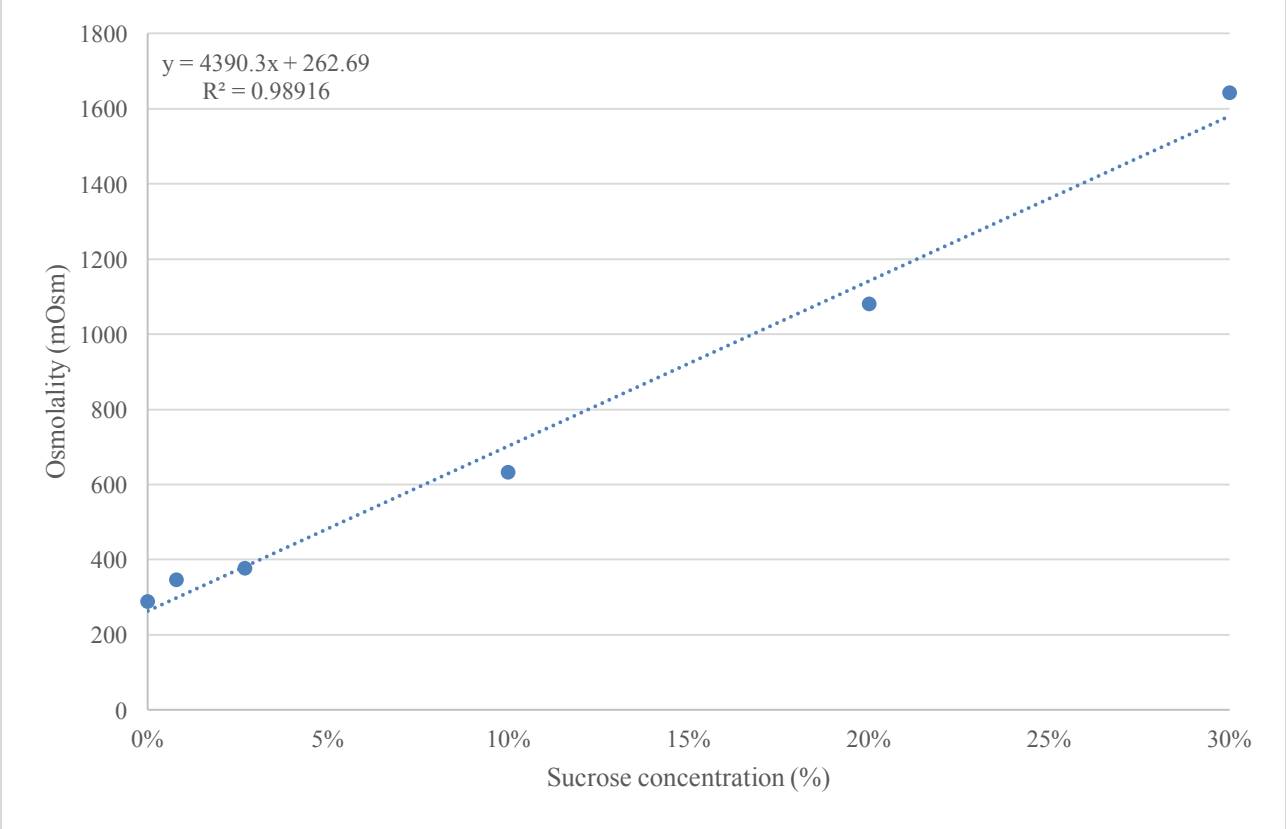

Fig. 2.16. Osmolality of PBS with Tween 80 (1% v/v) with the addition of sucrose

2.3.6.4. Effect of dialysis membrane length

At 8-h, the dissolution of TA from the formulation with the 1.5 cm membrane was 4% compared to 7% from the 10 cm ($f_{2_{1.5-10}}$ = 79.23) and 9% from the 20 cm ($f_{2_{1.5-20}}$ = 73.11) membrane (Fig. 2.17). The highest noticeable difference between the TA dissolution from the formulation with 10 and 20 cm membranes is at 24-h, as there is a TA dissolution from the formulation of 9 and 16% respectively ($f_{2_{10-20}}$ = 74.71). Having a larger membrane contact surface area increased drug permeation, as it may be partially dependent on the contact area of the sample with the membrane [27, 62, 63]. Similar results were shown with added medium in the donor phase [1 mL Adcortyl® + 9 mL of PBS with Tween 80 (1% v/v)] comparing TA dissolution from the formulation with dialysis membrane lengths of 10 and 20 cm ($f_{2_{10-20}}$ = 82.49) (Fig. 2.17).

2.3.6.5. Effect of temperature of medium

Increasing the temperature of the medium to 60 ^{o}C, at 24-h shows a clear difference in % of drug dissolved comparing the methods with increasing surface area. In the 1.5 cm membrane, there was a 12.5% of TA dissolved, compared to 23% from the 10 cm ($f_{2_{1.5-10}}$ = 59.98) and 34.5% from the 20 cm ($f_{2_{1.5-20}}$ = 44.34) (Fig. 2.17) proving that an increase in the temperature of the setup leads to a more accelerated dissolution of TA from the formulation and diffusion through the membrane as high temperature increases molecular mobility and subsequently drug dissolution [26, 64].

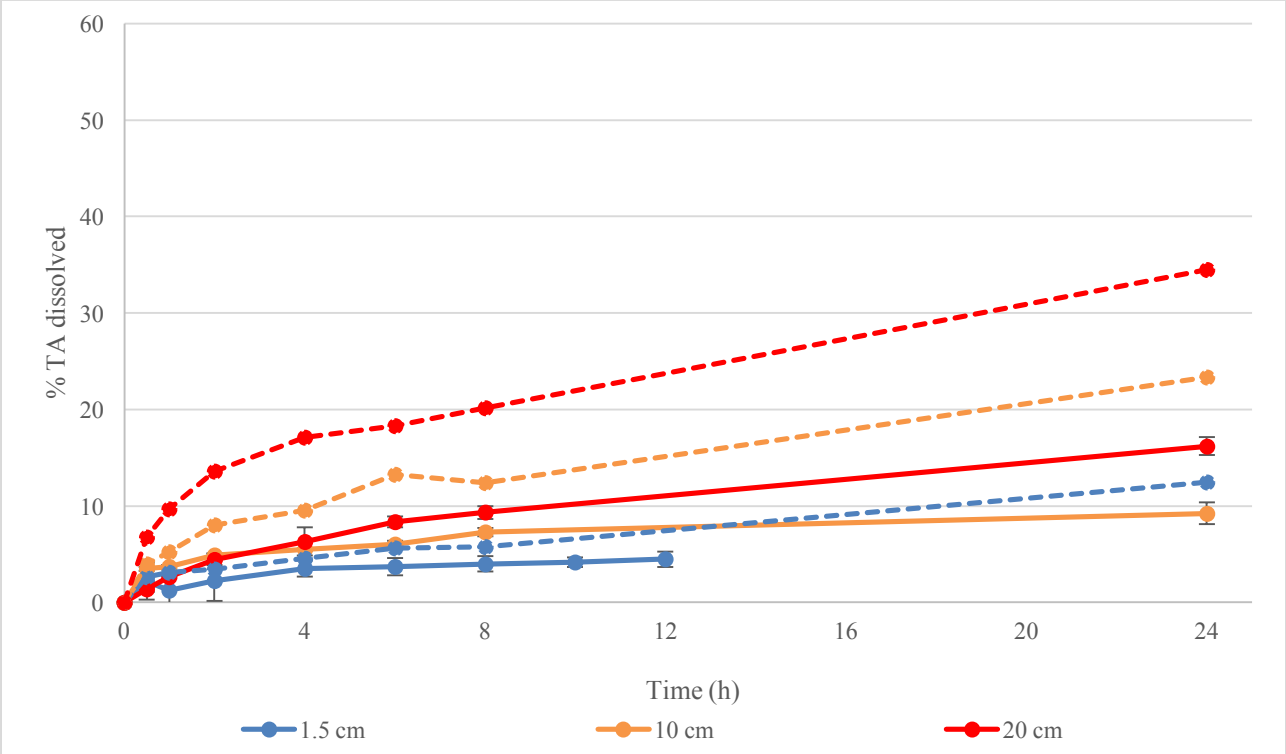

Fig. 2.17. Mean ± SD of TA dissolved from Adcortyl® (1 mL) in 1000 mL PBS with Tween 80 (1% v/v) with different lengths of dialysis membrane at 37 °C (solid lines) and at 60 °C (dashed lines)

2.3.6.6. Effect of increased volume of the donor phase (medium added to donor phase)

Comparing TA dissolution between the donor phase containing Adcortyl® (1 mL) or Adcortyl® with the addition of PBS with Tween 80 (1% v/v) (1 + 9 mL), showed TA dissolution of 16% and 13% respectively in 24-h ($f_{2_{1-1+9}}$ = 85.92) (Fig. 2.18). Theoretically, as medium is added in the donor phase, more drug can dissolve from the suspension and permeate through the membrane to the receptor phase. As a higher amount of drug is dissolved with Adcortyl® (1 mL) compared to Adcortyl® with additional medium (1 + 9 mL), adding medium inside the dialysis membrane did not lead to higher TA dissolution and diffusion through the membrane [27], with the diffusion possibly being the rate-limiting step for the method [24].

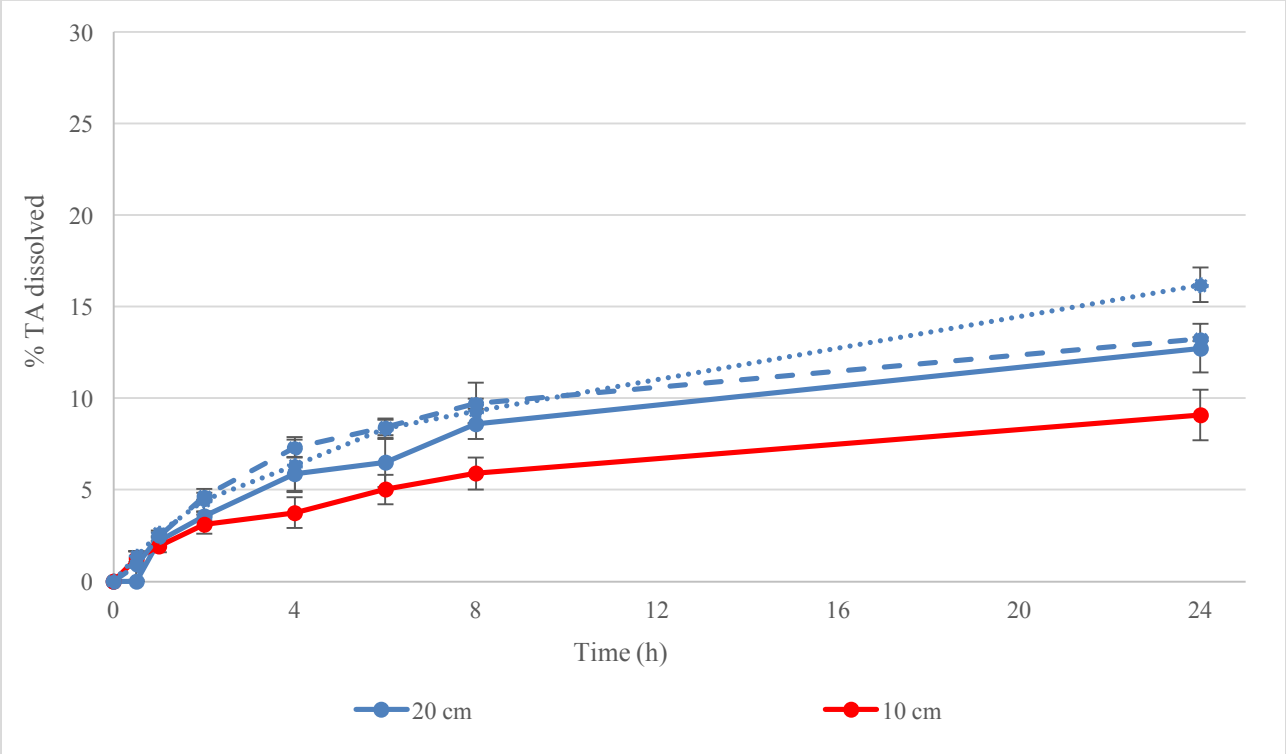

Fig. 2.18. Mean ± SD of TA dissolved from Adcortyl® with additional medium in the donor phase (1 mL + 9 mL) (solid lines), Adcortyl® (1mL) (dotted line) and Adcortyl® (1 mL with 2000 mOsm) (dashed lines) in 1000 mL PBS with Tween 80 (1% v/v) with different length of dialysis membrane

2.3.6.7. Organic solvent in receptor phase

2.3.6.7.1. Effect of drug concentration in the suspension

Comparing the amount of drug dissolved from a dose of 1 mL of TA suspension [10 mg/mL (Adcortyl®) and 40 mg/mL (Kenalog 40®)] and diffused from the dialysis membrane in PBS with methanol (50% v/v) became evident after 2-h ($f_{2_{Adcortyl-Kenalog\ 40}}$ = 35.01) (Fig. 2.19). In order to accelerate drug dissolution, adding an organic solvent in the aqueous buffer medium has proven to be advantageous [26]. With the 1 mL dose containing Kenalog 40® compared to Adcortyl®, drug permeation rate increased indicating a passive diffusion process, with the concentration driving force playing the important role, following the 1st Fick's law [27].

2.3.6.7.2. Effect of formulation type

2.3.6.7.2.1. TA solution vs. suspension

Comparing TA dissolution from a dose of 1 mL solution of 5 mg/mL TA in MeOH with a dose of 0.5 mL of suspension [Adcortyl® (5 mg TA)] showed that the dissolved drug compared to the drug in suspension, permeates through the semi-permeable membrane faster ($f_{2_{solution-suspension}}$ = 18.72) (Fig. 2.19). This can be explained as the drug in solution is already dissolved and able to permeate through the membrane, while the drug in suspension as will have to first dissolve and then permeate through the membrane [27, 65].

2.3.6.7.2.2. TA suspension with different volume of methanol

Results between TA suspensions of 10 mg/mL with a different methanol volume, [TA powder in 1 mL PBS with MeOH (90% v/v) and TA powder in 1 mL PBS with MeOH (50%) v/v], showed that the suspension with a higher amount led to higher percentages of drug dissolved at the end of 12-h ($f_{2_{10/90-50/50}}$ = 27.16) (Fig. 2.19). This can be explained as the suspension with a higher amount of methanol contains a higher amount of dissolved drug which can permeate through the membrane more rapidly [27, 65].

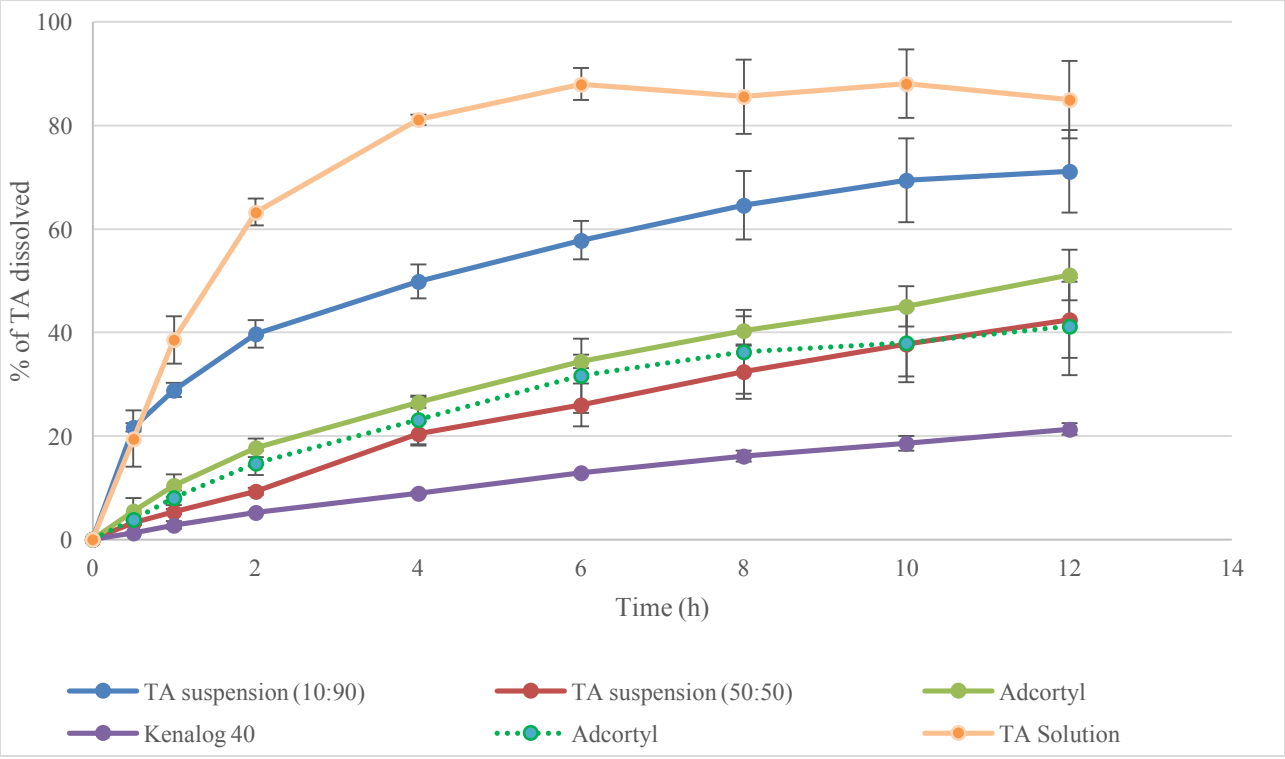

Fig. 2.19. Mean ± SD of TA % dissolved from formulations with the dialysis membrane method [100 mL PBS with MeOH (50% v/v), membrane length: 1.5 cm, volume: 1 mL (solid line), 0.5 mL (dotted line)]

2.3.6.7.3. Effect of organic solvent type

Increasing the % of ethanol added to PBS leads to slightly higher amounts of TA diffused from the dialysis membrane although results is of non-significance (data not shown). The dissolution of TA is significantly higher with the use of methanol in the medium, as a co-solvent system has a reduction of water-to-water interactions due to the presence of hydrogen bond donating or accepting regions and also hydrocarbon regions. This leads to the system being more favourable for non-polar solutes [42].

2.4. Conclusions

The effect of various factors on drug dissolution from parenteral suspensions was successfully evaluated with the selected dissolution methods. Using the USP apparatus II revealed that placing the suspension directly in PBS will lead to a plateau in dissolution after the first 10 min according to the solubility of the drug in the medium. In the USP apparatus I and III, with the use of float-A-lyzers, there was no drug dissolution from the formulation measured. With the use of the USP apparatus IV open system, the parameters tested, including hydrodynamics (flow rate and cell size), sample position, different type and amount of surfactants added to the medium, the type of filter used and the concentration of TA in the suspension had a significant effect on drug dissolution from the formulation. The discrimination power of the USP apparatus IV method was also shown by testing dissolution profiles of different microparticle sizes. The effect of glass bead size on the dissolution of TA was not significant. In the closed system, with the use of a bi-phasic setup, the factors tested seem to affect the partitioning of the drug to the organic phase without affecting the plateau reached in the aqueous phase. The change in the oil-water interface area compared to all the factors tested, seemed to lead to faster partitioning rather than dissolution of the drug. Using the dialysis membrane methodology, with PBS in the receptor phase and the donor phase of a short dialysis membrane length, the drug did not migrate through the membrane. Also, with increased surfactant in the receptor phase, increase osmolality in the donor phase and additional volume in the donor phase (addition of medium), there was no drug dissolution from the formulation. Results were promising when a significantly high difference of osmolality was present with the use of methanol in the receptor phase, with an increase in dialysis surface area and by accelerating the dissolution by increasing the temperature of the medium. The flow-through cell dissolution method provided an appropriate method to characterise parenteral formulations and set specifications, that could be used for the development of a compendial dissolution method for these intra-articular suspensions.

2.5. References

1. Kang, M.L. and Im G.I., *Drug delivery systems for intra-articular treatment of osteoarthritis.* Expert Opin Drug Deliv, 2014. **11**(2): p. 269-82.
2. Lavelle, W., E.D. Lavelle, and L. Lavelle, *Intra-articular injections.* Anesthesiol Clin, 2007. **25**(4): p. 853-62, viii.
3. Uthman, I., J.P. Raynauld, and B. Haraoui, *Intra-articular therapy in osteoarthritis.* Postgrad Med J, 2003. **79**(934): p. 449-53.
4. Gerwin, N., C. Hops, and A. Lucke, *Intraarticular drug delivery in osteoarthritis.* Adv Drug Deliv Rev, 2006. **58**(2): p. 226-42.
5. Rodriguez-Merchan, E.C., *Intra-articular Injections of Hyaluronic Acid and Other Drugs in the Knee Joint.* HSS Journal, 2013. **9**(2): p. 180-182.
6. Moreland, L.W., *Intra-articular hyaluronan (hyaluronic acid) and hylans for the treatment of osteoarthritis: mechanisms of action.* Arthritis Research & Therapy, 2003. **5**(2): p. 54-67.
7. Edwards, S.H., *Intra-articular drug delivery: the challenge to extend drug residence time within the joint.* Vet J, 2011. **190**(1): p. 15-21.
8. Allen, K.D., S.B. Adams, and L.A. Setton, *Evaluating intra-articular drug delivery for the treatment of osteoarthritis in a rat model.* Tissue Eng Part B Rev, 2010. **16**(1): p. 81-92.
9. Bédouet, L., Pascale, F., Moine, L., Wassef., M., Ghegediban, S.H., Nguyen, V.N., Bonneau, M., Labarre, D., Laurent, A., *Intra-articular fate of degradable poly(ethyleneglycol)-hydrogel microspheres as carriers for sustained drug delivery.* International Journal of Pharmaceutics, 2013. **456**(2): p. 536-544.
10. Edwards, S.H., Cake, M.A., Spoelstra, G., Read, R.A., *Biodistribution and clearance of intra-articular liposomes in a large animal model using a radiographic marker.* J Liposome Res, 2007. **17**(3-4): p. 249-61.
11. Thakkar, H., R. Kumar Sharma, and R.S. Murthy, *Enhanced retention of celecoxib-loaded solid lipid nanoparticles after intra-articular administration.* Drugs R D, 2007. **8**(5): p. 275-85.
12. Rothenfluh, D.A., Bermudez, H., O'Neil, C.P., Hubbell, J.A., *Biofunctional polymer nanoparticles for intra-articular targeting and retention in cartilage.* Nat Mater, 2008. **7**(3): p. 248-54.
13. Burt, H.M., Tsallas, A., Gilchrist, S., Liang L.S., *Intra-articular drug delivery systems: Overcoming the shortcomings of joint disease therapy.* Expert Opin Drug Deliv, 2009. **6**(1): p. 17-26.
14. Liang, L.S., Jackson, J., Min, W., Risovic, V., Wasan, K.M., Burt, H.M., *Methotrexate loaded poly(L-lactic acid) microspheres for intra-articular delivery of methotrexate to the joint.* J Pharm Sci, 2004. **93**(4): p. 943-56.
15. Larsen, C., Ostergaard, J., Larsen, S.W., Jensen, H., Jacobsen, S., Lindergaard, C., Andersen, P.H., *Intra-articular depot formulation principles: role in the management of postoperative pain and arthritic disorders.* J Pharm Sci, 2008. **97**(11): p. 4622-54.
16. Brown, C.K., Friedel, H.D., Barker, A.R., Buhse, L.F., Keitel, S., Cecil, T.L., Kraemer, J., Morris, J.M., Reppas, C., Stickelmeyer, M.P., Yomota, C., Shah, V.P., *FIP/AAPS joint workshop report: dissolution/in-vitro release testing of novel/special dosage forms.* AAPS PharmSciTech, 2011. **12**(2): p. 782-94.
17. Wang, Q.X., N. Fotaki, and Y. Mao, *Biorelevant Dissolution: Methodology and Application in Drug Development.* Dissolution Technologies, 2009. **16**(3): p. 6-12.

18. Siewert, M., Dressman, J., Brown, C.K., Shah, V.P., FIP, AAPS, *FIP/AAPS guidelines to dissolution/in-vitro release testing of novel/special dosage forms.* AAPS PharmSciTech, 2003. **4**(1): p. 43-52.
19. D'Souza, S.S. and P.P. DeLuca, *Methods to assess in-vitro drug release from injectable polymeric particulate systems.* Pharm Res, 2006. **23**(3): p. 460-74.
20. Butoescu, N., Jordan, O., Burdet, P., Stadelmann, P., Petri-Fink, A., Hofmann, H., Doelker, E., *Dexamethasone-containing biodegradable superparamagnetic microparticles for intra-articular administration: physicochemical and magnetic properties, in-vitro and in-vivo drug release.* Eur J Pharm Biopharm, 2009. **72**(3): p. 529-38.
21. Kawadkar, J. and M.K. Chauhan, *Intra-articular delivery of genipin cross-linked chitosan microspheres of flurbiprofen: preparation, characterisation, in-vitro and in-vivo studies.* Eur J Pharm Biopharm, 2012. **81**(3): p. 563-72.
22. Sterner, B., Harms, M., Weigandt, M., Windbergs, M., Lehr, C.M., *Crystal suspensions of poorly soluble peptides for intra-articular application: A novel approach for biorelevant assessment of their in-vitro release.* Int J Pharm, 2013.
23. Dong, J., Jiang, D., Wang, Z., Wu, G., Miao, L., Huang, L., *Intra-articular delivery of liposomal celecoxib–hyaluronate combination for the treatment of osteoarthritis in rabbit model.* International Journal of Pharmaceutics, 2013. **441**(1–2): p. 285-290.
24. D'Souza, S.S. and P.P. DeLuca, *Development of a dialysis in-vitro release method for biodegradable microspheres.* AAPS PharmSciTech, 2005. **6**(2): p. E323-8.
25. Seidlitz, A. and W. Weitschies, *In-vitro dissolution methods for controlled release parenterals and their applicability to drug-eluting stent testing.* J Pharm Pharmacol, 2012. **64**(7): p. 969-85.
26. Shen, J. and D.J. Burgess, *Accelerated in-vitro release testing methods for extended-release parenteral dosage forms.* J Pharm Pharmacol, 2012. **64**(7): p. 986-96.
27. Gao, Z. and B. Westenberger, *Dissolution testing of acetaminophen suspension using dialysis adapter in flow-through apparatus: a technical note.* AAPS PharmSciTech, 2012. **13**(3): p. 944-8.
28. Phillips, D.J., Pygall, S.R., Cooper, V.B., Mann, J.C., *Overcoming sink limitations in dissolution testing: a review of traditional methods and the potential utility of biphasic systems.* J Pharm Pharmacol, 2012. **64**(11): p. 1549-59.
29. Bhattachar, S.N., Wesley, J.A., Fioritto, A., Martin, P.J., Babu, S.R. , *Dissolution testing of a poorly soluble compound using the flow-through cell dissolution apparatus.* Int J Pharm, 2002. **236**(1-2): p. 135-43.
30. Fotaki, N., *Flow-Through Cell Apparatus (USP Apparatus 4): Operation and Features.* Dissolution Technologies, 2011.
31. Hoa, N.T. and R. Kinget, *Design and evaluation of two-phase partition-dissolution method and its use in evaluating artemisinin tablets.* J Pharm Sci, 1996. **85**(10): p. 1060-3.
32. Ungphaiboon, S., Nittayananta, W., Vuddhakul, V., Maneenuan, D., Kietthubthew, S., Wongpoowarak, W., Phadoongsombat, N. , *Formulation and efficacy of triamcinolone acetonide mouthwash for treating oral lichen planus.* Am J Health Syst Pharm, 2005. **62**(5): p. 485-91.
33. Kadam, R.S., Tyagi, P., Edelhauser, H.F., Kompella, U.B., *Influence of choroidal neovascularization and biodegradable polymeric particle size on transscleral sustained delivery of triamcinolone acetonide.* Int J Pharm, 2012. **434**(1-2): p. 140-7.
34. Kulkarni, S.S. and U.B. Kompella, *Nanoparticles for Drug and Gene Delivery in Treating Diseases of the Eye*, in *Ocular Pharmacology and Toxicology*, B.C. Gilger, Editor. 2014, Humana Press: Totowa, NJ. p. 291-316.

35. Tomaszewska, I., Karki, S., Shur, J., Price, R., Fotaki, N., *Pharmaceutical characterisation and evaluation of cocrystals: Importance of in-vitro dissolution conditions and type of coformer.* Int J Pharm, 2013. **453**(2): p. 380-8.
36. Jantratid, E., De Maio, V., Ronda, E., Mattavelli, V., Vertzoni, M., Dressman, J.B., *Application of biorelevant dissolution tests to the prediction of in-vivo performance of diclofenac sodium from an oral modified-release pellet dosage form.* Eur J Pharm Sci, 2009. **37**(3-4): p. 434-41.
37. Vertzoni, M., Symillides, M., Iliadis, A., Nicolaides, E., Reppas, C., *Comparison of simulated cumulative drug versus time data sets with indices.* European Journal of Pharmaceutics and Biopharmaceutics, 2003. **56**(3): p. 421-428.
38. Zhang, Y., Huo, M., Zhou, J., Zou, A., Li, W., Yao, C., Xie, S., *DDSolver: An Add-In Program for Modeling and Comparison of Drug Dissolution Profiles.* The AAPS Journal, 2010. **12**(3): p. 263-271.
39. Park, S.H. and H.K. Choi, *The effects of surfactants on the dissolution profiles of poorly water-soluble acidic drugs.* Int J Pharm, 2006. **321**(1-2): p. 35-41.
40. Fotaki, N., Brown, W., Kochling, J., Chokshi, H., Miao, H., Tang, K., Gray, V., *Rationale for selection of dissolution media: three case studies.* Dissolution Technologies, 2013. **20**(3): p. 6-13.
41. Balakrishnan, A., Rege, B. D., Amidon, G. L., Polli, J. E., *Surfactant-mediated dissolution: contributions of solubility enhancement and relatievely low micelle diffusivity.* J Pharm Sci., 2004. **93**(8): p. 2064-75.
42. Walden, M., Nicholls, F.A., Smith, K.J., Tucker, G.T., *The effect of ethanol on the release of opioids from oral prolonged-release preparations.* Drug Dev Ind Pharm, 2007. **33**(10): p. 1101-11.
43. Martinez, M., Rathbone, M., Burgess, D., Huynh, M., *In-vitro and in-vivo considerations associated with parenteral sustained release products: a review based upon information presented and points expressed at the 2007 Controlled Release Society Annual Meeting.* J Control Release, 2008. **129**(2): p. 79-87.
44. Zhang, G.H., Vadino, W.A., Yang, T.T., Cho, W.P., Chaundry, I.A., *Evaluation of the Flow-Through Cell Dissolution Apparatus: Effects of Flow Rate, Glass Beads and Tablet Position on Drug Release from Different Type of Tablets.* Drug Development and Industrial Pharmacy, 1994. **20**(13): p. 2063-2078.
45. Kastellorizios, M. and D.J. Burgess, *In-vitro Drug Release Testing and In-vivo/In-vitro Correlation for Long Acting Implants and Injections*, in *Long Acting Injections and Implants*, J.C. Wright and D.J. Burgess, Editors. 2012, Springer US: Boston, MA. p. 475-503.
46. Shah, V.P., J. DeMuth, and D.G. Hunt, *Performance Test for Parenteral Dosage Forms.* Dissolution Technologies, 2015. **22**(4): p. 16-21.
47. D'Arcy, D.M., Liu, B., Bradley, G., Healy, A.M., Corrigan, O.I., *Hydrodynamic and species transfer simulations in the USP 4 dissolution apparatus: considerations for dissolution in a low velocity pulsing flow.* Pharm Res, 2010. **27**(2): p. 246-58.
48. Kakhi, M., *Classification of the flow regimes in the flow-through cell.* European Journal of Pharmaceutical Sciences, 2009. **37**(5): p. 531-544.
49. Abdel-Mottaleb, M.M. and A. Lamprecht, *Standardized in-vitro drug release test for colloidal drug carriers using modified USP dissolution apparatus I.* Drug Dev Ind Pharm, 2011. **37**(2): p. 178-84.
50. Brown, W., *Apparatus 4 Flow Through Cell: Some Thoughts on Operational Characteristics.* Dissolution Technologies, 2005. **12**(2): p. 28-30.
51. Kerns, E.H. and L. Di, *Chapter 7 - Solubility*, in *Drug-like Properties: Concepts, Structure Design and Methods*. 2008, Academic Press: San Diego. p. 56-85.

52. Qureshi, S.A., Caille, G., Brien, R., Piccirilli, G., Yu, V., McGilveray, I.J., *Application of Flow-Through Dissolution Method for the Evaluation of Oral Formulations of Nifedipine.* Drug Development and Industrial Pharmacy, 1994. **20**(11): p. 1869-1882.
53. Savjani, K.T., A.K. Gajjar, and J.K. Savjani, *Drug Solubility: Importance and Enhancement Techniques.* ISRN Pharmaceutics, 2012. **2012**: p. 195727.
54. Thakur, A., R.S. Kadam, and U.B. Kompella, *Influence of drug solubility and lipophilicity on transscleral retinal delivery of six corticosteroids.* Drug Metab Dispos, 2011. **39**(5): p. 771-81.
55. Mudie, D.M., Shi, Y., Ping, H., Gao, P., Amidon, G.L., Amidon, G.E. , *Mechanistic analysis of solute transport in an in-vitro physiological two-phase dissolution apparatus.* Biopharm Drug Dispos, 2012. **33**(7): p. 378-402.
56. Grassi, M., N. Coceani, and L. Magarotto, *Modelling partitioning of sparingly soluble drugs in a two-phase liquid system.* Int J Pharm, 2002. **239**(1-2): p. 157-69.
57. Braun, R.J. and E.L. Parrott, *Influence of Viscosity and Solubilisation on Dissolution Rate.* Journal of Pharmaceutical Sciences, 1972. **61**(2): p. 175-178.
58. Xu, X., M.A. Khan, and D.J. Burgess, *A two-stage reverse dialysis in-vitro dissolution testing method for passive targeted liposomes.* Int J Pharm, 2012. **426**(1-2): p. 211-8.
59. Aulton, M.E., Properties of solutions, in Aulton's Pharmaceutics. The design and manufacture of medicines, M.E. Aulton, Editor. 2007, Churchill Livingstone, Elsevier. p. 33-42.
60. Gupta, B.P., Thakur, N., Jain, N.P., Banweer, J., Jain, S., *Osmotically controlled drug delivery system with associated drugs.* J Pharm Pharm Sci, 2010. **13**(4): p. 571-88.
61. Keraliya, R.A., Patel, C., Patel P., Keraliya, V., Soni, T.G., Patel, R.C., Patel, M.M., *Osmotic drug delivery system as a part of modified release dosage form.* ISRN Pharm, 2012. **2012**: p. 528079.
62. Larsen, D.H., K. Fredholt, and C. Larsen, *Assessment of rate of drug release from oil vehicle using a rotating dialysis cell.* Eur J Pharm Sci, 2000. **11**(3): p. 223-9.
63. Thing, M., Larsen, C., Ostergaard, J., Jensen, H., Larsen, S.W., *In-vitro release from oil injectables for intra-articular administration: Importance of interfacial area, diffusivity and partitioning.* Eur J Pharm Sci, 2012. **45**(3): p. 351-7.
64. Kamberi, M., Nayak, S., Myo-Min, K., Carter, T.P., Hancock, L., Feder, D., *A novel accelerated in-vitro release method for biodegradable coating of drug eluting stents: Insight to the drug release mechanisms.* Eur J Pharm Sci, 2009. **37**(3-4): p. 217-22.
65. Ostergaard, J., Larsen, S.W., Parshad, H., Larsen, C., *Bupivacaine salts of diflunisal and other aromatic hydroxycarboxylic acids: aqueous solubility and release characteristics from solutions and suspensions using a rotating dialysis cell model.* Eur J Pharm Sci, 2005. **26**(3-4): p. 280-7.

Chapter 3: Characterisation of *in-vivo* disease state synovial fluid towards the development of simulated synovial fluid

Overview

Purpose: To develop and characterise biorelevant media that simulate the environment of healthy and disease state synovial fluid, based on the physicochemical properties of the corresponding *in-vivo* fluids and reveal the similarity of drug solubilisation in the *in-vivo* and biorelevant synovial fluids.

Methods: The characterisation of *in-vivo* Osteoarthritis (OA) and Rheumatoid Arthritis (RA) synovial fluids and developed Biorelevant Synovial Fluids (BSFs) took place by measuring their physicochemical properties (pH, viscosity, surface tension, osmolality). Viscosity was measured against shear rate using a cone and plate viscometer, pH was measured with a pH/Ion meter, surface tension with the Du Nouy ring method and osmolality by freezing-point depression. Based on the properties of the *in-vivo* fluids, biorelevant media were designed to reflect conditions in the synovial joint cavity during healthy state, OA and RA. Solubility studies of Triamcinolone Acetonide (TA) were also performed in the *in-vivo* and *in-vitro* synovial fluid with the shake flask method in a temperature controlled water bath.

Results: Measurements of OA and RA *in-vivo* synovial fluids formed the basis for the development of the three BSFs (healthy state, OA and RA), with solubility studies performed to show biorelevance between *in-vivo* and *in-vitro* synovial fluid. Viscosity of the biorelevant media was not in accordance to the *in-vivo* measurements with the use of the average amounts of HA, and so Carboxymethylcellulose (CMC) or an increased amount of HA were used as viscosity enhancers. Solubility of TA in the *in-vivo* and *in-vitro* synovial fluid were increased with the addition of phospholipids in the developed media. Comparing solubility results of the *in-vivo* and *in-vitro* disease state (OA and RA) revealed that the latter were slightly lower.

Conclusions: The developed media with the addition of a viscosity enhancer, reflect the physicochemical properties of the *in-vivo* fluids, and present a higher physiological relevance to previously used artificial synovial fluid.

3.1. Introduction

In recent years, there has been a strong interest in the pharmaceutical industry for the development of parenteral formulations. Their various advantages, compared to the oral administration route that is mostly preferred due to its convenience in drug delivery, have resulted in a high number of marketed products [1]. A vital part in the development of these drugs and formulations is assessing their dissolution behaviour in an environment simulating *in-vivo* conditions, such as conditions in the joint cavity. The physiological environment of synovial fluid determines significantly the *in-vivo* performance of the drug administered through the IA route with factors such as pH, osmolality, surface tension and especially viscosity being of primary importance [2].

The lubricating and viscoelastic ability of HA has been determined from a variety of studies [3-8]. Viscosity has an important effect on dissolution rate and by following the Noyes–Whitney equation (Eq. 1) where the diffusion coefficient, D, is partly related to the solvent viscosity, the dissolution rate will decrease with the increasing viscosity of the medium; as D is inversely proportional to the viscosity [9]. This is shown in the Stokes–Einstein equation (Eq. 2), as the viscosity of the medium, among other parameters affects the diffusion coefficient D and consequently the dissolution rate with an inverse proportional correlation:

$$\frac{dm}{dt} = A\frac{D}{d}(C_s - C_b) \qquad \text{(Eq. 1)}$$

where

dm/dt = solute dissolution rate (kg x s^{-1})
m = mass of dissolved material (kg)
t = time (s)
A = surface area of the solute particle (m^2)
D = diffusion coefficient (m x s^{-1})
d = thickness of the concentration gradient (m)
C_s = particle surface (saturation) concentration (kg or moles/L)
C_b = concentration in the bulk solvent/solution (kg or moles/L)

and

$$D = \frac{kT}{6\pi\eta r} \quad \text{(Eq. 2)}$$

where

D = diffusion coefficient of the solute in solution
k = Boltzmann constant
T = absolute temperature
η = viscosity of the solvent
r = radius of the solute molecule

Proteins such as albumin and γ-globulin in synovial fluid have been a subject of discussion on how they affect viscosity and dissolution as the presence of the HA-protein complex has not been fully understood. There have been different opinions expressed in various studies on the bounding of HA with proteins and how this HA protein complex affects the non-Newtonian or Newtonian character of the synovial fluid. Fam, in his review [5], explains that initial studies [10-12] showed that hydrolysing the proteins in the complex, with the use of papain, would lead to a reduced viscosity of the modified synovial fluid. A later study though [13] revealed that ethylenediaminetetraacetic acid (EDTA) (used for producing papain) could be the responsible component for degrading the complex and leading to the reduced viscosity. Results from that study showed that the physicochemical properties of the complex are not dependent on the protein content and so it would not influence the complex viscosity, which was apparent in other studies as well [14, 15]. Further research [16] suggests that while plasma proteins were considered to bind to HA irreversibly forming a complex, albumin binds to HA in pH lower than 5 and so in the pH of physiological conditions there will be no binding present. A later study suggested that albumin may self-bind leading to multi-protein polymeric aggregates, while HA entangles in the protein aggregate [17, 18] proving that the proteins are important for the synovial fluid mechanical properties [19]. Further research has shown that components such as synthetic HA and proteins in BSF have a strong effect in increasing viscosity at low shear rates which would have an effect on the dissolution of drugs [20]. From these studies it is understood that the formation of HA-protein complexes takes place either because of protein aggregates or due to the complex between proteins and HA, without yet having an extended knowledge of the macromolecules involved [17]. The presence of proteins has also proven to affect the surface tension of synovial fluid [21].

The presence of lipids in the synovial fluid can be essential, as it is proven that they form multi-bilayers [22, 23] that affect surface tension while offering improvement in wetting characteristics. These components manage to transform a hydrophobic surface into a hydrophilic one by an aggregation process. The lipids are arranged into energetically favourable vesicles and lamellar spheres, to form a type of reservoir for surfactants in the lubrication process [22, 23]. Lipids also act as the body's natural surfactants and so may substantially contribute to the enhancement of the solubility and dissolution of poorly soluble drugs in the fluid.

There has been a small number of artificial synovial fluids developed (containing mainly HA), mostly used for viscosity, tribological and rheological testing purposes [17, 24-26], with some additional studies assessing dosage form performance [27-30]. Artificial synovial fluid has been developed [30] in order to investigate the influence of specific components present in the synovial fluid (HA and albumin) on the dissolution characteristics of crystal suspensions. Results showed that these components do influence drug dissolution and that an artificial synovial fluid may be able to provide similar dissolution characteristics in comparison with bovine synovial fluid. A review by Marques [29] has highlighted the use of a simulated synovial fluid with PBS and HA which has been used in the following *in-vitro* studies: dysprosium borate glass microspheres *in-vitro* were immersed in the mentioned simulated synovial fluid for up to 64 days at 37 ^{o}C [27], while in another study [28], bilayered chitosan based scaffolds were developed to investigate the cytotoxicity of composite scaffolds using unsintered hydroxyapatite. The mentioned simulated synovial fluid was also used in bioactivity studies for examining the possibility of the polymeric component for the chondrogenic part, to not mineralize in various immersion periods. In all occasions, the amount of the components added, would be chosen according to the average values present in synovial fluid found in literature, for a healthy individual. The components chosen for addition would be the HA, BSA and in some occasions γ-globulin.

Up to date there is no proposed BSF media reflecting the physiological parameters of the synovial fluid composition in healthy and disease state for assessing dissolution behaviour in the synovial joint. To develop these media and to be able to predict drug dissolution and solubility, it is vital to consider the physiological components that may affect the process of dissolution while evaluating physiologically relevant concentrations. In this study the physicochemical properties of the *in-vivo* disease state (OA and RA) synovial fluid were

characterised in terms of the pH, osmolality, surface tension, viscosity vs. shear rate, in order to obtain data that would be useful for the development of BSF. As several media would need to be developed in order to reflect changes in composition during disease stages, two disease states, OA and RA were taken into account in this study. A healthy state (HS) BSF was also developed according to the values reported in the literature. With the measurements performed on the disease state in-vivo synovial fluid, we were able to establish the values of the physicochemical properties, by considering how they affect the dissolution of the drug in the joint. In addition, the solubility of a model drug for IA use, TA, in the in-vivo pathogenic (OA and RA) synovial fluid was measured to show biorelevance with respect to how the drug would solubilise in both the in-vivo fluids and the developed BSF media.

3.2. Materials and methods

3.2.1. Materials

TA (98+%, fine chemical) was purchased from Alfa Aesar (UK). For the development of the BSFs, Hank's Balanced Salt Solution (HBSS), 1X, without calcium, magnesium, phenol red Thermo Scientific HyClone was purchased from Fisher Scientific (UK), the 0.1 M phosphate buffer contained 0.1 M Na_2HPO_4, 0.1 M HCl, bovine serum albumin powder, fraction V and sodium hyaluronate 95% were purchased from Fisher Scientific (UK), γ-globulin from bovine blood was purchased from Sigma-Aldrich (UK), phosphatidylcholine (PC) from egg was purchased from Lipoid (Germany) and carboxymethylcellulose (CMC) sodium salt was purchased from Fisons (Fisons Scientific Equipment, UK). Hyaluronidase from bovine tests, Type VIII, lyophilized powder (300-1000 U/mg) was purchased from Sigma-Aldrich (UK). For all media, ultra-pure water was obtained from a Milli-Q purification device.

3.2.2. Collection and handling of synovial fluid samples from patients with OA and RA

OA and RA synovial fluid was collected from volunteers through aspiration of excess synovial fluid present in the affected joint at the Orthopaedic centre, Attikon University Hospital, Athens, Greece. Fourteen volunteers (from three of which double samples were withdrawn) with OA aged 50-86 years old and ten volunteers with RA were included in the study. The volunteers all gave their written informed consent for being part of the experimental procedure. The study was approved by the Ethics Committee of the Attikon University Hospital, Athens, Greece. The aspirated synovial fluid samples, were kept in a freezer at -80 ^{o}C. Before measuring physicochemical properties and performing the solubility studies, the samples were left to reach room temperature. For the OA synovial fluid experiments, 14 samples were used for the pH, osmolality measurements and solubility studies, 13 for the surface tension measurements as for one sample there was not enough volume to perform the measurement and for the viscosity measurements 10 samples were used for the similar reason. For the RA synovial fluid experiments, 10 samples were used for all measurements and solubility studies (Table 3.1).

Table 3.1. OA and RA synovial fluid samples used for each study

Physicochemical Study	No. of OA samples	No. of RA samples
pH	14	10
Osmolality	14	10

Surface Tension	13	10
Viscosity	10	10
Solubility	14	10

3.2.3. Physicochemical characterisation of *in-vivo* and *in-vitro* biorelevant synovial fluid

3.2.3.1. pH

The pH values were measured by a freshly calibrated pH electrode connected to a S220 Seven Compact pH/Ion pH meter (Mettler-Toledo) at room temperature (25 ^{o}C). The measurements were performed in triplicates.

3.2.3.2. Osmolality

Osmolality values were measured by freezing-point depression of the media using an Advanced Micro-Osmometer Model 3300 (Advanced Instruments Inc.). The measurements were performed in triplicates.

3.2.3.3. Surface Tension

The surface tension was determined with the Du Nouy ring method by using a Force Tensiometer – Sigma 700/701 (Dyne Testing) at room temperature (25 ^{o}C). A standard Du Nouy Ring was used while the medium was placed in a small vessel with a diameter of 46 mm. The measurement lasted for 5 minutes or until a stable surface tension was indicated. The measurements were performed in triplicates.

3.2.3.4. Shear Rheometry (Viscosity)

The rheological properties of the *in-vivo* samples and the developed *in-vitro* BSFs were measured using a Bohlin C-VOR rheometer (Malvern Instruments Ltd, UK) at 25 ^{o}C with a stainless-steel cone and plate geometry technique (40 mm diameter cone with a 4^{o} cone angle) due to small volumes. Shear rates ranging from 0.07 to 1000 s^{-1} were applied for each measurement. The measurements were performed in triplicates with three measurements made for each sample.

3.2.4. Development of Healthy and Disease State Biorelevant Synovial Fluids

Biorelevant healthy and disease state synovial fluids were prepared with the addition of main components affecting dissolution, according to average values found in the literature. The

addition of CMC sodium salt or an increased amount of HA was used to enhance the viscosity value of the developed media. The buffers were chosen according to their ability to maintain the aimed pH value while providing osmolality values close to the measured *in-vivo* values. The biorelevant media were prepared according to the method proposed by Jantratid et al. [31]. The HBSS buffer was adjusted to a pH of 6.8 by adding 0.1 M of HCl before the addition of further components while the phosphate buffers for the OA and RA BSFs were made by adding 0.1 M Na_2HPO_4 (955.1 mL/L) and 0.1 M HCl (44.9 mL/L) for 1 L of a 0.1 M buffer. The phosphate buffer was then adjusted to pH 8.1 (for OA) and 8 (for RA) with addition of 0.1 M HCl to result to the targeted pH.

To prepare all three biorelevant media (HS, OA and RA), the following procedure was followed with different amounts added, according to the media developed (Table 3.2)

1) The buffer was prepared and adjusted to the appropriate pH
2) HA is added under continuous stirring and then the viscous solution is transferred to a round-bottom flask with the appropriate amount of PC (Stock solution: 100 mg/mL PC in dichloromethane) added
3) The dichloromethane is driven off by using a rotary evaporator (Buchi Rotovapor R-114 and Buchi Waterbath B-480, Buchi Labotechnik, Flawil, Switzerland) and vacuum (PC 2001 Vario and control system CVC 2II, Vacuubrand GMBH, Wertheim, Germany) at 40 ^{o}C for 15 min starting at 650 mbar and decreasing the pressure gradually to 100 mbar which is then maintained for a further 15 min. This led to a slightly cloudy micellar solution having no odour of dichloromethane
4) The γ-globulin and BSA are then added under continuous stirring
5) Finally, additional buffer is used to adjust the volume
6) The medium is stored at 5 ^{o}C until used (within 3 days)

3.2.5. Importance of components in the Biorelevant Synovial Fluid development

3.2.5.1. Selection of buffer species

During the development of the media, the PBS was found to be commonly used for simulating synovial fluid [29] as the ion concentrations are close to the literature data [32] leading to values of osmolality close to the *in-vivo* measurements. Alternatively, the HBSS was found to have salts very similar to those present in the plasma and also contained sodium bicarbonate, which is the body's original buffer (together with carbonic acid) and that is why it was chosen for the development of the HS synovial fluid [33, 34]. The pH of the HBSS was altered in the

beginning of the development with the addition of 0.1 M hydrochloric acid for the final pH of the medium to be 7.4. The same buffer (HBSS) was initially tested for developing the disease state BSFs (OA and RA) but due to the additions, the buffer solution would "break" and lose its properties. Thus, a different phosphate buffer was chosen according to the final pH of the disease state media (OA and RA) (Table 3.2). The selection was made according to the ability of the buffer to combine the targeted pH and osmolality instead of physiological relevance [35].

3.2.5.2. Hyaluronic acid

The lubricating and viscoelastic ability of HA has been determined from a variety of studies [3-8] and so its presence in the BSF is vital as a primary determinant for viscosity. Considering that the molecular weight and concentration would affect the viscosity of the medium [5, 24], as the HA used during the development has a molecular weight of 1.5-2.2 M Da, different amounts than the physiological should be used to have the appropriate viscosity according to the *in-vivo* measurements (Healthy: 8.1 mg/mL, OA: 4.8 mg/mL and RA: 3.5 mg/mL, compared to *in-vivo* amounts (Healthy: 3 mg/mL, OA: 1.5 mg/mL and RA: 1.3 mg/mL, Table 3.2).

3.2.5.3. Proteins (Bovine Serum Albumin and γ-globulin)

As proteins seem essential components of synovial fluid, γ-globulin and bovine serum albumin (BSA) due to their potential effect in viscosity, they were included into the medium. The presence of proteins has also proven to affect the surface tension of synovial fluid [21].

3.2.5.4. Phospholipid PC

The presence of lipids in the synovial fluid can be essential as they can act as the body's natural surfactants, although there have not been any previously reported studies involving this component in the development of artificial synovial fluid. The addition of phospholipid PC would also improve the biorelevance of the media.

Based on the decision to include these components, a HS BSF and two disease state (RA and OA) BSFs were developed with amounts added according to the average findings in the literature for each, as several media were needed to be developed in order to reflect changes in composition during disease stages (Table 3.2).

3.2.6. Composition of healthy state biorelevant medium

The amounts of the components and the ranges of the physicochemical measurements reported in the literature seem to have a high variability. This may be explained by the variability in measuring techniques, aspiration techniques (leading to oxygenation of samples) [36] and biological variation, as different volunteers included in studies may differ in data involving age, disease progression and treatment during the time of aspiration, as injections in synovial fluid may affect the measurements performed. The average amounts of components added in the HS BSF shown in the "IN-VIVO" section of Table 3.2, were according to documented measurements found in the literature, with Version 1 (Table 3.2, orange) developed according to these average values of chosen components. The pH of HBSS had to be reduced to 6.8 instead of its initial value of 7.4, before the addition of components, in order for the developed final product to acquire the targeted pH value. The adjustment took place with the addition of 0.1 M HCl to the buffer, before the addition of any further components, as proteins precipitated from the added acid. In Version 2 (Table 3.2, orange), CMC sodium, a viscosity enhancer, was chosen to be added to the medium to reflect the effect of a viscosity enhancer, while measurements with the removal of HA (containing only CMC as the viscosity enhancer) were also performed. Different concentrations of CMC sodium were tested in order to find the appropriate amount, with 25 mg/mL chosen for further testing (Fig. 3.1). Regarding the HA used in this study, it has a molecular weight of 1.5 to 2.2 million Da with the HA contained in HS synovial fluid being 6.3 to 7.6 million Da [5]. Version 3 (Table 3.2, orange) shows the addition of HA in an appropriate amount according to the equation derived from the exponential fitting from the viscosity measurements with different HA amounts added to the buffer [Data fitted with Eq. Y=0.03947 * exp (0.6348*X)] (Prism Version 7, GraphPad) (Fig. 3.2), as the molecular weight of HA plays a significant role in the effect it has on the viscosity of the medium [5, 24].

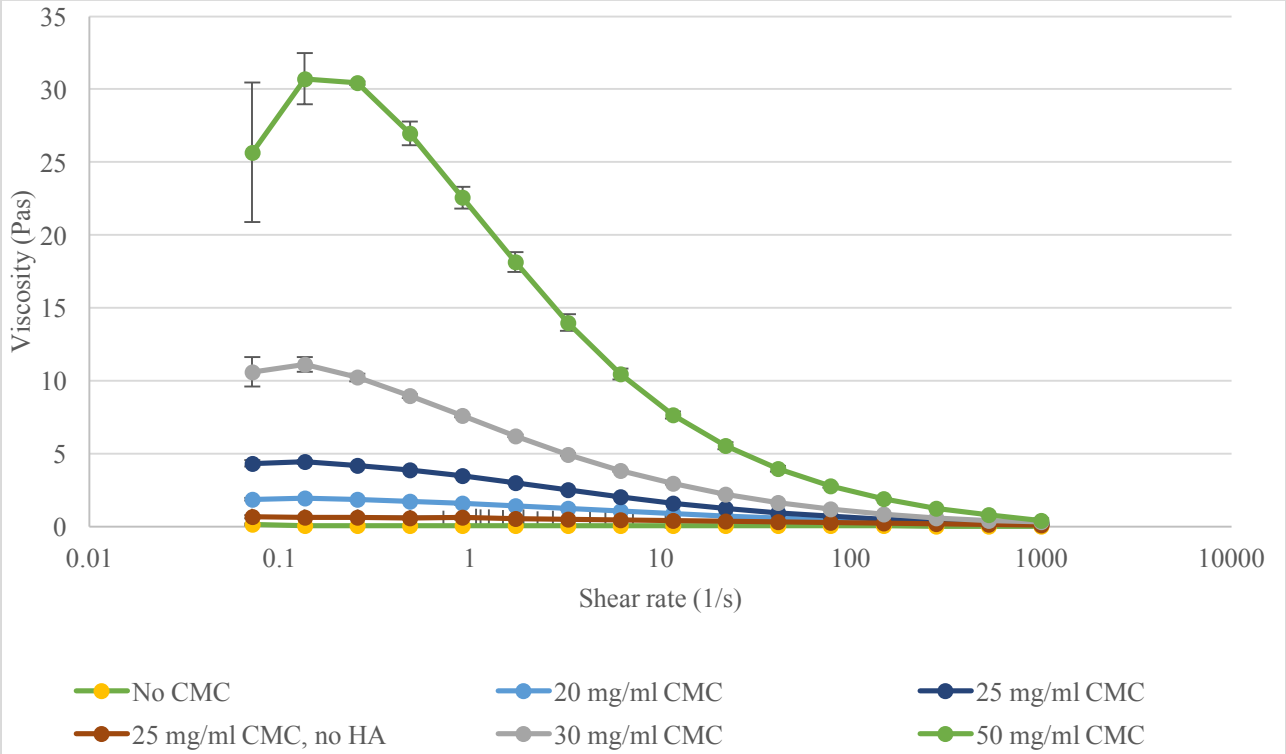

Fig. 3.1. HS BSF viscosity measurements with the addition of CMC in HBSS

3.2.7. Composition of OA biorelevant medium

Table 3.2 (*In-vivo* OA, green) summarizes the average values of the *in-vivo* components found from the literature. Starting with measurements in each step addition of a component, in order to see their effect on the physicochemical properties, Version 1 was developed with a phosphate buffer of 0.05 M (Table 3.2, green). The phosphate buffer also includes the addition of salts according to the ion concentrations of the initial buffer (0.05 M) and the ion concentrations of the synovial fluid from the literature data, to increase osmolality to the aimed value [32]. In Version 2 (Table 3.2, green), the effect of CMC sodium as a viscosity enhancer was tested (Fig. 3.2) similarly to the HS BSF. As both osmolality and ionic strength have a strong impact on drug release, it is of importance to investigate the effect of different strengths of Molar concentration of the buffer, for concluding to the optimal level (Table 3.2, green, Version 2). 0.05 M was tested with the addition of salts and in versions without HA or without CMC or without both; 0.06 and 0.07 M were tested with or without salts and 0.1, 0.12 and 0.13 M were tested without salts. In Version 3 (Table 3.2, green), the addition of HA is considered for increasing viscosity according to the equation derived from the exponential fitting of viscosity measurements with different HA amounts added to the buffer [Data fitted with Eq. Y=0.03947 * exp (0.6348*X)] (Prism, Version 7, GraphPad) (Fig. 3.4). An increased Molarity was chosen without the addition of salts as the buffer for the performed measurements.

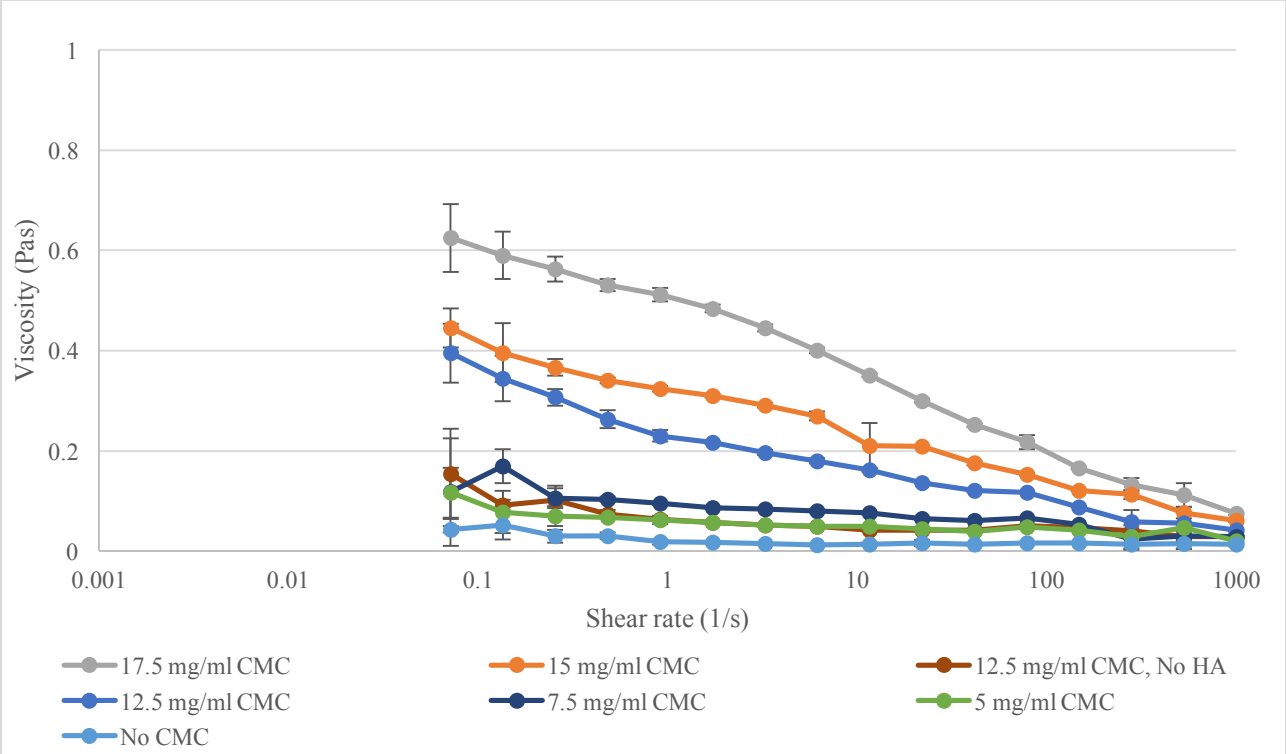

Fig. 3.2. OA BSF viscosity measurements with the addition of CMC in Phosphate buffer

3.2.8. Composition of RA biorelevant medium

For the RA BSF development, as with the Healthy state and OA BSF, the *in-vivo* average amounts of components found in the literature were taken into account for the amounts of the components added in the developed biorelevant media. The similar buffer used for OA was chosen and in Version 1 (Table 3.2, purple), with the addition of salts, the presence of CMC sodium for increasing viscosity was evaluated (Fig. 3.3). Similarly with before, the addition of HA (Fig. 3.4) was tested instead of CMC sodium (Version 2, Table 3.2, purple).

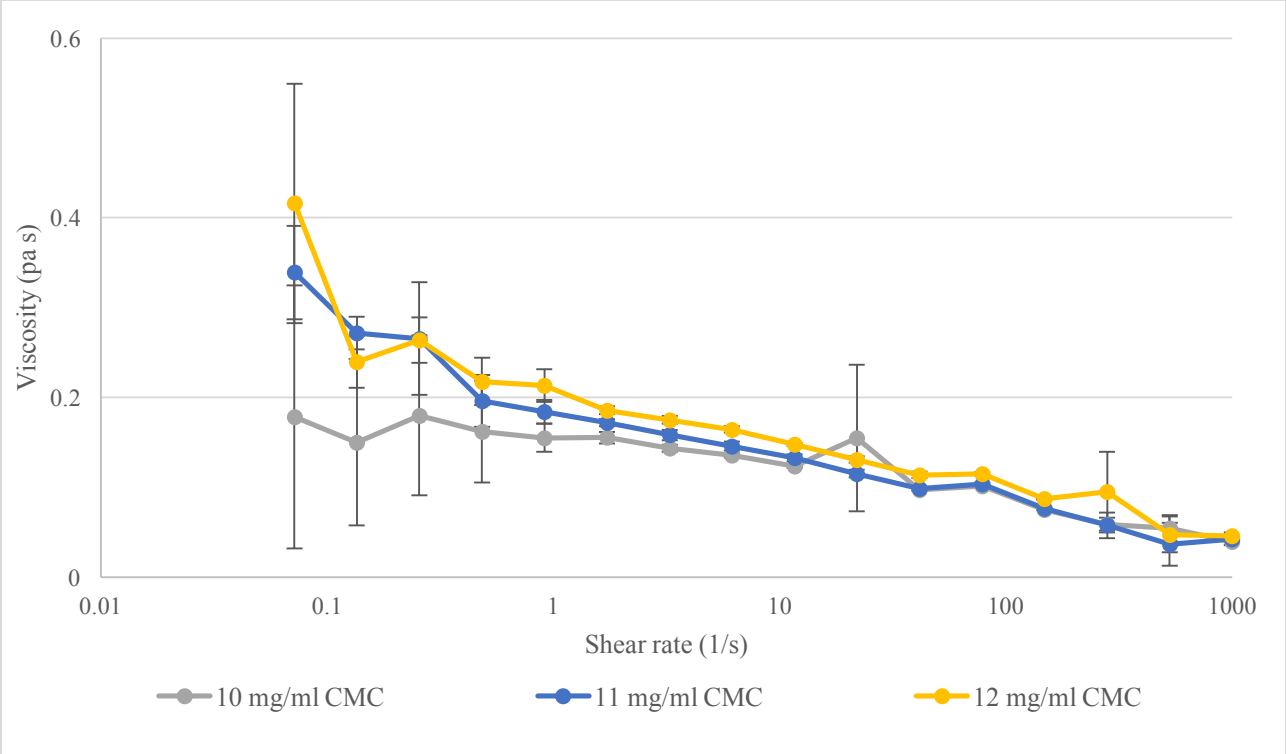

Fig. 3.3. RA BSF viscosity measurements with the addition of CMC in Phosphate buffer

Table 3.2. Composition of Healthy (orange), OA (green) and RA (purple) BSF

Components BSF (mg)	IN-VIVO (Healthy)	Version 1	Version 2	Version 3	IN-VIVO (OA)	Version 1	Version 2	Version 3	IN-VIVO (RA)	Version 1	Version 2
Buffer	-	HBSS	HBSS	HBSS	-	0.05 M $NaHPO_4$ + HCl (+salts)	0.05, 0.06, 0.07, 0.1, 0.12, 0.13 M $NaHPO_4$ + HCl (+salts)	0.1 M $NaHPO_4$ + HCl	-	0.1 M $NaHPO_4$ + HCl (+ salts)	0.1 M $NaHPO_4$ + HCl
HA	3	3	3 and 0	8.1	1.5	2	1.5 and 0	4.8	1.3	1.3	3.5 and 0
BSA	11.5	11.5	11.5	11.5	11.5	11.5	11.5	11.5	20.25	20.25	20.25
γ-globulin	1.7	1.7	1.7	1.7	1.7	1.7	1.7	1.7	24.75	24.75	24.75
PC	0.15	0.15	0.15	0.15	0.25	0.25	0.25	0.25	0.9	0.9	0.9
CMC sodium	-	-	25	-	-	-	5, 7.5, 12.5, 15, 17.5	-	-	10, 11 and 12	-
Salts	-	-	-	-	-	2.9 mg/mL NaCl 0.3 mg/mL KCl	2.9 mg/mL NaCl 0.3 mg/mL KCl	-	-	2.9 mg/mL NaCl 0.3 mg/mL KCl	-

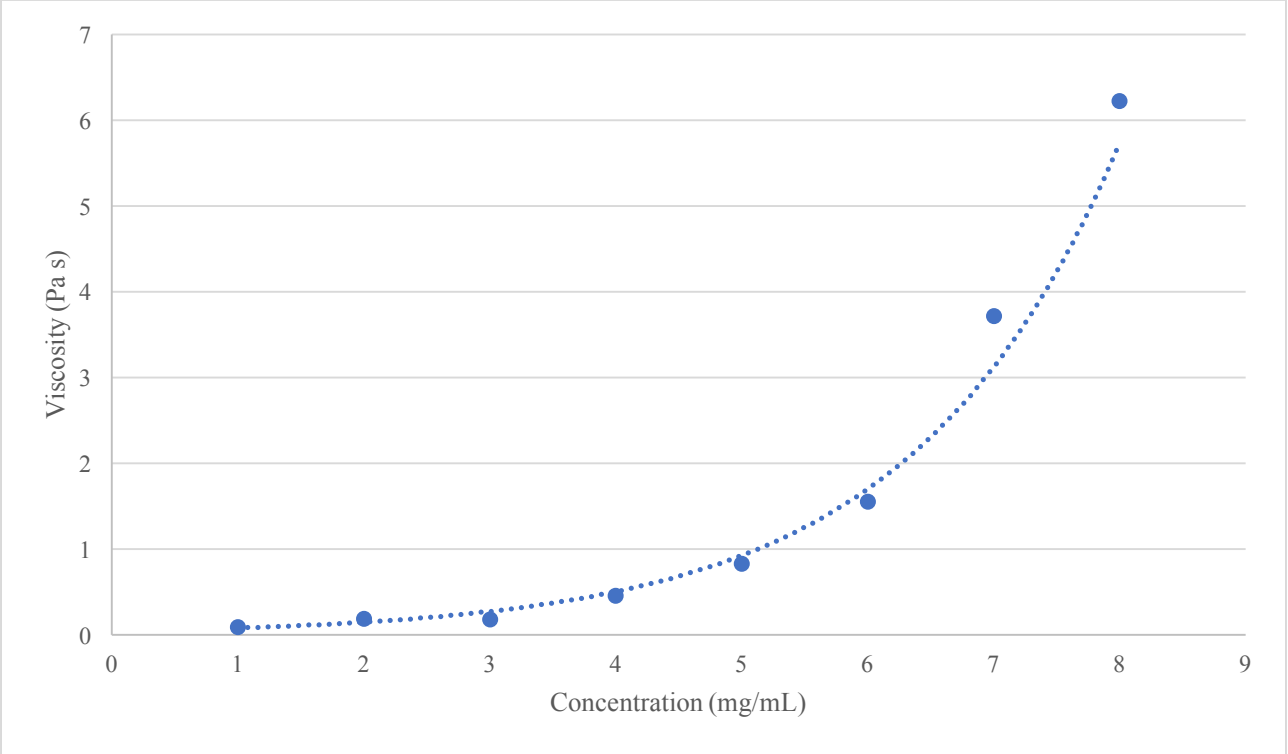

Fig. 3.4. Equation derived from exponential growth fitting of 8 samples of Phosphate buffer with HA.

3.2.9. Solubility studies of TA in *in-vivo* disease state (OA and RA) and biorelevant synovial fluid in healthy state and disease state (OA and RA)

The solubility of TA in the *in-vivo* disease state synovial fluid (OA and RA), the *in-vitro* developed BSFs (HS, OA and RA) and in the widely used artificial synovial fluid [PBS with HA (3 mg/mL) at pH 7.4] [29] was determined at 37 ^{o}C. The *in-vitro* BSFs that were tested to determine TA solubility, contained additional HA to reach the viscosity of the *in-vivo* results. In addition, the solubility of TA was determined in the *in-vitro* BSF of HS and OA with the average amounts of HA found from the literature, for the biorelevant medium after the addition of each component. The studies were performed with the shake flask method by adding an excess amount of TA to the medium in test. The suspensions were then shaken in a water bath at 37 ± 0.5 ^{o}C (Grant SBB Aqua Plus, UK) for 24-h (achieved equilibrium). Samples were then withdrawn, filtered with 2.7 μm GF filters, diluted with the corresponding medium where appropriate before analysis and then treated with hyaluronidase solution. The amount of TA was then quantified in the HPLC [37].

3.2.10. Sample Preparation

Synovial fluid sample preparation took place according to the method described by Sottofattori et al. [38]. An amount of hyaluronidase solution prepared based on manufacturer (initial concentration of 300-1000 U/mg) were added to the *in-vivo* and *in-vitro* developed synovial fluid samples to reach a final concentration of 150 U/mL which degraded HA and decrease the viscosity of the sample leading to an easier filtration and analysis. Hyaluronidase was reconstituted at 1 mg/mL in 0.02 M sodium phosphate buffer, pH 7, containing 77 mM sodium chloride and 0.01 % BSA.

3.2.11. Triamcinolone Acetonide HPLC Analysis

The solubility samples and standard solutions were analysed using an Agilent 1100 series HPLC system (Agilent, UK) consisting of a G1329A autosampler, a G1330A ALS thermostat, a G1316A thermostatted column compartment, a G1315A DAD, a G1322A degasser and a G1311A quaternary pump. A modification of a published method was used [64]. Reversed phase chromatography was performed using an Agilent Eclipse XDB-C18 column (2.6 x 250 mm, 5μm pore size) (Agilent, UK). The flow rate was set at 1 mL/min, temperature at 25 ^{o}C, the UV detection signal was set at 240 nm, stop time at 24 min and injection volume 20 μL. The HPLC method included a gradient with increased water % in the beginning of each run (methanol:water at 10:90 for 8 min and then at 65:35 for 16 min).

Samples were diluted with the corresponding medium, where appropriate, before analysing with the HPLC to determine the amount of TA dissolved. Working calibration standards from a range of concentrations (2-10 μg/mL) were composed with a solution of hyaluronidase being added to the sample. The hyaluronidase solution was added to the sample and then a 20 μg/mL aqueous intermediate (PBS) of the stock solution of TA in methanol (5 mg/mL) was added to the synovial fluid-enzyme solution in appropriate volumes to prepare the spiked standards following the sample preparation technique. Adding the stock solution directly into the blank BSF caused protein precipitation due to the strong effect of the organic solvent. The drug amount was chosen to be included before the addition of the hyaluronidase, to follow the same process observed in the solubility studies; the sample including the drug and the addition of the degrading enzyme following afterwards. The % dissolved was calculated according to a calibration curve (2-10 μm) in the corresponding medium [39].

3.3. Results and Discussion

3.3.1 Physicochemical properties of *in-vivo* disease state Synovial Fluid (OA and RA)

3.3.1.1. pH and osmolality

The mean pH of the OA samples was at 8.04 ± 0.41 making it slightly basic. The pH of the RA samples was 7.56 ± 0.11 which is close to the value of the synovial fluid in physiological conditions. The osmolality of the RA and OA samples was similar and close to isosmotic values (299.5 ± 9.87 and 301.89 ± 9.55 mOsm/kg, respectively) (Table 3.4 and 3.5, IN-VIVO).

The measurement of pH is of primary importance as it can have a significant effect on the dissolution of drug products. Comparing these results to literature data, the OA pH measured seems to be in accordance with most published data [40] but also slightly higher than other recorded results [41]. Studies conducted with different aspiration and measurement techniques may lead to non-correlating results [2] and so this difference in values may be explained by the variability in measuring techniques and aspiration techniques (leading to oxygenation of samples) [36]. Biological variation may also be the cause, as different volunteers included in studies may differ in data involving age, disease progression and treatment during the time of aspiration, as injections in synovial fluid may affect measurements performed [2, 40, 42, 43]. An explanation has also been given involving the measurement of the hydrogen ion concentration determining the pH value; as the samples are withdrawn from the synovial cavity, oxygenation may take place, changing the hydrogen ion concentration and showing higher pH values, as pH measurements involve the measurement of the hydrogen ions concentration in the solution [36]. This indicates that pH results should be closer to physiological values (pH: 7.5) as synovial fluid is an ultrafiltrate of the blood [7, 32, 44] and so values should be similar to the pH of blood. This was also suggested from the synovial fluid pH of RA patients, as measured results show a value close to physiological (7.56 ± 0.11) (Table 3.5). Although previously documented results are in good correlation with these measurements from RA patients [40], data from other studies have shown lower values. A lower value of pH for RA synovial fluid was justified from a topical lactic-acid acidosis taking place in the joint due to the inflammation caused by the disease. In addition, the position of the needle while withdrawing fluid, has proven to be of importance for the reproducibility of readings in RA measurements, which was not an issue for normal joints. In RA, the synovial membrane has acid producing villi formed in its surface that may entrap synovial fluid in its folds and if synovial fluid is withdrawn from those positions, the pH will be lower than the actual value

[36, 45]. Similarly to the OA samples, oxygenation of the withdrawn samples can be the reason for the measurements being of a higher value [40].

Osmolality measurements showed isosmotic values of approximately 300 mOsm for OA and RA synovial fluids (Table 3.4 and 3.5, IN-VIVO). The principal cation affecting osmolality in synovial fluid is sodium (approx. 145 mM) and the principal anion is chloride (approx. 107.4 mM) [32]. Results for the OA synovial fluid were consistent with earlier results [46] while another study showed lower values [47]. In disease state, the HA present in synovial fluid changes in amount and form. According to the progression of the disease, the conformation may be different and so patients may have differing values. Due to the conformational change and the difference in molecular weight of the HA (in HS: 6.3-7.6 MDa compared to 1.06-3.48 MDa in OA and 3.2-6.8 MDa in RA [5]), there is an increase of bound water instead of salt leading to decreased osmolality [42, 46]. Differences in osmolality may also be explained by the presence of chondrocytes in the articular cartilage, as they seem to be affected by the difference in osmolarity while regulating the gene expression of chondrogenic transcription factors together with ECM constituents [47]. The osmolality of RA samples recorded in earlier studies are consistant with the measurements our group has recorded, with a mean value of 280 ±7.7 mOsm [46] and a range of 273-283 mOsm [47]. A slight difference which may be considered between the two disease states is explained by the change of the constituent concentrations through the disease, such as total protein being lower in OA and also due to the extra enzymes and debris present in the joint during RA [46].

3.3.1.2. Surface tension

The surface tension of RA was 47.6 ± 2.2 mN/m and 45.4 ± 3.8 mN/m for OA (Table 3.4 and 3.5, IN-VIVO). The value measured for the RA fluid was in accordance to previously recorded measurements in the literature [48]. Different amounts of phospholipids are present in OA and RA synovial fluids due to the degeneration of the synovium, on which the surface-active phospholipids are bound. Although the surface tension is primarily affected by their presence, the values measured seem to be similar in the OA and RA synovial fluids with no significant difference observed between the two disease states. The measurements are lower than healthy state synovial fluid values found in the literature [24] as disease state synovial fluids contain a higher amount of phospholipids [22, 23, 49, 50]. The RA synovial fluid contains larger amounts of immunoglobulin complexes, fibrin and fibrinogen than serum and healthy state synovial fluid which is also partly responsible for lower surface tension values in comparison [51].

3.3.1.3. Viscosity vs. shear rate

Our measurements showed that for shear rates from 0.07 to 1000 1/s the viscosity values for RA fluid had an average value of 0.36 to 0.01 Pa s and the OA fluid had an average value of 0.88 to 0.01 Pa s while a higher variability was apparent in the lowest shear rates (Table 3.4 and 3.5, IN-VIVO). OA synovial fluid has non-Newtonian shear thinning properties which means that the viscosity will decrease as the shear rate becomes higher [5, 24, 52, 53] compared to the Newtonian properties of the RA synovial fluid [54]. Hence, it is common in the literature to present viscosity values against shear rates, as a specific viscosity or values over time are difficult to interpret [55]. Studies comparing the viscosity of OA with RA synovial fluid showed lower viscosity at the same shear rates [52, 53, 56] for the latter.

The primary component affecting viscosity in synovial fluid is the HA [7, 26, 32, 44, 50]. While a higher concentration or molecular weight of hyaluronic acid increases viscosity [5, 24], increasing the concentration in an aqueous solution above 1 mg/mL or by increasing the molecular weight from 0.15 x 10^6 Da to 1.2 x 10^6 Da [24, 57] leads to the formation of an entanglement network, enhancing the increase of viscosity [24]. The viscosity of OA and RA synovial fluids have been measured in earlier studies and are in accordance with the measurements performed; showing that the viscosity in OA samples is higher than in RA at the measured shear rates [5, 24, 41, 52, 58] although varying according to the type of rheometer used and shear rates chosen. From our results, it is noticeable that the difference in viscosity measurements between OA and RA synovial fluid is more significant in low shear rates while there is no difference in the highest shear rate tested due to shear-thinning abilities of the synovial fluid [5]. The importance of the leading effect of HA on viscosity was also shown in tests during which HA was degraded with the use of an enzyme, such as hyaluronidase [38], and showed a significant decrease in viscosity and elasticity [59]. As the concentration of HA affects viscosity, data from literature shows that the amount in OA synovial fluid is higher compared to RA, due to the damaged synovial membrane which produces HA, and also due to dilution with blood in the synovial cavity [5, 56, 60]. As for the molecular weight of HA, it has lower values for the disease states compared to the HS synovial fluid, due to depolymerisation [5]. More specifically this reaction is caused by certain components present in blood, such as ascorbic acid, produced by the increased amount of leukocytes in the diseased synovial joint [58].

3.3.2. Physicochemical properties of Biorelevant Synovial Fluid (Healthy state, OA and RA)

3.3.2.1. Healthy state biorelevant synovial fluid (HS BSF)

Table 3.3. Physicochemical properties of developed HS BSF

Components HS BSF	**IN-VIVO**	**Version 1**				**Version 2**		**Version 3**
		Buffer + HA	+ PC	+ BSA	+g-glob	+CMC	+CMC -HA	
pH	**7.46**	**7.86**± 0.02	**8.68**± 0.02	**7.8**± 0.03	**7.35**± 0.02	**7.5**± 0.02	**7.41**± 0.01	**7.35**± 0.03
Osmolality (mOsm)	363.5± 53.5	**281.67**± 0.58	**288.33**± 5.77	**295.33**± 2.89	**306**± 11.36	**360.3**± 0.58	**349**± 3.61	**318.33**± 11.68
Viscosity (Pa s) at 0.07 and	**6.9**± 4.25	**0.1**± 0.01	**0.1**± 0.02	**0.08**± 0.06	**0.08**± 0.06	**4.32**± 0.22	**0.67**± 0.12	**5.96**± 0.63
at 1000 Shear rate (1/s)	**0.01**± 0.01	**0.02**± 0.002	**0.01**± 0.004	**0.005**± 0.004	**0.01**± 0.0014	**0.19**± 0.005	**0.11**± 0.002	**0.07**± 0.01
Surface Tension (mN/n)	**50.6**± 0.19	**53.35**± 3.9	**55.9**± 0.52	**51.24**± 1.11	**51.82**± 0.4	**44.42**± 0.44	**47.42**± 0.32	**50.52**± 0.51

The amounts of the components and the ranges of the physicochemical measurements reported in the literature seem to have a high variability. This may be explained by the variability in measuring techniques, aspiration techniques (leading to oxygenation of samples) [36] and biological variation, as different volunteers included in studies may differ in data involving age, disease progression and treatment during the time of aspiration, as injections in synovial fluid may affect measurements performed.

The physicochemical properties in Version 1 (Table 3.3) were measured in each addition step in order to see the effect each component may have. During the addition of each component, noticeably, the pH was more affected by the addition of HA and then PC, as the pH value increased by approximately 1 unit with each addition, while it reduced to the intended value with the addition of BSA and γ-globulin. The osmolality of the medium in Version 1 reflected the iso-osmolal values of the *in-vivo* literature data. Regarding the surface tension, although the addition of PC potentially reduces its value [22], the difference seen was not significant,

while the addition of proteins had a slightly stronger effect [21] resulting to the value of the literature. The viscosity, although increased with the addition of HA, does not seem to be significantly influenced by the addition of the extra components. While HA was added in the correct average amount, the viscosity did not seem to be close to the anticipated value. This is because the molecular weight of HA plays a significant role in the effect it has on the viscosity of the medium [5, 24]. Measurements in Version 2 (Table 3.3) show the effect of the addition of CMC in viscosity, while measurements with the removal of HA were also performed. Different concentrations of CMC sodium were tested in order to find the appropriate amount, with 25 mg/mL chosen for further testing (Fig. 3.1). Results showed that the addition of CMC sodium led to an exponential increase in viscosity [61-64]. Results with the addition of CMC sodium and removal of HA, showed that the presence of CMC sodium does affect the viscosity significantly, by enhancing rather than replacing the viscosity effect of HA. The addition of CMC in its sodium salt form also has a significant impact on the osmolality of the medium as it causes an increase while the surface tension seems to slightly reduce (Table 3.3).

Version 3 (Table 3.3) shows the addition of HA in an appropriate amount according to the equation derived from the exponential fitting from the viscosity measurements with different HA amounts added to the buffer (Fig. 3.4) [5, 24]. In addition, the presence of HA as the viscosity enhancer compared to the use of CMC leads to the viscosity and surface tension values being of accordance with the *in-vivo* data with a slight decrease in osmolality which reached a value similar to Version 1 (Table 3.3), as the sodium salt of CMC, increasing the osmolality, is not present. Version 1 (Table 3.3) was chosen to test the solubility of TA and according to the relevance of the physicochemical property results with the *in-vivo* results from literature, Version 3 was tested as well.

3.3.2.2. Osteoarthritis biorelevant synovial fluid (OA BSF)

Table 3.4 summarizes the measured physicochemical properties used for the development of the OA BSF. Starting with measurements in each step addition of a component, in order to see their effect on the physicochemical properties, Version 1 with a phosphate buffer of 0.05 M was developed. The differences observed between the HS and OA BSF (Version 1, Table 3.4) seem to be significant in the way the components added affect the change in the pH. This can be explained due to the strength of the buffer used, as the HBSS is at 0.1X and the phosphate buffer is at 0.05 M and so a stronger buffer would be more resistant to changes in pH when small quantities of components which may affect it, are added.

In Version 2 (Table 3.4), the effect of CMC sodium as a viscosity enhancer was tested (Fig. 3.2), showing that with this addition, the osmolality and viscosity increases while the pH and surface tension remains constant. Removing the HA shows that the effect of CMC sodium enhances rather than replaces the viscosity. This may be due to the different processes followed to increase viscosity. CMC sodium, compared to HA, when dissolved in the medium separates into sodium cations and a polymer anion due to an electrolytic process which then interact with each other through electrostatic forces. Also electrostatic interactions (hydrogen bonds) take place as the water molecule and OH groups on the CMC molecule exhibit electric dipole which have a vital importance in the viscosity effect [63].

Having no presence of a component primarily affecting the viscosity (removal of CMC sodium and HA), led to a value close to the viscosity of the buffer although slightly increased due to the presence of proteins and their aggregation [65-68]. A difference in buffer Molarity did not seem to have a significant effect on the pH or the viscosity of the medium while with increasing Molarity, the surface tension slightly rose (Version 2, Table 3.4). Changing the concentration of the solutes in the buffer, by increasing sodium and potassium ions, led to the increase of the buffer osmolality. This is shown as media with similar Molarities have different osmolality values with the addition or removal of salts and also by increasing the strength of the buffer (Version 2, Table 3.4). In Version 3 (Table 3.4), the addition of HA is considered for increasing viscosity according to the equation derived from the exponential fitting of viscosity measurements with different HA amounts added to the buffer (Table 3.4, Fig. 3.4). An increased Molarity was chosen without the addition of salts as the phosphate buffer (0.1 M) and all the physicochemical properties measured were of accordance with the *in-vivo* data. Version 1 (Table 3.4) was chosen to test the solubility of TA and according to the relevance of the physicochemical property results with the *in-vivo* fluid, Version 3 was tested as well.

Table 3.4. Physicochemical properties of developed OA state BSF

Components OA BSF	IN-VIVO	Version 1				Version 2										Version 3
Additions (Salts)		Buffer +HA	+ PC	+BSA	+g-glob	0.05M (+) - CMC	0.05M (+)	0.05M (+) - HA	0.05M (+) - CMC - HA	0.06M (+)	0.06M (-)	0.07M (+)	0.07M (-)	0.1M (-)	0.12M (-)	0.13M (-)	0.1M (-)
pH	**8.04**± 0.41	**8.35**± 0.02	**8.31**± 0.015	**8.06**± 0.035	**8.02**± 0.006	**7.96**± 0.015	**7.95**± 0.005	**7.89**± 0.01		**8**	**8**	**8**	**8**	**8**	**8**	**8**	**7.88**± 0.04
Osmolality (mOsm)	**301.9**± 9.55	**218.3**± 2.08	**225.7**± 9.87	**249.7**± 14.5	**245.3**± 9.24	**232.3**± 0.577	**265.7**± 1.155	**256.7**± 1.53		**290.3**± 0.57	**191**± 1.2	**310**± 0.6	**214**± 1.15	**269**± 0.58	**319**± 0.43	**335.3**± 0.58	**270**± 16.5
Viscosity (Pa s) at 0.07 and	**0.88**± 0.2	**0.1**± 0.04	**0.2**± 0.14	**0.14**± 0.03	**0.09**± 0.08		**0.4**± 0.06	**0.15**± 0.09	**0.04**± 0.007		**0.45**± 0.11	**0.42**± 0.08			**0.45**± 0.09	**0.43**± 0.08	**0.89**± 0.08
at 1000 Shear rate (1/s)	0.01± 0.004	**0.01**± 0.002	**0.02**± 0.001	**0.01**± 0.003	**0.01**± 0.002		**0.04**± 0.002	**0.03**± 0.004	**0.01**± 0.005		**0.05**± 0.003	**0.05**± 0.005			**0.005**± 0.001	**0.05**± 0.003	**0.03**± 0.0026
Surface Tension (mN/n)	**45.44**± 3.78	**56.33**± 3.23	**58.23**± 3.32	**46.89**± 0.24	**45.66**± 0.35		**48.63**± 0.31	**48.8**± 0.44	**49.48**± 0.25		**48.77**± 0.23	**50.93**± 0.67			**52.12**± 0.42	**53.7**± 0.21	**53.59**± 0.49

3.3.2.3. Rheumatoid Arthritis biorelevant synovial fluid (RA BSF)

In Version 1 (Table 3.5), the average component amounts together with added salts and the presence of CMC sodium for increasing viscosity, show that a small increase in CMC amount might affect the viscosity but the osmolality, pH and surface tension may stay unaffected. Similarly to before, the addition of HA (Fig. 3.4) was tested instead of CMC sodium (Version 2, Table 3.5) with the final measurements being in accordance with the *in-vivo* data. According to the relevance of the physicochemical property results with the *in-vivo* fluid, Version 2 (Table 3.5) was chosen for testing solubility with TA.

Table 3.5. Physicochemical properties of developed RA state BSF

Components RA BSF	**IN-VIVO**	**Version 1**			**Version 2**
Additions		+ CMC 10 mg/mL	+ CMC 11 mg/mL	+ CMC 12 mg/mL	
pH	**7.56**± 0.11	**7.5**± 0.1	**7.5**± 0.1	**7.5**± 0.1	**7.49**± 0.031
Osmolality (mOsm)	**299.5**± 9.87	**337**± 1.56	**338**± 1.43	**336**± 0.78	**329.67**± 20.82
Viscosity (Pa s) at 0.07 and at 1000 Shear rate (1/s)	**0.36**± 0.13 0.01± 0.003	**0.18**± 0.15 **0.04**± 0.004	**0.34**± 0.05 **0.04**± 0.006	**0.42**± 0.13 **0.05**± 0.004	**0.42**± 0.04 **0.02**± 0.003
Surface Tension (mN/n)	**47.66**± 2.19	**46.38**± 3.89	**45.67**± 2.11	**46.08**± 0.66	**52.48**± 0.34

3.3.3. Solubility studies

The solubility studies of TA in the *in-vivo* disease states showed that, in RA, the drug has a solubility of 54.15 ± 19.1 µg/mL and in OA 29.84 ± 9.46 µg/mL (Fig. 3.5). The solubility of TA in RA synovial samples is higher suggesting that the amounts of components added to the two pathogenic synovial fluids affect the solubility and probably the dissolution rate of the drug in the joint [9]. The component most likely affecting solubility is the lipids present in different concentrations in the disease state media as they act as the body's natural surfactants. The lipids manage to transform a hydrophobic surface into a hydrophilic one by an aggregation process. The molecules are arranged into energetically favourable vesicles and lamellar spheres

to form a type of reservoir for surfactants in the lubrication process [22, 23] leading to the fact that they may substantially contribute to the enhancement of the solubility and dissolution of poorly soluble drugs in the fluid.

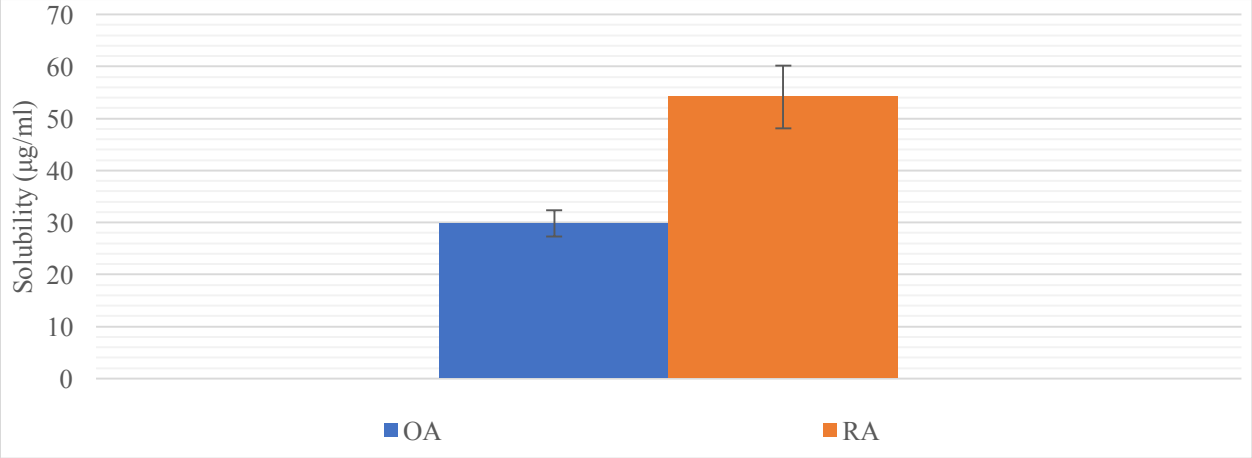

Fig. 3.5. Mean ± SEM solubility of TA in synovial fluid of OA and RA patients (OA, n=14, RA, n=10)

Regarding studies with the *in-vitro* fluid, measuring the solubility of TA in each step addition of the components, in the HS and OA BSF, the addition of PC increased the solubility significantly compared to the addition of the proteins (Table 3.6). Comparing the TA solubility values in the *in-vivo* disease state results (Fig. 3.5) with the *in-vitro* disease state results (Table 3.7) (OA 29.8 µg/mL to 17.4 µg/mL and for RA 54 µg/mL to 19.4 µg/mL respectively) *in-vivo* results were higher. Although the components added to the BSF and the physicochemical properties tested are similar, the solubility seems to differ. Comparing the developed BSFs between them and with the widely used artificial synovial fluid [PBS with HA (3 mg/mL)], showed slight differences. The solubility of the developed BSFs seems to be lower in HS<OA<RA which would be explained primarily by the amount of PC phospholipids contained in the media, following the same pattern. There does not seem to be a significant difference with the widely used artificial synovial fluid although it does not contain any of the physiological components present in the developed media apart from HA. Despite this, the developed media may well have a significant effect on the solubilisation and dissolution rate of drugs, as they have different viscosities. Considering the macroviscosity of the solution, a more viscous fluid will slow down the diffusional mass transport and according to microviscosity and the Stokes-Einstein equation, this parameter has vital importance in the dissolution process (Eq. 2) [9].

Table 3.6. Solubility of TA in HS BSF (Version 1 Table 3.3) and OA BSF (Version 1 Table 3.4) after each component addition

Components added to BSF	HBSS + HA (HS) or Phosphate Buffer + HA (OA)	+ PC	+ BSA	+ γ-globulin (Completed BSF)
TA Solubility in HS (µg/mL)	**16.41**± 0.73	**25.47**± 1.3	**27.74**± 0.6	**26.89**± 1.34
TA Solubility in OA (µg/mL)	**13.86**± 0.09	**17.16**± 0.32	**19.4** ± 0.52	**19.82**± 0.42

Table 3.7. Solubility of TA in *in-vivo* OA, RA synovial fluid and in *in-vitro* HS BSF (Version 3 Table 3.3), OA BSF (Version 3 Table 3.4), RA BSF (Version 2 Table 3.5) and artificial synovial fluid [PBS + HA)3 mg/mL)]

Synovial Fluid	HS BSF	OA BSF	RA BSF	PBS + HA Artificial Synovial Fluid	OA *in-vivo*	RA *in-vivo*
TA Solubility (µg/mL)	**15.6**± 0.6	**17.4**± 2.1	**19.4**± 1.5	**16.7**± 1.4	**29.8**± 2.5	**54.2**± 6

3.4. Conclusions

Three BSFs were developed (HS, OA and RA) with their physicochemical parameter values being in accordance with the *in-vivo* measurements of disease state synovial fluid by taking into consideration the average values of the component amounts found in literature. Development of the media was according to the components that would have a strong effect in drug dissolution in these media. As the molecular weight of HA has a significant importance in viscosity enhancement and each synovial fluid state has HA of different molecular weights, using the average amount found in literature, did not provide the expected viscosity according to the *in-vivo* study measurements. By testing viscosity enhancers such as CMC or with additional amounts of HA, the appropriate viscosity for the developed BSFs could be achieved. According to the solubility studies performed, TA solubility in the developed BSFs were slightly below the values of TA solubility in the *in-vivo* OA and RA synovial fluids. Comparing the developed media to the widely used artificial synovial fluid, showed that there are differences between disease and healthy state. The developed BSFs reflect the influence of the altered component amounts and the difference in viscosity. These media can be recommended for the prediction of drug dissolution from IA formulations in the healthy and diseased joints, while they may provide further insight during biorelevant dissolution testing.

3.5. References

1. Seidlitz, A. and W. Weitschies, *In-vitro dissolution methods for controlled release parenterals and their applicability to drug-eluting stent testing.* J Pharm Pharmacol, 2012. **64**(7): p. 969-85.
2. Pedersen, B.T., Vilmann, P., Bar-Shalom, D., Mullertz, A., Baldursdottir, S. *Characterisation of fasted human gastric fluid for relevant rheological parameters and gastric lipase activities.* Eur J Pharm Biopharm, 2013. **85**(3 Pt B): p. 958-65.
3. Balazs, E.A., Watson, D., Duff IF., Roseman, S., *Hyaluronic acid in synovial fluid. I. Molecular parameters of hyaluronic acid in normal and arthritis human fluids.* Arthritis Rheum, 1967. **10**(4): p. 357-76.
4. Decker, B., McGuckin, W.F., McKenzie, B.F., Slocumb, C.H., *Concentration of hyaluronic acid in synovial fluid.* Clin Chem, 1959. **5**: p. 465-9.
5. Fam, H., J.T. Bryant, and M. Kontopoulou, *Rheological properties of synovial fluids.* Biorheology, 2007. **44**(2): p. 59-74.
6. Hamerman, D. and H. Schuster, *Hyaluronate in normal human synovial fluid.* Journal of Clinical Investigation, 1958. **37**(1): p. 57-64.
7. Larsen, C., Ostergaard, J., Larsen, S.W., Jensen, H., Jacobsen, S., Lindergaard, C., Andersen, P.H., *Intra-articular depot formulation principles: role in the management of postoperative pain and arthritic disorders.* J Pharm Sci, 2008. **97**(11): p. 4622-54.
8. Stafford, C.T., Niedermeier, W., Holley, H.L., Pigman, W., *Studies on the Concentration and Intrinsic Viscosity of Hyaluronic Acid in Synovial Fluids of Patients with Rheumatic Diseases.* Annals of the Rheumatic Diseases, 1964. **23**(2): p. 152-157.
9. Smith, B., *Chapter 3. Solubility and dissolution*, in *Remington Education: Physical Pharmacy*. 2015, Pharmaceutical Press.
10. Blumberg, B.S. and A.G. Ogston, *The effects of proteolytic enzymes on the hyaluronic acid complex of ox synovial fluid.* Biochemical Journal, 1957. **66**(2): p. 342-346.
11. Blumberg, B.S. and A.G. Ogston, *Further evidence on the protein complexes of some hyaluronic acids.* Biochemical Journal, 1958. **68**(1): p. 183-188.
12. Ogston, A.G. and J.E. Stanier, *On the state of hyaluronic acid in synovial fluid.* Biochemical Journal, 1950. **46**(3): p. 364-376.
13. Ogston, A.G. and T.F. Sherman, *Degradation of the hyaluronic acid complex of synovial fluid by proteolytic enzymes and by ethylenediaminetetra-acetic acid.* Biochemical Journal, 1959. **72**(2): p. 301-305.
14. Sandson, J. and D. Hamerman, *Isolation of hyaluronate protein from human synovial fluid.* Journal of Clinical Investigation, 1962. **41**(10): p. 1817-1830.
15. Scher, I. and D. Hamerman, *Isolation of human synovial-fluid hyaluronate by density-gradient ultracentrifugation and evaluation of its protein content.* Biochemical Journal, 1972. **126**(5): p. 1073-1080.
16. Grymonpré, K.R., Staggemeier, B.A., Dubin, P.L., Mattison, K.W., *Identification by Integrated Computer Modeling and Light Scattering Studies of an Electrostatic Serum Albumin-Hyaluronic Acid Binding Site.* Biomacromolecules, 2001. **2**(2): p. 422-429.
17. Oates, K.M.N., Krause, W.E., Jones, R.L., Colby, R.H., *Rheopexy of synovial fluid and protein aggregation.* J R Soc Interface, 2006. **3**(6): p. 167-74.
18. Rinaudo, M., *Rheological investigation on hyaluronan-fibrinogen interaction.* International journal of biological macromolecules, 2008. **43**(5): p. 444-450.
19. Tirtaatmadja, V., D.V. Boger, and J.R.E. Fraser, *The dynamic and steady shear properties of synovial fluid and of the components making up synovial fluid.* Rheologica Acta, 1984. **23**(3): p. 311-321.

20. Oates, K.M.N., W.E. Krause, and R.H. Colby, *Using Rheology to Probe the Mechanism of Joint Lubrication: Polyelectrolyte/protein interactions in Synovial Fluid.* MRS Proceedings, 2001. **711**.
21. Regev, O., Vandebril, S., Zussman, E., Clasen, C., *The role of interfacial viscoelasticity in the stabilization of an electrospun jet.* Polymer, 2010. **51**(12): p. 2611-2620.
22. Hills, B.A. and B.D. Butler, *Surfactants identified in synovial fluid and their ability to act as boundary lubricants.* Ann Rheum Dis, 1984. **43**(4): p. 641-8.
23. Pawlak, Z., W. Urbaniak, and A. Oloyede, *Natural articular joints: model of lamellar-roller-bearing lubrication and the nature of the cartilage surface.* 2013: p. 253-310.
24. Bingol, A.O., Lohmann, D., Puschel, K., Kulicke, W.M., *Characterisation and comparison of shear and extensional flow of sodium hyaluronate and human synovial fluid.* Biorheology, 2010. **47**(3-4): p. 205-24.
25. Smith, A.M., Fleming, L., Wudebwe, U., Bowen, J., Grover, L.M., *Development of a synovial fluid analogue with bio-relevant rheology for wear testing of orthopaedic implants.* J Mech Behav Biomed Mater, 2014. **32**: p. 177-84.
26. Zhang, Z., S. Barman, and G.F. Christopher, *The role of protein content on the steady and oscillatory shear rheology of model synovial fluids.* Soft Matter, 2014. **10**(32): p. 5965-73.
27. Conzone, S.D., Brown, R.F., Day, D.E., Ehrhardt, G.J., *In-vitro and in-vivo dissolution behavior of a dysprosium lithium borate glass designed for the radiation synovectomy treatment of rheumatoid arthritis.* J Biomed Mater Res, 2002. **60**(2): p. 260-8.
28. Malafaya, P.B. and R.L. Reis, *Bilayered chitosan-based scaffolds for osteochondral tissue engineering: influence of hydroxyapatite on in-vitro cytotoxicity and dynamic bioactivity studies in a specific double-chamber bioreactor.* Acta Biomater, 2009. **5**(2): p. 644-60.
29. Marques, M.R.C., R. Loebenberg, and M. Almukainzi, *Simulated Biological Fluids with Possible Application in Dissolution Testing.* Dissolution Technologies, 2011.
30. Sterner, B., Harms, M., Weigandt, M., Windbergs, M., Lehr, C.M., *Crystal suspensions of poorly soluble peptides for intra-articular application: A novel approach for biorelevant assessment of their in-vitro release.* Int J Pharm, 2013.
31. Jantratid, E., Janssen, N., Reppas, C., Dressman, J.B., *Dissolution media simulating conditions in the proximal human gastrointestinal tract: an update.* Pharm Res, 2008. **25**(7): p. 1663-76.
32. Gerwin, N., C. Hops, and A. Lucke, *Intraarticular drug delivery in osteoarthritis.* Adv Drug Deliv Rev, 2006. **58**(2): p. 226-42.
33. Hanks, J.H., *Hanks' balanced salt solution and pH control.* TCA manual / Tissue Culture Association, 1975. **1**(1): p. 3-4.
34. Iyer, S.S., W.H. Barr, and H.T. Karnes, *Characterisation of a potential medium for 'biorelevant' in-vitro release testing of a naltrexone implant, employing a validated stability-indicating HPLC method.* J Pharm Biomed Anal, 2007. **43**(3): p. 845-53.
35. Boni, J.E., R.S. Brickl, and J. Dressman, *Is bicarbonate buffer suitable as a dissolution medium?* J Pharm Pharmacol, 2007. **59**(10): p. 1375-82.
36. Goldie, I. and A. Nachemson, *Synovial pH in rheumatoid knee-joints. I. The effect of synovectomy.* Acta Orthop Scand, 1969. **40**(5): p. 634-41.
37. Glomme, A., J. Marz, and J.B. Dressman, *Comparison of a miniaturized shake-flask solubility method with automated potentiometric acid/base titrations and calculated solubilities.* J Pharm Sci, 2005. **94**(1): p. 1-16.

38. Sottofattori, E., M. Anzaldi, and L. Ottonello, *HPLC determination of adenosine in human synovial fluid.* J Pharm Biomed Anal, 2001. **24**(5-6): p. 1143-6.
39. Tomaszewska, I., Karki, S., Shur, J., Price, R., Fotaki, N., *Pharmaceutical characterisation and evaluation of cocrystals: Importance of in-vitro dissolution conditions and type of coformer.* Int J Pharm, 2013. **453**(2): p. 380-8.
40. Kitano, T., Ohasi, H., Kadoya, Y., Kobayashi, A., Yutani, Y., Yamano, Y., *Measurements of zeta potentials of particulate biomaterials in protein-rich hyaluronan solution with changes in pH and protein constituents.* J Biomed Mater Res, 1998. **42**(3): p. 453-7.
41. Jebens, E.H. and M.E. Monk-Jones, *On the viscosity and pH of synovial fluid and the pH of blood.* J Bone Joint Surg Br, 1959. **41-B**(2): p. 388-400.
42. Baumgarten, M., Bloebaum, R.D., Ross, S.D., Campbell, P., Sarmiento, A., *Normal human synovial fluid: osmolality and exercise-induced changes.* J Bone Joint Surg Am, 1985. **67**(9): p. 1336-9.
43. Ropes, M.W., E.C. Rossmeisl, and W. Bauer, *The origin and nature of human synovial fluid.* J Clin Invest, 1940. **19**(6): p. 795-9.
44. Butoescu, N., O. Jordan, and E. Doelker, *Intra-articular drug delivery systems for the treatment of rheumatic diseases: a review of the factors influencing their performance.* Eur J Pharm Biopharm, 2009. **73**(2): p. 205-18.
45. Cummings, N.A. and G.L. Nordby, *Measurement of synovial fluid pH in normal and arthritic knees.* Arthritis Rheum, 1966. **9**(1): p. 47-56.
46. Shanfield, S., Campbell, P., Baumgarten, M., Bloebaum, R., Sarmiento, A., *Synovial fluid osmolality in osteoarthritis and rheumatoid arthritis.* Clin Orthop Relat Res, 1988(235): p. 289-95.
47. Bertram, K.L. and R.J. Krawetz, *Osmolarity regulates chondrogenic differentiation potential of synovial fluid derived mesenchymal progenitor cells.* Biochem Biophys Res Commun, 2012. **422**(3): p. 455-61.
48. Jeleniewicz, R., Majdan, M., Zwolak, R., Dryglewska, M., *Synovial fluid surface tension in inflammatory joint diseases.* Reumatologia, 2005. **43**(6): p. 331–334.
49. Kosinska, M.K., Liebisch, G., Lochnit, G., Wilhelm, J., Klein, H., Kaesser, U., Lasczkowski, G., Rickert, M., Schmitz, G., Steinmeyer, J., *A lipidomic study of phospholipid classes and species in human synovial fluid.* Arthritis Rheum, 2013. **65**(9): p. 2323-33.
50. Schmidt, T.A., Gastelum, N.S., Nguyen, Q.T., Schumacher, B.L., Sah, R.L., *Boundary lubrication of articular cartilage: role of synovial fluid constituents.* Arthritis Rheum, 2007. **56**(3): p. 882-91.
51. Fathi-Azarbayjani, A. and A. Jouyban, *Surface tension in human pathophysiology and its application as a medical diagnostic tool.* Bioimpacts, 2015. **5**(1): p. 29-44.
52. Bhuanantanondh, P., D. Grecov, and E. Kwok, *Rheological Study of Viscosupplements and Synovial Fluid in Patients with Osteoarthritis.* Journal of Medical and Biological Engineering, 2012. **21**(1): p. 12-16.
53. Cooke, A.F., D. Dowson, and V. Wright, *The Rheology of Synovial Fluid and Some Potential Synthetic Lubricants for Degenerate Synovial Joints.* Engineering in Medicine, 1978. **7**(2): p. 66-72.
54. Dintenfass, L., *Rheology of complex fluids and some observations on joint lubrication.* Fed Proc, 1966. **25**(3): p. 1054-60.
55. Barnett, C.H., *Measurement and interpretation of synovial fluid viscosities.* Ann Rheum Dis, 1958. **17**(2): p. 229-33.
56. Schurz, J. and V. Ribitsch, *Rheology of synovial fluid.* Biorheology, 1987. **24**(4): p. 385-99.

57. Ambrosio, L., Borzacchiello, A., Netti, P.A., Nicolais, L.,*Rheological study on hyaluronic acid and its derivative solutions.* Journal of Macromolecular Science, Part A, 1999. **36**(7-8): p. 991-1000.
58. Tercic, D. and B. Bozic, *The basis of the synovial fluid analysis.* Clin Chem Lab Med, 2001. **39**(12): p. 1221-6.
59. Thurston, G.B. and H. Greiling, *Viscoelastic properties of pathological synovial fluids for a wide range of oscillatory shear rates and frequencies.* Rheologica Acta, 1978. **17**(4): p. 433-445.
60. Schurz, J., *Rheology of Synovial Fluids and Substitute Polymers.* Journal of Macromolecular Science, Part A: Pure and Applied Chemistry, 1996. **33**(9): p. 1249-126.
61. Lopez, C.G., Rogers, S.E., Colby, R.H., Graham, P., Cabral, J.T., *Structure of sodium carboxymethyl cellulose aqueous solutions: A SANS and rheology study.* Journal of Polymer Science Part B: Polymer Physics, 2015. **53**(7): p. 492-501.
62. Stamatopoulos, K., Batchelor, H.K., Alberini, F., Ramsay, J., Simmons, M.J., *Understanding the impact of media viscosity on dissolution of a highly water soluble drug within a USP 2 mini vessel dissolution apparatus using an optical planar induced fluorescence (PLIF) method.* Int J Pharm, 2015. **495**(1): p. 362-73.
63. Yang, X.H. and W.L. Zhu, *Viscosity properties of sodium carboxymethylcellulose solutions.* Cellulose, 2007. **14**(5): p. 409-417.
64. Zorba, M. and G. Ova, *An improved method for the quantitative determination of carboxymethyl cellulose in food products.* Food Hydrocolloids, 1999. **13**(1): p. 73-76.
65. Eastham, R.D., *The Serum Viscosity and the Serum Proteins.* Journal of Clinical Pathology, 1954. **7**(1): p. 66-68.
66. Gonçalves, A.D., Alexander, C., Roberts, C.J., Spain, S.G., Uddin, S., Allen, S., *The effect of protein concentration on the viscosity of a recombinant albumin solution formulation.* RSC Adv., 2016. **6**(18): p. 15143-15154.
67. Sapmaz, I., Manduz, S., Sanri, U.S., Karahan, O., Dogan, K., *Influence of albumin concentration in priming solution on blood viscosity under hypothermic conditions.* Cardiovascular Journal of Africa, 2009. **20**(3): p. 168-169.
68. Yadav, S., S.J. Shire, and D.S. Kalonia, *Viscosity analysis of high concentration bovine serum albumin aqueous solutions.* Pharm Res, 2011. **28**(8): p. 1973-83.

Chapter 4: Development of biorelevant dissolution tests for intra-articular formulations

Overview

Purpose: To develop biorelevant drug dissolution tests for IA formulations and define the effect of setup parameters and hydrodynamics on drug dissolution and permeation.

Methods: TA dissolution and permeation was investigated from an IA suspension using Side-Bi-Side cells and a bi-phasic setup. The amount of drug applied to the methods was based on the *in-vivo* clinical dose. Side-Bi-Side cells were used in three different setups with a static flow simulating the permeation of the drug through the synovial membrane (Setup I), a flow through the receptor phase simulating the blood circulation on the outer part of the synovial cavity (Setup II) and a flow from the donor to the receptor simulating the transynovial flow (Setup III). In static flow, the simultaneous measurement of dissolution and permeation of the drug was enabled. With a flow present, the permeation of the drug through the membrane was assessed, mimicking the permeation of the drug from the synovial cavity to the blood circulation through the synovium. Parameters such as the membrane [GF/F, GF-6, GF-10, a combination of GF-6 and GF-10, Polytetrafluoroethylene (PTFE), cellulose acetate (CA) membrane], the medium [PBS with Tween 80 (1% v/v), organic solvent (methanol, 1-octanol), biphasic setup with PBS with Tween 80 (1% v/v) and 1-octanol and also biorelevant media such as healthy state BSF, PBS with HA and HS, OA and RA BSFs without HA], the flow rate (0.1 and 0.2 mL/min) and also the drug amount (0.3 and 1 mg TA) were tested in order to assess their effect on drug dissolution and permeation. In the bi-phasic setup, drug dissolution and permeation was also assessed with the use of developed BSFs without HA (HS, OA and RA), with 1-octanol as the organic phase, acting as the reservoir for the dissolved drug. Measurements took place from both phases.

Results: Using the side-Bi-side setup, in Setup I, the PTFE membrane did not allow permeation of the drug compared to GF/F and CA, while the organic solvents tested showed no significant difference to the permeation of TA compared with PBS with Tween 80 (1% v/v), apart from methanol. With setup II, a flow present in the receptor phase showed a higher % of permeation of TA compared to the static flow in setup I. In setup III, less drug in the donor phase reached full permeation faster and a higher flow rate also led to increased permeation. Comparing media, the use of non-biorelevant PBS with Tween 80 (1% v/v) led to higher TA permeation. Membranes with higher pore size and loading capacity (GF-6 and GF-10) also led to a higher

amount of TA permeation. Between biorelevant media, there was no significant difference comparing HS BSF and PBS with HA. With BSF without HA, the HS and OA state led to higher TA permeation than with the use of RA state BSF. With the bi-phasic setup, discrimination in TA dissolution between the BSFs without HA tested, was not significant although difference in dissolution profiles was observed in comparison to testing TA dissolution in PBS.

Conclusions: The tested systems allow better simulation of the physiological variables of the synovial cavity in comparison to compendial dissolution apparatus. This may become quite useful to predict *in-vivo* behaviour of IA formulations after joint injection while it can also have application in the parenteral administration of suspensions.

4.1. Introduction

IA administration has proven to be a very attractive drug delivery approach for conditions affecting the joints, due to the multiple advantages offered and especially the direct application to the main site of the developed disease [1]. Compared to the delivery of conventional products such as tablets and capsules, this type of administration provides the possibility of high initial drug concentrations at the site of action with just a low amount of drug injected as exposure to non-related sites is minimised [2]. With limited systemic toxicity, this route is suitable for drugs with good efficacy but a low bioavailability, such as proteins or low solubility drugs [3]. Due to these advantages, there is a vast amount of IA formulations in the market, with an extensive number in the current pipeline of major pharmaceutical companies [2, 4, 5].

Drug dissolution testing is an important evaluation tool for measuring the rate and extent of drug dissolution from a dosage form. It has also been used for quality control evaluation during early and late stages of drug and formulation development, acting as a vital factor for the approval of newly marketed drug products [6, 7]. Standardised, official dissolution methods could be used for these purposes and for the optimization of therapeutic effectiveness during product development, but these compendial dissolution tests would not offer an assessment of biopharmaceutical properties, bioequivalence and predictive results of *in-vivo* bioavailability and behaviour due to their lack of biorelevance [6, 8]. Although there is a high unmet need for an official dissolution test in accordance with regulatory authorities, at the moment, there is no standardised official dissolution method for testing drug dissolution for parenteral and more specifically for IA products [9, 10]. Methodologies such as sample and separate, dialysis and continuous flow have been widely used conventional systems for parenteral formulations [11, 12], but with no sufficient simulation of the physiological environment and hydrodynamics of the synovial cavity, providing a weak prediction of *in-vivo* behaviour. Biorelevant dissolution for IA drugs would be performed under simulated *in-vivo* conditions for predicting the dissolution of drugs administered into the joint and subsequently the synovial fluid. This research tool may be able to reduce the amount of bioequivalence studies performed in various stages of the drug/formulation approval process, improve product quality and reduce relevant regulatory procedures [6]. It is crucial for the dissolution tests to be performed under exact simulated conditions of the synovial fluid physiology, with the choice of media and suitable instrument parameters mimicking hydrodynamics being of vital importance to be able to predict *in-vivo* bioavailability [13]. As there is no compendial setup simulating hydrodynamics

and resembling *in-vivo* conditions, modified setups could be of better use. A combination of a widely acceptable apparatus simulating the hydrodynamics of the joint with an appropriate setup with a suitable dissolution method and a medium that would simulate the synovial fluid conditions, would have the potential to provide efficient *in-vivo* predictive biorelevance.

For a more predictive biorelevant test of *in-vivo* conditions, a biorelevant fluid should simulate the synovial fluid in HS and in disease states, during which parameters affecting drug dissolution may change. Many of the biorelevant dissolution media used in various studies simulating the synovial fluid, may not be adequate for this purpose as they may not contain all the appropriate key components affecting drug dissolution and so being appropriate for predictive models [14-18]. Although several attempts have been made to simulate the conditions in the synovial cavity, in most media, attention is given to the addition of HA which provides viscoelastic properties to the fluid. Although viscosity does affect dissolution rate as it partly determines the diffusion coefficient in the Noyes-Whitney equation (Chapter 3) [19], there are components that provide solubilising effects to the tested drug such as phospholipids [20, 21] which have not been added to developed biorelevant fluid before. To have a better prediction of drug solubility and dissolution rate in the synovial cavity, an updated version of the widely used simulated synovial fluid [14] containing valuable components affecting solubilisation and dissolution was evaluated in Chapter 3, considering the missing physiological relevance of the composition.

The volume of synovial fluid in the knee would be 0.5-2 mL for a HS individual and more than 3.5 mL for a patient with OA [1]. The synovial fluid is an ultrafiltrate of the blood, being filtered from the blood circulation towards the inside of the synovial cavity through the synovial membrane; then the created synovial fluid is also filtered outside of the synovial cavity and again into the blood stream through the synovial membrane (transynovial flow). The synovial membrane (synovium) is quite thin (15-20 μm in the rabbit knee and 60 μm in the human knee [22]) and has an ECM of collagen and glycosaminoglycans [23] and the fluid flows through its 1-2 μm gaps between the synovial lining cells [24]. The aqueous transynovial flow is normally 5-10 μL/min for a flexed knee joint, with an IA pressure of approximately 2 cmH_2O inside the cavity [23]. With increased fluid volume inside the joint due to conditions such as chronic joint effusion, the IA pressure increases to approximately 20 cmH_2O affecting the transynovial flow that also increases to 20-40 μL/min [25]. The flow causes the volume of the synovial fluid in the cavity to be replaced (refreshed) multiple times during the day with

water and proteins replaced in less than 2 hours and HA in 38 hours in a normal individual and in patients with OA [1, 26]. In patients with RA due to the extensive damage of the synovial membrane, the proteins that enter and are cleared from the synovial cavity is up to three times more than in healthy individuals [1].

In order to evaluate permeation through membranes, *in-vitro* diffusion has been studied throughout the years, with setups involving the placement of the drug in the donor chamber, an artificial or biological membrane, a fluid passing through and the measurement of the flux from the receptor chamber. These type of configurations have been applied for the study of various drug delivery systems with a biorelevant approach depending on the type of membrane and type of medium used. Diffusion cells have been applied for studying diffusion in numerous delivery systems: for oral formulations, by measuring oral absorption from permeation across Caco-2 cell monolayers [27] and mimicking the physiological conditions of the human GI tract [28]; for drug delivery through the blood-brain barrier (BBB) by studying permeation effects through microvessel endothelial cells [29] and the involvement of the neurokinin (NK-1) receptor in the permeation of Substance P across the BBB with bovine brain microvessel endothelial cells (BBMEC) monolayers grown on polycarbonate membranes mounted on the diffusion apparatus [30]; for delivery through buccal absorption by studying the permeability characteristics of cultured buccal epithelial cells used as the membrane in the diffusion apparatus [31] and examining drug permeation across porcine buccal mucosa [32, 33]; and for pulmonary delivery by testing permeability through cystic fibrosis mucus solution for simulating disease state mucus [34] while the application of iontophoretic transport of drugs across a biological membrane has also been applied [35].

The application of a bi-phasic setup has also been suggested for simulating biorelevance of drug partitioning through a membrane. The setup involves the use of an upper organic layer which would be in equilibrium with the aqueous layer in test [36]. The drug which would be placed in the aqueous layer, would dissolve and by exploiting its lipophilicity (logP) it would partition into the organic layer which would act as a reservoir for the dissolved drug. This way, sink conditions would be maintained in the system until complete dissolution. The biorelevance in this model was initially reported by Gibaldi and Feldman [37], who suggested that the partitioning of the drug after dissolving in the aqueous phase, would be analogous to the absorbance of the drug from the gastrointestinal (GI) tract during the dissolution rate-limited absorption. This setup has been used since in multiple studies and has also been considered for

coupling with USP apparatus such as the USP apparatus IV [38, 39] and the USP apparatus II [40, 41]. The biorelevance noted in this setup may also be considered for an IA drug delivery system as the removal of the drug from the GI tract may reflect the permeation of the drug through the synovial membrane and into the sub-synovium and the blood circulation.

The aim of our research was to develop an *in-vitro* biorelevant dissolution test that can be used for the characterisation of drug dissolution and diffusion according to the physiological conditions present in the synovial joint. To achieve this aim, the objectives were to simulate the conditions in the synovial cavity by considering and evaluating the media used and the composition of the synovial fluid in healthy and disease state on drug dissolution, the hydrodynamics of the joint in terms of the volume of the fluid, the flow present in the synovial cavity in three membrane diffusion setups (static flow, blood circulation flow and transynovial flow), the effect of drug amount on the tested setups and the effect of the membrane applied. With a bi-phasic model we evaluated the effect of developed BSF in Chapter 3, on drug dissolution. TA was used as a model drug for the development of the dissolution method.

4.2. Materials and methods

4.2.1. Materials

TA (98+%, fine chemical) was purchased from Alfa Aesar (UK), Kenalog 40® (TA 40 mg/mL) and Adcortyl® (TA 10 mg/mL) were purchased from Bristol-Myers Squibb (UK). For all experiments, ultra-pure water was used obtained from a Milli-Q purification device. The phosphate buffers were made with sodium chloride (≥99.9%), potassium dihydrogen orthophosphate (≥99.5%), di-sodium hydrogen orthophosphate, anhydrous dried (≥99.5%) and potassium chloride (≥99.5%) which were purchased from Sigma-Aldrich (UK). The BSF produced, was made with HBSS 1X without calcium, magnesium, phenol red; bovine serum albumin powder, fraction V; sodium hyaluronate 95%, all purchased from Fisher Scientific (UK), γ-globulin from bovine blood purchase from Sigma-Aldrich (UK) and phospholipid PC from Egg purchased from Lipoid (Germany). Hyaluronidase from bovine tests, type VIII, lyophilized powder (300-1000 U/mg) was purchased from Sigma-Aldrich (UK). Tween 80 was bought from VWR (UK) and 1-Octanol (99%, pure) was purchased from Fisher Scientific (UK), while methanol was purchased from Sigma-Aldrich (UK). The membranes used, were ordered from Whatman (GE Healthcare Life Sciences) and include different types of glass microfiber filters (GF) GF/F, GF-6, GF-10 and membranes from CA (0.45 µm) and PTFE (0.45 µm) (Whatman, GE Healthcare Life Sciences, UK).

4.2.2. Methods

4.2.2.1. Media evaluated in biorelevant dissolution studies

4.2.2.1.1. Non-biorelevant media

In the setups involving the side-Bi-side cells, the media tested in the static flow (Setup I, Table 4.1) were PBS with Tween 80 (1% v/v), methanol, 1-octanol and a biphasic system containing PBS with Tween 80 (1% v/v) and 1-octanol. In setup II and III (Table 4.1), the non-biorelevant medium tested was PBS with Tween 80 (1% v/v).

4.2.2.1.2. Biorelevant media of Healthy and Disease State Synovial Fluid

BSFs were tested with the side-Bi-side setup III (Table 4.1) in three states, healthy, OA and RA and also in the widely used artificial synovial fluid containing PBS with HA (3 mg/mL) [14]. The BSF media were prepared with the addition of main components affecting

dissolution, excluding HA, with average values found in the literature (Table 4.2) in accordance with Chapter 3. The healthy state BSF was also evaluated with the addition of HA according to the values found in the literature. In the monophasic and bi-phasic setups, the similar BSFs simulating the healthy state, OA and RA, excluding the component HA, were tested. To prepare the media, the procedure followed was according to the development of BSFs in Chapter 3, and the methodology published by Jantratid et al [42].

Table 4.1. Side-Bi-Side setups and parameters tested

Setup	I (Static Flow)	II (Mimicking blood circulation)	III (Mimicking transynovial flow)
Flow rate	0 mL/min	0.2 mL/min	0.1 - 0.2 mL/min
Membrane	Glass microfiber (GF/F) Cellulose Acetate (CA) Polytetrafluoroethylene (PTFE)	Glass microfiber (GF/F)	Glass microfiber (GF/F, GF-6, GF- 10, GF-6 + GF-10) Cellulose Acetate (CA)
Medium (donor and receptor compartment)	PBS + Tween 80 (1% v/v) Methanol 1-octanol Biphasic: PBS with Tween 80 (1% v/v) and 1-octanol	PBS + Tween 80 (1% v/v)	PBS + Tween 80 (1% v/v) BSF with HA (Healthy state) BSF without HA (Healthy state, OA and RA) PBS + HA (3 mg/mL)
Sampling times	Every 30 min up to 1 hour, then every 2 hours up to 12 hours and then 24 hours	Every 30 min up to 1 hour, then every 2 hours up to 12 hours	Every 30 min up to 1 hour, then every 2 hours up to 8 or 12 hours
Sampling points	Donor and receptor phase	Receptor phase	Receptor phase
Volume of medium (Donor - Receptor)	3.5 mL	1.5 mL	1.5 mL
Amount of drug	1 mL of TA suspension 10 mg/mL (Adcortyl®)	1 mL of TA suspension 10 mg/mL (Adcortyl®)	0.1 and 1 mL of TA suspension 10 mg/mL (Adcortyl®)

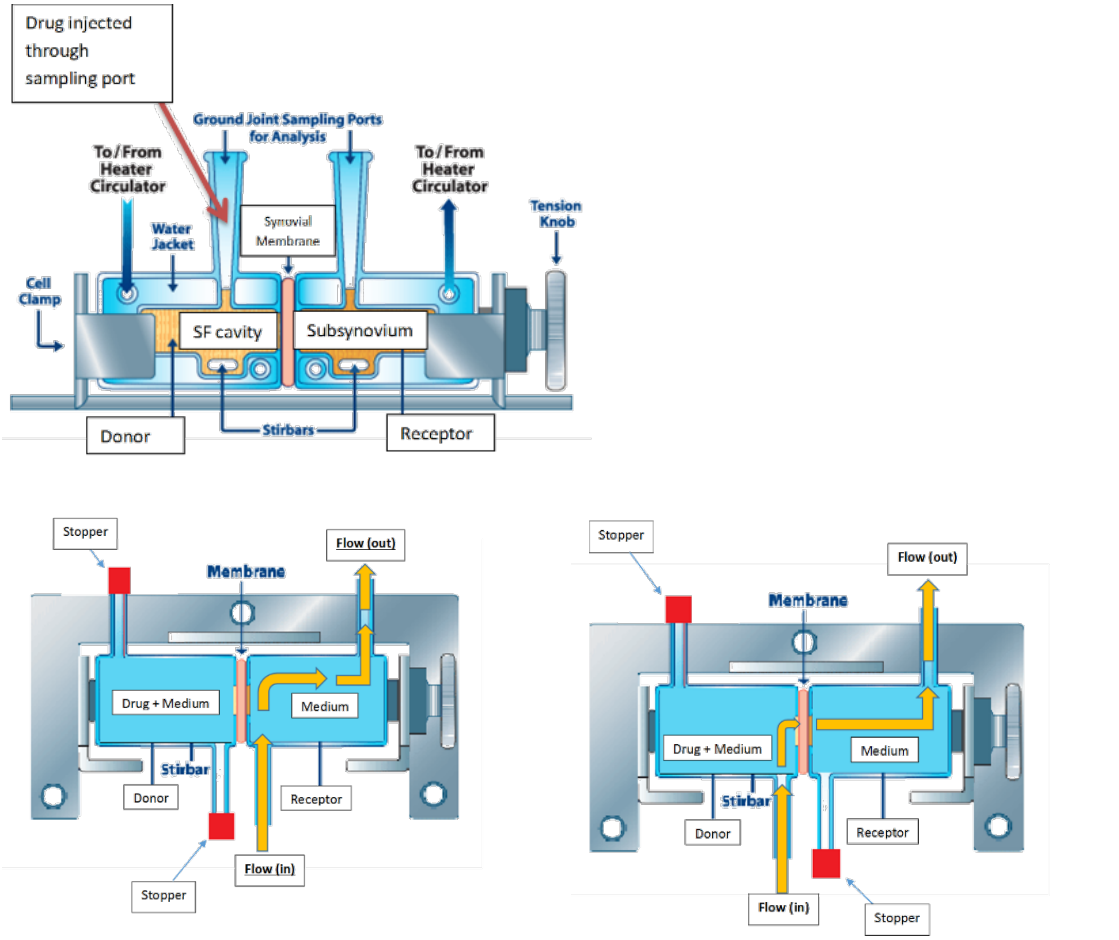

Fig 4.1. Side-Bi-Side setups in this study. Setup I (above), setup II (bottom, left), setup III (bottom, right)

Table 4.2. Composition of Biorelevant media simulating synovial fluid in healthy state, OA and RA

Components (mg/mL)	Healthy State	Osteoarthritis (OA)	Rheumatoid Arthritis (RA)
Buffer	HBSS	0.1 M $NaHPO_4$ + HCl	0.1 M $NaHPO_4$ + HCl
HA	3 or 0	0	0
BSA	11.5	11.5	20.25
γ-globulin	1.7	1.7	24.75
PC	0.15	0.25	0.9

4.2.2.2. Solubility studies

The solubility of TA in the developed biorelevant media (Healthy state, OA and RA) without HA, was determined at 37 ^{o}C. The study was performed with the shake-flask method by adding an excess amount of the drug to the medium in test. The suspensions were then shaken in a

water bath at 37 ± 0.5 ^{o}C (Grant SBB Aqua Plus, UK) for 24-h. Samples were then withdrawn, filtered with 0.45 μm RC filters, diluted with the corresponding medium where appropriate before analysis and then the TA amount was quantified in the HPLC.

4.2.2.3. Biorelevant in-vitro dissolution/permeation testing

4.2.2.3.1. *In-vitro* dissolution/permeation setups with Side-Bi-Side cells

The dissolution and permeation of TA was studied from commercially available Side-Bi-Side diffusion cells (Permegear Inc., USA). A controlled stirring rate (300 rpm) was applied in both compartments with 7 mm stir bars (Sigma-Aldrich, UK) in each glass half cell and a temperature of 37 ^{o}C applied. The cells were placed on temperature controlled magnetic stirrers. A membrane or filter was then applied between the glass half cells, which were then tightened together with a cell clamp. The system mimics the structure of the joint [22, 43] which is represented by two cavities, the donor phase (synovial cavity) and receptor phase (subsynovial cavity – blood circulation) which are separated by the membrane/filter (synovial membrane). The donor compartment in the glass cell half, represents the synovial cavity in which the drug is administered, the membrane in the setup represents the synovial membrane, and the receptor compartment in the other glass cell half represents the sub-synovium cavity in which the blood circulation flows. The physiological environment is simulated with low volumes in each compartment and with an open system flow in the setup, mimicking the blood circulation (flow in receptor phase) or the transynovial flow (flow from donor to receptor phase). Fig. 4.1. illustrates the different setups of the Side-bi-Side cells tested according to the actions taking place in the synovial cavity during and after the IA injection process.

4.2.2.3.1.1. Setup I. Static flow

Setup I explores the dissolution and permeation of TA through the membrane with static medium flow; the parameters tested being described in Table 4.2. In this setup, sampling takes place in both compartments, measuring dissolution in the donor compartment, where the drug is placed and permeation through the examined membrane and at the other compartment (receptor). In Setup I, the effect of different membranes and media was evaluated. Glass microfiber filters (GF/F, GF-6, GF-10) were used as the membrane between the donor and receptor compartment, with CA and PTFE filters tested as well. The cells used in this setup did not have ports allowing a flow through the receptors (as in setups II and III) and the volume of medium in each compartment was 3.5 mL. 1 mL of the TA suspension 10 mg/mL (Adcortyl®)

with medium [PBS with Tween 80 (1% v/v)], organic solvent (methanol or 1-octanol) or a bi-phasic setup [PBS with Tween 80 (1% v/v) and 1-octanol) was placed in the donor and receptor compartment. 100 μL samples were taken in multiple time points up to 24-h, from both compartments, with syringes from a zone midway between the surface of the medium and the bottom of the glass cell, with volume replacement with fresh medium. Samples from both compartments were injected in the HPLC, with measurements showing the amount of drug dissolved (donor compartment) and drug diffused through the membrane (receptor compartment). The % dissolved was calculated according to a calibration curve (2-10 μg/mL) in the corresponding medium [44]. Results are presented as Mean (% dissolved over time) ± S.D.

4.2.2.3.1.2. Setup II. Flow of medium in receptor phase (Simulating blood circulation)

In setup II (Fig. 4.1), there is a continuous flow through the receptor phase of the Side-bi-Side glass half cell, mimicking the permeation of the drug from the synovial cavity to the flowing blood circulation with the diffusion of TA measured over time. This setup considers the simulation of the blood flow outside of the synovial cavity and resembles the process following an IA injection, as part of the formulation slowly exits the joint and enters the flowing blood circulation [22, 26, 45]. The receptor phase simulates the subsynovium of the synovial joint (the outside part of the synovial cavity, separated by the synovial membrane) leading to the blood circulation [1, 22, 23]. Because of the flowing medium present, an open system flow is generated in the receptor compartment.

The effect of flow present in the receptor phase was evaluated with this setup, in which sink conditions are present due to the existence of the open system in the receptor phase. Stoppers were placed in the side portings of the donor Side-Bi-Side glass half cell phase (Fig 4.1, Setup II). A syringe pump (Fusion 200, Chemyx Ltd.) was used to flow the medium through the receptor compartment with tubing connected to one port flowing the medium in and a small part of tubing connected to the other port of the same glass cell for collecting the sample in volumetric cylinders, with stoppers placed in both ports of the donor compartment glass half cell. The cells with ports allowing a medium to flow through both phases, were different from the cells used for the static flow setup, with an initial volume of medium in each compartment, 1.5 mL. 1 mL of TA suspension 10 mg/mL (Adcortyl®) with medium [PBS with Tween 80 (1% v/v)] was placed in the donor and receptor compartment with a constant medium flowing through (flow: 0.2 mL/min) the receptor compartment. Samples were collected from the

receptor compartment in volumetric cylinders as the medium was flowing through, measuring drug permeation through the membrane every half hour for 1 hour and then every 2 hours for 12 hours. Samples from the receptor compartment were injected in the HPLC, with measurements showing the amount of drug diffused through the membrane. The % dissolved and permeated was calculated according to a calibration curve (2-10 μm) in the corresponding medium [44]. Results are presented as Mean (% dissolved over time) ± S.D.

4.2.2.3.1.3. Setup III. Flow of medium from donor to receptor phase (Simulating transynovial flow)

The third setup (III) (Fig. 4.1) mimics the transynovial flow, as the medium in the cell flows from the compartment where the drug is placed, permeates through the membrane, and then exits through the compartment that mimics the exo-synovial space making the setup an open flow system. As the donor phase simulates the synovial cavity containing synovial fluid and the receptor phase simulates the subsynovium of the synovial joint connected to the blood circulation, the flow mimics the transynovial flow from the synovial cavity to the subsynovium through the synovial membrane [46, 47]. A syringe pump (Fusion 200, Chemyx Ltd.) was used to flow the medium from the donor phase through to the receptor phase with tubing connected to one port of the donor compartment and a small part of tubing connected to one port of the receptor compartment for collecting the sample in volumetric cylinders, with stoppers placed in the remaining ports of the donor and receptor compartment glass half cells. The cells with ports allowing a medium to flow through both phases, were different from the cells used for the static flow setup, with an initial volume of medium in each compartment, 1.5 mL.

Parameters such as the effect of flow rate from the donor to the receptor phase (0.1 and 0.2 mL/min), was tested on the diffusion of TA through the GF/F membrane, and PBS with Tween 80 (1% v/v) as the medium placed in both receptors and a dose of 1 mL of TA suspension 10 mg/mL (Adcortyl®) in the donor phase (Table 4.2) Also different membranes [Glass microfiber (GF/F, GF-6, GF-10, combination of GF-6 and GF-10), CA and PTFE] were tested in PBS with Tween 80 (1% v/v) and Healthy state BSF (with HA) in a flow of 0.1 mL/min and a dose of 1 mL of TA suspension 10 mg/mL (Adcortyl®) in the donor phase. In addition, the effect of different drug amounts (1 and 0.3 mg) of TA on the diffusion of the drug through the GF/F membrane was examined in PBS with Tween 80 (1% v/v) and a flow of 0.2 mL/min. The effect of different media [PBS with Tween 80 (1% v/v), Healthy state BSF (without HA) and the widely used dissolution medium PBS with HA (3 mg/mL) [14]) were also examined, with a

GF/F, GF-6, GF/10 and a combination of GF-6 + GF-10 membrane with a flow of 0.1 mL/min and a dose of 1 mL of TA suspension 10 mg/mL (Adcortyl®) in the donor phase. Finally, the effect of biorelevant media without HA (Healthy state, OA and RA) was evaluated with a flow of 0.1 mL/min, a combination of GF-6 + GF-10 membranes and a dose of 0.1 mL of TA suspension 10 mg/mL (Adcortyl®) in the donor phase. For the development of the BSF, the HA is responsible for the viscosity of the medium [48, 49]. BSFs were tested with and without HA as the addition of HA leads to a high viscosity which does not allow the medium to be used in this setup as the flow and permeation through the membrane is restricted. TA suspension was placed in the donor compartment together with the medium used, in volumes of 0.1 mL and 1.4 mL respectively or 1 mL and 0.5 mL medium respectively, with 1.5 mL of medium placed in the receptor phase. Samples were collected from the receptor compartment in volumetric cylinders as the medium was flowing through, measuring drug permeation through the membrane every half hour for 1 hour and then every 2 hours for 12 hours. Samples from the receptor compartment was injected in the HPLC directly or after treatment for BSF samples containing HA, with measurements showing the amount of drug diffused through the membrane. The % dissolved and permeated was calculated according to a calibration curve (2-10 μm) in the corresponding medium [44]. Results are presented as Mean (% dissolved over time) ± S.D.

4.2.2.3.2. *In-vitro* dissolution/permeation set ups with glass bottles

The simulation of the synovial cavity from a biorelevant dissolution aspect can also be expressed with the use of a biphasic model. The monophasic and biphasic dissolution system experiments were performed with the use of glass bottles (Duran HPLC bottle, Fisher Scientific, UK). In both setups, there was an agitation of 300 rpm with the bottles placed on a magnetic hotplate stirrer. For the monophasic setup, 50 mL of PBS, HS and OA BSF (without HA) were tested and for the bi-phasic setup 50 mL of aqueous phase [(PBS, HS, OA and RA BSF (all BSFs without HA)] and 10 mL of organic phase (1-octanol). The experiments were performed at 37 ± 0.5 ^{o}C in triplicate. 1 mL samples were collected from a zone midway between the surface of the medium and the bottom of the glass bottle every 30 minutes for one hour and then each hour until 8 hours from the aqueous phase in the monophasic and from both phases in the biphasic setup (with volume replacement with fresh corresponding medium) to measure the amount dissolved in the aqueous compartment and the amount that partitions into the organic phase. Samples were then diluted with the corresponding medium where

appropriate, before analysing with the HPLC to determine the amount of TA dissolved and permeated. The % dissolved was calculated according to a calibration curve (2-10 μm) in the corresponding medium [44]. Results are presented as Mean (% dissolved over time) ± S.D.

4.2.2.4. Biorelevant media (containing HA) sample treatment

Synovial fluid sample preparation took place according to the method described by Sottofattori et al. [50]. An amount of hyaluronidase solution prepared based on manufacturer (initial concentration of 300-1000 U/mg) was added to the *in-vitro* BSF samples to reach a final concentration of 150 U/mL which degraded HA and decrease the viscosity of the sample leading to an easier filtration and analysis. Hyaluronidase was reconstituted at 1 mg/mL in 0.02 M sodium phosphate buffer, pH 7, containing 77 mM sodium chloride and 0.01 % BSA. For the spiked working calibration standards, the diluted TA solution was added afterwards.

4.2.2.5. Triamcinolone Acetonide HPLC Analysis

The solubility samples and standard solutions were analysed using an Agilent 1100 series HPLC system (Agilent, UK) consisting of a G1329A autosampler, a G1330A ALS thermostat, a G1316A thermostatted column compartment, a G1315A DAD, a G1322A degasser and a G1311A quaternary pump. A modification of a published method was used (Chapter 2). Reversed phase chromatography was performed using an Agilent Eclipse XDB-C18 column (2.6 x 250 mm, 5μm pore size) (Agilent, UK). The flow rate was set at 1 mL/min, temperature at 25 ^{o}C, the UV detection signal was set at 240 nm and injection volume 20 μL. The HPLC method for the analysis of the biorelevant samples had a stop time of 24 min and include a gradient with increased water % in the beginning of each run (methanol:water at 10:90 for 8 min and then at 65:35 for 16 min). For biorelevant samples, the HPLC method included the gradient with increased water % in the beginning of each run, in order to wash the column before each sample analysis. This reduced the build-up of impurities in the column which could lead to increased pressure. The HPLC method for the analysis of non-biorelevant samples had a stop time of 12 min and include the mobile phase running at an isocratic mode with 65:35 methanol:water. For non-biorelevant samples, calibration curves were prepared with the use of a stock solution of TA (100 μg/mL) in methanol. Working calibration standards from a range of concentrations (2-10 μg/mL) were composed after diluting the stock solution accordingly with the selected medium. For biorelevant samples, the samples were diluted with the corresponding medium where appropriate, before analysing with the HPLC to determine the

amount of TA dissolved. Working calibration standards from a range of concentrations (2-10 µg/mL) were composed with a solution of hyaluronidase being added to the sample. The hyaluronidase solution was added to the sample and then the 20 µg/mL aqueous intermediate (PBS) of the stock solution of TA in methanol (5 mg/mL) was added to the synovial fluid-enzyme solution to prepare the spiked standard following the sample preparation technique. Adding the stock solution directly into the blank BSF causes protein precipitation due to the strong effect of the organic solvent. The drug amount was chosen to be included before the addition of the hyaluronidase, to follow the same process observed in the solubility studies; the sample including the drug and the addition of the degrading enzyme following afterwards. The % dissolved was calculated according to a calibration curve (2-10 µm) in the corresponding medium.

4.2.2.6. Dissolution profile comparisons

The use of f_2 similarity factor was chosen for comparing dissolution profiles. The percentages of dissolution for all time points were considered until the drug reached 85% dissolution of the plateau value; in this occasion one time point after the 85% dissolution was taken into account. The similarity factor f_2 from 50-100 showed similarity of the compared dissolution profiles. The equation used was:

$$f_2 = 50 \times \log\left\{\left[1 + \left({}^{1}/_{n}\right)\sum_{t=1}^{n}\left(R_t - T_t{}^{2}\right)\right]^{-0.5} \times 100\right\} \quad \text{(Eq. 1)}$$

where:

n is the number of time points

Rt is the dissolution value of the reference at time t

Tt is the dissolution value of the test at time t.

The calculations were done with the DDsolver Add-In (DDsolver, Add-In, Microsoft Excel) software program using the dissolution profiles from the amount of drug dissolved over time.

4.3. Results and discussion

4.3.1. Solubility studies

Solubility studies performed in BSF without HA in three state (Healthy state, OA and RA, Fig. 4.2) showed similar results to the developed BSFs in Chapter 3, with RA BSF having the highest solubility followed by OA BSF and Healthy state BSF.

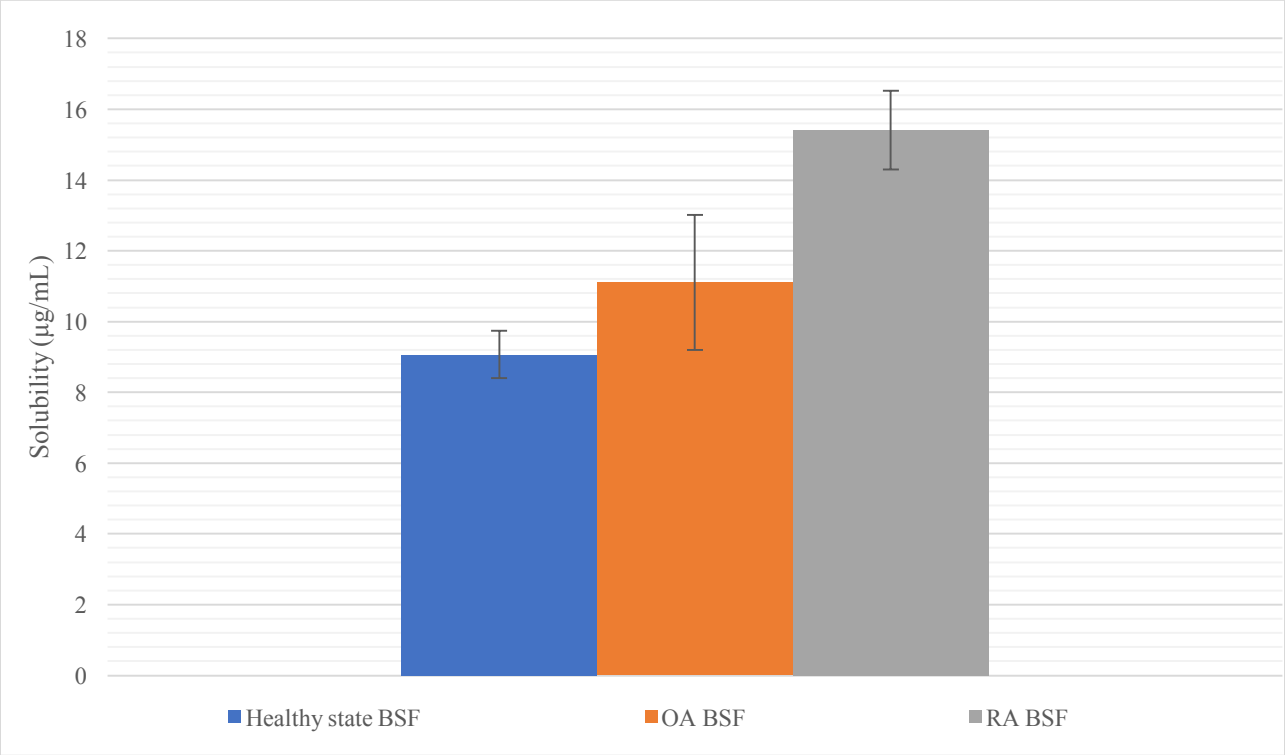

Fig. 4.2. Solubility of TA samples in BSF media without HA in three states (Healthy state, OA and RA) (n=3)

4.3.2. *In-vitro* dissolution and diffusion studies with Side-bi-Side setups

4.3.2.1. In-vitro dissolution and diffusion studies with Static Flow setup (I)

4.3.2.1.1. Effect of membrane

Three membranes were tested, GF, PTFE and CA. The TA dissolved in the donor phase reaches a plateau of ~ 2% and with the donor phase containing 3.5 mL, this demonstrates that 200 µg were dissolved from the 10 mg (1 mL Adcortyl®) injected. This plateau can be partially justified from the measured solubility of TA in PBS with Tween (1% v/v) (92 µg/mL) (Chapter 2). The percentage of drug dissolved (donor compartment) was higher than the amount of drug permeating through to the receptor compartment. The % of drug dissolved in the donor

compartment reached a 2% TA dissolved for all membranes tested, while the % drug diffused was less than 0.5% with the use of GF/F filter and CA membrane, whereas a negligible % of drug permeation to the receptor phase was observed with the use of the PTFE filter (Fig. 4.3). As permeation of the drug was evident with the use of a CA membrane and a GF/F filter, with the PTFE membrane there was an absence of permeation, making this type of membrane non-suitable. This may be explained due to the hydrophobicity (repulsion towards water) of the PTFE membrane, according to which the medium containing the drug was not able to permeate easily from the donor to the receptor phase. Further studies were conducted with the use of the GF filters as the diffusion rate might have been similar with CA, but these type of filters have a much higher loading capacity.

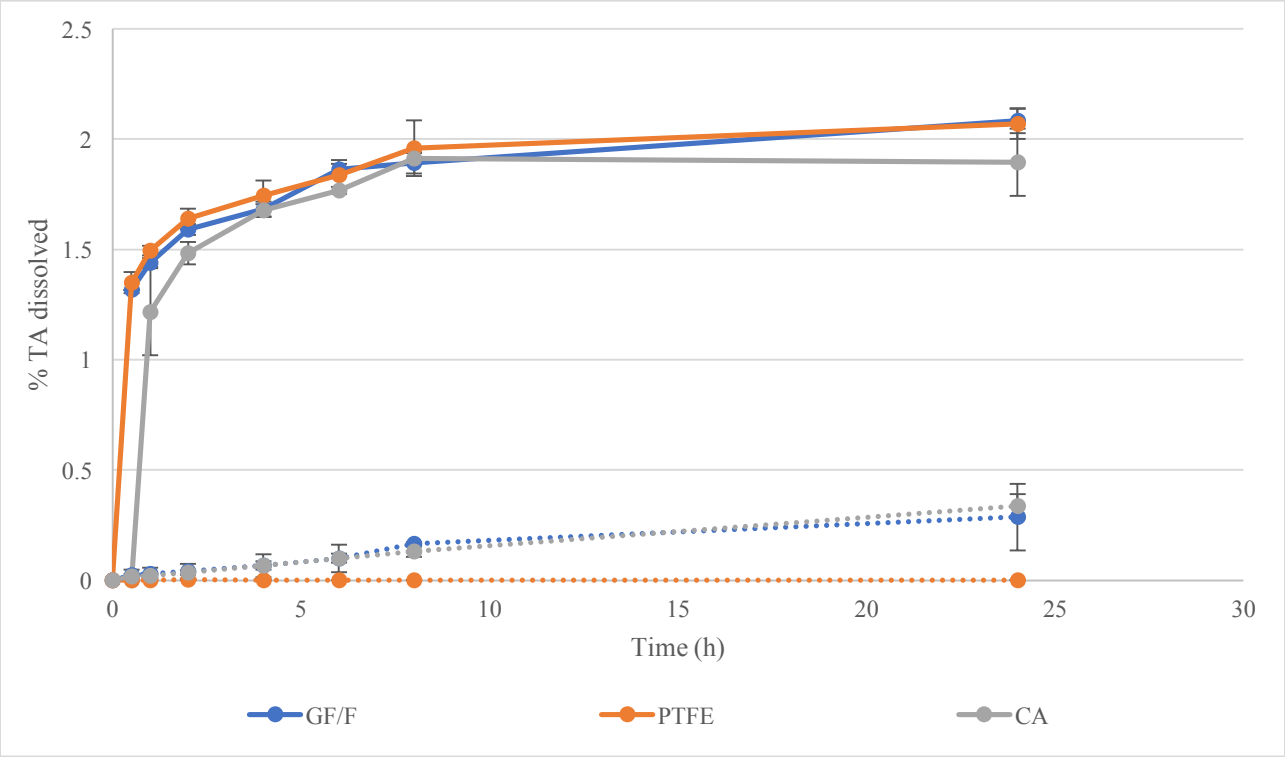

Fig. 4.3. Mean ± SD % TA dissolved from Adcortyl® in PBS with Tween 80 (1% v/v) in donor (solid line) and receptor (dotted line) compartment (dose: 1 mL of TA suspension 10 mg/mL)

4.3.2.1.2. Effect of organic medium

The % of drug dissolved (up to 2.6 %) and diffused (up to 0.3 %) in the system with the use of 1-octanol and with the bi-phasic system in the receptor compartment was similar with the results of PBS with Tween 80 (1% v/v) as the medium. The dissolution rate in the donor phase seems to be faster than the rate of drug permeation through the GF/F filter into the receptor

phase. The use of a bi-phasic system in the setup was assessed in order to increase the release of the drug in the aqueous phase as the organic phase would act as a "reservoir" due to the higher solubility of the drug in 1-octanol [36, 40] exploiting the lipophilicity (logP) of the drug. Also with the organic solvents used as media instead of PBS with Tween 80 (1% v/v) which was used in the first set of experiments, there is a higher drug solubility and so a higher dissolution in the donor phase should take place. With a higher amount of drug dissolved, there was a higher amount of drug available to diffuse through the membrane. Due to the limited sink conditions and the slow diffusion, this was not witnessed with 1-octanol being used as the medium, or as part of the bi-phasic system in the donor phase. With the use of methanol in the receptor compartment, a higher drug dissolution (up to 11 %) and drug diffusion (up to 13 %) was observed (Fig. 4.4). With methanol, as the organic solvent could be miscible with the medium in the donor phase, there was a higher diffusion of drug into the receptor phase. This way more drug dissolved in the donor phase leading to a higher dissolution measured in both compartments.

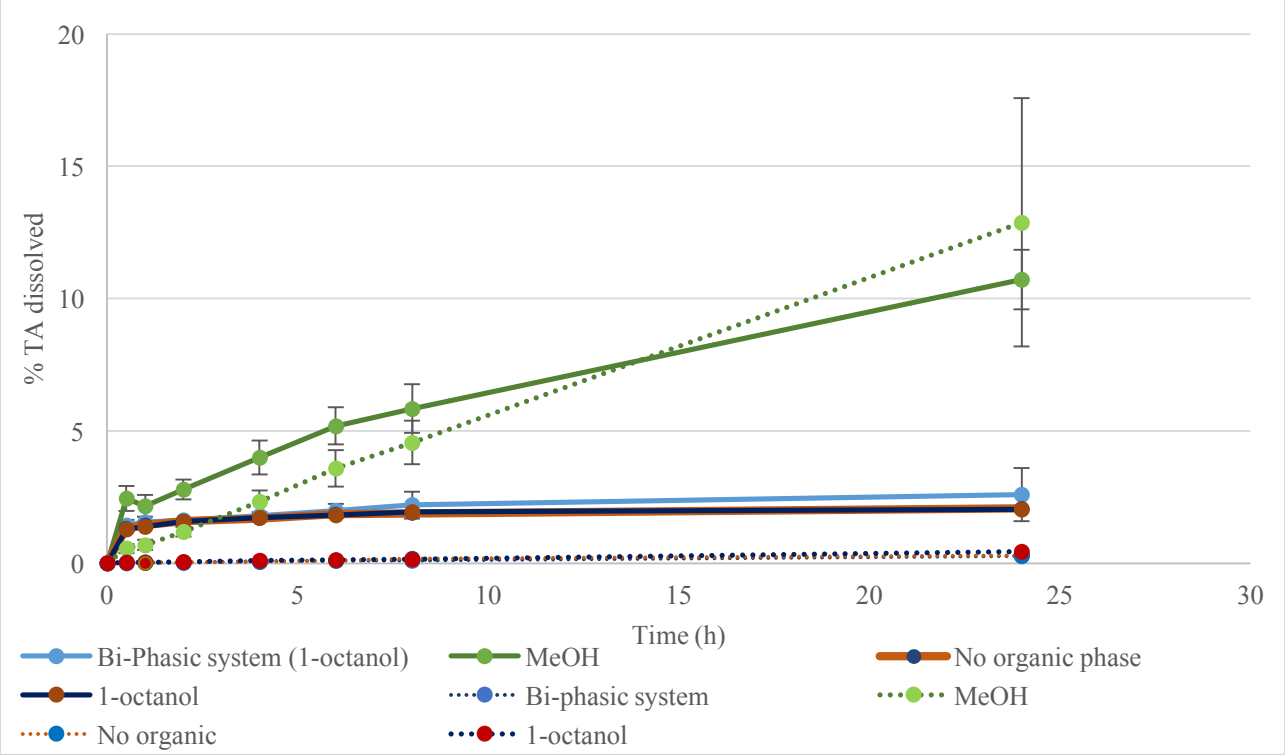

Fig. 4.4. Mean ± SD % TA dissolved from Adcortyl® in donor (solid line) and receptor (dotted line) compartment (membrane: GF/F, dose: 1 mL of TA suspension 10 mg/mL)

4.3.2.2. Blood circulation flow setup (II)

4.3.2.2.1. Effect of applied flow in receptor phase compared to Setup I and Setup III

When a constant flow of medium was applied in the receptor phase (0.2 mL/min), comparing setup I to setup II, the % of drug diffused was 0.34 % after 8-h, compared to 0.17 % in setup I.

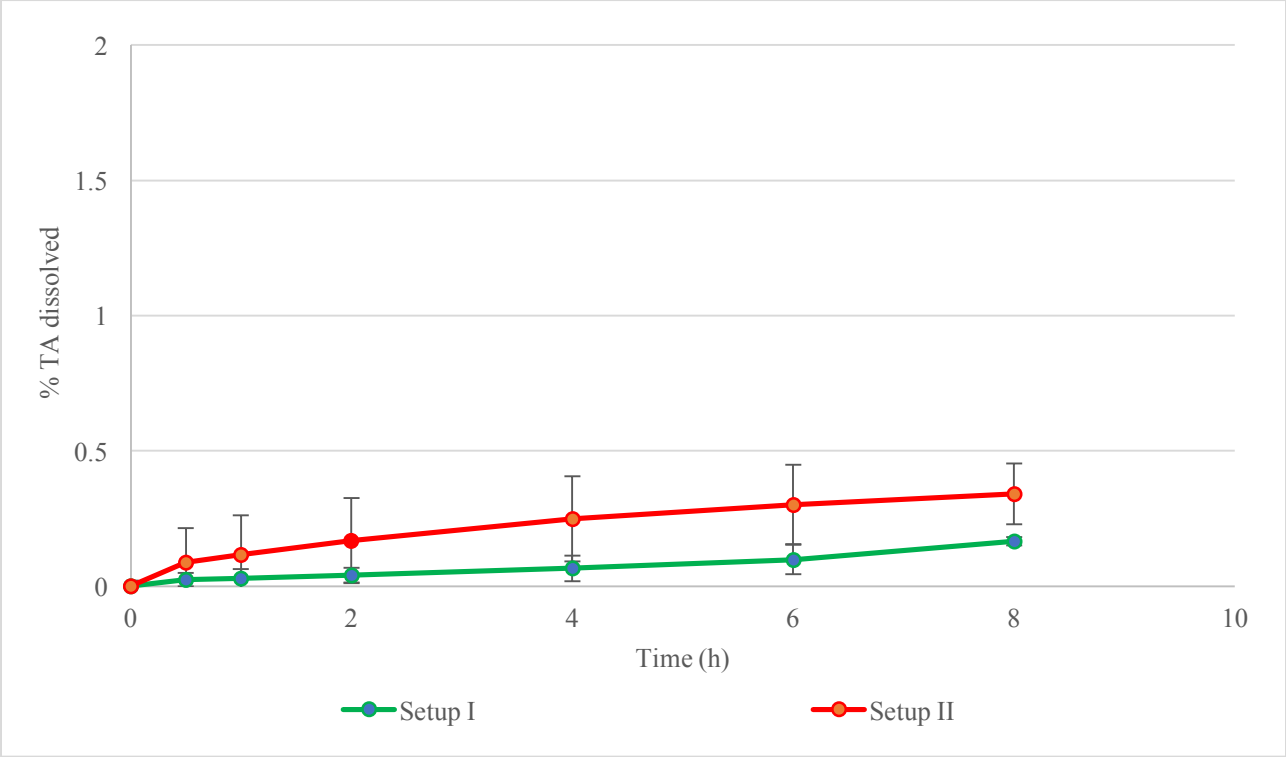

Fig. 4.5. Mean ± SD % TA dissolved though the membrane from Adcortyl® in PBS with Tween 80 (1% v/v) in Setup I and in Setup II (flow 0.2 mL/min) (Membrane: GF/F, dose: 1 mL of TA suspension 10 mg/mL)

With an open flow system having a flow rate of 0.2 mL/min in the receptor phase, the % of TA diffused through the membrane was twice the % compared to the static flow setup ($f_{2_{I-II}} = 99.76$) (Fig. 4.5). The continuous flow present in the receptor, provides sink condition in the receptor compartment and therefore a higher drug amount can diffuse through the membrane. Comparing flows applied in Setup II and III, led to a significant difference noted ($f_{2_{II-III}} = 19.24$). Comparing diffusion rate from 0.1 mL of Adcortyl, placed in the donor phase, at 8-h, in setup II there is a release of 6.4% compared to 71.4% in setup III (Fig. 4.6). With a flow set from the donor phase to the receptor phase and samples collected at the receptor phase means that the flow proceeds through the membrane aiding drug dissolution. Applying this flow, affects the hydration of the material in test. With a high volume of medium flown through the donor phase, an open system is present throughout the system allowing more drug to dissolve [54, 55].

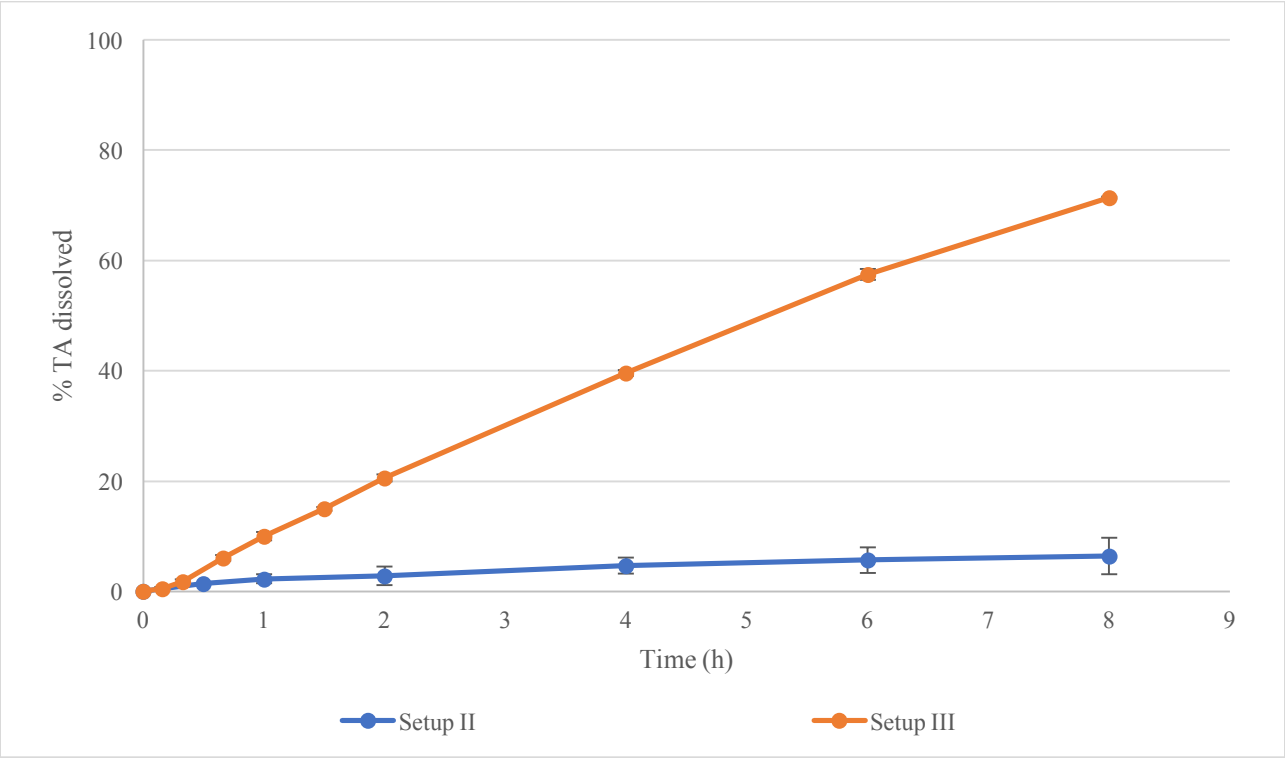

Fig. 4.6. Mean ± SD % TA dissolved though the membrane from Adcortyl® in PBS in Setup II and in Setup III (flow 0.1 mL/min) (Membrane: GF/F, dose: 0.1 mL of TA suspension 10 mg/mL)

4.3.2.3. Transynovial flow Setup (III)

4.3.2.3.1. Effect of drug amount

A suspension volume of 0.3 mL of Adcortyl® (3 mg of TA) led to complete drug dissolution (100%) after 10-h when PBS with Tween 80 (1% v/v) was used as the dissolution medium with a constant flow rate of 0.2 mL/min. A higher amount of drug present in the donor compartment (1 mL of Adcortyl®, 10 mg of TA) led to a 65% of the drug dissolved after 12-h ($f_{2_{1-0.3}} = 23.25$) (Fig. 4.7). Results can be justified according to the Noyes-Whitney equation (Eq. 1), as a higher amount of drug in the donor phase will take a longer time to dissolve in the open system compared to smaller drug concentration present [19].

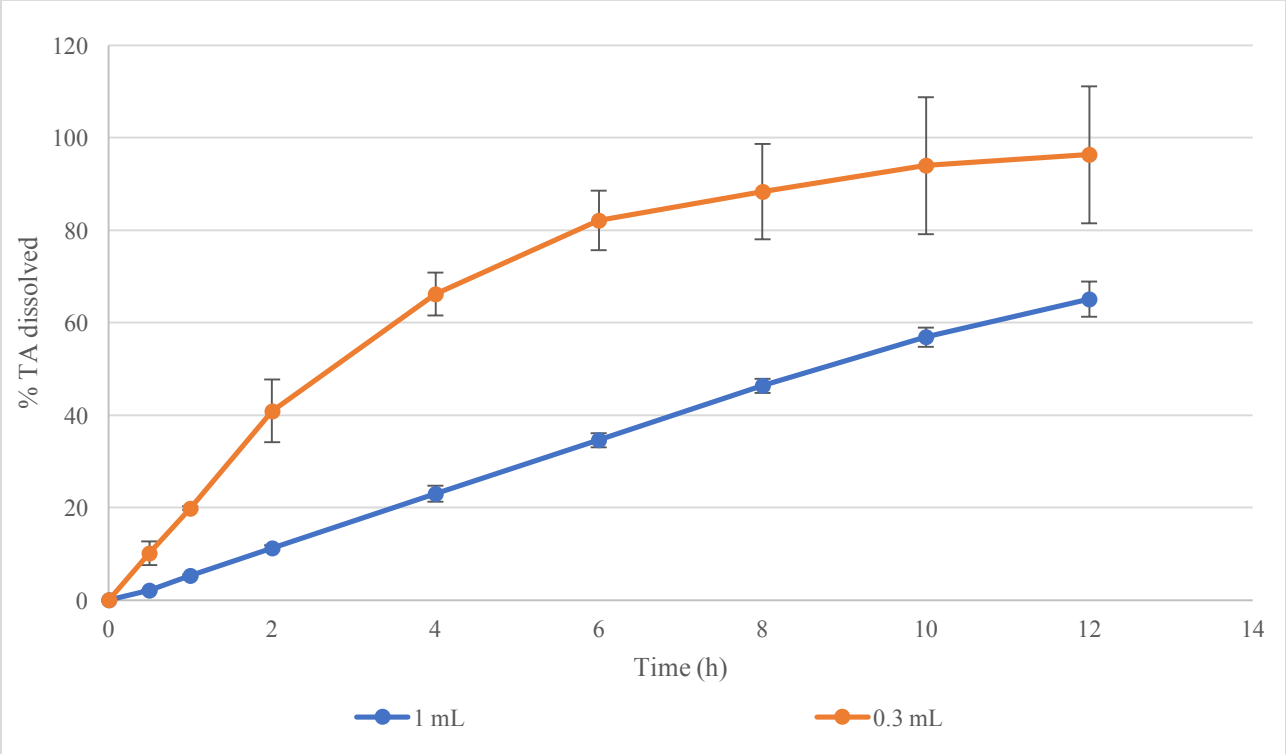

Fig. 4.7. Mean ± SD % TA dissolved though the membrane from different volumes of Adcortyl® (10 mg/mL) in PBS with Tween 80 (1% v/v) (flow: 0.2 mL/min, membrane: GF/F)

4.3.2.3.2. Effect of flow rate

Placing a dose of 1 mL of Adcortyl in the donor compartment and applying two constant flow rates, 0.1 and 0.2 mL/min, resulted in a 24% and 61% TA dissolved respectively after 12-h (Fig. 4.8). As the flow rate in the system increased, so did the percentage (%) of TA dissolved from the system ($f_{2_{1-0.3}} = 35$). As the flow rate is increased and more medium is flown from the donor to the receptor, the hydration of the material in test is affected, increasing the dissolution. As more medium is flown through, more drug is dissolved in the same amount of time [56].

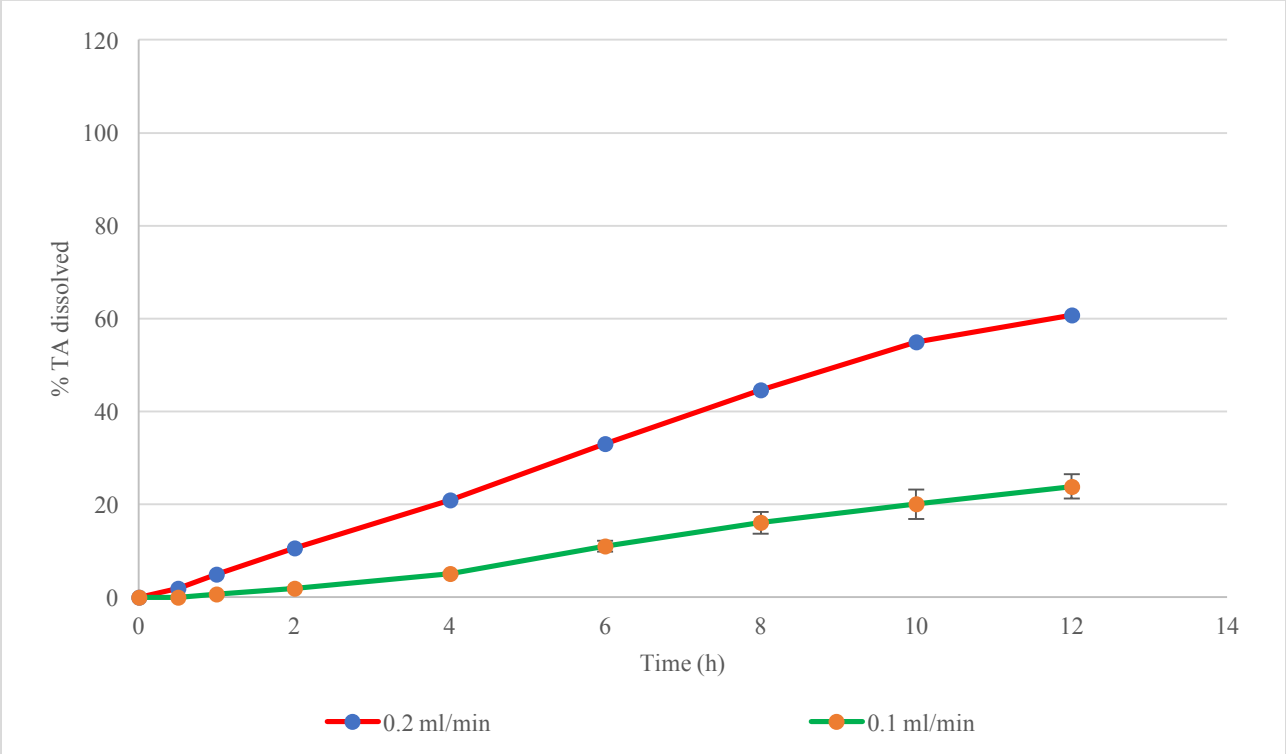

Fig. 4.8. Mean ± SD % TA dissolved through the membrane from Adcortyl® in PBS with Tween 80 (1% v/v) [membrane: GF/F, dose: 1 mL of TA suspension 10 mg/mL]

4.3.2.3.3. Effect of membrane and medium

The glass microfiber filters with binders providing extra mechanical strength [GF-6 (inorganic binder), GF-10 (organic binder) and GF-6 + GF-10 combined] have similar dissolution profiles up to ~45-50 % of drug dissolved in 12-h ($f_{2_{GF6-GF10}} = 93.61$, $f_{2_{GF6-GF6+GF10}} = 73.67$ and $f_{2_{GF10-GF6+GF10}} = 73.76$). The glass microfiber filter without binder tested (GF/F) and the CA membrane gave similar dissolution profiles but lower drug dissolution in 12-h, ~ 30-35% ($f_{2_{CA-GFF}} = 87.41$) (Fig. 4.9). The membranes were tested in order to evaluate their effect in drug dissolution at a flow of 0.1 mL/min. As the pore size of GF/F and GF-6 are similar (~ 0.7 µm), the difference in drug dissolved will be relevant to the inorganic binder present in the GF-6 filter increasing its mechanical and wet strength ($f_{2_{GFF-GF6}} = 52.17$). There are no significant differences between the GF filters with binders and their combination although particle retention between GF-6 and GF-10 is different, ~0.7 and ~2 µm respectively. CA (pore size: 0.45 µm) was not chosen for the subsequent studies with biorelevant media as it had a low retention capacity and the viscous biorelevant medium did not flow through it, even at a lower flow (0.05 mL/min, results not shown).

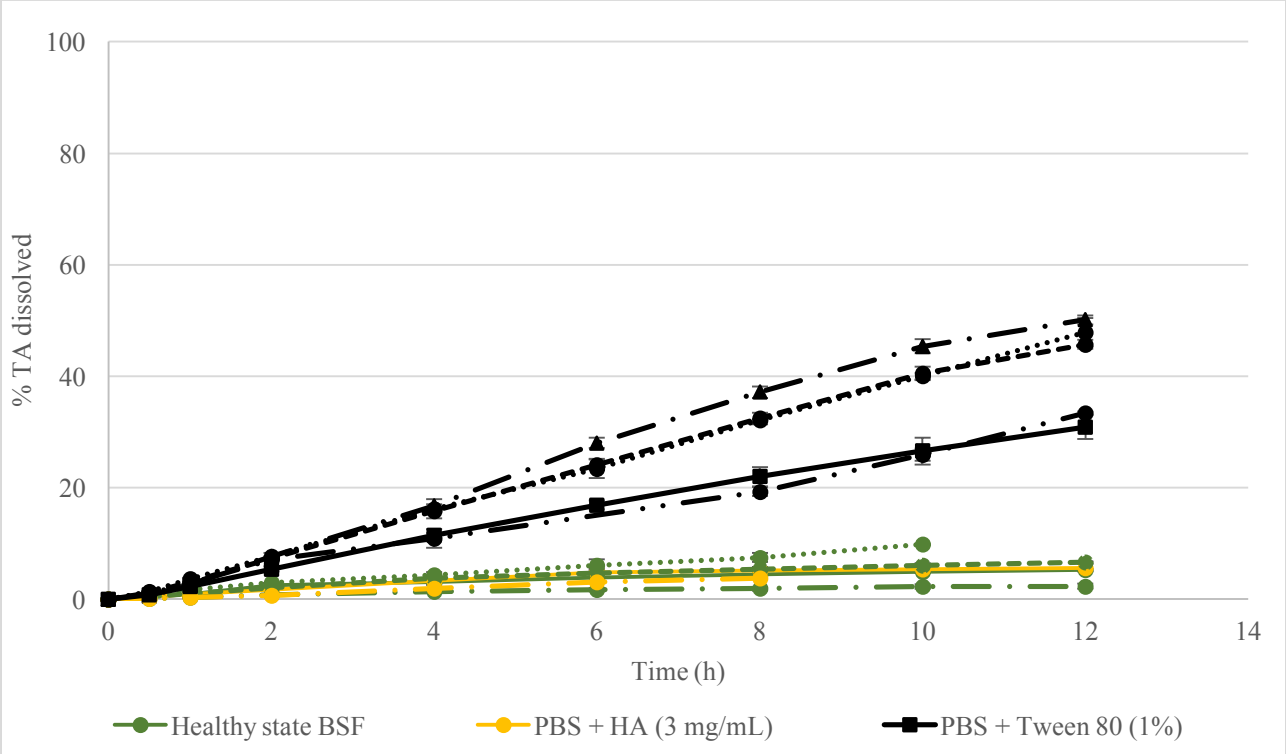

Fig. 4.9. Mean ± SD % TA dissolved through different membranes [GF/F (solid line), GF-6 (dotted line), GF-10 (dashed line), GF-6 + GF-10 (dashed and one dotted line) and CA (dashed and two dotted line)] from Adcortyl® in different media [PBS with Tween 80 (1% v/v), Healthy state BSF (with HA) and PBS with HA (3 mg/mL)] [flow 0.1 mL/min, dose 1 mL of TA suspension 10 mg/mL]

The widely-used PBS with HA (3 mg/mL) was compared with a healthy state BSF developed with a similar amount of HA and additional phospholipid PC and proteins (BSA and γ-globulin). The addition of phospholipids would theoretically increase the dissolution rate of TA as they act as natural surfactants [20] and consequently the permeation through the GF filters. Interestingly, the use of phospholipids in the HS BSF did not have any significant effect on the permeability of TA through the GF membranes compared to PBS containing HA with the use of GF/F ($f_{2_{HS\,BSF-PBS\,HA}} = 97.27$) or GF-6 + GF-10 ($f_{2_{HS\,BSF-PBS\,HA}} = 92.6$). Comparing dissolution with HS BSF and different types of GF filters showed that there is a slight increase with the GF/F compared to the GF filters with binders and finally with the combination of GF-6 and GF-10. This was also apparent with the use of PBS with HA. With the use of HA in the medium, the viscosity is increased leading to a more difficult permeation through the GF filter. As GF-6 and GF-10 have a higher mechanical and wet strength due to the binders present, they can withstand more pressure than the GF/F.

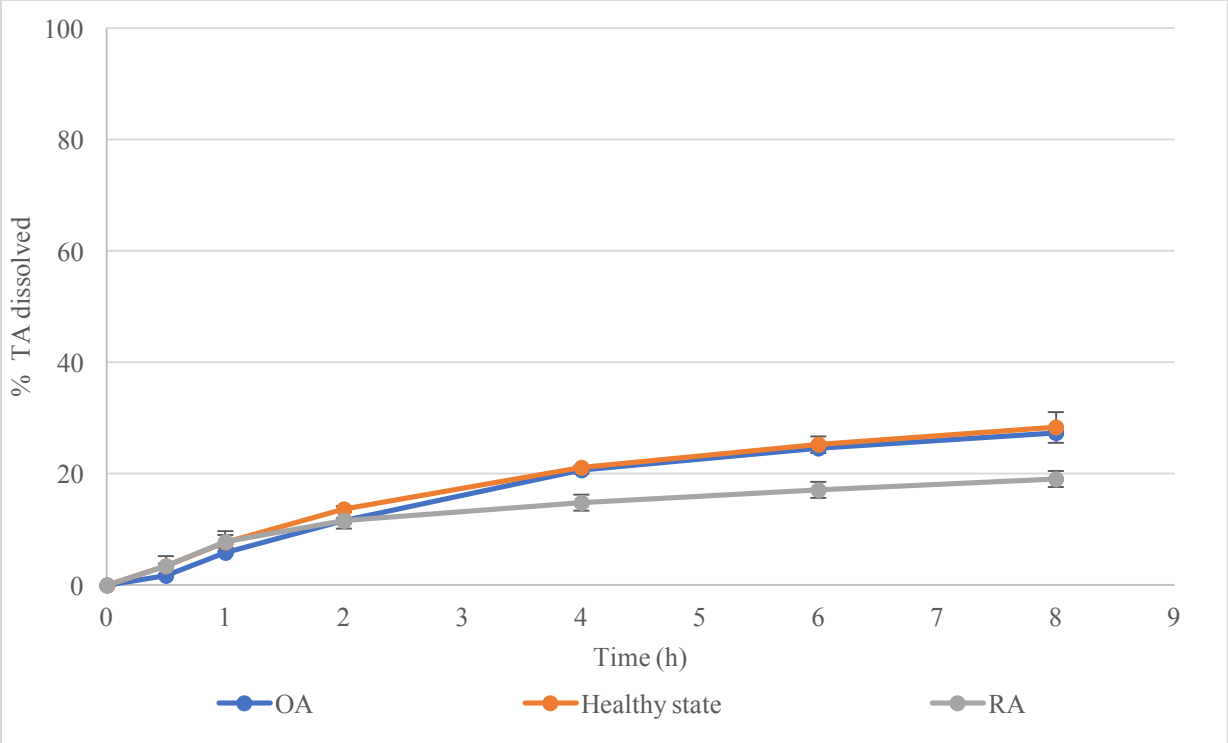

Fig. 4.10. Mean ± SD % TA diffused through the membrane from Adcortyl® with different biorelevant low viscosity media (no HA present) [flow 0.1 mL/min, dose: 0.1 mL of Ta suspension 10 mg/mL, membrane: GF-6 + GF-10]

In order to test a less viscous medium, with a value according to high shear rates (1000 1/s) assessed, BSF media without the addition of HA were developed. With the use of the GF-6 + GF-10 filter combination as the membrane in the setup, HS BSF and two disease state BSFs (OA and RA) were evaluated. Noticebly, the RA BSF, although contained a higher amount of phospholipids which would increase the solubility of the medium and lead to a higher dissolution of TA, had the lowest dissolution compared to HS ($f_{2_{HS-RA}} = 61.85$ and OA ($f_{2_{OA-RA}} = 63.66$). This could be due to the significantly high amount of proteins present in the RA BSF, as due to their size, they could accumulate and create a resistance to the diffusion of dissolved drug through the membrane [47]. The HS and OA BSF containt the same components in similar amounts except the phospholipid PC as OA contains an additional 0.1 mg/mL compared to the HS. Recording similar results with before, the increased amount of phospholipids does not lead to a significant difference between the TA dissolution in the two media ($f_{2_{HS-OA}} = 88.08$) (Fig. 4.10).

4.3.3. *In-vitro* dissolution with a monophasic set up with glass bottles

Dissolution testing in a monophasic setup was performed in PBS and BSF without HA in different states (HS and OA). The dissolution profiles reached different plateau values at 4-h and onwards, according to the solubility of TA determined experimentally in each one (Fig. 4.2) due to non-sink conditions. With a dose of 0.1 mL of Adcortyl (TA suspension, 10 mg/mL) in 50 mL of medium, the % of TA dissolved reached approximately 70% in 8-h; in the HS BSF the % of drug dissolved reached a plateau at an approximate dissolution of 53% due to TA solubility of 9.1 µg/mL and in the OA BSF the plateau reached was an approximate 47% due to TA solubility of 11.1 µg/mL (Fig. 4.2). Although the drug dissolution in HS BSF kept increasing until 4-h reaching a plateau, the TA dissolution in OA BSF seems to reach plateau from the first sampling point at 0.5-h. The dissolution rate of TA at 0.5-h seems to be faster in OA BSF than PBS and HS BSF with a difference of 10% TA release between them respectively (Fig. 4.11).

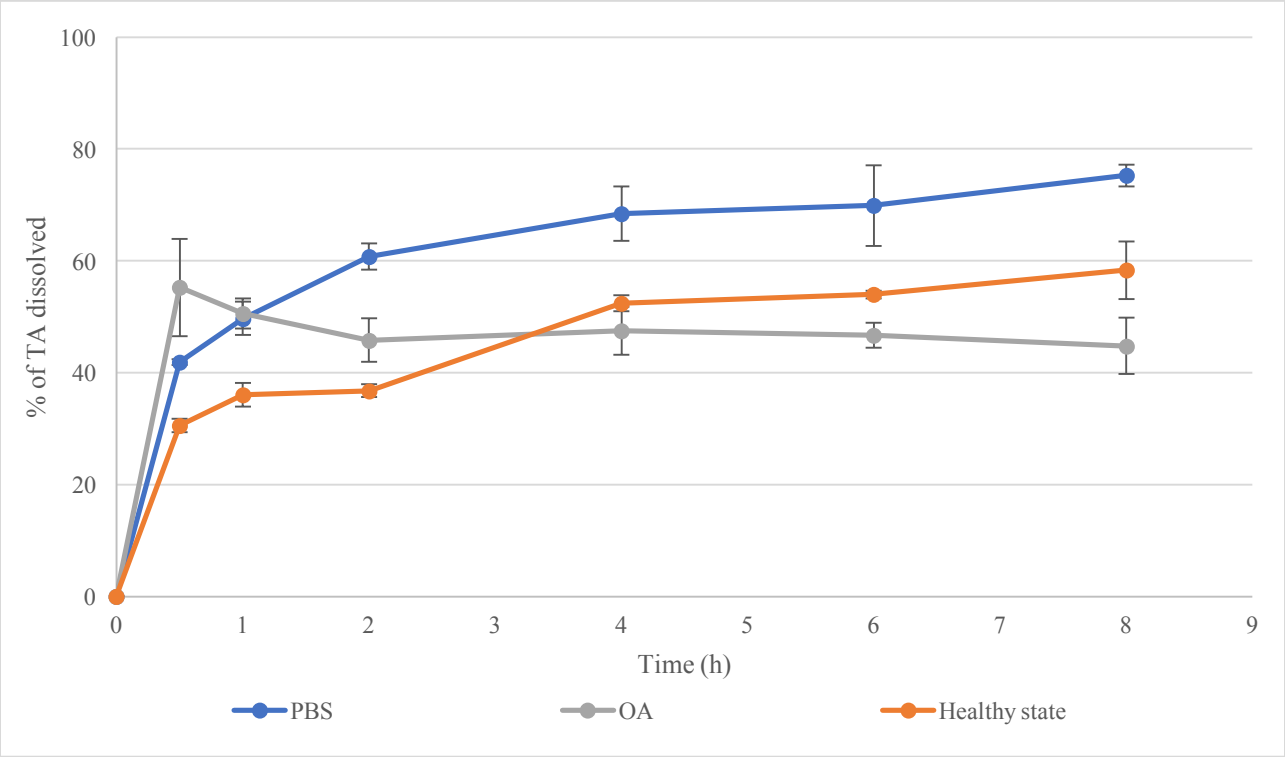

Fig. 4.11. Mean ± SD of TA dissolved from Adcortyl® in different BSF media without HA different in a monophasic setup with glass bottles (dose: 0.1 mL of TA suspension, 10 mg/mL)

4.3.4. *In-vitro* dissolution/permeation with a bi-phasic set up with glass bottles

Results showed that with the biphasic system, the drug reached complete dissolution in a 2-h time period, allowing more drug dissolution in the aqueous phase compared to the monophasic system over time. It was also shown that the partitioning of the drug to the organic layer took

place in a faster rate than the dissolution in the aqueous layer leading to low drug amounts left in the aqueous phase as the experiment would progress [40]. When testing a low solubility drug, a high volume of medium would be needed to offer these conditions. Using an organic immiscible layer would act as a reservoir for the drug which would dissolve in the aqueous layer and then partition through and so with this setup, more drug would then be able to dissolve in the aqueous layer and partition to the organic solvent.

It is important for the aqueous layer not to saturate and also for the total dose of drug studied to be less than 20% of its solubility in the volume of organic phase in the bi-phasic system [36, 40] for sink conditions to be maintained (10 mL of 1-Octanol in the organic phase and the solubility of TA in 1-octanol: 5.2 mg/mL [57]). The drug dissolved in a faster rate in the RA BSF compared to the OA and the HS BSF (Fig. 4.12). This is mainly due to the presence of phospholipids as they would increase drug dissolution over time, acting as the body's natural surfactants [20]. There is no significant difference in the dissolution between HS and OA which show that the small difference in phospholipids between them is not of primary importance.

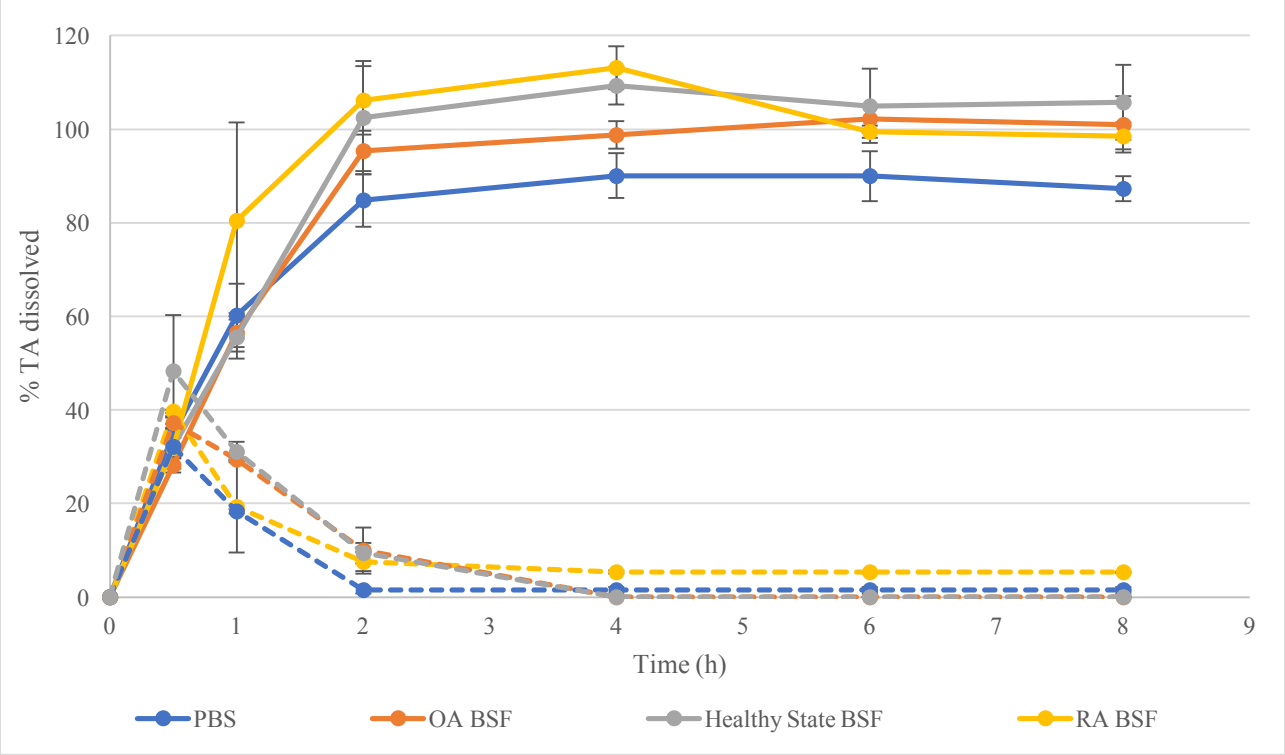

Fig. 4.12. Mean ± SD of TA dissolved from Adcortyl® in different BSF media without HA (dashed line) and partitioned in 1-octanol (solid line) in in a bi-phasic setup with glass bottles (dose: 0.1 mL of TA suspension, 10 mg/mL)

4.4. Conclusions

The biorelevant dissolution methods developed, take into consideration the *in-vivo* conditions of the synovial joint cavity. With the side-Bi-side cell, the setups mimic the volume of the synovial fluid and the flows applied, while the dissolution/permeation system would simulate the activities taking place in the joint after IA administration allowing the measurement of drug dissolution from the formulation in test. In the static flow, permeation through the membrane would not be significant, apart from the use of methanol in the donor and receptor phase. With Setup I, testing different membranes showed that there was no significant difference apart from the use of PTFE that seemed to not allow permeation. A higher permeation was apparent when flow was applied in the system (Setup II), while the highest permeation was evident with a flow applied from the donor phase through to the receptor phase (Setup III). Using a combination of glass microfiber membranes (GF-6 + GF-10), developed BSF tested in three states without HA (healthy, OA, RA), with low viscosity associated with high shear rates, showed significant differences between RA and the HS and OA BSF. With the bi-phasic dissolution in glass bottles, the organic solvent was used as a reservoir for the drug that would dissolve in the aqueous phase, providing sink conditions. There was no evident difference between the dissolution profiles in BSFs. These approaches provide a valuable tool to compare *in-vitro* drug release in a biorelevant environment and further studies (such as IVIVR or IVIVC) may also show its potential in predicting *in-vivo* dissolution profiles of IA formulations.

4.5. References

1. Gerwin, N., C. Hops, and A. Lucke, *Intraarticular drug delivery in osteoarthritis.* Adv Drug Deliv Rev, 2006. **58**(2): p. 226-42.
2. Kang, M.L. and G.I. Im, *Drug delivery systems for intra-articular treatment of osteoarthritis.* Expert Opin Drug Deliv, 2014. **11**(2): p. 269-82.
3. Abramson, S., *Drug delivery in degenerative joint disease: Where we are and where to go?* Advanced Drug Delivery Reviews, 2006. **58**(2): p. 125-127.
4. Butoescu, N., Jordan, O., Burdet, P., Stadelmann, P., Petri-Fink, A., Hofmann, H., Doelker, E., *Dexamethasone-containing biodegradable superparamagnetic microparticles for intra-articular administration: physicochemical and magnetic properties, in-vitro and in-vivo drug release.* Eur J Pharm Biopharm, 2009. **72**(3): p. 529-38.
5. Evans, C.H., V.B. Kraus, and L.A. Setton, *Progress in intra-articular therapy.* Nat. Rev. Rheumatol., 2014. **10**(1): p. 11-22.
6. Fotaki, N. and M. Vertzoni, *Biorelevant dissolution methods and their applications in in-vitroin-vivo correlations for oralformulations.* The Open Drug Delivery Journal, 2010. **4**(1): p. 2-13.
7. Klein, S., *The use of biorelevant dissolution media to forecast the in-vivo performance of a drug.* AAPS J, 2010. **12**(3): p. 397-406.
8. Reppas, C., Friedel, H.D., Barker, A.R., Buhse, L.F., Cecil, T.L., Keitel, S., Kraemer, J., Morris, J.M., Shah, V.P., Stickelmeyer, M.P., Yomota, C., Brown, C.K., *Biorelevant in-vitro performance testing of orally administered dosage forms-workshop report.* Pharm Res, 2014. **31**(7): p. 1867-76.
9. Brown, C.K., Friedel, H.D., Barker, A.R., Buhse, L.F., Keitel, S., Cecil, T.L., Kraemer, J., Morris, J.M., Reppas, C., Stickelmeyer, M.P., Yomota, C., Shah, V.P., *FIP/AAPS joint workshop report: dissolution/in-vitro release testing of novel/special dosage forms.* AAPS PharmSciTech, 2011. **12**(2): p. 782-94.
10. Shen, J. and D.J. Burgess, *Accelerated in-vitro release testing methods for extended-release parenteral dosage forms.* J Pharm Pharmacol, 2012. **64**(7): p. 986-96.
11. D'Souza, S.S. and P.P. DeLuca, *Development of a dialysis in-vitro release method for biodegradable microspheres.* AAPS PharmSciTech, 2005. **6**(2): p. E323-8.
12. Seidlitz, A. and W. Weitschies, *In-vitro dissolution methods for controlled release parenterals and their applicability to drug-eluting stent testing.* J Pharm Pharmacol, 2012. **64**(7): p. 969-85.
13. Wang, Q.X., N. Fotaki, and Y. Mao, *Biorelevant Dissolution: Methodology and Application in Drug Development.* Dissolution Technologies, 2009. **16**(3): p. 6-12.
14. Marques, M.R.C., R. Loebenberg, and M. Almukainzi, *Simulated Biological Fluids with Possible Application in Dissolution Testing.* Dissolution Technologies, 2011.
15. Oates, K.M.N., Krause, W.E., Jones, R.L., Colby, R.H., *Rheopexy of synovial fluid and protein aggregation.* J R Soc Interface, 2006. **3**(6): p. 167-74.
16. Smith, A.M., Fleming, L., Wudebwe, U., Bowen, J., Grover, L.M., *Development of a synovial fluid analogue with bio-relevant rheology for wear testing of orthopaedic implants.* J Mech Behav Biomed Mater, 2014. **32**: p. 177-84.
17. Sterner, B., Harms, M., Weigandt, M., Windbergs, M., Lehr, C.M., *Crystal suspensions of poorly soluble peptides for intra-articular application: A novel approach for biorelevant assessment of their in-vitro release.* Int J Pharm, 2013.
18. Zhang, Z., S. Barman, and G.F. Christopher, *The role of protein content on the steady and oscillatory shear rheology of model synovial fluids.* Soft Matter, 2014. **10**(32): p. 5965-73.

19. Smith, B., *Chapter 3. Solubility and dissolution*, in *Remington Education: Physical Pharmacy*. 2015, Pharmaceutical Press.
20. Hills, B.A. and B.D. Butler, *Surfactants identified in synovial fluid and their ability to act as boundary lubricants.* Ann Rheum Dis, 1984. **43**(4): p. 641-8.
21. Pawlak, Z., W. Urbaniak, and A. Oloyede, *Natural articular joints: model of lamellar-roller-bearing lubrication and the nature of the cartilage surface.* 2013: p. 253-310.
22. Burt, H.M., Tsallas, A., Gilchrist, S., Liang L.S., *Intra-articular drug delivery systems: Overcoming the shortcomings of joint disease therapy.* Expert Opin Drug Deliv, 2009. **6**(1): p. 17-26.
23. Larsen, C., Ostergaard, J., Larsen, S.W., Jensen, H., Jacobsen, S., Lindergaard, C., Andersen, P.H., *Intra-articular depot formulation principles: role in the management of postoperative pain and arthritic disorders.* J Pharm Sci, 2008. **97**(11): p. 4622-54.
24. Levick, J.R. and J.N. McDonald, *Viscous and Osmotically Mediated Changes in Fluid Movement across Synovium in Response to Intraarticular Albumin.* Microvascular Research, 1994. **47**(1): p. 68-89.
25. Blewis, M.E., Nugent-Derfus, G.E., Schmidt, T.A., Schumacher, B.L., Sah, R.L., *A model of synovial fluid lubricant composition in normal and injured joints.* Eur Cell Mater, 2007. **13**: p. 26-39.
26. Edwards, S.H., *Intra-articular drug delivery: the challenge to extend drug residence time within the joint.* Vet J, 2011. **190**(1): p. 15-21.
27. Udata, C., Patel, J., Pal, D., Hejchman, E., Cushman, M., Mitra, A.K., *Enhanced transport of a novel anti-HIV agent--cosalane and its congeners across human intestinal epithelial (Caco-2) cell monolayers.* Int J Pharm, 2003. **250**(1): p. 157-68.
28. Kataoka, M., Masaoka, Y., Yamazaki, Y., Sakane, T., Sezaki, H., Yamashita, S., *In-vitro System to Evaluate Oral Absorption of Poorly Water-Soluble Drugs: Simultaneous Analysis on Dissolution and Permeation of Drugs.* Pharmaceutical Research, 2003. **20**(10): p. 1674-1680.
29. Weber, S.J., Abbruscato, T.J., Brownson, E.A., Lipkowski, A.W., Polt, R., Misicka, A., Haaseth, R.C, Bartosz, H., Hruby, V.J., Davis, T.P., *Assessment of an in-vitro blood-brain barrier model using several [Met5]enkephalin opioid analogs.* J Pharmacol Exp Ther, 1993. **266**(3): p. 1649-55.
30. Chappa, A.K., K.L. Audus, and S.M. Lunte, *Characteristics of substance P transport across the blood-brain barrier.* Pharm Res, 2006. **23**(6): p. 1201-8.
31. Tavakoli-Saberi, M.R. and K.L. Audus, *Cultured buccal epithelium: an in-vitro model derived from the hamster pouch for studying drug transport and metabolism.* Pharm Res, 1989. **6**(2): p. 160-6.
32. Shojaei, A.H., B. Berner, and L. Xiaoling, *Transbuccal delivery of acyclovir: I. In-vitro determination of routes of buccal transport.* Pharm Res, 1998. **15**(8): p. 1182-8.
33. Shojaei, A.H., Khan, M., Lim, G., Khosravan, R., *Transbuccal permeation of a nucleoside analog, dideoxycytidine: effects of menthol as a permeation enhancer.* International Journal of Pharmaceutics, 1999. **192**(2): p. 139-146.
34. Bhat, P.G., D.R. Flanagan, and M.D. Donovan, *Drug diffusion through cystic fibrotic mucus: steady-state permeation, rheologic properties, and glycoprotein morphology.* J Pharm Sci, 1996. **85**(6): p. 624-30.
35. Wang, Y., L.V. Allen, Jr., and L.C. Li, *Effect of sodium dodecyl sulfate on iontophoresis of hydrocortisone across hairless mouse skin.* Pharm Dev Technol, 2000. **5**(4): p. 533-42.
36. Phillips, D.J., Pygall, S.R., Cooper, V.B., Mann, J.C., *Overcoming sink limitations in dissolution testing: a review of traditional methods and the potential utility of biphasic systems.* J Pharm Pharmacol, 2012. **64**(11): p. 1549-59.

37. Gibaldi, M. and S. Feldman, *Establishment of sink conditions in dissolution rate determinations. Theoretical considerations and application to nondisintegrating dosage forms.* Journal of Pharmaceutical Sciences, 1967. **56**(10): p. 1238-1242.
38. Sunesen, V.H., Pedersen, B.L., Kristensen, H.G., Mullertz, A., *In-vivo in-vitro correlations for a poorly soluble drug, danazol, using the flow-through dissolution method with biorelevant dissolution media.* Eur J Pharm Sci, 2005. **24**(4): p. 305-13.
39. Vangani, S., Li, X., Zhou, P., Del-Barrio, M.A., Chiu, R., Cauchon, N., Gao, P., Medina, C., Jasti, B., *Dissolution of poorly water-soluble drugs in biphasic media using USP 4 and fiber optic system.* Clinical Research and Regulatory Affairs, 2009. **26**(1-2): p. 8-19.
40. Hoa, N.T. and R. Kinget, *Design and evaluation of two-phase partition-dissolution method and its use in evaluating artemisinin tablets.* J Pharm Sci, 1996. **85**(10): p. 1060-3.
41. Phillips, D.J., Pygall, S.R., Cooper, B., Mann, J.C., *Toward biorelevant dissolution : application of a biphasic dissolution model as a discriminating tool for HPMC matrices containing a model BCS class II drug.* Dissolution Technologies, 2012. **19**(1): p. 25-34.
42. Jantratid, E., Janssen, N., Reppas, C., Dressman, J.B., *Dissolution media simulating conditions in the proximal human gastrointestinal tract: an update.* Pharm Res, 2008. **25**(7): p. 1663-76.
43. Butoescu, N., O. Jordan, and E. Doelker, *Intra-articular drug delivery systems for the treatment of rheumatic diseases: a review of the factors influencing their performance.* Eur J Pharm Biopharm, 2009. **73**(2): p. 205-18.
44. Tomaszewska, I., Karki, S., Shur, J., Price, R., Fotaki, N., *Pharmaceutical characterisation and evaluation of cocrystals: Importance of in-vitro dissolution conditions and type of coformer.* Int J Pharm, 2013. **453**(2): p. 380-8.
45. Ayral, X., *Injections in the treatment of osteoarthritis.* Best Pract Res Clin Rheumatol, 2001. **15**(4): p. 609-26.
46. Levick, J.R. and J.N. McDonald, *Synovial capillary distribution in relation to altered pressure and permeability in knees of anaesthetized rabbits.* J Physiol, 1989. **419**: p. 477-92.
47. Levick, J.R. and J.N. McDonald, *Fluid movement across synovium in healthy joints: role of synovial fluid macromolecules.* Annals of the Rheumatic Diseases, 1995. **54**(5): p. 417-423.
48. Bingol, A.O., Lohmann, D., Puschel, K., Kulicke, W.M., *Characterisation and comparison of shear and extensional flow of sodium hyaluronate and human synovial fluid.* Biorheology, 2010. **47**(3-4): p. 205-24.
49. Fam, H., J.T. Bryant, and M. Kontopoulou, *Rheological properties of synovial fluids.* Biorheology, 2007. **44**(2): p. 59-74.
50. Sottofattori, E., M. Anzaldi, and L. Ottonello, *HPLC determination of adenosine in human synovial fluid.* J Pharm Biomed Anal, 2001. **24**(5-6): p. 1143-6.
51. Jantratid, E., De Maio, V., Ronda, E., Mattavelli, V., Vertzoni, M., Dressman, J.B., *Application of biorelevant dissolution tests to the prediction of in-vivo performance of diclofenac sodium from an oral modified-release pellet dosage form.* Eur J Pharm Sci, 2009. **37**(3-4): p. 434-41.
52. Vertzoni, M., Symillides, M., Iliadis, A., Nicolaides, E., Reppas, C., *Comparison of simulated cumulative drug versus time data sets with indices.* European Journal of Pharmaceutics and Biopharmaceutics, 2003. **56**(3): p. 421-428.

53. Zhang, Y., Huo, M., Zhou, J., Zou, A., Li, W., Yao, C., Xie, S., *DDSolver: An Add-In Program for Modeling and Comparison of Drug Dissolution Profiles.* The AAPS Journal, 2010. **12**(3): p. 263-271.
54. Kastellorizios, M. and D.J. Burgess, *In-vitro Drug Release Testing and In-vivo/In-vitro Correlation for Long Acting Implants and Injections*, in *Long Acting Injections and Implants*, J.C. Wright and D.J. Burgess, Editors. 2012, Springer US: Boston, MA. p. 475-503.
55. Shah, V.P., J. DeMuth, and D.G. Hunt, *Performance Test for Parenteral Dosage Forms.* Dissolution Technologies, 2015. **22**(4): p. 16-21.
56. Gao, Z., *In-vitro dissolution testing with flow-through method: a technical note.* AAPS PharmSciTech, 2009. **10**(4): p. 1401-5.
57. Thakkar, H., R. Kumar Sharma, and R.S. Murthy, *Enhanced retention of celecoxib-loaded solid lipid nanoparticles after intra-articular administration.* Drugs R D, 2007. **8**(5): p. 275-85.

Chapter 5: Dissolution characterisation of intra-articular drugs with UV Surface Dissolution Imaging

Overview

Purpose: To investigate the real-time dissolution behaviour of IA drugs under UV imaging with the use of non-biorelevant and artificial synovial fluid (ASF) media.

Methods: The optimization of the dissolution process was done by testing drug amount (2 and 4 mg), flow rate (0.2 and 0.7 mL/min) and compression force (40 and 80 cN.m) with a two-level factorial design. To test the effect of surfactants, in static flow (0 mL/min), the media tested included PBS, PBS with Tween 80 (1% v/v), PBS with SLS (1% w/v) and PBS with CTAB (1% w/v). For evaluating the effect of viscosity on the dissolution of TA, three ASFs were tested, containing HA, simulating the viscosity of synovial fluid in HS, OA and RA state. The effect of surfactants was also tested with a continuous laminar channel flow of 0.2 mL/min with PBS, PBS with Tween 80 (1% v/v), PBS with SLS (1% w/v) and PBS with CTAB (1% w/v). TA was utilized as a model IA drug, with measurements involving surface concentration, Intrinsic Dissolution Rate (IDR) and TA mass dissolved.

Results: Optimizing the dissolution process, showed that the appropriate compression force to use for the analysis is 40 cN.m, the drug amount placed initially in the steel cup 6 mg (to have 4 mg left in the cup as the sample) and a flow rate of 0.2 mL/min. In static flow, surface dissolution was in accordance with visual representations of the dissolution of TA in the media. CTAB provided the highest drug dissolution followed by SLS, then Tween 80 and PBS without surfactant. With the use of the ASFs, increasing the viscosity led to lower dissolution rates with the surface concentration being higher in accordance with RA>OA>HS. With a flow applied in media with surfactants the IDR and TA mass dissolved was in accordance to visual representations.

Conclusions: The UV imaging system shows potential for *in-vitro* drug dissolution testing with IA drugs in PBS with surfactants and ASFs simulating the viscosity of synovial fluid.

5.1. Introduction

Corticosteroid drugs administered through the IA route provide symptomatic treatment while minimising overall systematic exposure, for chronic conditions such as OA and RA [1]. In the pharmaceutical industry, *in-vitro* dissolution testing has an important part in drug/formulation development and quality control with certain dissolution methods approved and in use. At the moment, there is no standard official dissolution method in the Pharmacopoieia for IA drugs [2]. This causes drawbacks to the establishment of the effect of variables in drug dissolution, which is of vital importance. Traditional dissolution testing methods such as sample and separate, dialysis membranes and continuous flow through apparatus (USP apparatus IV) [3, 4] have been used for measuring dissolution from parenteral formulations. With these methodologies, measuring dissolution of poorly water-soluble drugs might still present significant challenges and further difficulties related to dissolution [5].

An approach involving the use of UV imaging and visualisation of the dissolution procedure may help overcome these obstacles. The use of real-time information regarding solution concentration is provided [6], as the process is monitored exactly next to the surface of the drug. This way, dissolution is not focused on bulk solution concentration measurements over time. Being able to visualize the dissolution process is a promising and innovative tool offering a more detailed analysis of the drug particles dissolving in solution adjacent to the solid powder. UV imaging offers the potential to gain a great deal of information spectrally, spatially and temporally [7] by generating recordings of the continuous dissolution near the surface of the powder in test, with the chosen medium flowing through. For example, the surface concentration measured with the SDI provides real-time results of the dissolution process by monitoring the events taking place next to the surface of the tested drug powder [8]. Being able to understand in depth how different parameters of the system affect the surface concentration of the powder provides essential information about how drug would dissolve when in contact with the dissolution medium. The use of UV imaging provides the appropriate visualisation of the solute concentrations close to the surface of the powder. During the IA administration of a suspension, the drug particulates are injected into the synovial fluid with the possibility to follow different pathways. The major determinant according to which a specific pathway will be followed, is the size of the particulates. The drug particles may i) be phagocytosed by synovial fluid macrophages into the synovial membrane, ii) transfer in the articular cartilage of the bone, through convective transport due to change in pressure inside the synovial cavity

or iii) remain in the synovial fluid and attach to the articular cartilage or the synovial membrane [9]. In all occasions the transfer to the targeted location inside the synovial cavity involves the suspension being dispersed in the synovial fluid. With the use of simple buffer solutions *in-vitro*, the understanding of the dispersion, solubilisation and dissolution behaviour of the tested drug may provide essential information with the application of UV imaging. New insights of the dissolution process with images providing its initial stages, may contribute to understanding what kind of phenomena are taking place on the surface of the powder that may affect dissolution rate, which would be missed in the dissolution of bulk material with traditional apparatus [8].

Considering a more biorelevant dissolution approach, the viscosity of the synovial fluid in the healthy state and in disease states may have a significant effect on the solubilisation effect of the drugs given through the IA route. The HA is the main component responsible for the viscosity found in synovial fluid. The addition of this in buffer, with appropriate amounts according to the synovial fluid state, will provide a better prediction of the performance of the IA drug *in-vivo* [10, 11]. When the suspension of TA is injected in the synovial cavity, the suspended particles of the drug, according to the particle size, may dissolve in the synovial fluid [9]. The lubrication and viscoelastic ability of HA has been determined from a variety of studies [4, 11-15] and so its presence in the synovial fluid is vital as a primary determinant for viscosity. Being able to understand how the dissolution of TA will take place on the surface of the powder in real-time provides the opportunity to capture the initial stages of the dissolution process in real-time [16]. Although simulating the viscosity of the synovial fluid in test may create conditions physiologically relevant, the type of flow present in the synovial cavity should also be taken into account. The transynovial flow is present in the joint as the blood is filtrated inside the synovial cavity (with the addition of HA and lubricin forming the synovial fluid) and as synovial fluid drains out of the cavity through the terminal lymphatics. In normal conditions the transynovial flow is 0.005-0.01 mL/min in a flexed knee joint and up to 0.02-0.04 mL/min in chronic joint effusion conditions which would lead to approximately 1 mL of synovial fluid turn-over in 1- to 2-h [17]; and so an appropriate flow would provide additional biorelevance to the conditions tested.

The objective of this study was to investigate the real-time dissolution behaviour of IA drugs under UV imaging and evaluate the effect of surfactant in the medium (in static and continuous flow) and viscosity of ASFs (in static flow) while also optimising the method with the SDI

instrument. In the experiments conducted, we considered the surface concentration, IDR and TA mass dissolution from the surface of the sample cup containing the powder. TA, a poorly soluble model IA drug with a pKa of 11.75, was used for all experiments in PBS with surfactants and in artificial synovial fluid (simulating synovial fluid viscosity in Healthy state, OA and RA).

5.2. Materials and Methods

5.2.1 Materials

TA (98+%, fine chemical) was purchased from Alfa Aesar (UK). For all experiments ultra-pure water was used obtained from a Milli-Q purification device. The phosphate buffer saline (PBS) was made with sodium chloride (≥99.9%), potassium dihydrogen orthophosphate (≥99.5%), di-sodium hydrogen orthophosphate, anhydrous dried (≥99.5%) and potassium chloride (≥99.5%) which were purchased from Sigma-Aldrich (UK). HBSS, 1X, without calcium, magnesium, phenol red Thermo Scientific HyClone was purchased from Fisher Scientific (UK), while the 0.1 M phosphate buffer contained 0.1 M Na_2HPO_4 (14.2 g/L) and 0.1 M HCl, also purchased from Fisher Scientific. sodium hyaluronate 95% [hyaluronic acid, (HA)] was purchased from Fisher Scientific (UK). Tween 80 (polysorbate) was bought from VWR (UK) sodium dodecyl sulphate (≥99.0%) and CTAB (≥99.0%) were purchased from Sigma-Aldrich (UK).

5.2.2 Methods

5.2.2.1. Media used in the dissolution studies

5.2.2.1.1. Media with surfactants

The media used are PBS, PBS with Tween 80 (1% v/v), PBS with SLS (1% w/v) and PBS with CTAB (1% v/v). The media containing surfactants were tested in the static (0 mL/min) and the continuous (0.2 mL/min) flow.

5.2.2.1.2. Artificial synovial fluid (ASF) in different states

In order to evaluate the effect of the viscosity of the synovial fluid in HS and in disease state (OA and RA), the dissolution of TA was studied in media consisting of the buffers used for the development of the BSFs with the addition of the physiologically relevant amounts of HA for appropriate viscosity values (Table 5.1, in accordance with Chapter 3). The biorelevant media were prepared according to the method proposed by Jantratid et al. [18]. The HBSS buffer was adjusted to a pH of 6.8 by adding 0.1 M of HCl before the addition of further components while the phosphate buffers for the OA and RA biorelevant synovial fluids were made by adding 0.1 M Na_2HPO_4 (955.1 mL/L) and 0.1 M HCl (44.9 mL/L) in 1 L of 0.1 M buffer. The phosphate buffer was then adjusted to pH 8.1 and 8 respectively with addition of 0.1 M HCl. The amount

of HA added was 8.1 mg/mL for the healthy state, 4.8 mg/mL for the OA and 3.5 mg/mL for the RA. The media were tested under static flow (0 mL/min).

Table 5.1. Composition of Biorelevant media simulating synovial fluid viscosity in HS, OA and RA

Components (mg/mL)	HS ASF	OA ASF	RA ASF
Buffer	HBSS	0.1 M $NaHPO_4$ + HCl	0.1 M $NaHPO_4$ + HCl
HA	8.1	4.8	3.5

5.2.2.2. Surface Dissolution of TA with UV imaging

5.2.2.2.1. UV imaging setup

The UV imaging was performed with the use of an Actipix SDI 300 UV imaging system (Paraytec Ltd., York, UK) and with an Actipix flow through dissolution cartilage. The light source was a pulsed Xe lamp and the UV filter used had a detection wavelength of 254 nm. The UV imaging setup of the SDI system can be equipped with filters of different wavelengths but the detection in the analysis takes place with one single suitable filter. In order to decide which appropriate wavelength to use, a vital step was to determine the UV absorbance maxima of the drug in the medium tested (lambda max for TA= ~240 nm) [8]. The quartz cell (7.5 mm height, 3 mm width and 63 mm length) in which the dissolution cartridge is placed, contains a volume of approximately 0.56 mL media that may flow through [7]. The detection area available is 9 mm x 7 mm (1280 x 1024 pixels) with images recorded at a rate of 2.59 images per second and analysed with the Actipix D100 software, version 1.4 (Paraytex Ltd.) with a 10 x 1 horizontal pixel binning by converting pixel intensities into absorbance. The infusion of the dissolution media and standard solutions took place with a syringe pump (Fusion 200, Chemyx Ltd.) at specific flow rates at a temperature of 37^{o} C. The extinction coefficients were obtained by absorbance values from imaging of TA standard solutions in the media tested. Standard TA solutions (2-10 µg/mL) were infused for 5 min each at a flow of 1 mL/min with a blank buffer in the beginning of the run as a background reference and for detecting baseline drifts. The dissolution experiments were performed with the use of compacted TA samples in triplicates. The extinction coefficient used in all the analysis was of the PBS.

5.2.2.2.2. Preparation of compacts

For the dissolution studies in static and continuous flow, compacts were prepared by placing 6

mg of TA into stainless-steel cylinder sample cups (inner diameter 2 mm) which were then pressed in the manual press (316 SS compression rod and base insert, Paraytec, UK) for 1 min with a Quickset MINOR torque screwdriver (Torqueleader, M.H.H. Engineering Co., UK) by applying a pressure of 40 c.Nm, leaving approximately 4 mg of TA in the sample cup.

5.2.2.2.3. Dissolution studies

In all experimental runs, dark images were taken initially (with the lamp turned off, for 10 s) and reference images (with the lamp turned on, for 10 s) were recorded with the plastic cartilage placed in the flow cell, filled with blank buffer. After 10 s the data recording was paused and a compact containing TA was placed into the plastic cartilage, which was then placed again into the flow cell. The collection of data was then resumed after flushing the cell with medium 2 times in a rate of 2 mL/min for a total of 20 s, to ensure that the cell is filled and no bubbles are present in the imaging area.

The flow program then started with the experiments were performed in triplicates, at a temperature of 37^{o} C. The data collected in pixel intensities from the automatically adjusted measurement zones was converted into absorbance values by the software [Actipix D100 software version 1.5 (Paraytec, UK)], which were used for the calculation of surface concentration, IDR, and sample mass dissolved (SMD) over time. For the static flow, IDR and SMD were not considered, as the absorbance contour lines did not reach the measurement IDR zone of the UV image and the mass flux is also calculated by the system based on flow rate. For all the results given by the software, the pixel intensities are converted into absorbance values with the following equation:

$$A = \log\left(\frac{I_{ref} - I_o}{I_{sig} - I_o}\right) \qquad \text{(Eq. 1)}$$

where I_{ref}, I_o and I_{sig} are the pixel intensity which is measured when the buffer is flowing in the cell (reference signal), the pixel intensity because of the dark current (electronic noise which is measured with the Xe lamp turned off) and the pixel intensity which is measured as the experiment is running respectively.

5.2.2.2.3.1. Process optimisation with Design of Experiments (DoE)

A two-level factorial design was used in order to optimise the conditions used in the analysis of TA and the compact preparation in the experiments. Three factors were tested [drug amount

(2 and 4 mg in sample cup), flow rate (0.2 and 0.7 mL/min) and compression force (40 and 80 c.nm)] with PBS as the medium, developing a 2^3 factorial design, in order to evaluate their effect on surface concentration, IDR and TA mass dissolved. This process included eight runs in random order with 3 replications each, constituting 3 blocks of testing. Surface concentration, IDR and TA mass dissolved over time, showing the effect of each factor are presented in thermal analysis surface plots according to flow rate. The results (surface concentration, IDR and TA mass dissolved) were calculated by the SDI software, taking into account the extinction coefficient and according to the following equations [19]:

$$j = \frac{\sum_{z=0}^{H/2} v_z M c_z W \Delta z}{S} \quad \text{(Eq. 2)}$$

$$v_z = \frac{3Q}{2HW}\left[1 - \frac{(2z-H)^2}{H^2}\right] \quad \text{(Eq. 3)}$$

where:

j = IDR
v_z = velocity at z
M = molecular weight
c_z = concentration at z
W = width of the flow cell
Δz =effective pixel height
S = surface area of the sample
H =height of the flow cell in the observation region
Q = volume flow rate

Calculations of TA dissolution rates were done according to different absorbance values detected from specific detection areas in the UV image attained [7], located on the right end side of the image towards which the buffer would flow.

The ANOVA analysis in the optimisation of the SDI variables, was conducted using Statgraphics Centurion (Statgraphics, USA). The same program was also used to present results in 3D thermal analysis graphs showing the effect of variables on surface concentration, IDR and TA amount dissolved and Pareto charts showing the effect of each variable tested and also the effect of combined factors. In the Pareto charts, in which the ANOVA data is summarized, the x-axis presents the t-ratio of the variables tested, while the vertical line indicates statistical significance for the variable effect that has passed (P-value = 0.05) [20].

5.2.2.2.3.2. Studies in static flow

With a static flow (0 mL/min), the media used were PBS with surfactants and ASFs in three states (HS, OA and RA). The drug amount used was 4 mg and the compression force was 40 cN.m. The results measured were the surface concentration of TA as Mean (µg/mL) ± S.D.

5.2.2.2.3.3. Studies in continuous flow

With a continuous laminar channel flow of 0.2 µL/min the media used were non-biorelevant (PBS with surfactants). The drug amount used was 4 mg and the compression force was 40 cN.m. The results measured were the surface concentration of TA as Mean (µg/mL) ± S.D., the IDR as Mean (µg/min/cm^2) ± S.D. and TA mass dissolved as Mean (mg) ± S.D.

5.3. Results and Discussion

5.3.1. Dissolution studies

5.3.1.1. Process optimisation with the use of DoE

Table 5.2. Results from DoE

block	Drug amount	Flow rate	Compression force	Surface conc	IDR	SMD
	(mg)	(mL/min)	(cN.m)	(µg/mL)	(µg/min/cm^2)	(mg)
1	4.0	0.2	40.0	135	3.5	0.004
1	2.0	0.2	80.0	310	10	0.007
1	2.0	0.2	40.0	225	10	0.007
1	4.0	0.2	80.0	42.5	17.5	0.008
1	4.0	0.7	40.0	85	80	0.04
1	2.0	0.7	40.0	85	175	0.08
1	4.0	0.7	80.0	115	0	0
1	2.0	0.7	80.0	85	2.5	0.003
2	4.0	0.2	40.0	105	10	0.006
2	2.0	0.2	80.0	150	35	0.02
2	2.0	0.2	40.0	275	190	0.09
2	4.0	0.2	80.0	32	1	0.001
2	4.0	0.7	40.0	30	1	0.001
2	2.0	0.7	40.0	255	7	0.003
2	4.0	0.7	80.0	115	7.5	0.006
2	2.0	0.7	80.0	240	3	0.002
3	4.0	0.2	40.0	215	5	0.003
3	2.0	0.2	80.0	50	0	0.001
3	2.0	0.2	40.0	235	4	0.002
3	4.0	0.2	80.0	215	3	0.002
3	4.0	0.7	40.0	60	25	0.012
3	2.0	0.7	40.0	65	22.5	0.01
3	4.0	0.7	80.0	105	8.5	0.004
3	2.0	0.7	80.0	74	2.5	0.001

5.3.1.1.1. Surface Concentration

The effect of the variables tested on the dissolution of TA and the surface concentration results are shown in Fig. 5.2 and in Table 5.2. Increasing the drug amount (2 and 4 mg) in the stainless-steel compact reduced the average surface concentration, with a higher compression force making this effect less significant. According to the Pareto Chart, the highest significant effect is when the compression force is considered in combination with the drug amount (P-value = 0.0112) while the effect of the drug amount on its own is not of high significance (P-value = 0.1841). Comparing different flows (0.2 and 0.7 mL/min), it was observed that a lower flow

rate led to a higher total surface concentration when considered in combination with the compression force tested (Fig. 5.1). The flow rate alone had the less significant effect on surface concentration (P-value = 0.9295) while a higher effect was noted when combined with the drug amount, but again of low significance (P-value = 0.5229) (Fig. 5.1). To understand better how the factors tested (drug amount, flow rate and compression force) can affect surface dissolution we can consider the solvation of drug particles from the compact due to the presence of the medium and the dissolved molecules flown away from the surface of the compact due to the flow rate present in the system [21]. A higher flow led to a smaller amount of solvated drug particles accumulating in the powder surface and in combination with a high compression force of 80 cN.m, the powder is pressed with a higher packing force in the sample cup. Increasing the compression leads to increased surface energy, and so the drug dissolution rate will be decreased. A larger volume of medium would be required to come into contact with the powder surface to cause the dissolution of the drug and so with a higher compression force the differences noted in surface concentration are in a lesser effect. Considering the drug amount added in the sample cup, a higher drug amount increases the powder density and in both compression forces, leads to a smaller surface concentration (Fig. 5.1). As less drug is presented in the sample cup, surface concentration seems to be less significantly affected in both flows tested, showing that the density of the powder in the compact may not affect the solvated drug amount (Fig. 5.2).

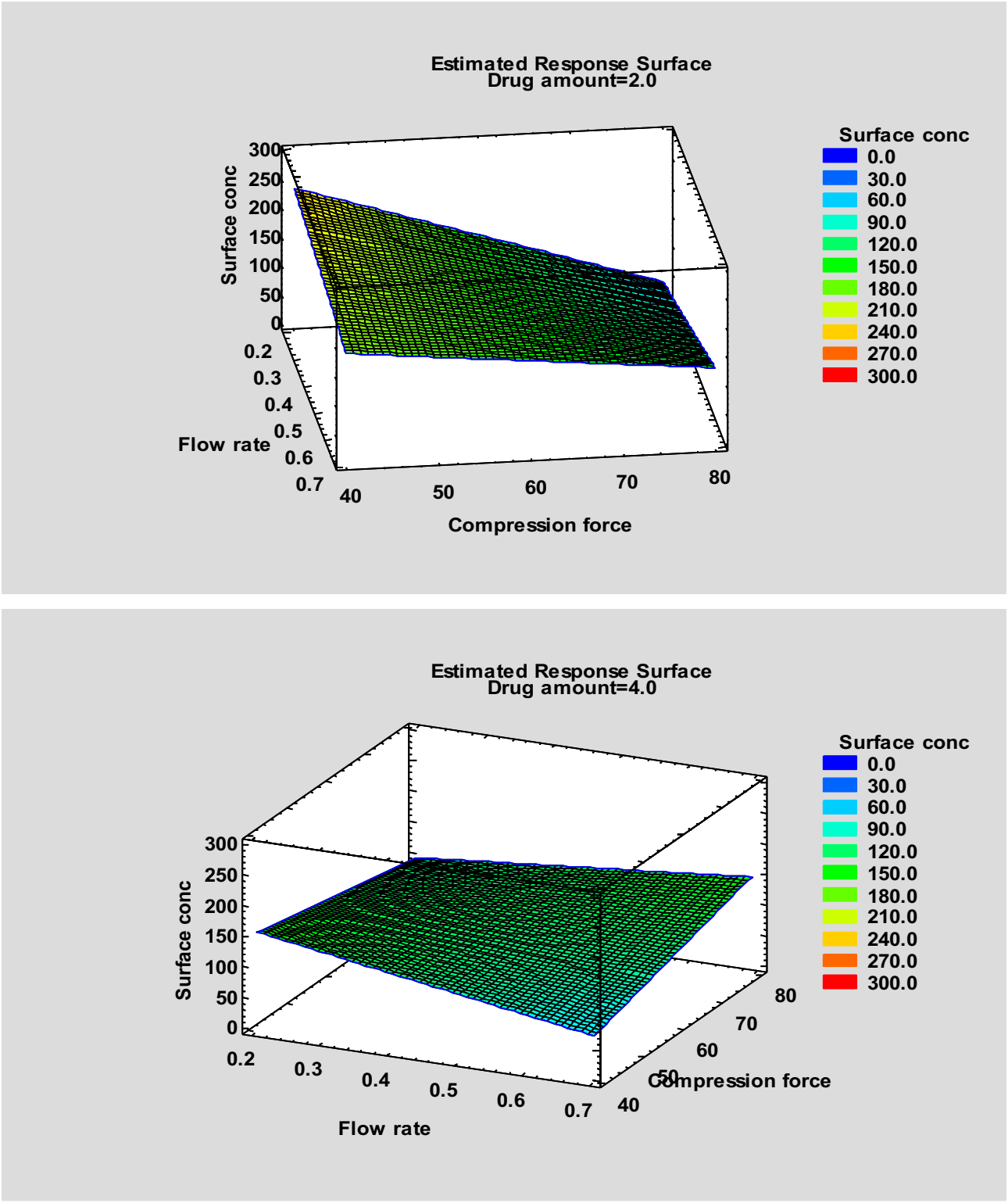

Fig. 5.1. Response surface showing the effect of the variables tested in the surface concentration in drug amounts of 2 mg (above) and 4 mg (below) tested.

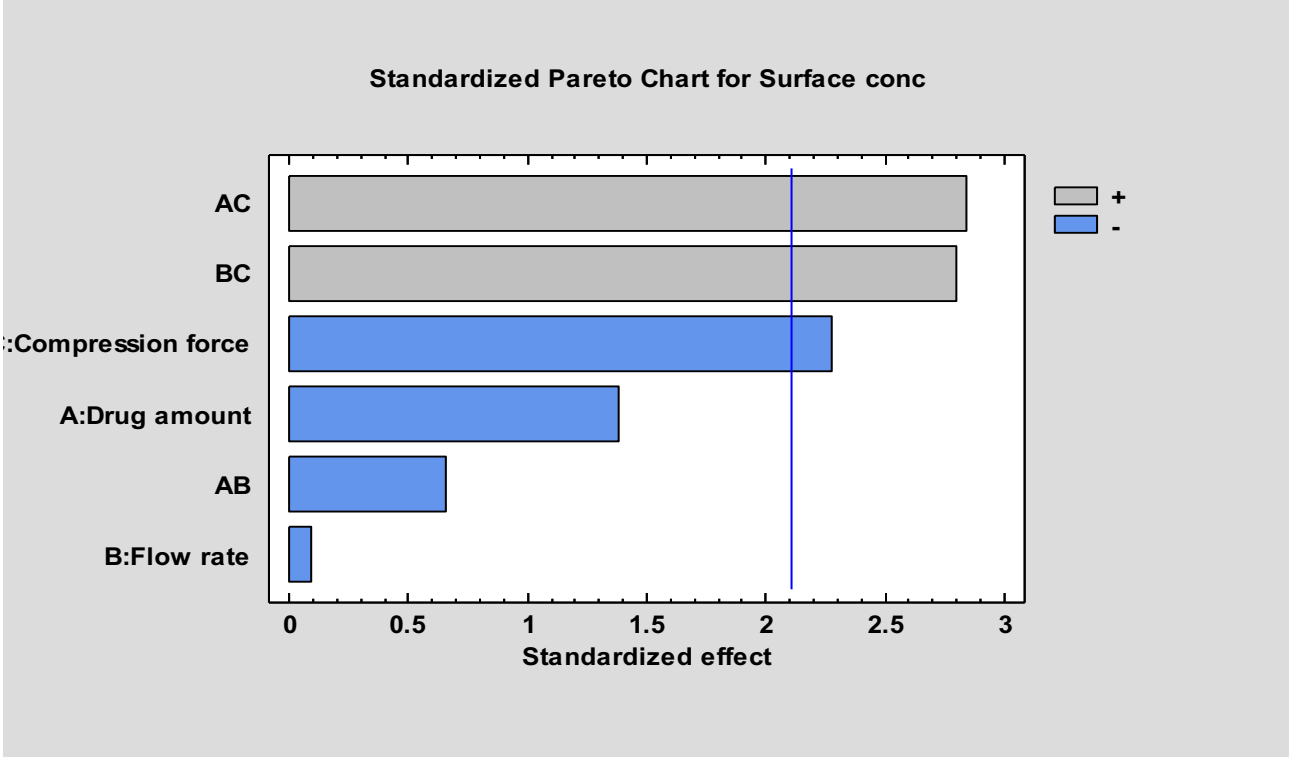

Fig. 5.2. Standardised Pareto Chart showing the standardized effect of the tested variables and their combinations on the surface concentration of the TA dissolved with UV imaging

5.3.1.1.2. Intrinsic Dissolution Rate (IDR)

Results regarding the IDR (Table 5.2), show that each factor tested provides a significant effect according to the Pareto Chart (Fig. 5.4). The highest effect was with different compression forces (P-value = 0.0008) with the effect of the flow rate and drug amount combination being of high significance as well (P-value = 0.001). With a lower compression force, the powder is more loosely packed with the compression rod in the stainless steel press and so dissociation from the surface and solvation into dissolved molecules can take place faster, leading to higher IDR (Fig. 5.3). In both flow rates and compression forces, a higher drug amount led to a higher dissolution rate with a more significant effect in the lower compression force (P-value = 0.0024). The IDR is affected mostly in combination of a variable with the flow rate which could be explained by the increased hydration of the material in test [8, 22]. With a higher volume flown through the cell, a higher amount of powder particles was dissolved, leading to the confirmation of the convective-diffusion theory (P-value = 0.0018); during which mass transport of a dissolved component will be a result of concentration gradients causing diffusion and convection due to bulk fluid motion [6, 23]. Significant effect is also shown with the

compression force in combination with the drug amount (P-value = 0.0055) and flow rate (P-value = 0.0088).

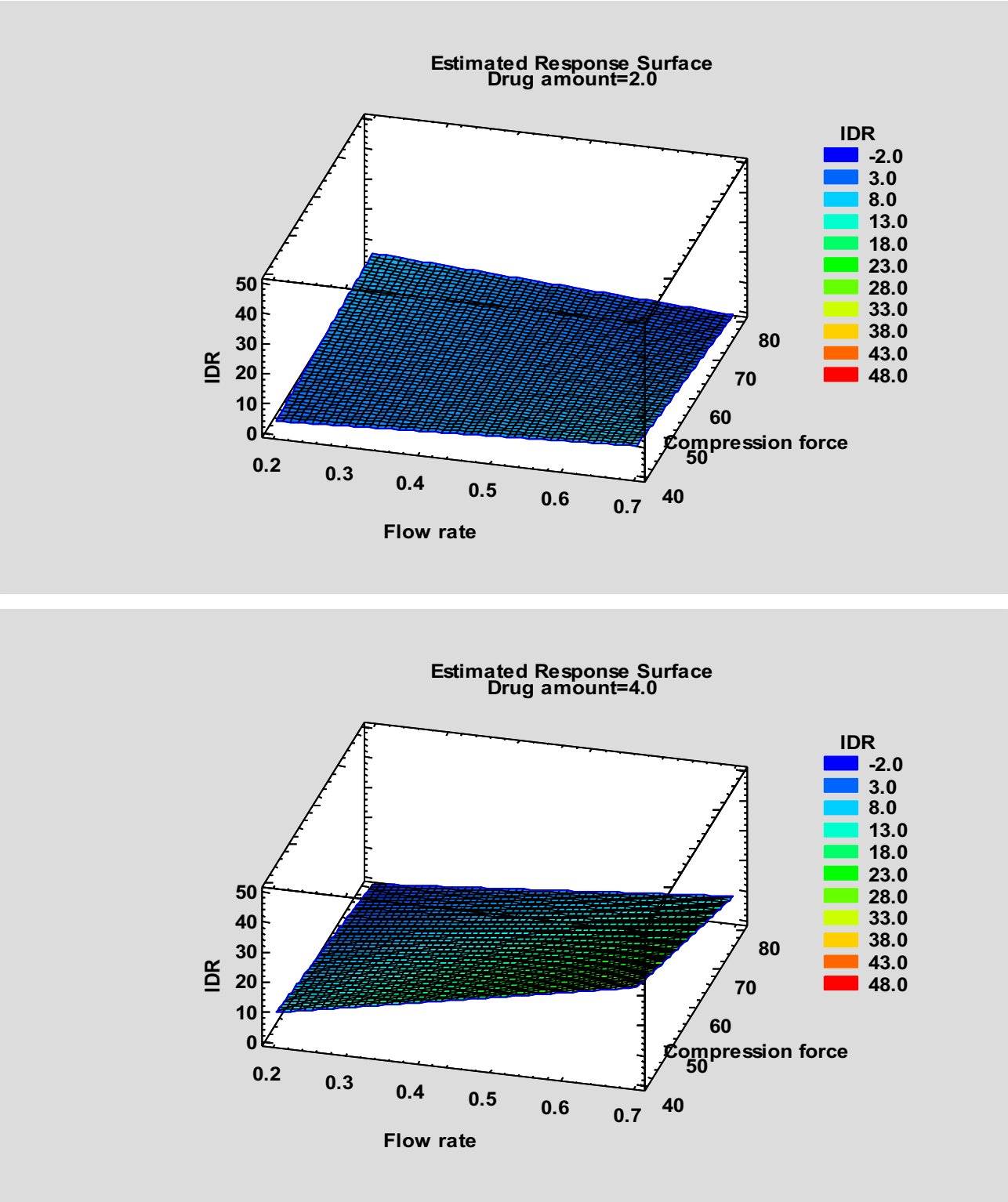

Fig. 5.3. Response surface showing the effect of the variables tested in the IDR in drug amounts of 2 mg (above) and 4 mg (below) tested

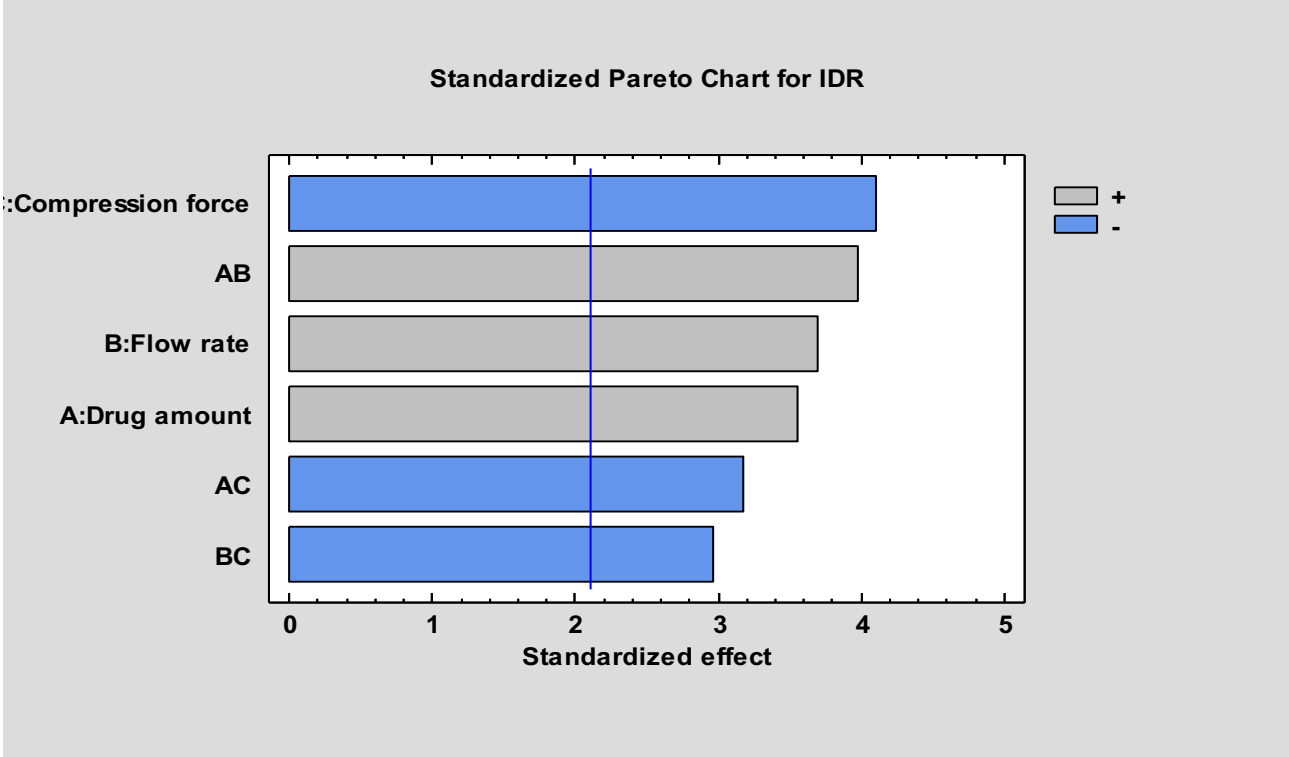

Fig. 5.4. Standardised Pareto Chart showing the standardized effect of the tested variables and their combinations on the IDR of the TA dissolved with UV imaging

5.3.1.1.3. Sample mass dissolved (SMD)

The difference noted in results for the TA mass dissolved (Table 5.2) might not be considered of high significance due to the low results measured from the dissolution of TA and the non-significant effect of the variables tested, as shown in the Pareto charts (Fig. 5.6). This is also justified due to TA being poorly soluble in PBS with SMD being low (Fig. 5.5) (Chapter 2). In a similar way to the results in surface concentration, the high compression force results in less drug being solvated from the powder surface (P-value = 0.1197). A more compact sample led to reduced amounts of TA dissolved (Fig. 5.5). In the higher flow rate, less compression force led to higher results (P-value = 0.1514) with a higher amount of drug in the sample cup, increasing the density of the compact powder (P-value = 0.097). The combination of drug amount leading to a different powder density in combination with the flow rate seems to affect the measurements of SMD conducted with the SDI having a stronger effect than powder density on its own (P-value = 0.0672). As a smaller amount of drug is packed with a similar compression force, there will be a difference in the porosity affecting the compaction of the powder in the sample cup. As the medium will enter the drug sample faster (increased hydration), this will increase the drug dissolution rate. Similar significance was depicted with

a combination of the compression force with the drug amount (P-value = 0.2324) and the flow rate (P-value = 0.5343).

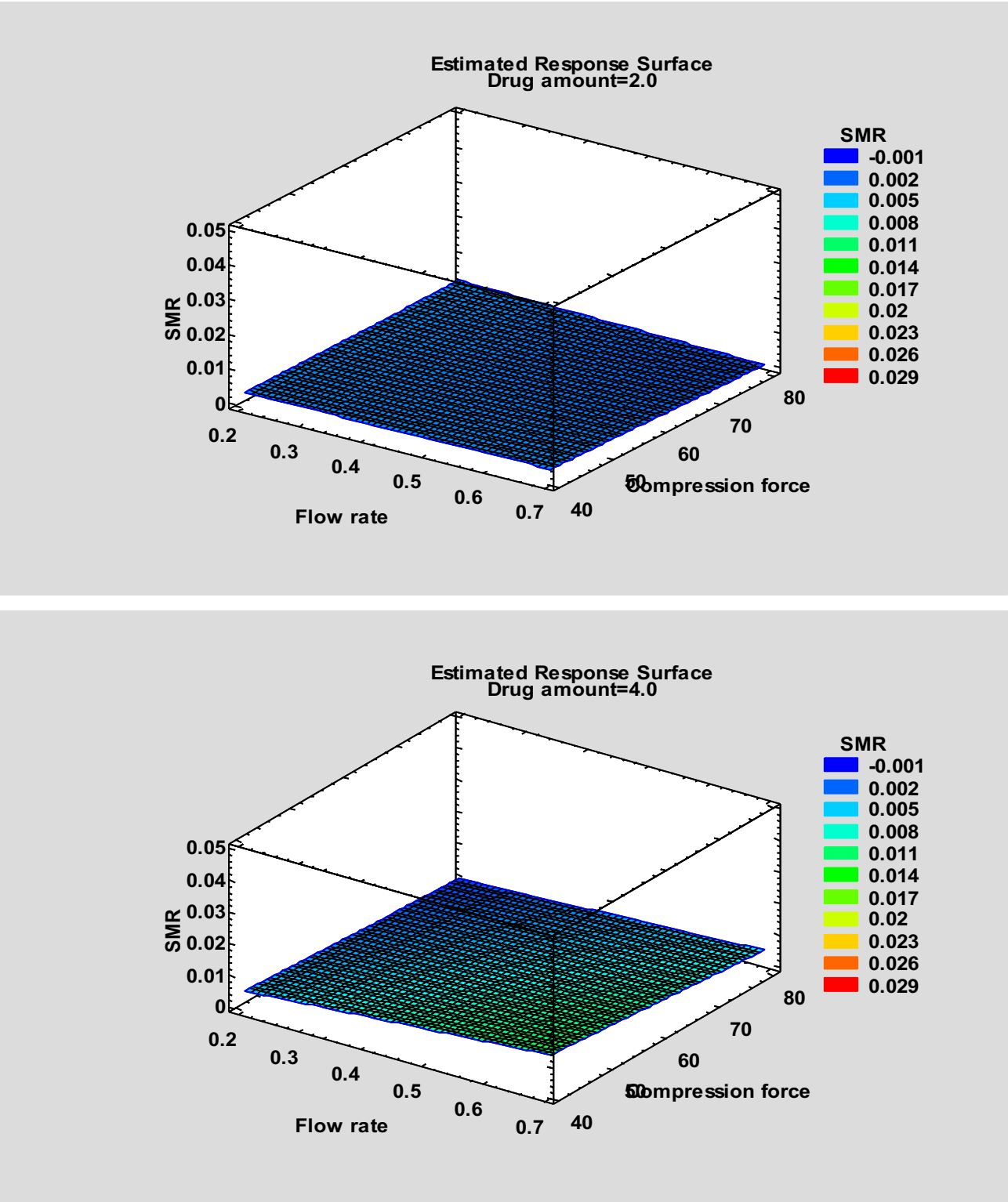

Fig. 5.5. Response surface showing the effect of the variables tested in the SMD in drug amounts of 2 mg (above) and 4 mg (below) tested

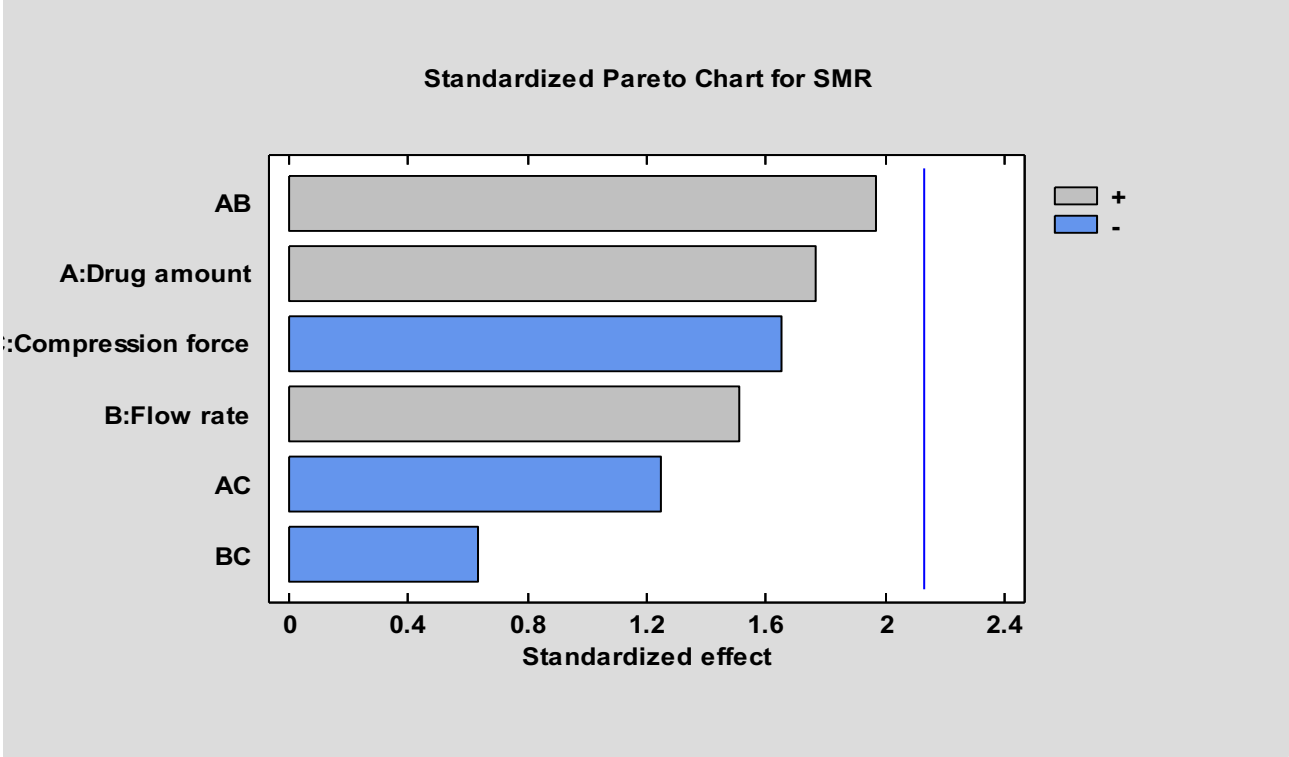

Fig. 5.6. Standardised Pareto Chart showing the standardized effect of the tested variables and their combinations on the SMD of the TA dissolved with UV imaging

5.3.1.2. Dissolution imaging in static flow conditions

5.3.1.2.1. Effect of type of surfactant in PBS on surface concentration

From the absorbance maps of the surface concentration of TA in media containing different types of surfactant (Fig. 5.13), it can be observed that dissolved TA shows an equivalent intensity with the solubility of the drug in each media and the dissolution rates of TA in the studies containing similar media (Chapter 2) [solubility of TA in: PBS, 28.52 μg/mL; PBS with Tween 80 (1% v/v), 91.6 μg/mL; PBS with SLS (1% w/v), 478.01 μg/mL; PBS with CTAB (1% w/v), 1041.226 μg/mL]. The intensity of the solvated molecules was obvious from the expansion of the absorbance area, contour lines and the absorbance value measured through the analysis over time (Fig. 5.13) [6]. Results of TA surface concentration show that the surfactants added, provide a different solubilisation capacity to the medium leading to the solubility of TA in ascending order: PBS (27.6 μg/mL) < PBS with Tween 80 (1% v/v) (58.3 μg/mL) < PBS with SLS (1% w/v) (86.5 μg/mL) < PBS with CTAB (1% w/v) (171.1 μg/mL) (Fig. 5.7). The differences in the surface concentrations of TA in the different media are also equivalent with the visual results recorded from the downstream absorbance tails (Fig. 5.13). As there is no flow in the system, the amount of drug dissolved from the surface of the powder

due to the presence of the medium, expanded above the surface, slowly diffusing. With static flow conditions, the dissolved drug particles stayed close to the surface of the dissolving powder which affects the local solution distribution within the cell, also obvious from the concentrated density gradients (Fig. 5.13) [6]. During dissolution, local supersaturated solutions may occur near the sample surface, which leads to the plateau of the surface concentration observed in Fig. 5.7. This may also limit the possibility of higher drug dissolution rates to be measured [16]. Swelling of the sample was also examined visually after each run, confirming that this was not the reason of the increased absorbance above the surface of the sample (Fig. 5.13).

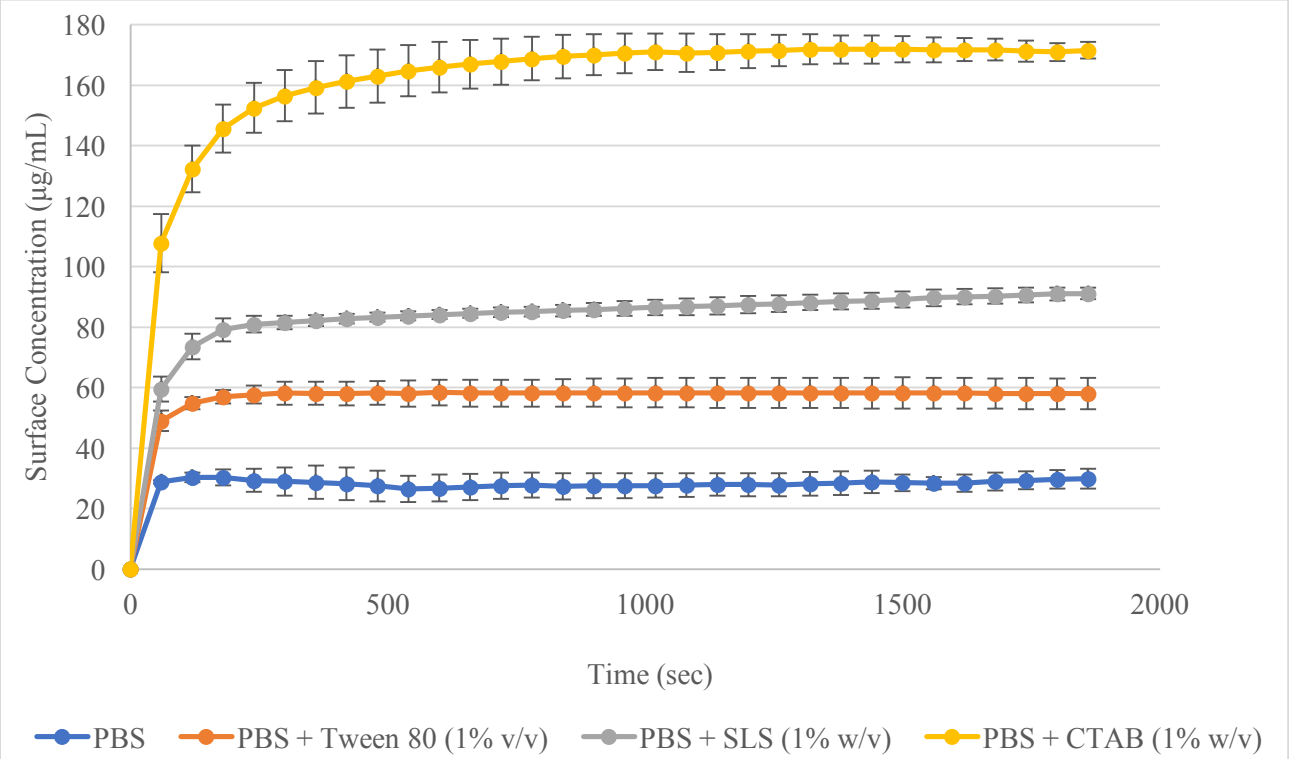

Fig. 5.7. Mean ± SD of TA surface concentration in different media over time in static flow

5.3.1.2.2. Effect of viscosity of ASFs on surface concentration

Results with ASFs showed that increasing the amount of HA in the medium leads to a lower dissolution with the surface concentration of TA in HS being 31.99 µg/mL, in OA 70.3 µg/mL and in RA being 78.7 µg/mL at 30 min (Fig. 5.8 and 5.14). Following the Noyes–Whitney equation expressing the dissolution rate, the diffusion coefficient D, is partly related to the solvent viscosity; and the dissolution rate will decrease with increasing medium viscosity as D is inversely proportional to the viscosity [24]. This is shown in the Stokes–Einstein equation,

as the viscosity of the medium, among other parameters affects the diffusion coefficient and so the dissolution rate (Chapter 3, 4). In addition, more viscous fluid will slow down the diffusional mass transport of the drug.

Results confirm that with no flow present in the system (Fig. 5.8), the media with increasing viscosity have the least amount of drug dissolved. Visually, from the absorbance maps depicted in Fig. 5.9, it was noticed that drug powder aggregates that were dissolving on the surface of the powder, detached and separated from the surface. This could be noticed for the ASFs tested and while it took place, the surface concentration would slightly reduce and then would start to increase again, which can also be noticed in Fig. 5.8 when values drop slightly [e.g. OA ASF at 1260 sec (Fig. 5.8) depicted in Fig. 5.9].

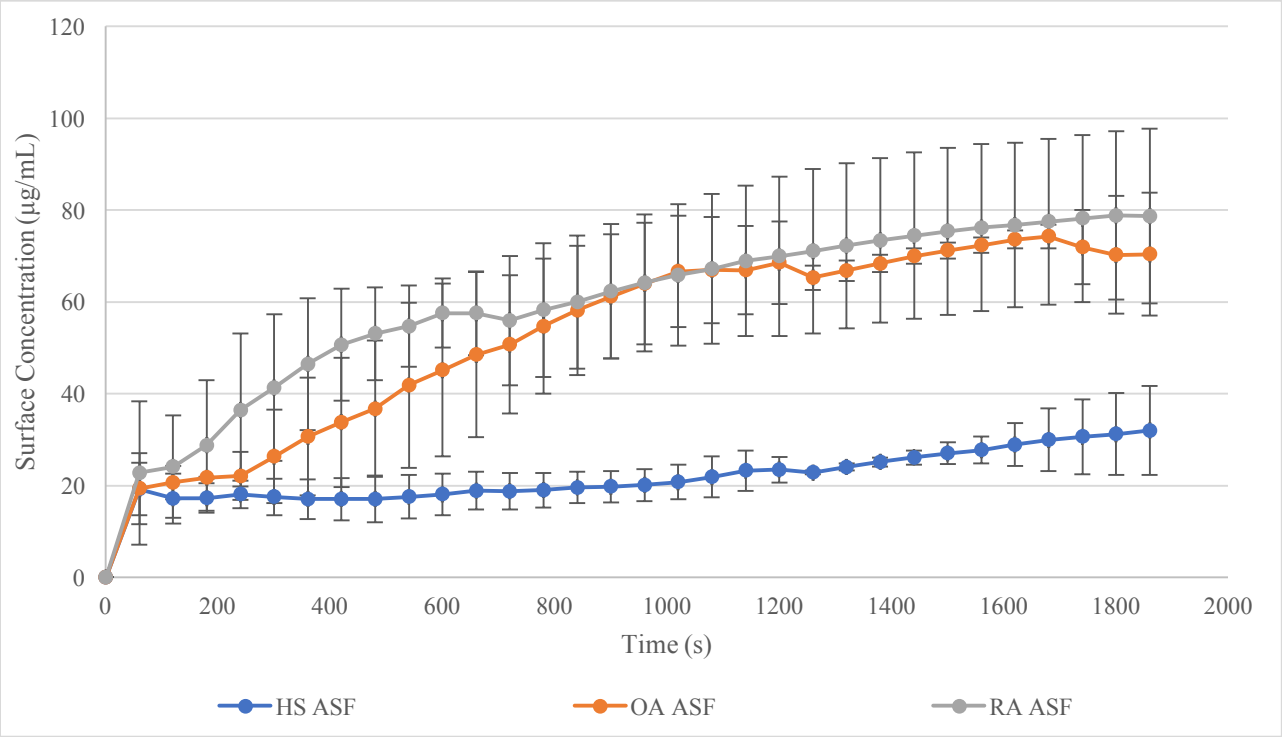

Fig. 5.8. Mean ± SD of TA surface concentration in different BSF containing only HA, over time in static flow

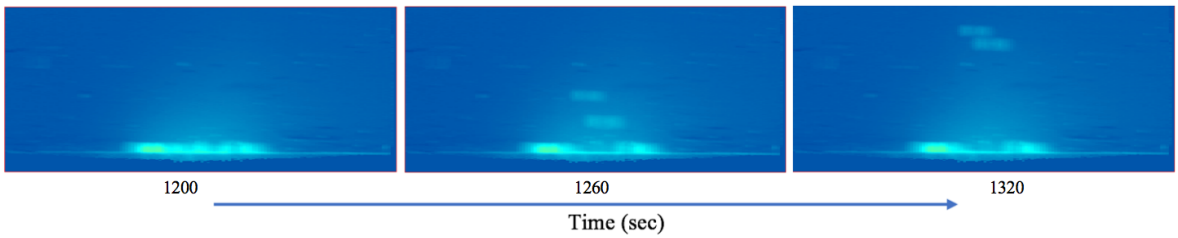

Fig. 5.9. Absorbance maps of TA in OA ASF (static flow)

5.3.1.3. Dissolution imaging in continuous flow conditions

5.3.1.3.1. Effect of type of surfactant in PBS

5.3.1.3.1.1. Surface Concentration

Although visual representations of the experiments with a flow present (Fig. 5.15), show a higher absorbance and wider quantification region downstream in the analysis of TA in PBS with CTAB (1% w/v) and in PBS with SLS (1% w/v) [8], the results of the TA surface concertation show a higher value for TA in PBS with SLS (1% w/v) at 66.85 µg/mL followed by TA in PBS with CTAB (1% w/v) at 60.05 µg/mL and TA in PBS with Tween 80 (1% v/v) at 57.8 µg/mL (Fig. 5.10). Comparing these results shows small difference, although being of higher values than the TA surface concentration in PBS without a surfactant (25.5 µg/mL) (Fig. 5.10). Results according to visual representations in Fig. 5.15, can be explained as the dissolved drug will be transferred from the area above the surface of the powder and towards the direction of the flow [6], away from the surface of the sample.

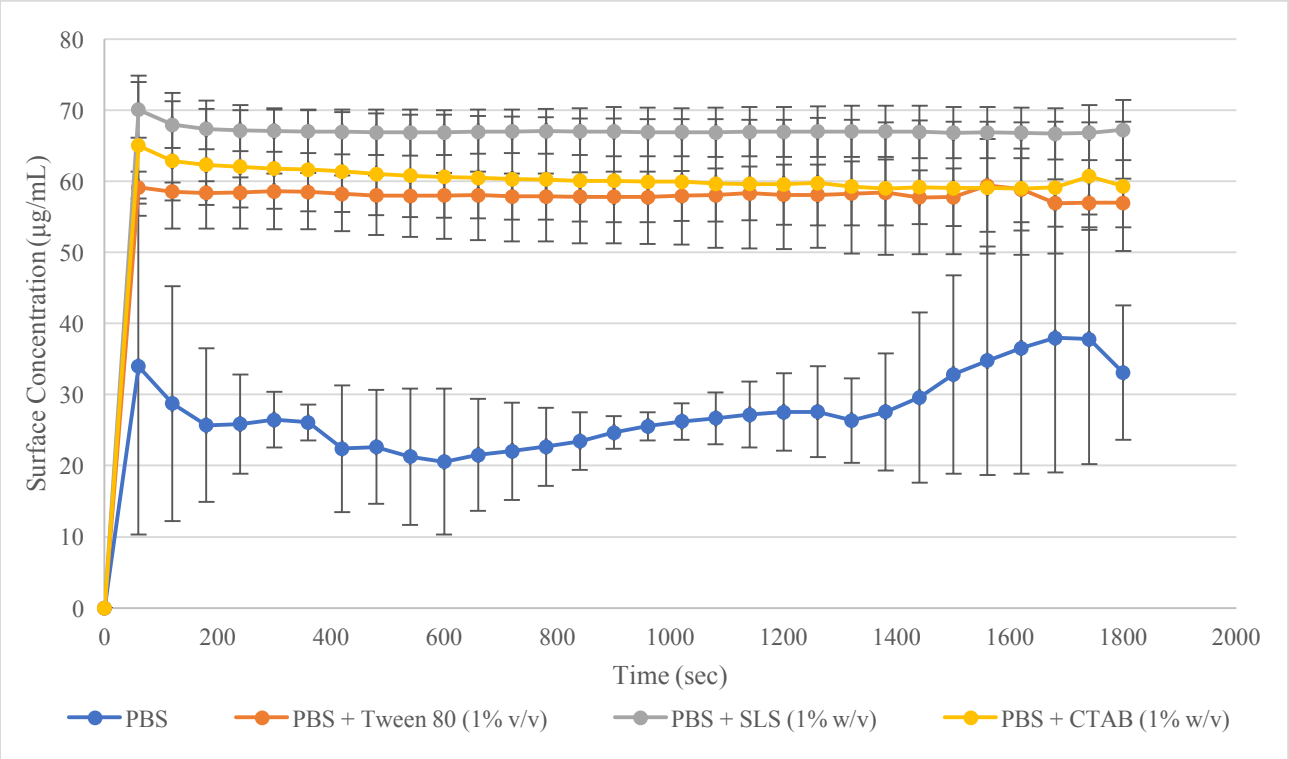

Fig. 5.10. Mean ± SD of TA surface concentration in different media over time with a flow of 0.2 mL/min.

5.3.1.3.1.2. Intrinsic Dissolution Rate (IDR)

The rate of intrinsic dissolution of TA seems to be lower in PBS with an average of 0.47 µg/min/cm^2 while with a surfactant in the medium, in PBS with Tween 80 (1% v/v) and PBS with SLS (1% w/v) it seems to be higher than in PBS with an average rate of 1.39 and 2.91 µg/min/cm^2 respectively (Fig. 5.11). The rate of TA in PBS with CTAB (1% w/v) is even higher with an average of 3.7 µg/min/cm^2. As TA in PBS with CTAB (1% w/v) has the highest dissolution rate compared to other media (Chapter 2), similar results are noted in this experiment with the visualisation of the dissolution showing a thicker downstream "tail" in the flow rate used [8] (Fig. 5.15). With surfactant added to the medium, there is reduced surface tension with the creation of micelles, while improving wetting properties and increasing the dissolution rate of the drug [25]. The molecular weight of Tween 80 is larger compared to the molecular weight of the anionic surfactants used [26] and so with similar surfactant molar concentrations, more drug molecules will be encapsulated in the SLS micelles, leading to lower diffusivity of the drug-micelle complex and so less drug was dissolved from the formulation. Furthermore, ionic surfactants such as SLS and CTAB have higher surface activities with a stronger solubilising effect than non-ionic surfactants such as Tween 80, leading to higher drug solubilisation [27].

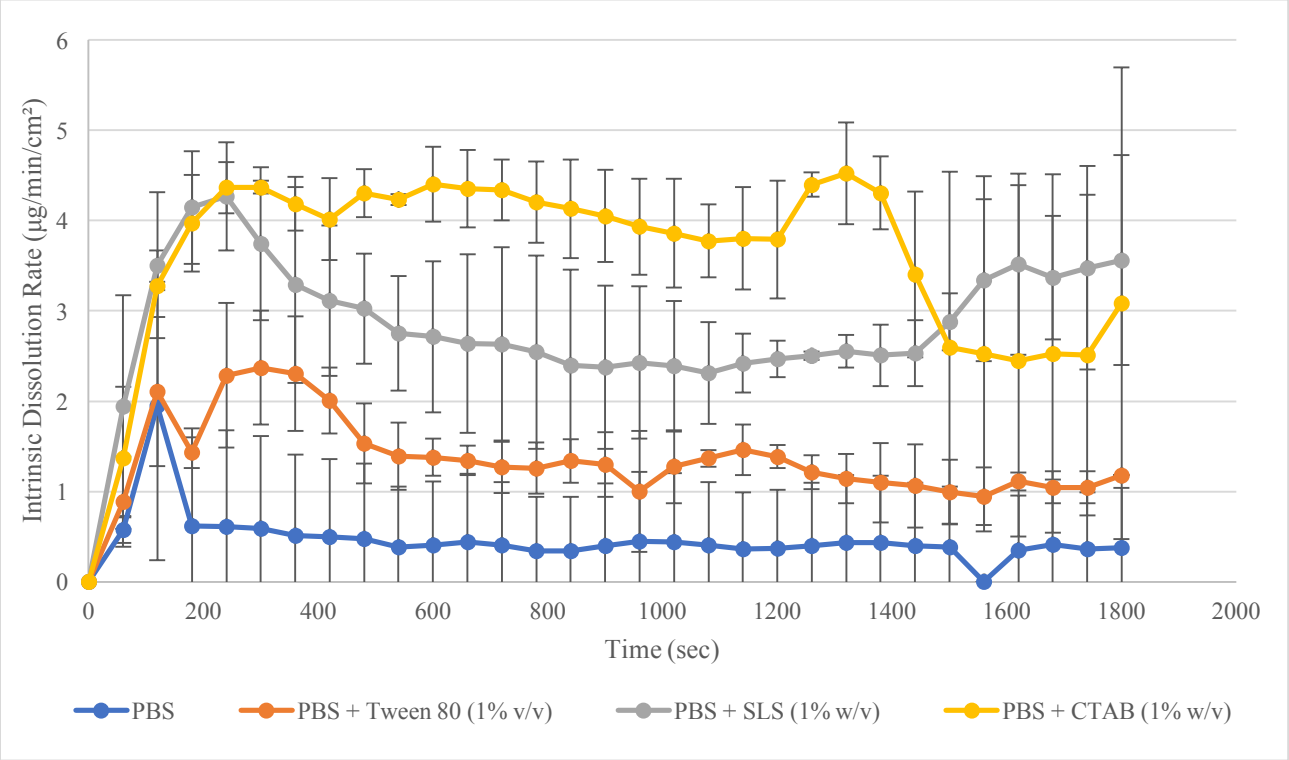

Fig. 5.11. Mean ± SD of TA IDR in different media over time with a flow of 0.2 mL/min.

5.3.1.3.1.3. Sample mass dissolved (SMD)

More drug seems to be dissolved with PBS with CTAB (1% w/v) running through the system (0.0036 mg in 30 min) rather than with PBS with SLS (1% w/v) (0.0027 mg in 30 min) and PBS with Tween 80 (1% v/v) (0.0012 mg in 30 min) but with no significant difference noted between them (Fig. 5.12). The results can be justified from the visual representation of the analysis, with the downstream tail showing higher absorbance in accordance with the TA dissolved (Fig. 5.15). TA in PBS had the least amount of TA dissolved (0.0004 mg in 30 min) which can be also be justified from the dissolution experiments of TA in buffers with surfactants (Chapter 2) showing similar results.

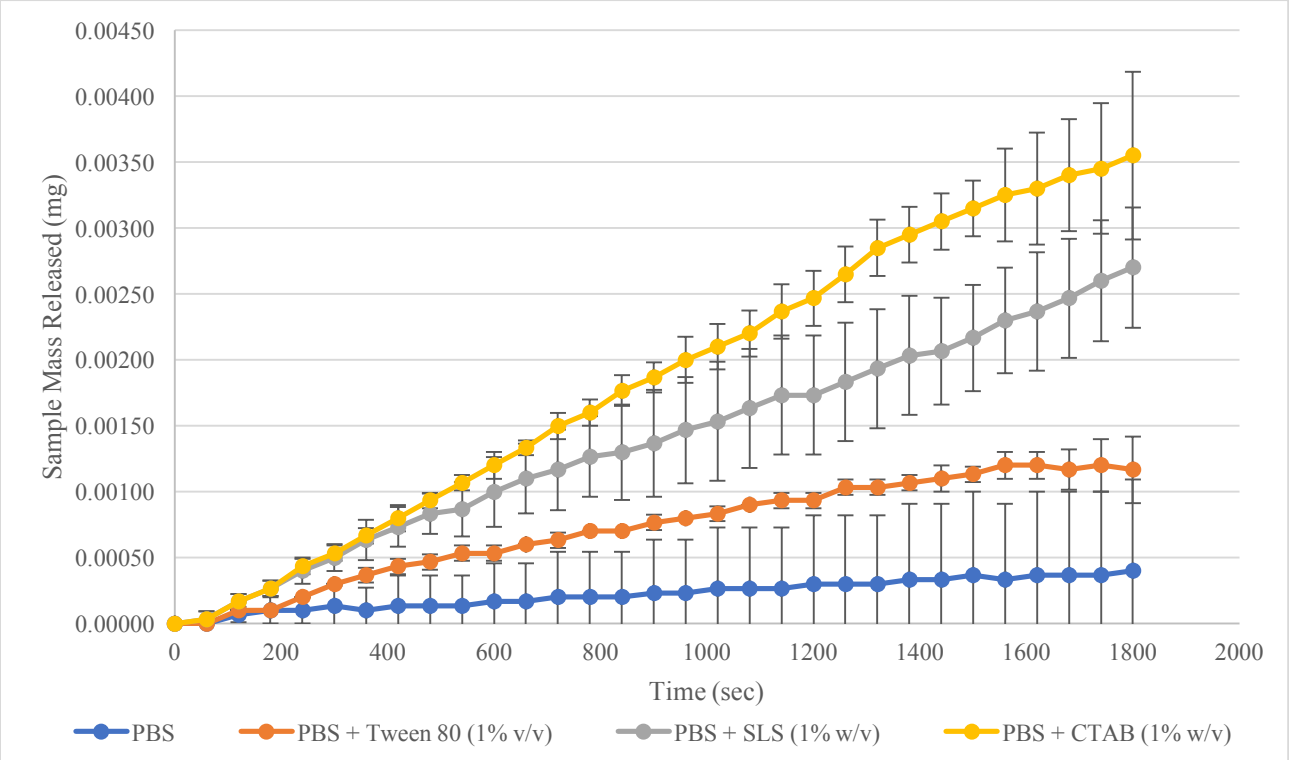

Fig. 5.12. Mean ± SD of TA mass dissolved in different media over time with a flow of 0.2 mL/min

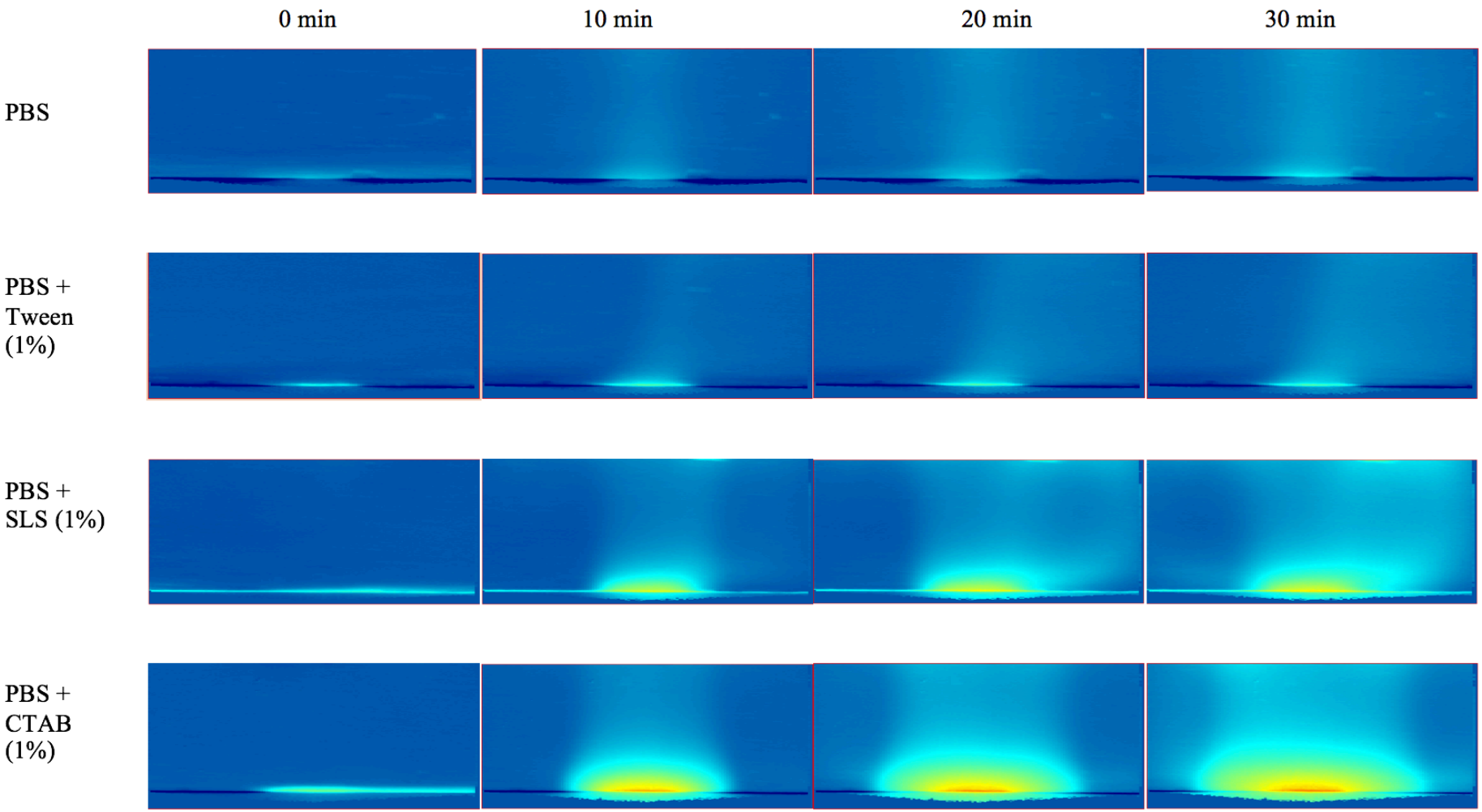

Fig. 5.13. Absorbance maps of TA in PBS with surfactants (static flow)

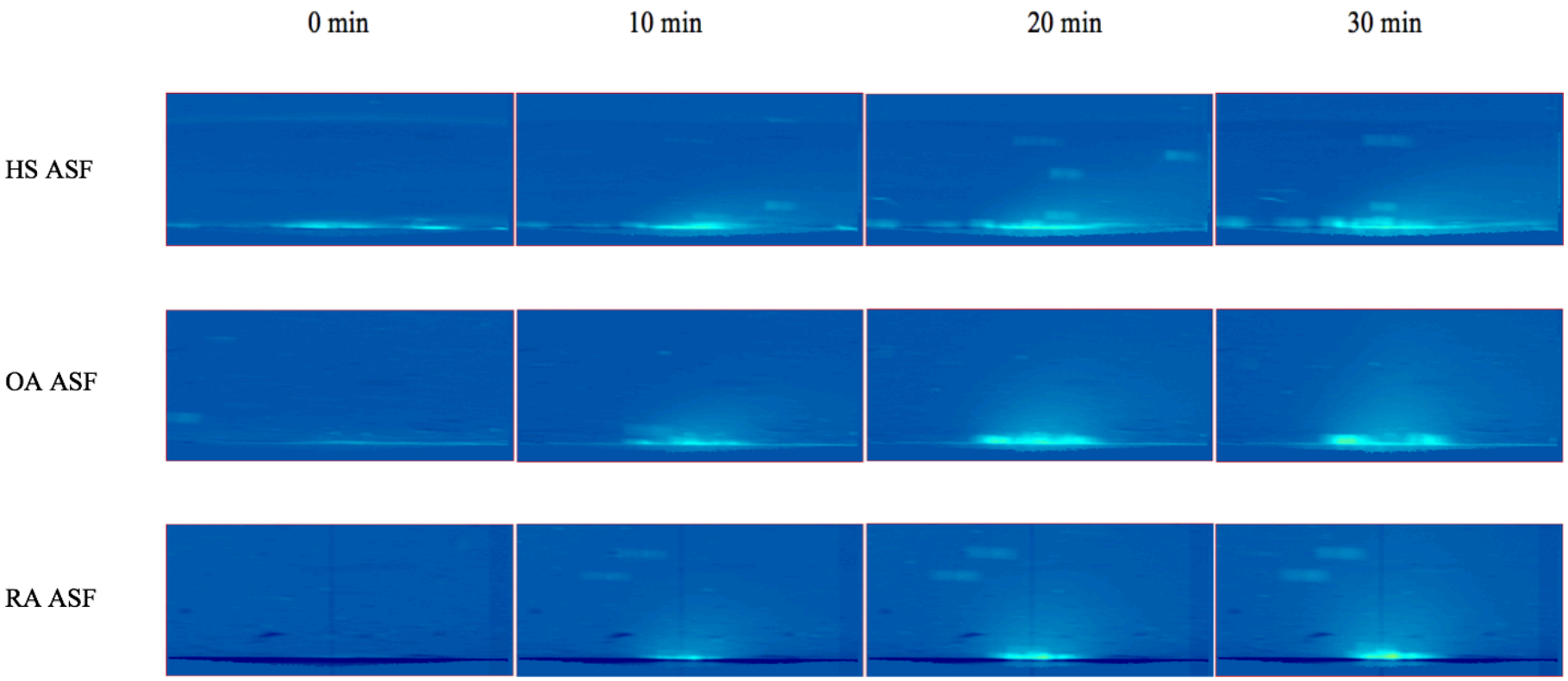

Fig. 5.14. Absorbance maps of TA in ASFs in different states (HS, OA and RA) (static flow)

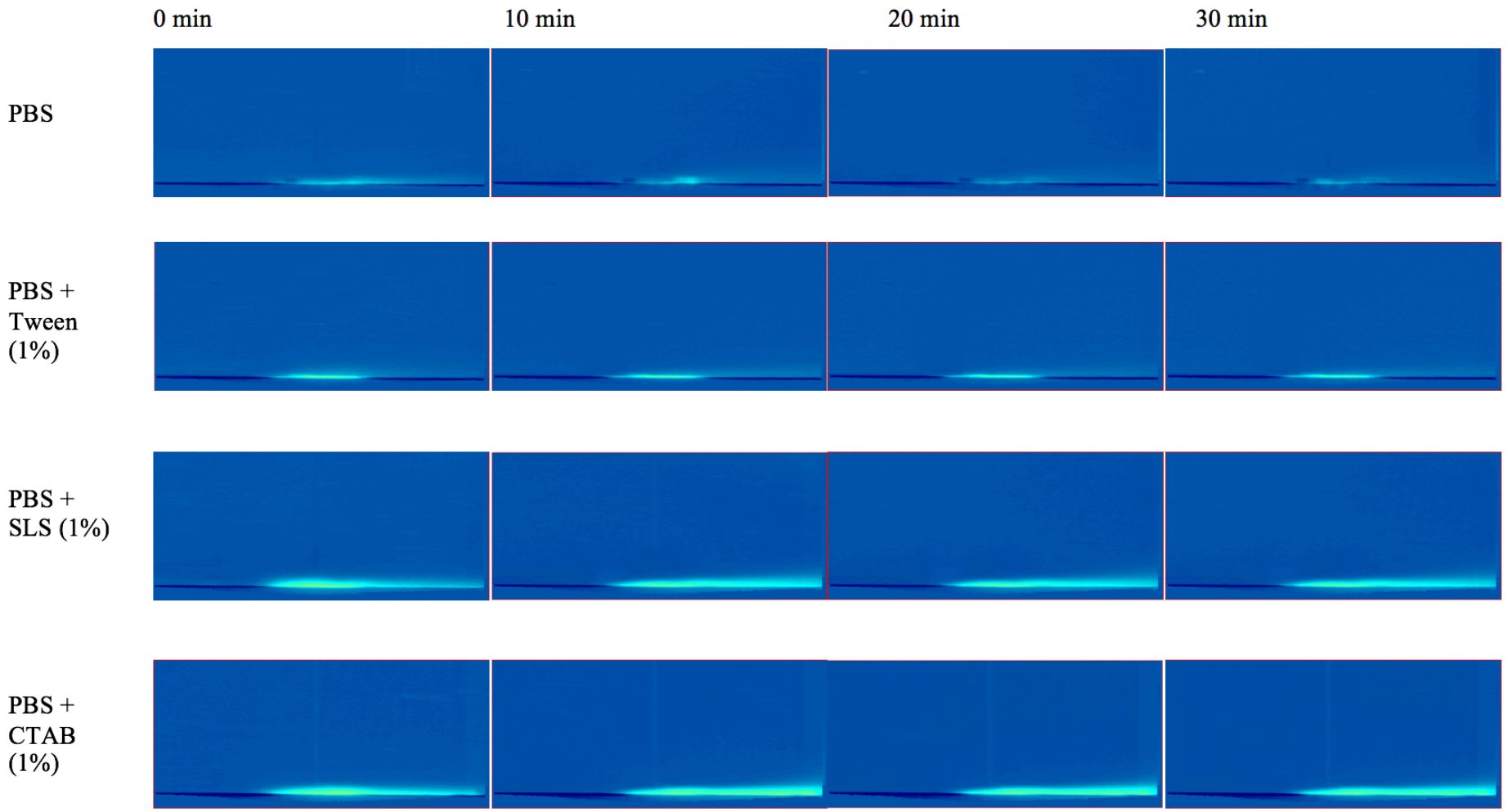

Fig. 5.15. Absorbance maps of TA in PBS with surfactants (continuous flow 0.2 mL/min)

5.4. Conclusions

In this study, the use of UV surface dissolution imaging is studied as a promising tool for predictive *in-vitro* dissolution testing of IA drugs. The process optimization was of significant importance to understand which are the optimal conditions of drug amount, flow rate and compression force for further experiments. In static flow, testing TA in PBS containing different surfactants with increasing solubility showed that results were in accordance with what visual representations of the analysis and the dissolution of TA in the media (Chapter 3). When flow was applied, visually it was apparent that the highest drug mass dissolved and IDR was in the buffer with the highest solubility and the quantified results led to similar conclusions. The use of ASFs was also proven successful and the media were compatible with the utilized UV surface dissolution imaging setup and showed that increased viscosity of the medium leads to a slower dissolution rate. Using the UV imaging detector assists in monitoring drug dissolution adjacent to the surface of the drug powder in spatially and temporally conditions and results have shown that the media have a significant effect on the dissolution behaviour of TA. The UV imaging seems to have vast potential as a future tool for drug dissolution testing, involving biorelevant media as well.

5.5. References

1. Edwards, S.H., *Intra-articular drug delivery: the challenge to extend drug residence time within the joint.* Vet J, 2011. **190**(1): p. 15-21.
2. Brown, C.K., et al., *FIP/AAPS joint workshop report: dissolution/in-vitro release testing of novel/special dosage forms.* AAPS PharmSciTech, 2011. **12**(2): p. 782-94.
3. D'Souza, S.S. and P.P. DeLuca, *Methods to assess in-vitro drug release from injectable polymeric particulate systems.* Pharm Res, 2006. **23**(3): p. 460-74.
4. Larsen, C., et al., *Intra-articular depot formulation principles: role in the management of postoperative pain and arthritic disorders.* J Pharm Sci, 2008. **97**(11): p. 4622-54.
5. Seidlitz, A. and W. Weitschies, *In-vitro dissolution methods for controlled release parenterals and their applicability to drug-eluting stent testing.* J Pharm Pharmacol, 2012. **64**(7): p. 969-85.
6. Boetker, J.P., et al., *Insights into the early dissolution events of amlodipine using UV imaging and Raman spectroscopy.* Mol Pharm, 2011. **8**(4): p. 1372-80.
7. Ostergaard, J., et al., *Monitoring lidocaine single-crystal dissolution by ultraviolet imaging.* J Pharm Sci, 2011. **100**(8): p. 3405-10.
8. Gordon, S., et al., *Real-time dissolution behavior of furosemide in biorelevant media as determined by UV imaging.* Pharm Dev Technol, 2013. **18**(6): p. 1407-16.
9. Burt, H.M., et al., *Intra-articular drug delivery systems: Overcoming the shortcomings of joint disease therapy.* Expert Opin Drug Deliv, 2009. **6**(1): p. 17-26.
10. Bingol, A.O., et al., *Characterisation and comparison of shear and extensional flow of sodium hyaluronate and human synovial fluid.* Biorheology, 2010. **47**(3-4): p. 205-24.
11. Fam, H., J.T. Bryant, and M. Kontopoulou, *Rheological properties of synovial fluids.* Biorheology, 2007. **44**(2): p. 59-74.
12. Balazs, E.A., et al., *Hyaluronic acid in synovial fluid. I. Molecular parameters of hyaluronic acid in normal and arthritis human fluids.* Arthritis Rheum, 1967. **10**(4): p. 357-76.
13. Decker, B., et al., *Concentration of hyaluronic acid in synovial fluid.* Clin Chem, 1959. **5**: p. 465-9.
14. Hamerman, D. and H. Schuster, *Hyaluronate in normal human synovial fluid.* Journal of Clinical Investigation, 1958. **37**(1): p. 57-64.
15. Stafford, C.T., et al., *Studies on the Concentration and Intrinsic Viscosity of Hyaluronic Acid in Synovial Fluids of Patients with Rheumatic Diseases.* Annals of the Rheumatic Diseases, 1964. **23**(2): p. 152-157.
16. Sarnes, A., et al., *Dissolution study of nanocrystal powders of a poorly soluble drug by UV imaging and channel flow methods.* Eur J Pharm Sci, 2013. **50**(3-4): p. 511-9.
17. Blewis, M.E., et al., *A model of synovial fluid lubricant composition in normal and injured joints.* Eur Cell Mater, 2007. **13**: p. 26-39.
18. Jantratid, E., et al., *Dissolution media simulating conditions in the proximal human gastrointestinal tract: an update.* Pharm Res, 2008. **25**(7): p. 1663-76.
19. Missel, P.J., Stevens, L.E., Mauger, J.W.: *Re-examination of convective diffusion/drug dissolution in a laminar flow channel: Accurate prediction of dissolution rate*. Pharm. Res., 2001, 24, 2300- 2306.
20. Meng, J., T.F. Sturgis, and B.-B.C. Youan, *Engineering Tenofovir Loaded Chitosan Nanoparticles: To Maximize Microbicide Mucoadhesion.* European Journal of Pharmaceutical Sciences, 2011. **44**(1-2): p. 57-67.
21. Shah, A.C. and K.G. Nelson, *Evaluation of a convective diffusion drug dissolution rate model.* J Pharm Sci, 1975. **64**(9): p. 1518-20.

22. Kastellorizios, M. and D.J. Burgess, *In-vitro Drug Release Testing and In-vivo/In-vitro Correlation for Long Acting Implants and Injections*, in *Long Acting Injections and Implants*, J.C. Wright and D.J. Burgess, Editors. 2012, Springer US: Boston, MA. p. 475-503.
23. Missel, P.J., L.E. Stevens, and J.W. Mauger, *Reexamination of convective diffusion/drug dissolution in a laminar flow channel: accurate prediction of dissolution rate.* Pharm Res, 2004. **21**(12): p. 2300-6.
24. Smith, B., *Chapter 3. Solubility and dissolution*, in *Remington Education: Physical Pharmacy*. 2015, Pharmaceutical Press.
25. Savjani, K.T., A.K. Gajjar, and J.K. Savjani, *Drug Solubility: Importance and Enhancement Techniques.* ISRN Pharmaceutics, 2012. **2012**: p. 195727.
26. Fotaki, N., et al., *Rationale for selection of dissolution media: three case studie.* Dissolution Technologies, 2013. **20**(3): p. 6-13.
27. Park, S.H. and H.K. Choi, *The effects of surfactants on the dissolution profiles of poorly water-soluble acidic drugs.* Int J Pharm, 2006. **321**(1-2): p. 35-41.

Chapter 6: Conclusions and Perspectives

In this thesis, various dissolution testing methods were used to assess drug dissolution from a model IA drug. The objectives were to study and define the effect of various factors of dissolution methods affecting drug dissolution from the formulation and use this information i) to design appropriate *in-vitro* compendial tests for IA formulations; ii) to design appropriate *in-vitro* biorelevant tests for IA formulations by using developed BSF media and iii) to use UV imaging for characterizing the dissolution process for IA drugs in buffer with surfactants and ASFs. The ultimate goal was the development of appropriate and validated *in-vitro* predictive models of the absorption of a drug after IA administration by taking into account the physiological factors that affect the absorption process. The methods developed will be used for defining critical variables and setting specifications and may also be applied to other injectable formulations.

In this work, the continuous flow through cell, the dialysis membrane and the bi-phasic setup were evaluated according to their potential as compendial dissolution tests, while side-Bi-side diffusion cells and the bi-phasic setup were evaluated for their potential as biorelevant dissolution tests for IA formulations. BSFs of different physiological states (healthy, OA and RA) were developed according to the physicochemical characterisation of *in-vivo* disease state synovial fluid, and were also used in the biorelevant dissolution tests. The SDI was also evaluated for its potential to provide deeper insights into the early events of the dissolution process of IA drugs. In the following parts we summarize the conclusions and perspectives of the various aspects of this research.

6.1. Compendial Tests for IA formulations

Evaluating the effect of various parameters of the tested dissolution methods on the drug dissolution of IA formulations, provided important information related to the potential of each method to be used as a compendial dissolution test. With the USP apparatus I and III, there was no dissolution measured, due to the non-permeation of the drug through the dialysis membrane of the Float-A-lyzers used within the apparatus. With the the USP apparatus II, the suspension dissolved immediately reaching a plateau in the % of drug dissolved before complete dissolution, due to the absence of sink conditions. Using the USP apparatus IV in open system, to examine the continuous flow through cell method, showed that the system is sensitive to the different parameters, with high significance established between the variables.

The promising results were confirmed by establishing the discriminating ability of the setup with drug microparticles of different size. With the use of the bi-phasic method with the USP apparatus IV in closed system, the parameters tested affected the rate of drug permeation to the organic phase, with the drug dissolving in the aqueous phase almost immediately, up to the amount allowed due to the solubility limit, presenting a plateau of % drug dissolved in results. Changing the oil-water interface area led to a faster partitioning rather than dissolution of the drug, showing the potential of the method to be used as a compendial dissolution test. The dialysis membrane method presented many difficulties with the dissolution and permeation of the drug through the membrane. In most setups evaluating various parameters there was no drug dissolution measured, similarly to the use of dialysis membranes with the Float-A-lyzers, probably due to an evident particle agglomeration of the flocculated suspension. The evaluation of various parameters including the length of the dialysis sac, increased temperature and the presence of an organic solvent in the receptor phase, enhanced drug permeation through the membrane showing that the dialysis membrane method has potential in drug dissolution of IA formulations. As these findings form a useful basis for further fundamental research, an important future step is to validate the optimal conditions of the tested dissolution methods. Testing a higher number of IA drugs and showing the discrimination power of these methods will further prove the potential they have, to be established as compendial methods.

6.2. *In-vivo* synovial fluid measurements and development of Biorelevant Synovial Fluid (healthy state, OA and RA)

The BSFs were developed by taking into consideration the *in-vivo* measurements of the disease state synovial fluids and the average amount of key components affecting dissolution, found in literature. The buffers chosen, maintained the desired pH, while Molarity was chosen for appropriate osmolality values of the developed media. For having appropriate viscosity of the developed BSFs, HA was used in higher amounts than the average values found in literature, as the three states, *in-vivo* contain, HA in different molecular weights (which plays an important role in enhancing viscosity). To choose the appropriate amount with the HA used, a calibration curve was done with the HA in use, at different concentrations vs. viscosity at a low shear rate (0.07 s^{-1}). CMC was also tested as a viscosity enhancer to reach the targeted values. Regarding the solubility studies performed, Also the addition of the hyaluronidase solution in the sample was chosen to be added after the addition of the drug solution in the calibration standards. This was decided, to follow the same order of hyaluronidase solution addition as in

the experimental samples in which the drug is already dissolved in the synovial fluid (in-vivo or *in-vitro* biorelevant). Comparing the solubility of TA in the developed BSFs and in the in-vivo disease state, results show that there are still biorelevant aspects of the synovial fluid affecting dissolution, to be understood. The potential exists, however, for the developed media to be useful for predicting in-vivo behaviour. This is based on their biorelevance compared to other existing media simulating synovial fluid and the differences in TA solubility noticed between the healthy state and the disease states developed and also in comparison to the widely used PBS with HA (3 mg/mL).

6.3. Biorelevant Tests for intra-articular formulations

Both *in-vitro* biorelevant systems involving the side-Bi-side cells and the bi-phasic setup studied have shown great potential in discrimination between dissolution rates of the setup parameters tested. The dissolution/permeation methods tested simulated successfully the permeation of the synovial fluid through the synovial membrane, the transfer of the dissolved drug to the flowing blood circulation and the transynovial flow mimicking the pathway that the synovial fluid follows. The transynovial flow setup with the side-Bi-side cells specifically has shown great biorelevance by mimicking the condition in the joint (hydrodynamics of setup and BSF) and the dissolution of the drug in different states of BSF media. Using TA as the model drug, discrimination between the biorelevant media could only be evident between the RA BSF and the healthy state and OA BSF. As the BSF tested did not contain HA which affects dissolution rate, the difference in composition between the healthy state BSF and the OA BSF was 0.15 and 0.25 mg/mL of PC respectively and the different buffers used. Using the BSFs in the bi-phasic model tested, did not show any significant differences in the TA dissolution rate. Although the systems showed significant promise, testing more drugs and also proving the discrimination power of the systems with the use of different drug particle sizes may also provide extra insights in the full potential of the systems. Furthermore, more *in-vivo* work can be performed in order to establish pharmacokinetic parameters and then related them with the *in-vitro* data from these biorelevant dissolution methods. This may lead to the development of *in-vitro-in-vivo* relationships (IVIVR) which can be used for the mechanistic understanding and development of *in-vitro – in-vivo* correlations (IVIVC).

6.4. Dissolution testing with UV imaging

Optimising the UV imaging process for testing IA drugs, showed that the compression force is significantly important for the results obtained, as a more compacted powder will not allow drug particles to solvate and dissolve easily. The TA mass released did not seem to be affected by any of the variables in test as results were very low and possibly of non-significance due to the low solubility of the drug in the medium tested. This study also contains an attempt to evaluate the effect of viscosity of ASFs simulating different states of the synovial fluid. In static flow, with less viscosity, dissolution rate of TA was higher, as viscosity is part of the diffusion coefficient according to the Noyes – Whitney dissolution rate equation affecting the process. Using PBS with surfactants, drug dissolution took place in accordance to the visual representations of the dissolution process. With the applied flow of 0.2 mL/min, visually, the surface concentration, IDR and TA mass released in PBS with CTAB (1% w/v) seemed to be higher than the other media, in accordance with quantified results. UV imaging has proved to be a promising technique for analysing the dissolution properties of drugs given through the IA route and as a future tool for biorelevant dissolution testing, studies may provide further significance to these applications. Understanding the effect of flow in the ASFs tested will also help to study the dissolution properties of the drug in more detail. Additionally, testing the developed BSF in different states, containing all chosen components (HA, proteins and phospholipids) could provide a better insight in how the drug dissolves in synovial fluid. Also, applying a flow in the cell with the use of BSFs, would show the full potential of this new perspective for *in-vitro* testing of drug dissolution for IA drugs.